

# **Development of generic methods for the analysis and purification of polar compounds by high performance liquid chromatography**

Joseph Jonathan Russell

A thesis submitted in partial fulfilment of the requirements of the University of the West of England, Bristol for the degree of Doctor of Philosophy

This research programme was carried out in collaboration with GlaxoSmithKline, Stevenage, UK

Faculty of Health and Applied Sciences, University of the West of England

16 May 2016

## Abstract

Generic methods were developed using different columns for analysis and purification of hydrophilic compounds by hydrophilic interaction chromatography (HILIC). Mobile phases were investigated in detail, and across each column chemistry tested (BEH Amide, Atlantis bare silica, ZIC-HILIC and Cogent Hydride), salt-buffered mobile phase offered good to excellent peak shape for acids, bases and neutral solutes with a range of hydrophilicities. Additionally, cation exchange occurred on the bare silica column even when rubidium nitrate was added to the mobile phase, which should block all cation exchange sites. Measurement of mobile phase pH in hydroorganic solvent (ACN-water mixture with buffer) better represented the environment solutes experience on column than fully-aqueous pH measurement. The performance of HILIC with Charged Aerosol Detection (CAD) was evaluated with a hydrophilic acid, a hydrophobic base and a hydrophilic neutral solute; limits of detection and quantitation were 1-3 ng and 5-9 ng on column, respectively. This compared favourably to literature values for other universal detectors. HILIC-CAD was further investigated by flow injection analysis (FIA) using 29 solutes containing acids, bases and neutrals. HILIC and CAD had excellent compatibility: peak areas were double compared to reversed-phase conditions, response was reasonably uniform for 21 non-volatile solutes considering the

solutes' diversity. HILIC-CAD was viable for retention and detection of highly hydrophilic species without chromophores: salts, sugars and amino acids. Salts travelled down the column as independent cations and anions. Resolution of sugars and amino acids was challenging and was incomplete due to project time constraints. Generic methods were developed on an analytical system in the labs of the industrial collaborator and applied to purifications on wide-bore columns at scaled-up flow rates (21mm id, 20mL/min prep vs. 4.6mm id 1 mL / min analytical analytical). A standard prep system was capable of usable productivity using HILIC with 1mL injections (22 mg of crude purified per hour) and use of At-Column Dilution enhanced this around 10-fold with scope for 4mL injections (223 mg of crude purified per hour).

## Acknowledgements

I thank Professor David McCalley for his support throughout the project. His expertise in HPLC and guidance in preparing papers worthy of high-impact journals has been invaluable. I would also like to thank Dr James Heaton, who has given me reasoned critique with loyal friendship.

I offer thanks to Dr Bob Boughtflower and Tim Underwood at GlaxoSmithKline for preparing the bid for my CASE studentship in collaboration with Professor McCalley. The intense HPLC training they gave me at the start of my project and supervision of my prep work in a second placement set me in good stead, with their balance of sound theory and hard-nosed pragmatism. I thank Simon Readshaw at GlaxoSmithKline for supporting my project from start to finish.

I thank ThermoFisher Scientific for the loan of UHPLC instrumentation and Charged Aerosol Detectors, especially Dr Frank Steiner, Dr Tony Edge and Dr Norman Ramsey.

Thanks also to the Chromatographic Society for providing financial support to attend meetings in the UK and International HPLC conferences in New Orleans, USA and Geneva, Switzerland, in particular Dr John Lough. I hope to continue as a UK researcher who produces chromatography publications and play a future role in this field.

I would like to thank the Royal Society of Chemistry for providing financial support to attend meetings and the opportunity to learn management skills by becoming an Early Career Network Representative in the Bristol & District local section. I thank Colin Chapman for bringing me onto the local committee and Giovanni Depietra and Niamh Brannelly for collaborating in the revival of the Early Career Network in our local area.

Finally, I thank Professor John Hart for being my second supervisor. As part of such a large and eminent supervisory team, John has been a friend throughout the project.

This project was funded by an EPSRC CASE studentship award with GlaxoSmithKline (GSK). Initial HPLC training was done at GSK Stevenage during a three week placement Oct-Nov 2012 and a purification study in a placement Sep-Oct 2015. A UHPLC system with CAD detection was provided by ThermoFisher Scientific, with beta-testing of a new CAD Veo detector (Chapter 5).

## **Dedication**

This thesis is dedicated to my wife Lisa. She keeps me looking up; with her I can see that the chasm is but a crack.

# Contents

Acknowledgements.....	4
Dedication .....	5
Contents.....	6
Chapter 1.....	10
1. High-Performance Liquid Chromatography.....	11
2. HPLC separation .....	13
3. Polarity and Hydrophilicity.....	18
4. HPLC of polar pharmaceuticals .....	20
5. Ion pair chromatography .....	22
6. Hydrophilic Interaction Chromatography .....	22
7. HPLC detection.....	27
8. Charged Aerosol Detection .....	28
9. Purification of polar pharmaceuticals.....	30
10. Focused Gradient Liquid Chromatography and At-Column Dilution .....	31
11. Objectives.....	33
Chapter 2.....	36
1. Instrumentation .....	37
a. HILIC buffer experiments .....	37
b. Charged Aerosol Detector experiments .....	37
c. HILIC Generic and focused method development.....	38
d. HILIC prep experiments.....	38
2. Conditions .....	38
a. Injection .....	38
3. Chemicals and reagents .....	39
4. Probe solutes .....	40
Chapter 3.....	41
Abstract.....	42
1. Introduction .....	43
2. Experimental .....	45
3. Results and discussion .....	49
3.1. Buffer and solute properties.....	49

3.2 Initial studies to establish a generic HILIC mobile phase buffer: performance of four different phases with three mobile phase buffers .....	51
3.3. Detailed studies to elucidate phenomena responsible for results in 3.2 .....	57
3.3.1 Comparison of performance of four different stationary phases with three different buffers .....	57
3.3.2. Effect of mobile phase water concentration and buffer on retention and peak shape .....	68
3.3.3. Causes of poor peak shape for cationic solutes in formic acid .....	72
3.3.4. Effect of buffer salt concentration and salt cation on retention of cationic compounds .....	74
Conclusions .....	75
Chapter 4.....	77
Abstract.....	78
1. Introduction .....	79
2. Experimental .....	82
2.1 Chemicals and reagents .....	82
2.2 Equipment and methodology .....	86
3. Results and discussion .....	88
3.1.1 Detection limits (HPLC) .....	88
3.1.2 Calibration curves (HPLC).....	90
3.2 Response universality and uniformity. ....	96
3.2.1 Flow injection analysis .....	96
3.2.2 Effect of solute salt composition on response (HPLC; FIA) .....	96
3.2.3 Response Uniformity (FIA)-dependence on solute and mobile phase buffer .....	103
3.2.4 Effect of solute volatility on response .....	108
3.2.5 Effect of organic modifier (FIA) .....	111
3.2.6 Effect of elevated temperature (FIA) .....	116
3.3 Analysis of salts (HPLC) .....	119
4. Conclusions .....	121
Chapter 5.....	123
Abstract.....	124
1. Introduction .....	125
2. Experimental .....	128
2.1 Chemicals and reagents .....	128
2.2 Equipment and methodology .....	128
3. Results and discussion .....	130

3.1 Viability of sugar analysis using an alternative stationary phase (BEH Amide) and CAD Veo detection .....	130
3.2 Comparison of Ultra and Veo CAD .....	135
3.2.1 Noise in buffered and unbuffered mobile phase.....	136
3.3 Analysis of Simple Sugars in Beer and Cider .....	142
3.4 Analysis of underivitisised Amino Acids .....	146
4. Conclusions .....	149
Chapter 6.....	150
Abstract.....	151
1. Introduction .....	152
2. Theory .....	153
2.1 Loadability .....	153
2.2 Peak shape .....	155
2.3 Solubility.....	155
2.4 Productivity .....	156
3. Experimental .....	158
3.1 Chemicals and reagents .....	158
3.2 Apparatus and methodology .....	160
4. Results and discussion .....	161
4.1 Choosing separation conditions with alternate selectivity.....	161
4.1.1 Changing the selectivity using the organic solvent.....	161
4.1.2 Changing the selectivity by changing the stationary phase in generic HILIC methods.....	165
4.1.3 Focused analytical 'zone' methods .....	170
4.1.3 Changing the selectivity using RPLC toolbox methods at low pH and high pH .....	174
4.2 Sample preparation using different injection solvents to improve analyte solubility.....	175
4.3 Purification by HILIC.....	177
4.3.1 Generic vs. focused methods on an Atlantis column.....	177
4.3.2 Generic vs. focused methods on a BEH Amide column .....	181
4.3.3 Purification by HILIC using an At-Column Dilution (ACD) system .....	184
4.3.4 Preparative productivity .....	188
4.3.5 Purification of zwitterion(s) .....	193
4.4 Possible explanations for poor ACD performance using DMSO or TFA.....	195
4.4.1 Characterising of the effect of DMSO on peak shape using an analytical system.....	195
4.4.3 Loss of resolution in ACD with 10% TFA diluent .....	201



5. Conclusion.....	202
Chapter 7.....	205
1. Overall Conclusion .....	206
2. Further Work.....	211
References .....	215
Appendix I .....	226
Figures, Tables, Equations, Symbols and Abbreviations.....	226
I.1 List of Figures .....	227
I.2 List of Tables .....	231
I.3 List of Equations.....	232
I.4 List of Symbols .....	234
3. I.5 List of abbreviations.....	239
Appendix II .....	242
Presentations and Publications.....	242
1. II.1 Poster Presentations .....	243
2. II.2 Oral Presentations .....	244
3. II.3 Second Author Oral Presentations.....	245
4. II.4 Publications.....	246

## **Chapter 1**

# **General Introduction**

# **1. High-Performance Liquid Chromatography**

Chemical analysis and purification of complex mixtures is challenging, and chromatography has been developed to address that. The technique of chromatography was originally developed by Tswett in the early 1900's to purify coloured plant extracts. Tswett's technique is similar to modern use: a mobile phase transports the sample through a stationary phase to a detector. In Tswett's analysis, the column was open and the human eye was the detector. A detector has only limited ability to perform chemical analysis of multiple analytes simultaneously, therefore a chemical separation pre-detector, due to the column, provides assurance that the correct substance is analysed or collected. The stationary phase is a column comprised of a packed bed of solid particles, which perform a chemical separation of components in sample mixture, whereby each solute retains then elutes from the column. Chromatography advanced when in 1941 the theory of modern liquid chromatography (LC) was first described by Martin and Synge, applying plate theory from the fractional distillation used to purify petroleum extracts to describe the bands which develop in a separation (Martin, Synge 1941). In the 1970's, Huber, Kirkland and Horvath introduced the principle of using small particles as column packing, and the technique progressed to be called high pressure liquid chromatography or high-performance liquid chromatography (HPLC). In HPLC, the column is filled with a sorbent, which is typically silica-based due to its high thermal mechanical stability, chemical resistance at moderate pH (3-7) (Berthod 1991) although alternative sorbents are also used (e.g. porous graphitic carbon). The sorbent is typically a packed bed of porous particles (diameter 1 – 50µm) where the stationary phase is the pore surface within the particles themselves. Since around the 1980's, the stationary phase has been chemically bonded to

the pore surface, most commonly as a Reversed Phase Liquid Chromatography (RPLC) stationary phase, or unbonded as a bare silica. In RPLC the stationary phase is a hydrocarbon chain attached to a triethoxysilyl moiety, which bonds to the silica surface via a condensation reaction to give a surface with the ligand bonded to it (Fig. 1.1); the mobile phase is highly aqueous which favours retention of hydrophobic solutes into the stationary phase pores.

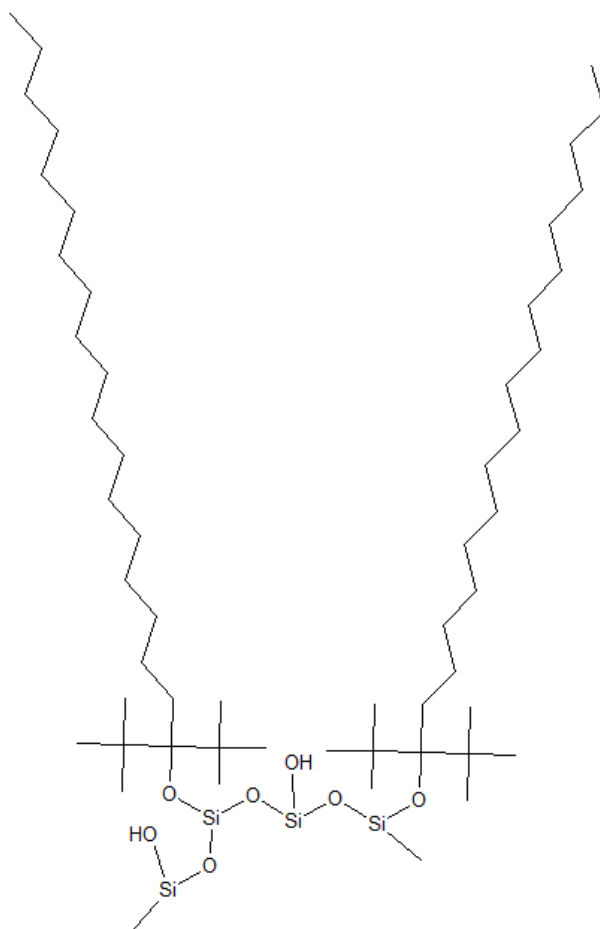


**Figure 1.1 : Octadecylsilyl ligand with isopropyl protection bonded to silica stationary phase**

In the earlier stages of HPLC, the stationary phase was prepared in-house, but this leads to inherent variability of performance, due to a variety of factors which require strict control e.g. ligand density on the surface, packing of the particles. Packing is itself a challenging

process to control, and a study by Kirkland summarises the journey from packing as a 'dark art' to a scientific process (Kirkland *et al.* 2006). Modern HPLC columns are purchased with the stationary phase prepared and pre-packed.

The coupling of ultraviolet absorbance (UV) detectors in the 1960's (Kirkland 1968) and mass spectrometers (MS) in the 1970's (Niessen 2003) to HPLC systems made these techniques powerful with scope for automation. HPLC is near-ubiquitously the technique used to measure and attain acceptable purity of non-volatile substances (Espada *et al.* 2008, Korfmacher 2005). Generic methods allow the application of a relatively small set of analytical methods to a wide variety of compound structures. For example the pharmaceutical company GlaxoSmithKline quality-control tested a library of >700,000 compounds using a single RPLC method (Lane *et al.* 2006). This is very attractive industrially, as the alternative is method development for each compound of interest which can be time-consuming. The ubiquitous RPLC is used to a high degree of sophistication in generic methods as part of Open access (OA, 'walk-up') in drug development (Mallis *et al.* 2002). The user prepares a sample and follows on-screen instructions, the OA method analyses it and emails them the result. Major pharmaceutical companies have invested in this approach (Mallis *et al.* 2002, Korfmacher 2005, Espada *et al.* 2008, Dunn April 2013).

## 2. HPLC separation

In a HPLC separation, the sample is injected into the flow of mobile phase. The amount of mobile phase needed to do that depends on retentivity of the solute in the column and how much mobile phase is delivered by the pump during the separation.

$$V_m = t_0 F \quad (1.1)$$

$$V_r = V_m(1 + k) \quad (1.2)$$

The volume of mobile phase in one column volume ( $V_m$ ) is a function of the time taken by an unretained species to pass through the column ( $t_0$ ) and the volumetric flow rate ( $F$ ) (Equation 1.1). The volume of mobile phase required to elute a peak is the retention volume ( $V_r$ ) (Equation 1.2); this is proportional to the flow rate, which can vary between separations. Guiochon commented that absolute retention times are poorly reproducible and retention factors are the favourable measure of solute retentivity (Guiochon *et al.* 2013).

$$k = \frac{t_R - t_0}{t_0} \quad (1.3)$$

The retention factor ( $k$ ) is a dimensionless measure of solute retention, describing the retention of a solute relative to the passage of an unretained volume of mobile phase through the column (Equation 1.3). Samples typically contain greater than one chemical component; therefore retention must be different for each component to achieve separate peaks and allow the detector to interpret a single signal at a time.

$$\alpha = \frac{k_2}{k_1} \quad (1.4)$$

The relative retention of two peaks is the selectivity factor ( $\alpha$ ), described by the relative retention of two closely-eluting peaks (Equation 1.4). This must be greater than one to achieve separation, and as an approximate rule of thumb, good separations are obtained for selectivity factors above 1.5.

$$N_{0.5} = 5.54 \left( \frac{t_R}{W_{0.5}} \right)^2 \quad (1.5)$$

To separate complex mixtures, each peak must be sufficiently narrow. Ideally peak widths would be infinitesimally small, however band broadening occurs both outside the column due to dead volumes in the instrument, e.g. tubing, and inside the column due to mass transfer and diffusion. To understand band broadening, the concept of theoretical plates was derived by Martin and Synge (Martin *et al.* 1941), where each solute band is analogous to a plate used to capture distillate in fractional distillation of petroleum components. Peak efficiency ( $N_{0.5}$ ) is the peak width at half-height ( $W_{0.5}$ ) relative to the retention time (Equation 1.5), units are number of theoretical plates per column.

$$N = \frac{H}{L} \quad (1.6)$$

The height equivalent to one theoretical plate is the efficiency divided by the column length ( $L$ ) (Equation 1.6). State of the art Ultra High Performance Liquid Chromatography (UHPLC) systems are specially designed to minimise the extra-column band broadening due to e.g. excess tubing length.

$$u = \frac{L}{t_0} \quad (1.7)$$

$$H = A + \frac{B}{u} + Cu \quad (1.8)$$

Intra-column band broadening, represented by  $H$ , can be described by three processes: axial diffusion ( $A$ ), longitudinal diffusion ( $B$ ) and mass transfer ( $C$ ), which are a function of the mobile phase velocity ( $u$ , equation 1.7) as described by the theory of J J Van Deemter (van Deemter *et al.* 1956) (Equation 1.8). The  $A$  term is supposedly unaffected by average mobile phase velocity (1.7) and can be used as a measure of packing quality. The  $B$  term dominates

at low flow rates when (B/u) is large and the solute band is allowed excessive time to diffuse along the column bed. The C term is dominant at high flow rates when (B/u) is small. To achieve good efficiency in analysis, plate heights (H) around 2-20  $\mu\text{m}$  are required, which is slightly larger than the diameter of common stationary phase particles in those columns (1-5  $\mu\text{m}$ ).

$$h = \frac{H}{d_p} \quad (1.9)$$

$$h = a + \frac{b}{u} + cu \quad (1.10)$$

Particle diameters vary between columns, therefore in kinetic studies reduced plate height (h) is considered (1.9), which corrects for the particle size to give (1.10). An ongoing objective of column manufacturers is to produce reduced plate heights below around 1, corresponding to a solute band equilibrating within the diameter of a single particle (1.9).

$$\Delta P = \frac{2500L\eta F}{d_p^2 d_c^2} \quad (1.11)$$

Smaller H values can be achieved using smaller particles, as the shorter distance into and out of the particles allows for better mass transfer (1.8). However the system backpressure affected by particle size (1.11), column dimensions (length L and diameter  $d_c$ ), mobile phase viscosity ( $\eta$ ) and flow rate (F). Modern UHPLC systems are designed to cope with high backpressures (around 1000 bar) when small particles ( $d_p < 2 \mu\text{m}$ ), narrow columns (2.1 mm i.d.) and high flow rates are used for fast analysis on short columns ( $L \leq 5\text{cm}$ ).

In generic methods, bespoke method development is discouraged in favour of using optimal conditions for the majority of analyses. Therefore flow rate is kept constant and this project



hasn't focused on kinetic investigations involving varied flow rate. It is attractive industrially to use an analytical method which scales up to purify compounds without the need for further method development. Therefore this project focuses on HPLC methods that can be scaled up to preparative systems for purification. Preparative separations require the use of much higher flow rates (see 9 below) and therefore to avoid excessive backpressures, very small particles and high analytical flow rates are avoided in this project since these both contribute to high system backpressures (1.11). For a detailed discussion of kinetics in hydrophilic interaction chromatography, studies by Heaton (Heaton *et al.* 2014a, 2014c), McCalley (McCalley 2007) and Gritti/Guiochon (Gritti *et al.* 2013c, 2015) give this topic thorough consideration.

$$R_s = \left(\frac{1}{4}\right) \left[\frac{k}{1+k}\right] (\alpha - 1) \sqrt{N} \quad (1.12)$$

If there is sufficient selectivity ( $\alpha$ ) between peaks, efficiency has limited effect on separation power. It can be shown using the equation for chromatographic resolution ( $R_s$ ; Equation 1.12) that  $R_s$  is optimal at moderate retention ( $1 \leq k \leq 5$ ), good spacing ( $\alpha \geq 1.5$ ) and high efficiency ( $N \approx 10,000$  or above).

$$\log k = \log_{EB} + \eta' H - \sigma S^* + \beta' A + \alpha' B + \kappa' C \quad (1.13)$$

The basis of retention in RPLC is the interaction of the solute with the stationary phase. A central tenet of that is solute partition from a mostly aqueous mobile phase into a layer of octadecylsilyl (ODS, also known as C-18) ligands. This is ideal for non-polar solutes with low affinity for aqueous media and high affinity for the hydrophobic environment inside the column pores. Different interactions between solute and stationary phase are possible and Carr, Snyder *et al.* described those by the Hydrophobic-Subtraction model (Equation 1.13),

where the effect of each interaction on retention is considered (Carr *et al.* 2011, 2015, Marchand *et al.* 2011). Retention ( $\log k$ ) is a function of: partitioning from the mobile to stationary phase (represented by the  $\log$  of retention of a neutral solute ethylbenzene (EB)), hydrophobic interactions ( $\eta'H$ ), steric interactions ( $\sigma S^*$ ), hydrogen bonding of a basic solute to an acidic stationary-phase group ( $\beta'A$ ), hydrogen bonding of an acidic solute to a basic stationary-phase group ( $\alpha'B$ ) and ion-exchange between an ionic solute and a charge-bearing column ( $\kappa'C$ ).

However highly polar solutes are either not retained by RPLC or resolved poorly (McCalley 2010a) due to a low affinity for hydrophobic C18 stationary phase relative to a highly aqueous mobile phase. Therefore alternative separation modes have been considered.

### 3. Polarity and Hydrophilicity

To establish if a solute is hydrophilic and unlikely to retain by RPLC, it is possible to measure a solutes' hydrophilicity using two immiscible solvent phases, normally water and an organic solvent such as n-octanol.

$$X_{(aq)} \leftrightarrow X_{(org)} \quad (1.14)$$

A hydrophilic species will partition into the aqueous phase ( $X_{(aq)}$ ) and a hydrophobic species will partition into the non-aqueous phase ( $X_{(org)}$ ) (Equation 1.14).

$$P = \frac{C(X_{aq})}{C(X_{org})} \quad (1.15)$$

The partition coefficient of this process (P) is calculated by measuring the concentration of the solute in the aqueous [C(aq)] and organic phases [C(org)] (Equation 1.15), for a solute in its neutral form which can be achieved by adjusting the pH.

$$\log P = \log (C_{Xaq}) - \log(C_{Xorg}) \quad (1.16)$$

However P can vary over several orders of magnitude depending on the solute. Log P (Equation 1.16) is a simple value that is increasingly positive for hydrophobic solutes that partition into the organic solvent and increasingly negative for hydrophilic solutes that partition into the organic solvent. However for complex mixtures each solute may be neutral or charged and measuring P is difficult.



$$Ka = \frac{[H_3O^+][A^-]}{[HA]} \quad (1.18)$$

$$pH = pKa + \log \frac{[A^-]}{[HA]} \quad (1.19)$$

To calculate the acidity or basicity of a solution and calculate the solute charge state requires pH and pKa calculations. For the dissociation of an acid (HA) to hydroxonium (H<sub>3</sub>O<sup>+</sup>) and its anion (A<sup>-</sup>) in the presence of water (Equation 1.17), the dissociation constant (Ka) is described by equation 1.18, the concentration of each species shown in square brackets. The negative of the log hydroxonium concentration is equivalent to the pH, and -logKa is the pKa, which relate as shown in equation 1.19.

$$\log D = \log P + \log \left[ \frac{1}{1 + 10^{pKa - pH}} \right] \quad (1.20)$$

The distribution coefficient (D) calculates the partitioning of a solute in its native form whether ionised or neutral, and log D this takes into account the solute pKa, solution pH and log P (equation 1.20). The log D value positive for hydrophobic species that partition into the non-aqueous portion or negative for hydrophilic species that partition into the aqueous portion (equation 1.20). Log D correlates well with hydrophobic retention in RPLC, where a more-positive log D value corresponds to stronger retention on those columns (Poole 2009).

#### **4. HPLC of polar pharmaceuticals**

RPLC is highly productive using modern columns and modern systems that can cope with high backpressures from fast-flowing mobile phase through small particles on narrow columns, however its application is limited to hydrophobic solutes. Fragment-based drug discovery uses small molecules as potential new drugs, described in a seminal paper by Jencks in 1981 (Jencks 1981). This strategy focuses on optimising interactions between chemical species and proteins, and these small molecules (<300 Da) can then be chemically modified to improve physico-chemical properties such as bioavailability. This strategy has since been adopted across the pharmaceutical industry, and was described by Scott *et al.* as ‘firmly established in drug discovery’ (Scott *et al.* 2012). A problem with this strategy is these small molecules can be hydrophilic, with weakly basic or zwitterionic chemical functional groups providing potential biological activity and capacity for formation of C-X bonds in further synthesis (Scott *et al.* 2012, Jencks 1981). This poses a problem for laboratories that synthesise drug-fragments: reliable purity measurements are essential for their quality control prior to high-throughput screening for biological activity (Espada *et al.* 2008). The hydrophilicity of Molecular ‘building blocks’ used in fragment-based drug design

is a serious problem since well-established RPLC requires a solute to be hydrophobic in order to retain on those columns. Polar compounds aren't retained by RPLC and chromatographic separation can be impossible by this somewhat traditional method. Some alternative variations of RPLC have been developed to manipulate the hydrophobicity of the solute and gain retention on those columns. Low pH mobile phase can be prepared by adding a weak or strong acid such as formic (FA) or trifluoroacetic acid (TFA), respectively. When an acidic solute is deprotonated it is negatively-charged and more hydrophilic. Conversely, adding a strong acid to this will protonate, thus neutralise, the acid, and it is more hydrophobic. Therefore FA and TFA are used to retain some acids by RPLC. A similar strategy is used for basic solutes: the protonated form of a base is positively-charged and more-hydrophilic; the unprotonated form is neutral and more-hydrophobic. Thus adding a strong base to RPLC mobile phase raises the pH, neutralises basic species and enhances hydrophobic retention on those columns (McCalley 2004, Davies *et al.* 2008). A potential flaw in the high pH technique is the liability of silica to dissolve through hydrolysis by hydroxyl ions ( $\text{OH}^-$ ). This can be overcome using hybrid silica, which substitutes ethylene bridges for siloxane bonds between silanols in the underlying structure (see poi. This hybrid silica is somewhat resistant to high pH (see point 2 on p. 24). These strategies can be successful for analysis of simple acids and bases by RPLC, but hydrophilic neutral species and zwitterions are unsuitable for high and low pH RPLC, since their  $\text{pK}_a$ 's don't allow for enhanced hydrophobicity at extremes of pH.

## 5. Ion pair chromatography

Addition of Ion-Pairing (IP) agents such as trifluoroacetic acid (TFA) also facilitate retention of charged polar species. A drawback of IP is a reduction of detector sensitivity, especially in Electrospray Mass Spectrometry (ESI-MS) where IP agents can suppress analyte ionisation (Heaton *et al.* 2011). Additionally, it is unclear what the precise retention mechanism is in IP, for example Dai *et al.* reported for basic solutes that approximately 3% of molecules associate with the 'ion pair' agent TFA in aqueous solution (Dai *et al.* 2005).

## 6. Hydrophilic Interaction Chromatography

Polar solutes are hydrophilic and require separation on stationary phases that can attract such species. Hydrophilic Interaction Chromatography (HILIC) is a variant of HPLC has been used to separate sugars since at least the 1970's and in 1990 Alpert coined the name HILIC, which coincided with the release of columns specifically designed to use this separation mode to analyse e.g. phosphorylated amino acids and peptides (Alpert 1990). In HILIC the stationary phase is either bare silica or a bonded polar ligand. The mobile phase has high organic solvent content (>70% ACN) with small water content and buffer. Water forms a stagnant layer on the stationary phase; this allows solutes to partition between a hydrophobic mobile phase and a hydrophilic stationary phase (Figure 1.2).

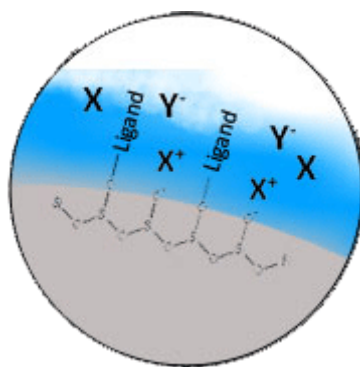


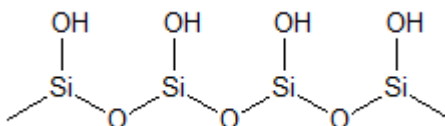
**Figure 1.2. Simple scheme of HILIC retention with neutral (X), basic (X<sup>+</sup>) and acidic (Y<sup>-</sup>) solutes**

The specific interactions between solute and stationary phase have been debated in the literature (Irgum *et al.* 2006, 2011, Kawachi *et al.* 2011, McCalley *et al.* 2010, 2013, 2014, Gritti 2013c, Guo *et al.* 2005, Laemmerhofer *et al.* 2008, Bicker *et al.* 2008). That discussion primarily discussed whether or not partitioning is the dominant retention mechanism in HILIC, as proposed by Alpert (Alpert 1990). A 2006 review by Irgum of HILIC literature was inconclusive, with some of the authors covered suggesting surface-solute interactions, e.g. on Amino columns (Irgum *et al.* 2006). It was suggested by Laemmerhofer Lindner and Bicker that the retention mechanism is complex, with contributions from partitioning, ion-exchange and hydrogen-bonding (Laemmerhofer *et al.* 2008, Bicker *et al.* 2008). McCalley demonstrated that ion-exchange can be mediated by the buffer salt concentration, with high buffer concentration shielding the solute from stationary phase charges (McCalley 2010b). In that study it was noted by the author that ion-exchange differs greatly between HILIC columns (McCalley 2010b).

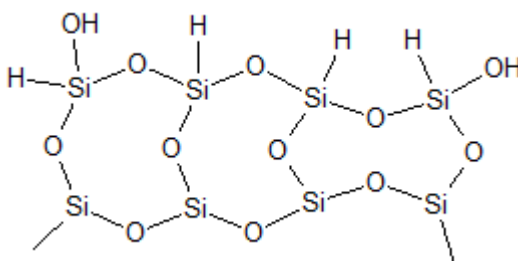
Studies by Irgum, Ikegami and McCalley attempted to categorise HILIC columns according to their retention behaviour (Dinh *et al.* 2011, Kawachi *et al.* 2011, Kumar *et al.* 2013). There

was good agreement that HILIC columns can be described as four broad categories (ligand chemistry described in brackets, approximate structures shown):

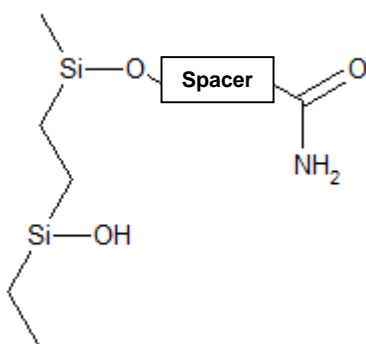
1. Cation-exchangers (e.g. Bare Silica)



(e.g. Silica Hydride)

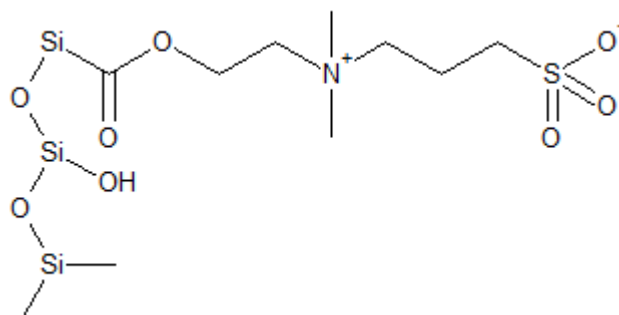


2. Neutral polar bonded ligand (e.g. Amide, BEH Amide)

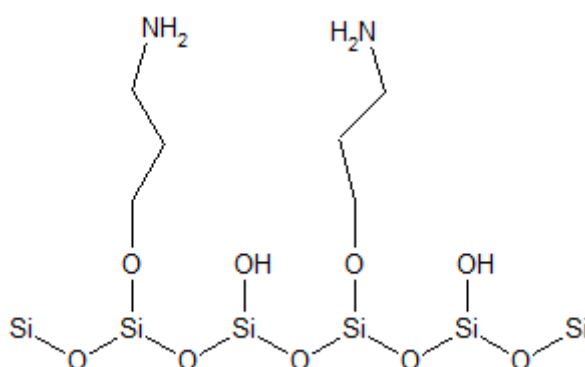


3. Zwitterionic polar bonded bonded ligand (e.g. ZIC-HILIC)





#### 4. Anion Exchangers (e.g. Amino)



The Tanaka group were critical of ion-exchange in HILIC, commenting that reducing ion-exchange interactions is important to obtain better column efficiency in HILIC, with apparent peak tailing when this interaction is employed (Kawachi *et al.* 2011). However Kumar *et al.* observed higher theoretical plate numbers on bare silica than bonded-phase columns (Kumar *et al.* 2013). Ikegami noted that retention differences could be observed between neutral nucleosides and their corresponding nucleobase (e.g. k (uridine)/ k (uracil) reported as 1.81 on an Amide ligand-bonded silica column). The authors commented that the number of hydroxyl groups on the ribose moiety has a great influence on the retention of nucleosides on HILIC columns, suggesting uridine series are suitable probes for HILIC studies (Kawachi *et al.* 2011). Exceptionally high retention of the nucleoside cytidine on Amide and ZIC-HILIC columns was reported by Kumar *et al.* and those authors suggested this

solute can hydrogen-bond with the stationary phase (Kumar *et al.* 2013). An alternative type of silica was developed around 1991 and has been developed by Pesek as 'type C' silica. On these columns, acidic silanols groups are replaced by 'silica hydride' groups and there ought to be virtually no exposed silanols (Yang *et al.* 2013). Applications using type C silica use formic acid as a mobile phase additive, which is reasonable given the manufacturer's claim of an inert stationary phase. However, a report from Watson concluded that 'type C' silica behaves remarkably similar to bare silica (Bawazeer *et al.* 2012) and this phase has shown poor peak shapes in some literature when using Formic Acid as buffer (Yang *et al.* 2013). It is unclear if type C silica offers alternate selectivity compared to bare silica and therefore that was considered in this study. Acetone has been used as a mobile phase organic modifier in place of acetonitrile by the Haddad group (Hutchinson *et al.* 2012) and by Heaton for its use in MS (Heaton *et al.* 2011), but it is unclear how retention compares in acetone to the more typical acetonitrile.

Some more recent fundamental studies into HILIC focused on mass transfer (Gritti *et al.* 2013b, 2013c, Heaton *et al.* 2014a). Solute mass transfer occurs in the mobile phase and the stationary phase (1.18). The contribution of each can be determined in kinetic studies, where theoretical plate heights (1.6) are plotted over a range of average mobile phase velocities and the results fitted to equations such as van Deemter equations (1.8) or (1.10). Mass transfer in the mobile phase is perhaps expected to be high in HILIC due to the low viscosity of organic solvent-rich mobile phase providing relatively free movement of solutes. A 2010 study reported somewhat high mobile phase mass transfer in HILIC using a bare silica column compared to RPLC on a C18 column (McCalley 2010b). Gritti and Guiochon also reported higher van deemter 'B' terms in HILIC compared to RPLC (Gritti *et al.* 2013c).

However when those authors used 'peak parking' to monitor solute movement in the stationary phase, where solute band diverted is diverted to a second column with no mobile phase flow and allowed to diffuse along the column bed, they found diffusivity was low, in contrast to high diffusivity in the mobile phase. The authors attributed that to a relatively high microviscosity of the water layer held to the stationary phase (Gritti *et al.* 2013c). Heaton *et al.* measured diffusion of hydrophilic species on comparable columns with matched retention factors and observed a similar effect, suggesting that adsorption via possible hydrogen bonding between solute and stationary phase surface can contribute to retention (Heaton *et al.* 2014a).

HILIC is compatible with polar compounds, although is yet to be incorporated into a generic method scheme for the analysis of polar pharmaceuticals. The retention mechanism in HILIC is complex and poorly understood, therefore research into the HILIC retention mechanism, with a focus on selectivity and peak efficiency, should lead to a polar 'tool box' of generic methods. The role of buffers in HILIC is unclear, and requires investigation on a range of modern HILIC columns. Detection by MS is less effective in the buffers typically used for HILIC methods, due to analyte signal suppression (Kostiainen *et al.* 2009, Mallet *et al.* 2004, Law *et al.* 2000). An objective of this project is therefore to investigate if formic acid can be used as a buffer in HILIC generic methods, as opposed to buffers.

## **7. HPLC detection**

Batches of drug leads are often products of one-off syntheses, containing impurities which are unknown and standards are thus unavailable. Detection is typically by UV which is cheap and simple to operate or Mass Spectrometry which gives assurance of compound identity

via mass/charge data. Impurity compounds may not contain chromophores thus ultraviolet wavelength (UV) detectors are 'blind' to them. Using MS and UV, small peaks are not meaningful in the absence of reference standards and are not necessarily impurities. Therefore universal detectors, such as the charged aerosol detector (CAD) are a desirable component of a polar 'tool box'. However CAD is a new technology and although operation is very straightforward (Vehovec *et al.* 2010), it is poorly understood.

## 8. Charged Aerosol Detection

A prototype detector was built by Dixon and Peterson in 2002 (Dixon, *et al.* 2002) and since then CAD has been developed for use in HPLC. Around 100 publications to date have focused on CAD (e.g. (Cohen *et al.* 2012, Gamache *et al.* 2005, Web of Science search topic 'Chromatograph\*' AND TITLE 'Charged Aerosol\*'), but only a handful explored the fundamental properties of this relatively novel detector (Dixon *et al.* 2002, Gamache *et al.* 2005, Hutchinson *et al.* 2010, Hutchinson *et al.* 2012, Khandagale *et al.* 2013, Vervoort *et al.* 2008). Figure 1.3 shows a simplified schematic of the CAD. The CAD produces aerosol particles (Steps 1-2 in Figure 1.3) and positively-charged nitrogen gas. These mix such that the aerosol particles acquire positive surface charges (Step 3 in Figure 1.3), and are then transported to an electrometer which converts their charge to an electrical signal (Step 4 in Figure 1.3) via in-built hardware. In contrast to UV detectors, the CAD does not require a solute to contain a chromophore due to it forming physical particles of whatever solute is present. In MS, molecular ions are formed which is in contrast to CAD which forms charged particles. Although some aspects of CAD operation are already understood, it is not clear how it responds to semi-volatile and volatile solutes, which ought to be incapable of forming

aerosol particles. Other detectors which depend on the formation of aerosol particles, such as evaporative light scattering detection (ELSD) as developed by Charlesworth in 1970 (Charlesworth 1978), suffer from complex relationships between solute concentration and detector response (Guiochon *et al.* 1988). ELSD, which measures the light scattering of a laser when the aerosol particles cross the beam, is thought to change in detection mechanism with increasing size of particle. CAD is somewhat more straightforward but nonetheless also depends on aerosol particle formation. It is possible there is some commonality between the ELSD and CAD theory insofar as particle formation is concerned. Thus an empirical relationship between solute concentration and detector response might be achievable. A combination of universal detection and a universal response to solute concentration suggest CAD has potential as a HPLC detector in generic methods. Therefore an objective of this project was to evaluate the performance of CAD, in particular with the use of HILIC separations.

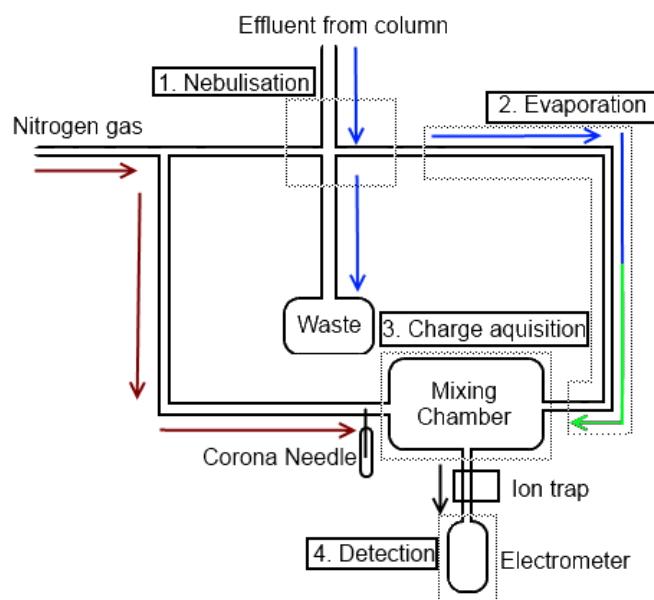


**Figure 1.3. The Charged Aerosol Detector**

## 9. Purification of polar pharmaceuticals

Purification by preparative HPLC uses wider-bore columns compared to analytical separations ( $\geq 10$  mm i.d. preparative,  $\leq 4.6$  mm i.d. analytical) to hold sufficient stationary phase so that larger samples can be loaded onto the column.

$$\text{Scale up factor} = \frac{dc_{\text{Prep}}^2}{dc_{\text{Analytical}}^2} \quad (1.21)$$

When scaling up a separation, to maintain the same average mobile phase velocity the flow rate is scaled up in proportion to the ratio of the squared column diameter (1.21). The injection volume is scaled up by the same factor (1.21) to maximise the loading of sample. Preparative HPLC commonly employs sample loads far above the column capacity, and separation performance is degraded as a result of shifts in retention and broad peaks with low efficiency.

Purification studies using HILIC are scarce in the scientific literature, although this is a necessary application of the technique. McCalley reported in 2007 that bare silica HILIC column(s) have capacity around ten times higher than RPLC for strong bases (McCalley 2007), which are particularly problematic in RPLC (McCalley 2010a). Gritti and Guiochon studied the overloading of strong bases propranolol and amitriptyline hydrochloride using a bridged ethylene hybrid (BEH) silica in HILIC (Gritti *et al.* 2015), reporting similar improvements over RPLC. This study used a charged surface hybrid (CSH)-C18 RPLC column, which contained positive charges to control solute repulsion, which is thought to be responsible for the tailing overload of charged bases even at low solute concentration (Gritti *et al.* 2015). Bonded phase columns are available with diverse chemistries in HILIC, which can provide substantial changes in selectivity (Kumar *et al.* 2013, Kawachi *et al.* 2011, Dinh

*et al.* 2011). However none of these columns have featured in HILIC purification or loadability studies.

## **10. Focused Gradient Liquid Chromatography and At-Column Dilution**

The majority of fundamental studies into HILIC have used isocratic conditions, whereby the mobile phase composition is held constant throughout the separation. This simplifies the methodology, however there are practical benefits from changing the mobile phase during the separation (Snyder *et al.* 2010). In RPLC, applying a gradient of mobile phase organic solvent content is common practise, starting from mostly-aqueous mobile phase to a more organic-rich mobile phase. The benefits from this are reduced run time, as the increased organic solvent content elutes strongly-retained solutes from the column. Additionally, peak shape is improved using a solvent gradient: once eluted the solute travels solely into the mobile phase and interactions with the stationary phase are minimal, therefore band broadening is less pronounced. Solvent gradients have been applied to HILIC separations (Karatapanis *et al.* 2009, Periat *et al.* 2013a, Tyteca *et al.* 2014), however in contrast to RPLC the starting conditions are an organic-rich mobile phase changing to a more-aqueous mobile phase. Focused gradients can be used to expand areas of the chromatogram and are used in day-to-day preparative work in industry, although publications on this technique are limited to application notes, e.g. (Tei *et al.* 2013). A recent study of optimisation of relevant parameters in preparative separations by Forssén and Fornstedt found that selectivity ( $\alpha$ ) was the most important factor to maximise productivity (Forssén *et al.* 2014). Focused methods are designed to improve the spacing between the peak of interest and the nearest-eluting species, although focused gradients have not been reported to been applied using

HILIC. Therefore that strategy was employed in this project to HILIC-prep separations. At-column dilution was described by Neue to aid loading of poorly-soluble compounds (Neue *et al.* 2003). In this technique, the sample is introduced onto the column slowly via a second pump, which is diluted at the column head by a second flow of weakly-eluting mobile phase mixed in to the sample flow using a T-piece (Fig. 1.4). This was employed in this project to further enhance preparative performance.

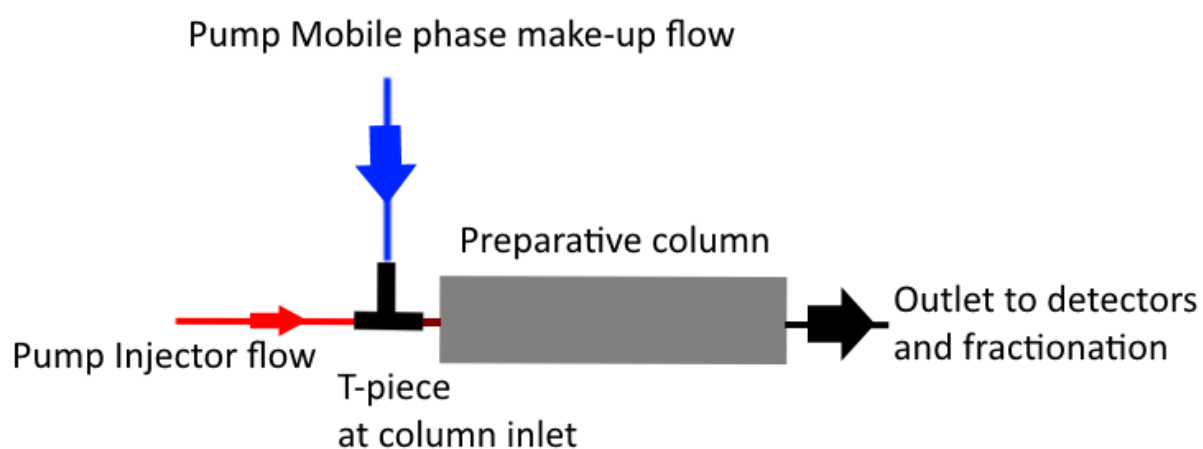


**Figure 1.4. At Column Dilution**



## 11. Objectives

The principle interest of this project is the analysis and purification of hydrophilic drug-like solutes and polar “building block” molecules. The present study evaluates HILIC in a generic method setup. Choice of some basic parameters is necessary before HILIC methods can be implemented in a generic setup, namely the following.

### 1. Suitable mobile phase buffer

A detailed study of mobile phase buffers including salt and simple acid buffers was necessary. Previous studies by Watson *et al.* have suggested simple acid buffers may not be suitable on type C silica phases (Bawazeer *et al.* 2012), thought to contain Si-H bonds as ligands (Yang *et al.* 2013). A study using a bare silica HILIC column suggested formic acid may not be suitable for basic solutes (McCalley 2007), but this has not been evaluated for alternative bonded-phase columns.

### 2. Suitable stationary phase

Studies by Irgum, Ikegami and Kumar have shown differences in the retentivity of HILIC stationary phases (Dinh *et al.* 2011, Kawachi *et al.* 2011, Kumar *et al.* 2013). Based on this, and the categories described in (6), a bare silica and BEH Amide column were chosen for generic HILIC use, as these give appreciably alternate selectivity (Kumar *et al.* 2013) and the BEH Amide has extra stability resulting from the bridged ethylene hybrid silica with potential for future alternative pH use (McCalley 2015).

### 3. Universal detection

Charged aerosol detection is supposedly a universal detector, responding to any non-volatile solute, with uniform response, independent of solute chemistry. The calibration curves of solute concentration vs. detector response ought to be simpler than established universal detectors such as ELSD. However these factors have not been evaluated with a sufficiently broad range of solute chemistries. Additionally, the organic-rich solvent used as HILIC mobile phase ought to give excellent detector response due to facile desolvation, as reported for MS elsewhere (Periat *et al.* 2013b). This has not been evaluated by HPLC for the CAD. It was therefore an objective of this project to elucidate the effect of various parameters and conditions on CAD response with a view to describe optimal use of this relatively novel detector.

### 4. Viability of HILIC purification.

It is industrially attractive to scale-up analytical methods directly to larger-bore preparative columns for purifications, and although this has been attempted for mixed-mode and aqueous normal phase methods, HILIC can be operated at lower mobile phase salt concentration than these modes (e.g. 5mM cf. 20mM) which simplifies work-up as the salt is removed to produce a pure product (Underwood May 2014). It was therefore an objective of this project to develop some generic HILIC analytical methods suitable for polar pharmaceuticals and apply those to purification in a proof-of-concept study.

### 5. Suitable sample diluent

A basic understanding of hydrophilic compound solubility in HILIC mobile phases has not been established in the literature. One study by Guillarme *et al.* reported the water content

of diluents used in sample preparation must be kept to a minimum for HILIC separations (Ruta *et al.* 2010) and alternative solvents may be possible diluents for HILIC (Ruta *et al.* 2010). Further work in this area is crucial if HILIC can be employed to purify polar solutes on the scale required by the pharmaceutical industry.

## **Chapter 2**

# **General Experimental**

## **1. Instrumentation**

### **a. HILIC buffer experiments**

These were performed with a 1290 binary high pressure mixing UHPLC instrument (Agilent, Waldbronn, Germany) with Chemstation, photodiode array UV detector (0.6  $\mu$ L flow cell) and 5  $\mu$ L injections.

### **b. Charged Aerosol Detector experiments**

These were performed with a Thermo UltiMate 3000 Rapid Separation Liquid Chromatography system. This was comprised of a quaternary pump, diode array detector (DAD) and either a Corona Ultra or Corona Veo CAD, with Chromeleon 7.2 software (Thermo, Germering, Germany). The CAD is a destructive detector, therefore the DAD and CAD detectors were connected in series in some experiments, with flow first through the DAD. Thermo Viper tubing (0.13 mm ID) was used as connection tubing. Data collection rates were 100 Hz for both DAD and CAD, due to narrow peak widths (typically 1 s at half height in flow injection analysis (FIA)). The Corona Ultra nebuliser (cross flow design similar to that used in atomic absorption spectrometry) was controlled at 22°C with the evaporator tube at ambient temperature, while the Veo (concentric flow design similar to those used in mass spectrometry) nebuliser was at ambient temperature and the evaporator tube set to 30°C. The Veo had a power function (PF) designed to 'linearise' data, which was set to either 0.67 (this simulates 'off'), 1.00 (the default) or 1.2 (optimised setting using experimental data, see below). Experiments on acetone as a HILIC mobile phase and dimethylsulfoxide (DMSO) as a diluent on analytical columns were also performed on this Thermo system.

### **c. HILIC Generic and focused method development**

These were performed at GlaxoSmithKline laboratories, using an Agilent 1100 system (Agilent, Waldbronn, Germany) with Chemstation, binary pump, UV Diode Array Detector (DAD) and 1  $\mu$ L injections.

### **d. HILIC prep experiments**

These were performed at GlaxoSmithKline laboratories, using a Waters prep system with Masslynx, quaternary pump, and automated fraction collection, QDa mass spectrometer with an electrospray interface, UV diode array detector and UV post-fraction detector. Fractionation was directed by the MS, which was set to sufficiently high sensitivity such that fractions were discarded to waste in this proof-of-concept study.

## **2. Conditions**

### **a. Injection**

Chromatographic peak shape can be sensitive to the injection volume used to introduce the sample. Dolan advised this be limited to around 15% of the peak volume (Dolan 2014) with a rough 'rule of thumb' to keep injection volumes below 16  $\mu$ L for the analytical column and particle dimensions used in these studies (Dolan 2014). Above this, volume overload can occur, which reduces peak efficiency thus reduces resolution ( $R_s$ ). Injection volumes were kept well below this, as the UV detectors offered sufficient sensitivity at 5  $\mu$ L injections. The CAD experiments used low injection volumes of typically 1  $\mu$ L, as an objective of those studies was to establish the detection limits of this relatively novel detector. This injection

volume (1  $\mu$ L) was also found suitable for flow injection analysis (Chapter 4, 5). Preparative experiments used custom injection volumes as described in Chapter 6.

### 3. Chemicals and reagents

All test solutes, and rubidium nitrate were obtained from Sigma-Aldrich (Poole, U.K.). Acetonitrile (ACN, far UV grade), ammonium formate (AF) and orthophosphoric acid (PA) were obtained from Fisher (Loughborough U.K.). AF buffers were prepared by adjusting aqueous solutions to pH 3.0 with formic acid such that the over-all concentration of AF in the mobile phase after organic solvent addition was 5 mM. The pH values of the mobile phase quoted are those either in the aqueous portion of the buffer ( $w^w$  pH) or alternatively as measured in the organic-aqueous combination with the electrode calibrated in aqueous buffers ( $w^s$  pH).

Standards for HILIC buffer experiments were prepared at a concentration of 50 mg/L and made up in the exact mobile phase. For CAD experiments these were prepared at a concentration of typically 10,000 mg / L in 50-50 ACN-water with 0.1% FA (v/v), then diluted with exact mobile phase to the required concentration. For HILIC generic method development, a combined standard of eight probe solutes was prepared at a concentration of 0.5 mg / mL in 50-50 ACN-water with 0.1% FA (v/v). For HILIC prep experiments, custom diluents and concentrations were used as described in Chapter 6.

## **4. Probe solutes**

To represent a variety of polarities, hydrophilicities and charge states, a selection of neutral, acid, basic and zwitterionic compounds were used as test probes. Each results chapter describes the solutes chosen for that particular study.



## **Chapter 3**

# **Comparison of peak shape in hydrophilic interaction chromatography using acidic buffers and simple acid solutions**

## Abstract

The retention and peak shape of neutral, basic and acidic solutes was studied on hydrophilic interaction chromatography (HILIC) stationary phases that showed both strong and weak ionic retention characteristics, using aqueous–acetonitrile mobile phases containing either formic acid (FA), ammonium formate (AF) or phosphoric acid (PA). The effect of organic solvent concentration on the results was also studied. Peak shape was good for neutrals under most mobile phase conditions. However, peak shapes for ionised solutes, particularly for basic compounds, were considerably worse in FA than AF. Even neutral compounds showed deterioration in performance with FA when the mobile phase water concentration was reduced. The poor performance in FA cannot be entirely attributed to the negative impact of ionic retention on ionised silanols on the underlying silica base materials, as results using PA at lower pH (where their ionisation is suppressed) were inferior to those in AF. Besides the moderating influence of the salt cation on ionic retention, it is likely that buffers improve peak shape due to the increased ionic strength of the mobile phase and its impact on the formation of the water layer on the column surface.

# 1. Introduction

Hydrophilic interaction chromatography (HILIC) is rapidly establishing itself as a complementary technique to reversed-phase separations (RP), particularly for polar and/or ionised compounds that are poorly retained using the latter method. It is a technique well-suited to the analysis of pharmaceuticals and compounds of biomedical significance (Olsen 2001, Periat *et al.* 2013b, Zhou *et al.* 2008). The stationary phase in HILIC is typically bare silica, or polar groups bonded to a silica or an organic polymer matrix (McCalley 2010b, Kawachi *et al.* 2011, Hemstrom *et al.* 2006). The hydro-organic mobile phase is similar to that used in RP, except typically employs much higher concentrations of acetonitrile (>70%). There is appreciable overlap in the applicability of these two techniques to compounds of moderate hydrophilicity, particularly for basic compounds. These can be retained by ionic interactions which occur on all silica-based phases as well as by hydrophilic interactions (McCalley 2010b, 2013, Kawachi *et al.* 2011, Hemstrom *et al.* 2006). Hydrophilic interactions are likely to result from a combination of solute partition between a water layer held on the surface of the column and the bulk mobile phase, and by adsorption onto polar groups that may be partially deactivated by the presence of the water layer (Hemstrom *et al.* 2006). HILIC separations are usually performed in ACN-water mobile phases containing additives or buffer components, particularly when the analysed solutes are ionogenic. The buffer serves to control the ionisation of the stationary phase surface groups and silanols in silica-based phases, as well as the ionisation of the solute. The choice of buffers for HILIC is limited to those that have sufficient solubility in high concentrations of ACN. Typically, ammonium acetate or ammonium formate (AF) is used; these salts have the additional advantage that they are volatile and thus compatible with nebuliser-based detectors e.g. electrospray

ionisation mass spectrometry. However, use of buffers can cause depression of the electrospray signal that increases with concentration over the typical range (5–50 mM) employed (Kostiainen *et al.* 2009, Mallet *et al.* 2004, Law *et al.* 2000). Even at the 5 mM level, it was shown that AF can cause greater signal suppression for acidic and basic pharmaceuticals compared with the use of simple acidic solutions of 0.1% formic acid (FA), which are commonly used. An added advantage of these acid solutions is that they are easier to prepare than mobile phases containing buffers. Nevertheless, it has been shown that ACN-water mixtures containing formic acid alone can give rise to poor peak shape in HILIC for acidic and basic solutes, whereas good peak shapes were obtained with AF buffers (McCalley 2007). However, these studies were performed solely on a bare silica column. It is possible that the strong ionic interactions with ionised silanols on this type of phase are contributory to this poor peak shape with FA, and that buffers are unnecessary with other types of HILIC columns (Kumar *et al.* 2013). For example, bonded phase (e.g. with amide ligands) materials prepared on inorganic–organic hybrid silicas show much reduced ionic interactions. Furthermore, silica hydride materials (Type C silica) are available for HILIC-type separations. It is claimed that this new type of stationary phase has significant differences in terms of chemical structure to traditional silicas, which are mainly populated with polar silanol groups. In contrast, Type C silica apparently has surface silicon-hydride groups (Pesek *et al.* 2008, Boysen *et al.* 2011). The term “aqueous normal phase” (ANP) has been suggested to describe separations on this type of silica phase to distinguish them from “classical” HILIC separations. Nevertheless, ANP is also a term more generally used as an alternative to HILIC for classical separations, reflecting the possibility that adsorption is at least a contributory mechanism along with partition to the overall retention mechanism. It could be supposed that these Type C stationary phases would contribute considerably less

ionic inter-actions, so the use of buffers might be unnecessary with such phases, if ionised silanol groups were the cause of peak shape problems. Indeed, separations on these phases are often reported with ACN-water mixtures containing only 0.1% formic or acetic acids (Boysen *et al.* 2011, Pesek *et al.* 2008, Bawazeer *et al.* 2012) although no comment has been made in these reports concerning the lack of use of buffers, or whether their absence gave rise to any detrimental (or even beneficial) effects. The aims of this paper were to compare the use of buffers with acid solutions for acidic, basic and neutral solutes separated on a variety of stationary phases, including bare silica, amide bonded onto hybrid silica, zwitterionic and silica hydride phases. These materials are considerably different in their retention characteristics towards ionised solutes, and therefore might produce different results in the various mobile phases. In this way we hoped to gain information to assist appropriate mobile phase selection for use in HILIC and HILIC with mass spectrometric detection. This study is divided between initial work to establish a pragmatic buffer choice for ongoing work in the project (Chapters 4-6), and detailed studies to further elucidate the phenomena responsible for those results.

## **2. Experimental**

Initial experiments were performed with an Agilent 1100 binary HPLC instrument (Agilent, Waldbronn, Germany) with Chemstation, UV variable wavelength detector and 5µL injections.

All experiments were performed with a 1290 binary high pressure mixing UHPLC instrument (Agilent, Waldbronn, Germany) with Chemstation, photodiode array UV detector (0.6 µL

flow cell) and 5  $\mu\text{L}$  injections. The columns used (all 25  $\times$  0.46 cm ID, except where stated) were Cogent Silica C (4  $\mu\text{m}$  particle size, pore size 100 $^{\circ}\text{\AA}$ , surface area 350  $\text{m}^2/\text{g}$ ) from Microsolv (Eatontown, USA), Atlantis silica (5  $\mu\text{m}$  particle size, pore Size 100  $\text{\AA}$ , surface area 360  $\text{m}^2/\text{g}$ ) from Waters (Milford, USA), ZIC-HILIC (5  $\mu\text{m}$  particle size, pore size 200  $\text{\AA}$ , surface area 140  $\text{m}^2/\text{g}$ ) from Merck-Sequant (Umeå, Sweden) and XBridge BEH Amide (15 cm  $\times$  0.46 cm, 3.5  $\mu\text{m}$  particle size, pore size 140  $\text{\AA}$ , surface area 190  $\text{m}^2/\text{g}$ ) from Waters. By replacing the column with a zero dead volume fitting, the extra-column bandspreading of the instrument was estimated to reduce column efficiency by less than 5% even for a non-retained peak on the most efficient column. Temperature was maintained at 30 $^{\circ}\text{C}$  using the Agilent column compartment. Acetonitrile (far UV grade), ammonium formate and orthophosphoric acid were obtained from Fisher (Loughborough U.K.). AF buffers were prepared by adjusting aqueous solutions to pH 3.0 with formic acid such that the over-all concentration of AF in the mobile phase after organic solvent addition was 5 mM. Standards were prepared at a concentration of 50 mg/L and made up in the exact mobile phase. The pH values of the mobile phase quoted are those either in the aqueous portion of the buffer ( $w^w$  pH) or alternatively as measured in the organic-aqueous combination with the electrode calibrated in aqueous buffers ( $w^s$  pH). All test solutes, and rubidium nitrate were obtained from Sigma-Aldrich (Poole, U.K.). Log D and log P values were calculated as the average from three different programs: ACD version 12.0 (ACD labs, Toronto, Canada), Marvin (ChemAxon, Budapest, Hungary) and MedChem Designer (Simulations Plus, Lancaster, USA). pKa and solute charge was calculated from the average estimate given by the first two calculators. For the initial studies column efficiency was measured at half-height. For the detailed studies to elucidate explanation for those data, column efficiency (N) was measured from the first and second statistical moments according to the relationship in 3.1.

Asymmetry factor was measured at 10% of peak height by dividing the width of the trailing edge of the peak by that of the leading edge. The columns were operated in the region of their optimum flow (1.0 mL/min for silica and hydride silica, 0.5 mL/min for zwitterionic and amide).

$$N = \frac{M_1^2}{M_2} \quad (3.1)$$

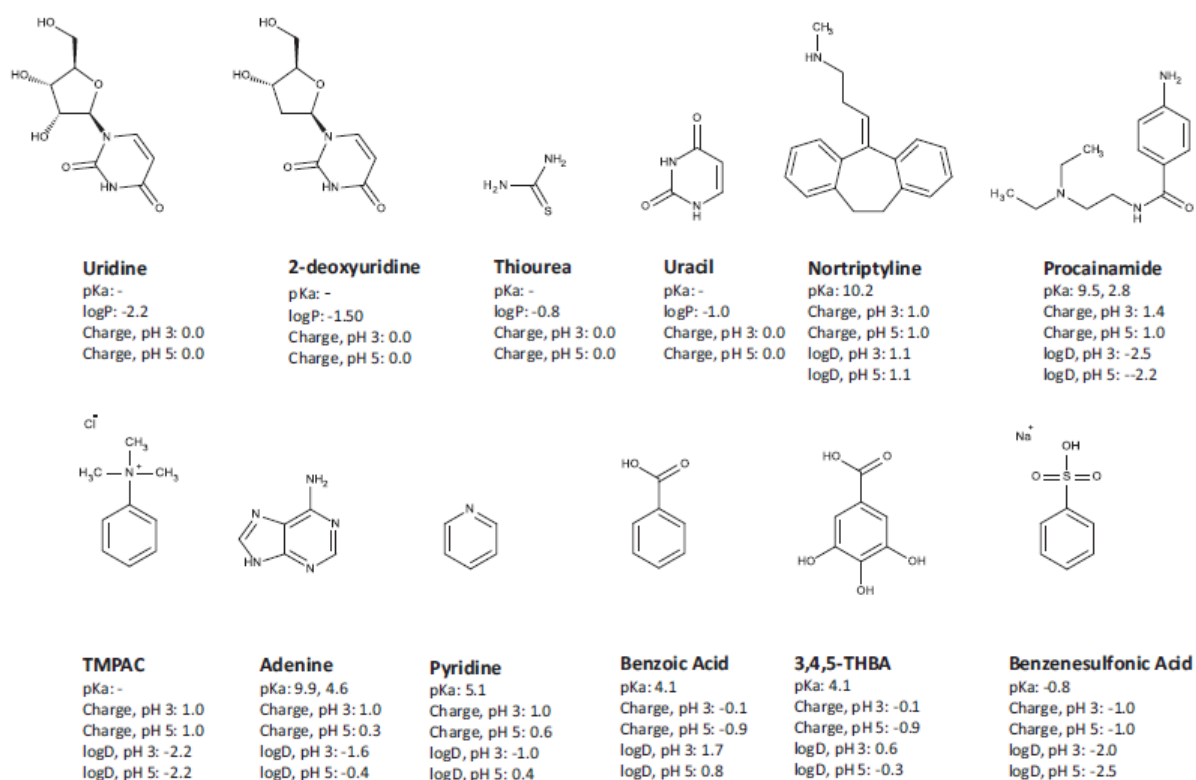


Fig. 3.1. Structures, pKa, log P/D and charge at  $w^w$  pH 3 and  $w^w$  pH 5 for the probe solutes



### 3. Results and discussion

#### 3.1. Buffer and solute properties.

Table 3.1 indicates the pH, ionic strength and buffer capacity of the three mobile phases used, 5 mM ammonium formate (AF) adjusted to pH 3.0 with formic acid, 0.1% (v/v) formic acid (FA), and 0.1%(v/v) orthophosphoric acid (PA), if prepared in aqueous solution. Ammonium formate and formic acid are soluble in high concentrations of ACN; they are also volatile additives and thus extremely suitable for use in HILIC with mass spectrometry detection (Periat *et al.* 2013b). PA is an alternative acid additive used by several column manufacturers e.g. (*Halo Penta-HILIC brochure* 2014). It was used successfully by Mant and Hodges for the HILIC separation of peptides using a 0.2% concentration in 85% ACN, using UV detection (Mant *et al.* 2008). These authors sought a more hydrophilic acid additive than trifluoroacetic acid (TFA). We showed by experiment in the present study that 0.1% PA was completely soluble even in 100% ACN, with no evidence of precipitation. PA is not volatile and is thus unsuitable for use with mass spectrometry detection. However, PA was studied due to the lower  $w^w$  pH and  $w^s$  pH given by this relatively strong acid, and thus its better ability to suppress the ionisation of residual silanol groups. PA is also not expected to give substantial ion pair effects (see the discussion of these effects in Section 3.2). Ion pairing could lead to lower retention of ionised bases due to reduction in ionic interactions with the stationary phase and the reduced hydrophilicity of the paired species. In contrast, trifluoroacetic acid, which is a stronger acid and is more hydrophobic than PA can give quite pronounced ion pair effects (McCalley 2007), which we believed might have confounded the interpretation of the results by affecting retention times.

A relatively low concentration of AF was employed, as such concentrations are generally preferred when mass spectrometry is used for detection. While the buffer capacity of formic acid in water is the least of the three solutions, it is still appreciable.  $w^s$  pH values (in the organic–aqueous mixture) are shown for 85% ACN solutions. The choice of this measurement as opposed to  $w^w$  pH in the aqueous fraction alone is not straightforward. Detailed computer modelling by Tallarek and co-workers (Melnikov *et al.* 2011, 2012), suggests that there is a layer exclusively of water molecules tightly bonded to the surface of bare silica; in this case the use of  $w^w$  pH may be more appropriate. However, other experimental work suggests there may be significant numbers of acetonitrile molecules in the interfacial region (Rivera *et al.* 2013). Fig. 3.1 shows the structure, pKa, charge and log D/log P values at  $w^w$  pH 3.0 and 5.0 for the 12 probe solutes used, which were a mixture of neutrals, strong and weak acids and bases, and a quaternary ammonium salt. Average values of these parameters from several different calculation programs were used in order to improve the accuracy of the estimations. Although the agreement of estimates from the programs was reasonable, there was some lack of consistency between the programs due to the use of different software algorithms (Kumar *et al.* 2013).

**Table 3.1 pH, molarity and buffer capacity of aqueous buffer solutions and dilute acids;  $w^s$  pH measured in 85% ACN. \*This was used as 0.1% of an 85% solution (14.6 mM/L).**

Buffer	$w^w$ pH	$w^s$ pH	Molarity (mmol/L)	Buffer capacity (mmol/L pH)
0.1% Formic Acid	2.7	2.9	2.2	9.7
5mM Ammonium Formate pH 3.0	3.0	5.2	6.1	14.7
0.1% Phosphoric Acid*	2.1	2.0	7.9	26.1

### **3.2 Initial studies to establish a generic HILIC mobile phase buffer: performance of four different phases with three mobile phase buffers**

Initially this study was performed on an Agilent 1100 system with a view to establish a generic mobile phase buffer system for the remainder of the project. Eleven solutes were used as probe compounds, shown in Fig. 3.1 with the exception of Uracil, which was added to later parts of this work (3.3) to characterise a somewhat broader selection of hydrophilic neutral solutes. Each solute was injected individually onto the respective column in mobile phase buffered either by ammonium formate (5mM  $w^w$  pH 3 with formic acid), formic acid (0.1% v/v) or phosphoric acid (0.1% v/v). Plots of column efficiency, measured at peak half-height, are shown in Fig. 3.2a-d for each column for the three buffer systems. Peak

asymmetry was measured at 10% peak height ( $As_{0.1}$ ). Peak shape in terms of efficiency and symmetry was superior in ammonium formate buffer on all columns for the majority of solutes compared to formic acid (0.1% v/v). Ionogenic solutes were strongly affected by the choice of buffer, whereas neutral solutes were relatively unaffected (Fig. 3.2). The overall peak shape recovered when phosphoric acid (0.1% v/v) was used as mobile phase buffer (Fig.3.2a-c). There were also shifts in retention between the buffers, for example on the Cogent column bases were more strongly retained in formic acid than in ammonium formate buffer (data not shown). These phenomena were elucidated in detail in a collaborative study, discussed in 3.3.

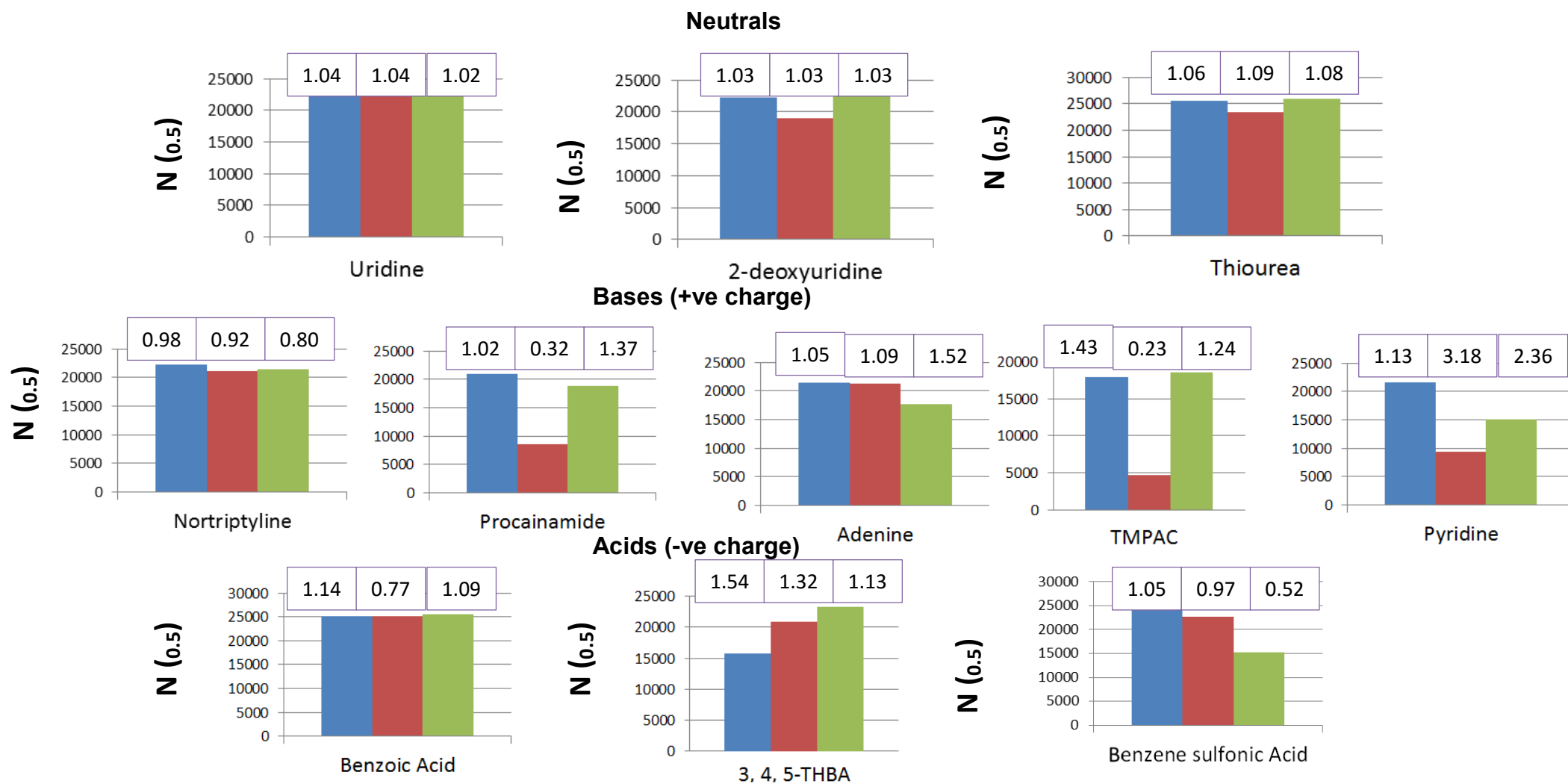


**Fig. 3.2a** Initial results for eleven probe compounds, Atlantis column. Vertical scale is peak efficiency at half-height in plates per column; peak asymmetry at 10% height shown in purple boxes above efficiency bar plots. Stationary phase Atlantis (4.6 x 250mm, 5 $\mu$ m) mobile phase 89.425% ACN with respective buffer. **Blue** = Ammonium Formate 5mM; **Red** = Formic Acid 0.1% v/v; **Green** = Phosphoric Acid 0.1% v/v

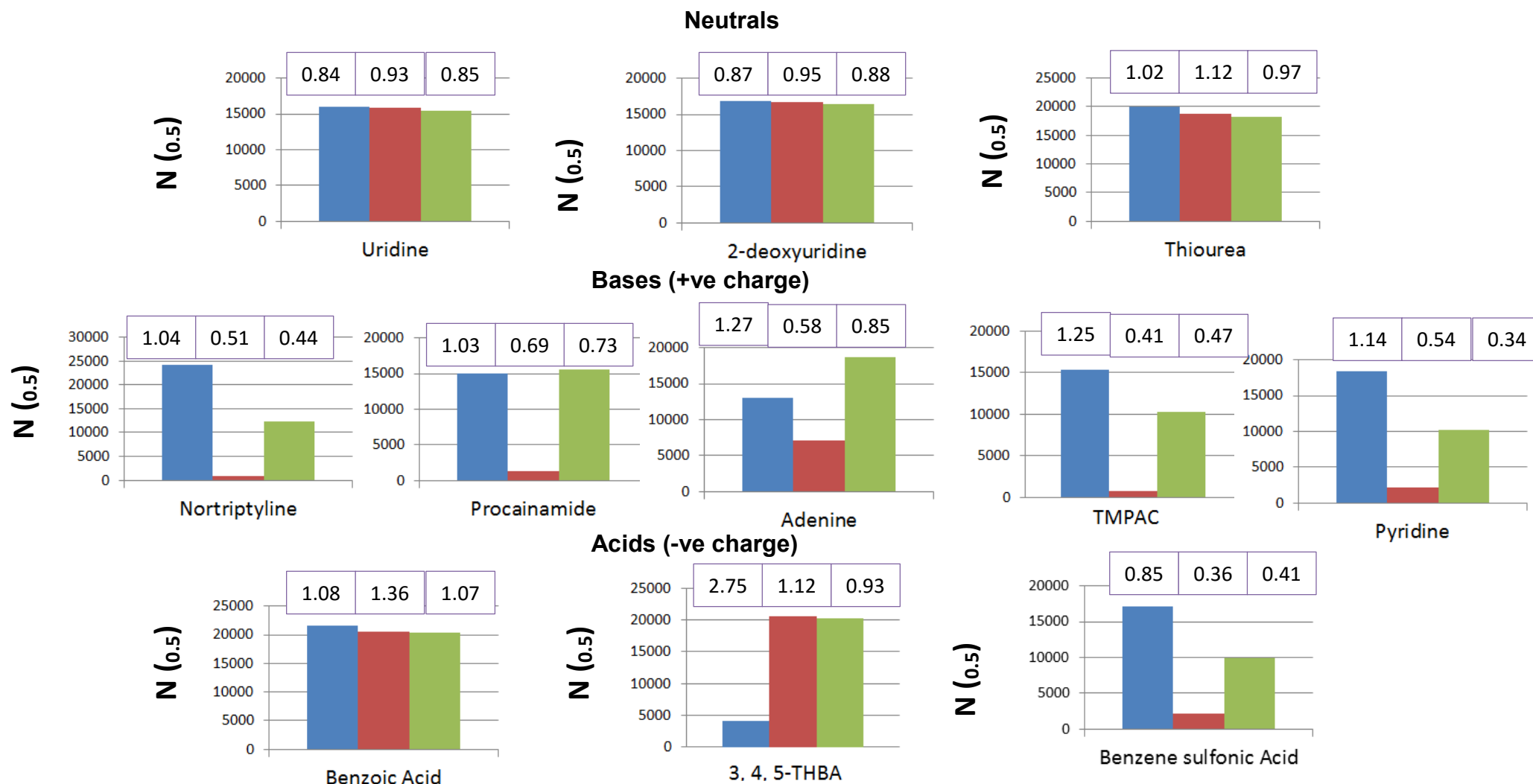


**Fig. 3.2b** Initial results for eleven probe compounds, BEH Amide column. Vertical scale is peak efficiency at half-height in plates per column; peak asymmetry at 10% height shown in purple boxes above efficiency bar plots. Stationary phase BEH Amide (4.6 x 150mm, 3.5 $\mu$ m) mobile phase 89.425% ACN with respective buffer. **Blue** = Ammonium Formate 5mM; **Red** = Formic Acid 0.1% v/v; **Green** = Phosphoric Acid 0.1% v/v

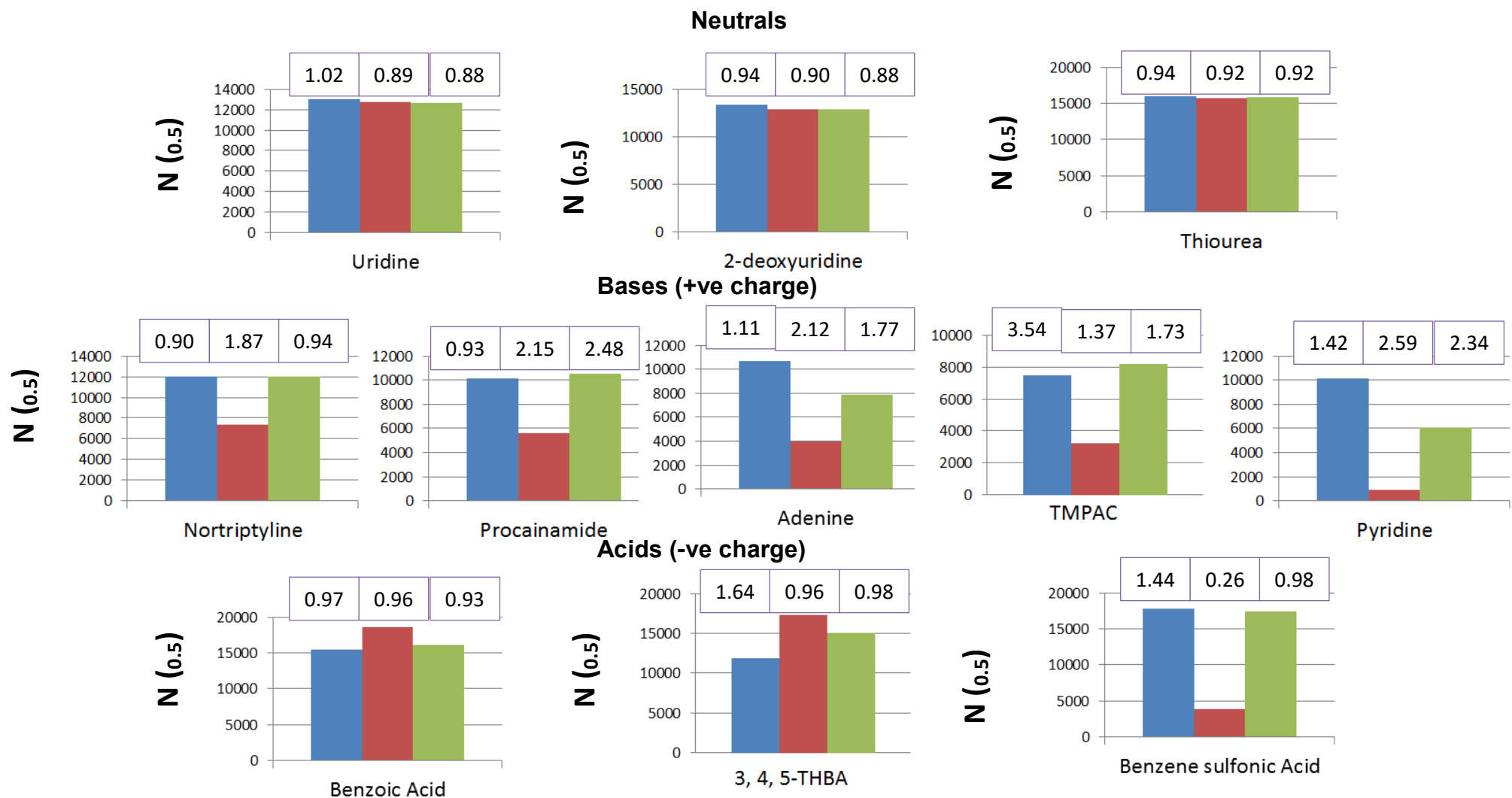


**Fig. 3.2c** Initial results for eleven probe compounds, Cogent Type C silica column. Vertical scale is peak efficiency at half-height in plates per column; peak asymmetry at 10% height shown in purple boxes above efficiency bar plots. Stationary phase BEH Amide (4.6 x 150mm, 3.5 $\mu$ m) mobile phase 89.425% ACN with respective buffer. **Blue** = Ammonium Formate 5mM; **Red** = Formic Acid 0.1% v/v; **Green** = Phosphoric Acid 0.1% v/v

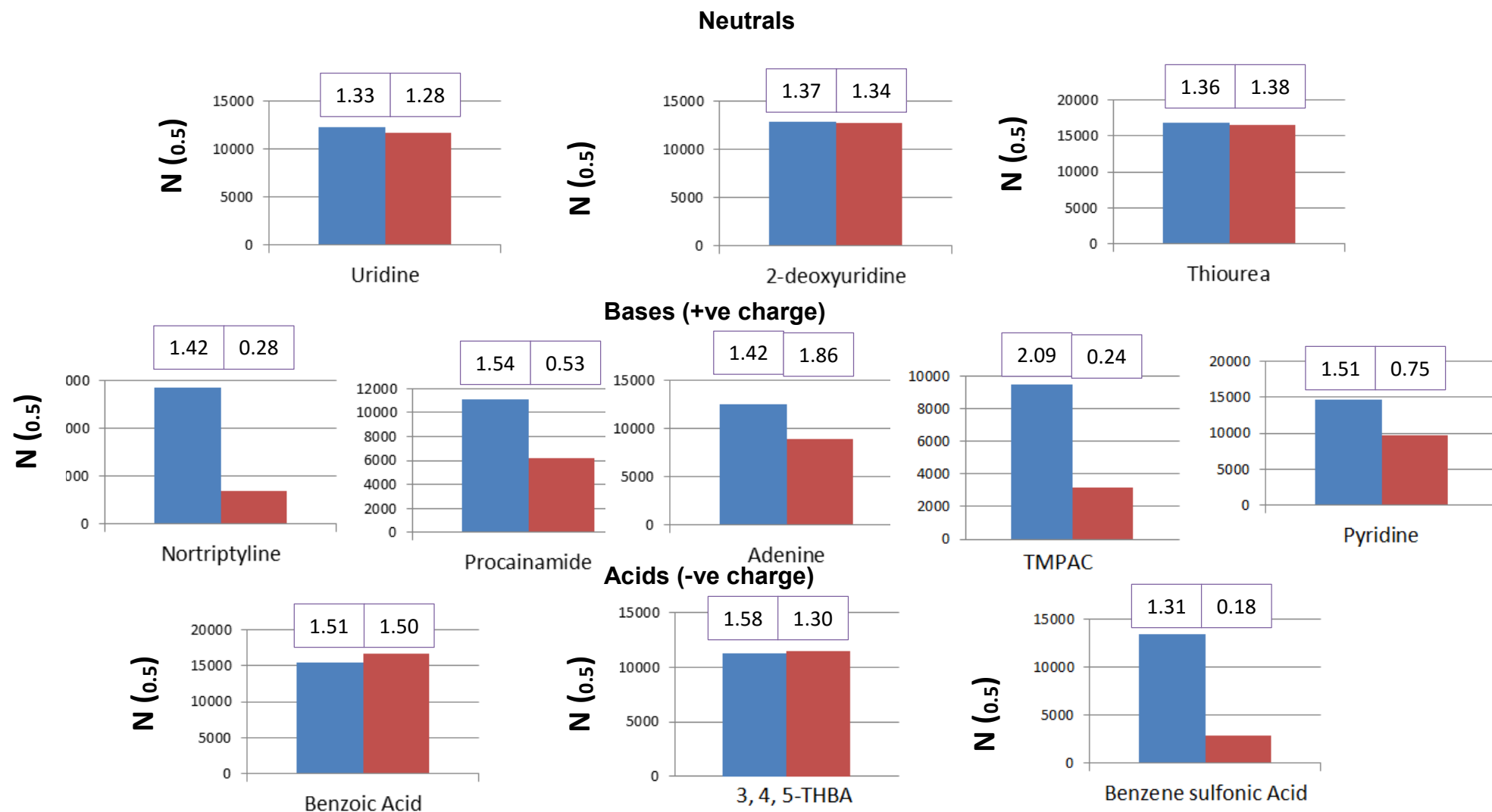


**Fig. 3.2d** Initial results for eleven probe compounds, ZIC-HILIC column. Vertical scale is peak efficiency at half-height in plates per column; peak asymmetry at 10% height shown in purple boxes above efficiency bar plots. Stationary phase BEH Amide (4.6 x 150mm, 3.5 $\mu$ m) mobile phase 89.425% ACN with respective buffer. **Blue** = Ammonium Formate 5mM; **Red** = Formic Acid 0.1% v/v.



### **3.3. Detailed studies to elucidate phenomena responsible for results in 3.2**

#### **3.3.1 Comparison of performance of four different stationary phases with three different buffers**

The silica and bridged ethyl hybrid (BEH) amide phases were chosen for their, respectively, high and low cationic selectivity (preferential retention of cationic compounds) indicated in previous work (Kawachi *et al.* 2011, Kumar *et al.* 2013). The silica hydride stationary phase was studied as it supposedly contains very few silanol groups. Thus, ionic retention should be considerably reduced and its influence on retention and peak shape using FA would be considerably lower. A popular zwitterionic phase which has been used to separate hydrophilic species such as metabolites (Zhang *et al.* 2015) was also included as it can give alternative selectivity compared with the other phases in this work. The columns were evaluated using 90% ACN containing each of the three buffers AF, FA and PA, giving the results shown in Fig. 3.3. 10% water (90% ACN) was chosen for the study as it gave reasonable retention for most compounds (see also Section 3.3.2). The bare silica phase was characterised by low retention of the neutral solutes (uridine–uracil) in both AF and FA (Fig. 3.3a). Retention of neutrals on this column was somewhat lower still in FA than AF, which might be attributed to a reduced water layer in the absence of the salt (Dinh *et al.* 2013). Greater retention of neutrals was obtained on both the zwitterionic and amide phases. This increased retention is likely to be related to the greater occupancy of the column pores with water on the ZIC phase (25%) and a TSK amide phase (21%) compared with Atlantis silica (9%) that have been measured using Karl-Fischer titration (data obtained in 80% ACN with 5 mM acetate, (Dinh *et al.* 2013)). This greater uptake of water is due to

the formation of swollen hydrogels on polymerically-functionalised phases like ZIC-HILIC (Dinh *et al.* 2011, 2013), and seems likely to emphasise the contribution of the partition mechanism to retention. With each mobile phase and each column, the retention of cationic solutes (nortriptyline to pyridine) was considerably higher than for neutrals. Preferential retention of cations compared with neutrals in AF or FA was shown for all columns, but was less pronounced on the amide phase. While the hydrophilicity of cations contributes to this increased retention, ionic interactions are likely to give a strong influence on retention. Thus nortriptyline ( $\log D_{w^w} \text{ pH } 3.0 = 1.1$ ) is only moderately hydrophilic, but its high  $pK_a$  (10.2) results in protonation in all mobile phases leading to additional ionic retention. TMPAC ( $\log D_{w^w} \text{ pH } 3.0 = -2.2$ ) is considerably more hydrophilic, which combined with similar ionic interactions (both nortriptyline and TMPAC are unipositively charged under the analysis conditions) leads to stronger retention than for nortriptyline. The retention of the weak base pyridine ( $pK_a$  5.1,  $\log D_{w^w} \text{ pH } 3.0 = -1.0$ ) was much greater in PA compared with AF. The lower pH of the PA mobile phase could result in greater protonation of this weak base in PA increasing its hydrophilicity and also increasing ionic retention caused by residual silanol ionisation (Fig. 3.3a). The persistence of ionic interactions on all columns at the low pH of PA is indicated by the observation that neutral uridine has a more negative  $\log D_{w^w} \text{ pH } 3.0$  value ( $-2.1$ ) but considerably smaller retention in the PA mobile phase than pyridine ( $-1.0$ ). Besides the effect of the different pH values of these mobile phases on retention, the competing effect of the ammonium ionic retention should also be considered. This factor most likely contributes to the smaller retention of cationic solutes using AF compared with FA, which is particularly evident for the hydride, silica and zwitterionic columns (Fig. 3.3a). While the silica column is known to give high ionic retention (Dinh *et al.* 2011), the same result is surprising for the hydride column, which supposedly has hydride

groups in place of silanols. The same observation of high retention of bases on hydride phases, and the possibility of ionic retention of these solutes, has also been noted by other authors (Bawazeer *et al.* 2012). Similarly, the low retention of the anionic solutes such as 3,4,5-trihydroxybenzoic acid ( $pK_a$  4.1,  $\log D_{w^w}$  pH 3.0 = 0.60) and particularly of benzenesulfonic acid, BSA ( $pK_a$  -0.8,  $\log D_{w^w}$  pH 3.0 = -2.0) on the silica and hydride columns (e.g. with AF) can be explained by repulsion of these species from ionised silanols. It seems that the positively charged ammonium ions cannot mask sufficiently the effects of the silanols, at least not with the low concentrations of AF used in this study. This repulsion must effectively counteract retention resulting from the partition mechanism, as BSA is appreciably hydrophilic. These anionic solutes only showed appreciable retention on the zwitterionic and amide phases, which have been shown to exhibit reduced ionic effects (Kumar *et al.* 2013). It is also possible that retention of acidic solutes is promoted by the presence of the quaternary ammonium functionality that is present on the zwitterionic phase. The continued low retention of BSA in PA on all columns is also suggestive of persistent silanol ionisation, even at lower pH. Fig. 3.3b indicates that the choice of buffer had relatively little effect on the efficiency of neutral compounds when 90% ACN was used (although lower efficiency was noted for some neutrals in FA using a lower water concentration -95% ACN—see following section). The silica column gave excellent efficiency for almost all solutes (neutral, cationic and anionic) in AF buffer, generating >25,000 plates for some compounds (reduced plate height  $h < 2.0$ ). High efficiency was also obtained for the amide column for all these solutes in AF, with  $h$  as low as 2.1 for the neutrals (note the dimensions and particle size of this column differed from the others). The lower plate count given by the zwitterionic column for neutrals was due to some peak tailing (see Fig. 3c), which influences the efficiency calculation, particularly when using the moments method.

While there was some decline in efficiency for the ionogenic solutes on all columns compared with the neutrals (especially for some of the cationic solutes with the hydride column, and for 3,4,5-THBA), efficiency was still broadly maintained at high levels for all columns when using AF. Clearly however, the most remarkable observation from Fig. 3.3b is the catastrophic loss in efficiency for the cationic solutes on all columns using FA, with plate counts in some cases only a tenth or less of their values in AF. Substantial deterioration in the efficiency of the acid BSA was also noted in FA; the high efficiency of benzoic acid in FA is attributable merely to the very low retention of this solute under the analysis conditions (see Fig. 3.3a). Clearly the problem with use of FA, noted previously only for a bare silica phase, is not connected merely with the strong ionic interactions of this material, as the amide phase (based instead on a hybrid organic–inorganic silica) has considerably reduced interactions of this type (Kumar *et al.* 2013). Fig. 3.3c indicates that the loss in efficiency is in most cases due to serious fronting of peaks. However in ammonium formate buffers, the ammonium cation is presumably able to act as a counter-ion in cation exchange with basic compounds and additionally shield surface negative charges from acidic solutes. This perhaps explains the improved overall peak shape in AF as opposed to FA mobile phase (Fig. 3.3a).

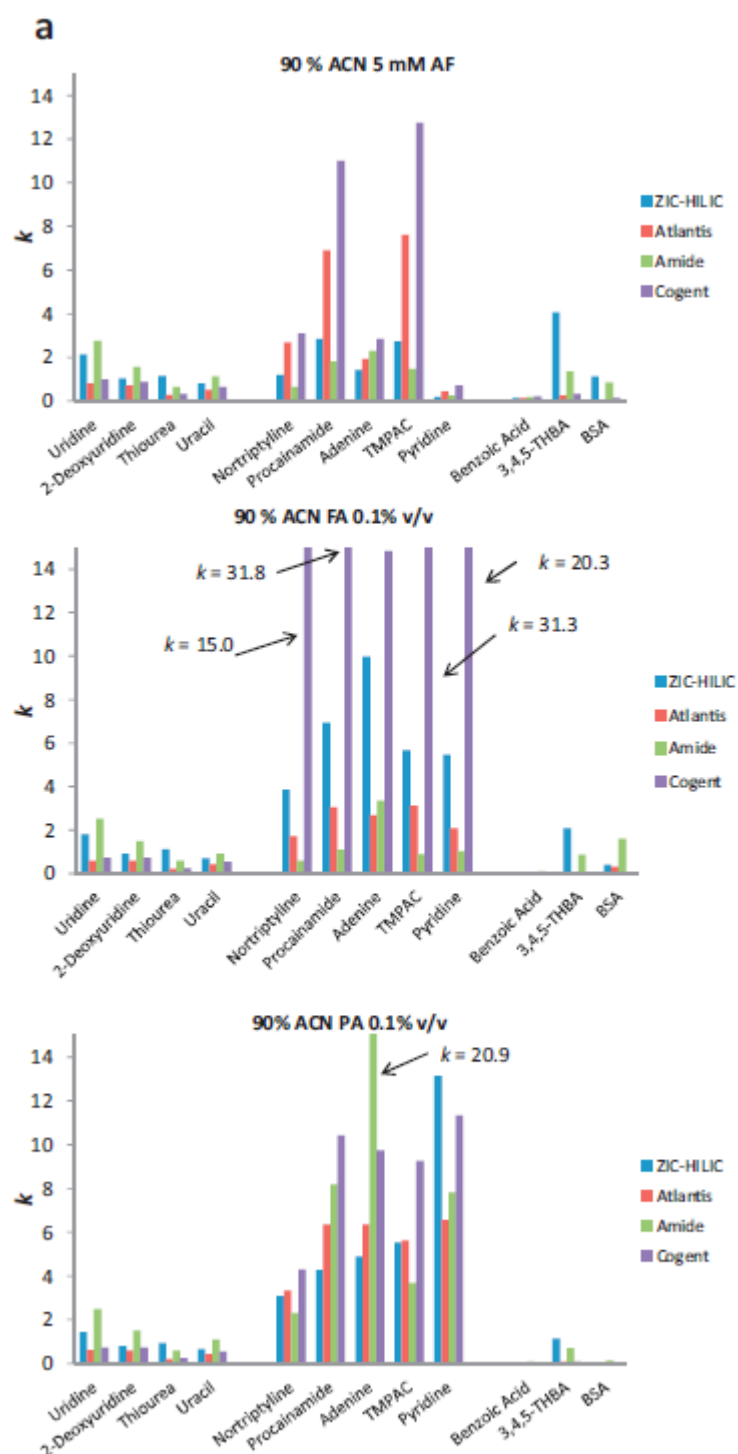


**Fig. 3.3a. Retention factor ( $k$ ), for neutrals (uridine–uracil), cationic(nortriptyline–pyridine) and anionic solutes (benzoic acid-BSA) on four different columns using mobile phases with 90% ACN and various buffers. Solutes TMPAC = trimethylphenylammonium chloride; THBA = trihydroxybenzoic acid; BSA = benzenesulfonic acid. Column temperature 30°C. Solute concentration 50 mg/L, injection volume 5  $\mu$ L. For other details, see Section 2.**

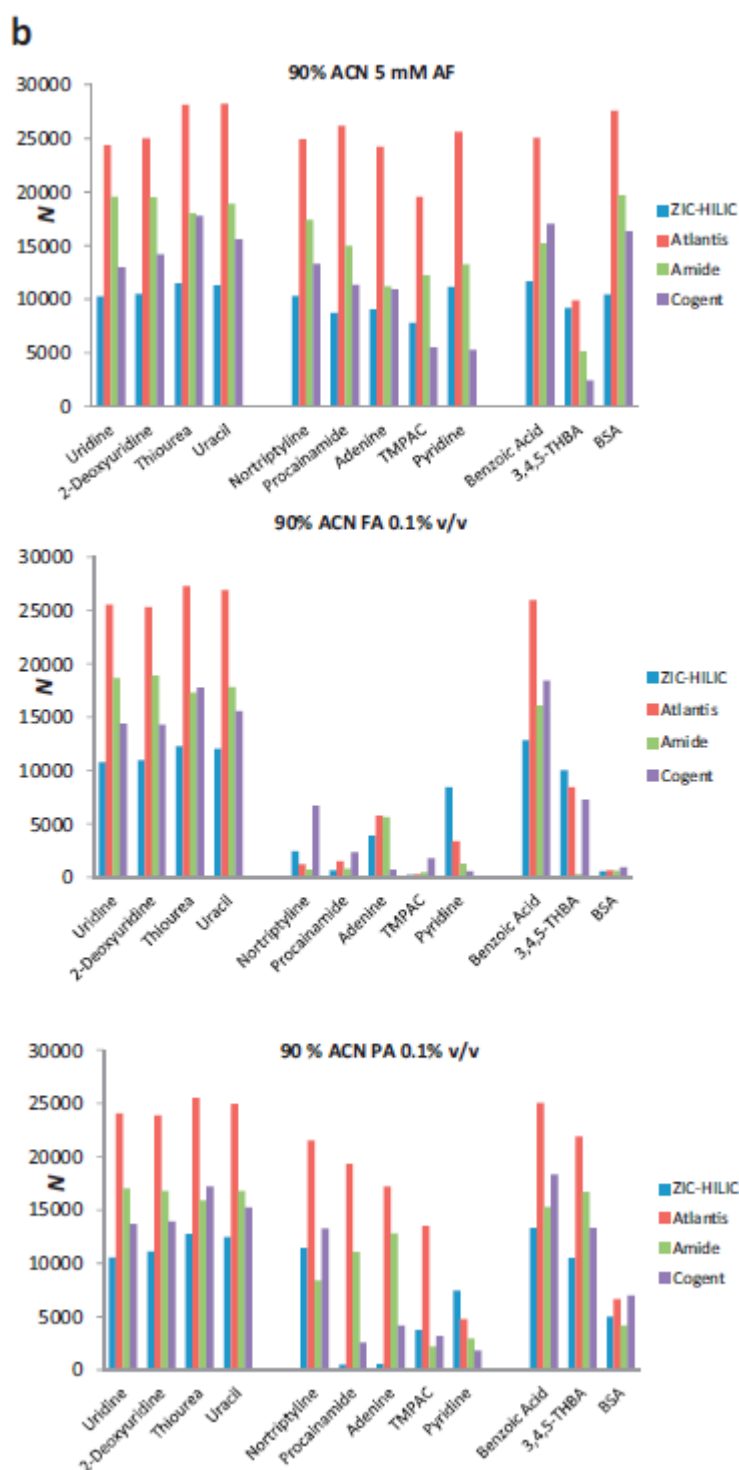


**Fig. 3.3b. Column efficiency (N, statistical moments method) for neutrals (uridine–uracil), cationic(nortriptyline–pyridine) and anionic solutes (benzoic acid-BSA) on four different columns using mobile phases with 90% ACN and various buffers. Solutes and conditions as per Fig 3.2a.**

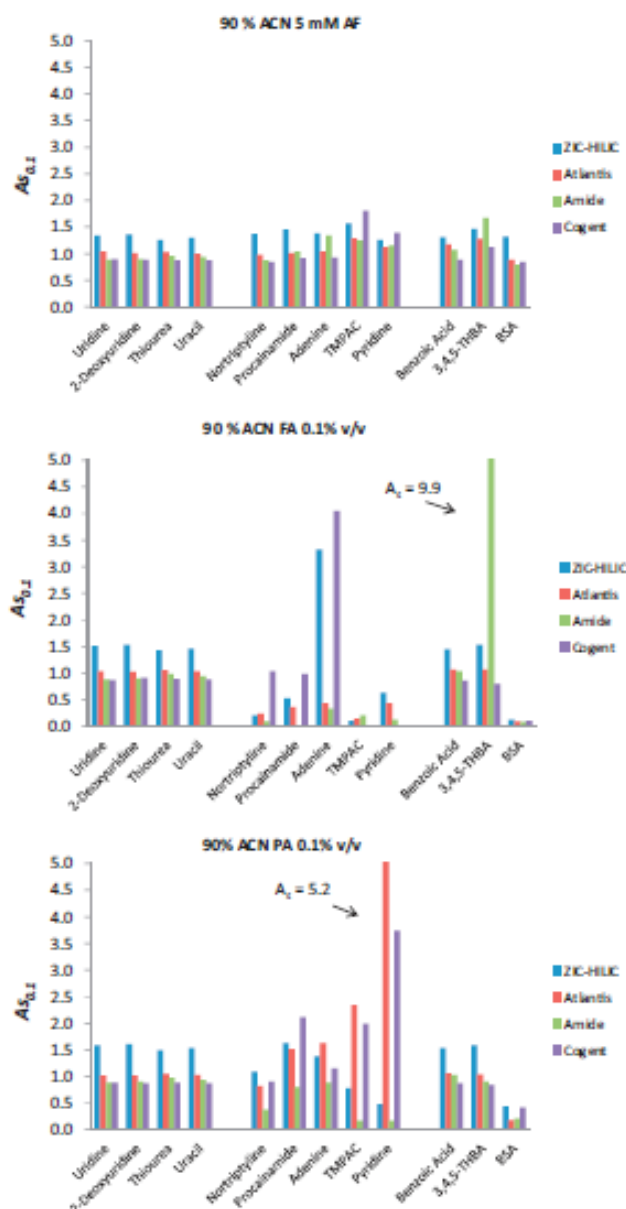
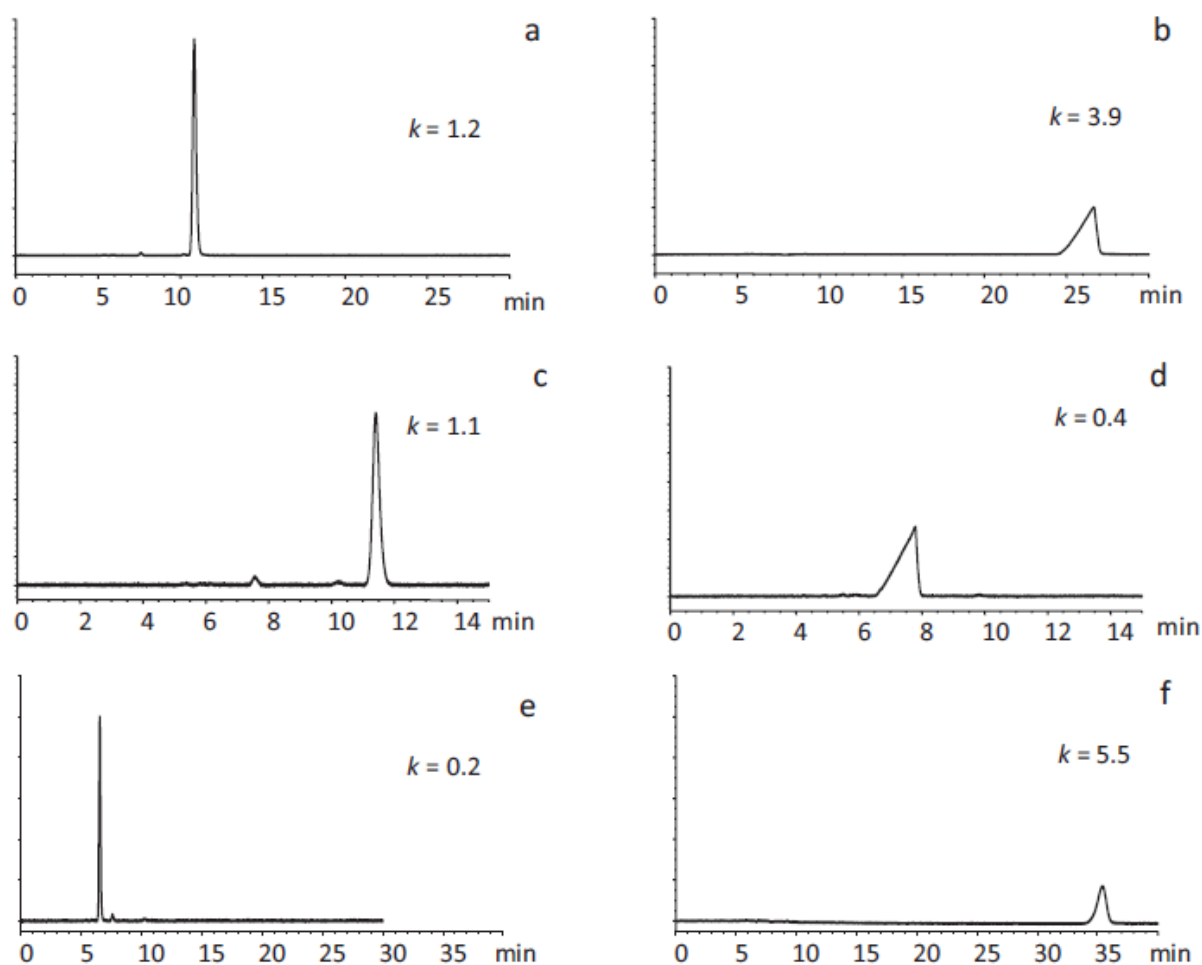


Fig. 3.3c asymmetry factor ( $As_{0.1}$ ) for neutrals (uridine–uracil), cationic(nortriptyline–pyridine) and anionic solutes (benzoic acid-BSA) on four different columns using mobile phases with 90% ACN and various buffers. Solutes and conditions as per Fig. 3.2a.

Fig. 3.3 (a) Retention factor ( $k$ ), (b) column efficiency ( $N$ , statistical moments method) and (c) asymmetry factor ( $As_{0.1}$ ) for neutrals (uridine–uracil), cationic(nortriptyline–pyridine) and anionic solutes (benzoic acid-BSA) on four different columns using mobile phases with 90% ACN and various buffers. Solutes TMPAC = trimethylphenylammonium chloride; THBA = trihydroxybenzoic acid; BSA = benzenesulfonic acid. Column temperature 30°C. Solute concentration 50 mg/L, injection volume 5  $\mu$ L. For other details, see Section 2.



**Fig. 3.4.** ZIC-HILIC column (a) nortriptyline with mobile phase 90% ACN, 5 mM overall AF pH 3; (b) nortriptyline with 90% ACN containing 0.1% FA; (c) BSA with AF; (d) BSA with FA; (e) pyridine with AF; (f) pyridine with FA. Flow rate 0.5 cm<sup>3</sup>/min.

Fig. 3.4 compares examples of the chromatograms for nortriptyline, BSA and pyridine in AF or FA mobile phase, showing peak fronting in the latter. Efficiency for cationic and anionic solutes was improved in PA compared with FA, but still inferior to that in AF for all columns. For this acid, either tailing or fronting caused loss inefficiency. Apparently, (partial) suppression of ionic interactions at low pH is not necessarily beneficial to obtaining good peak shapes for ionogenic solutes. Indeed it may be that the balance of ionic and



hydrophilic retention is the critical factor in determining peak shape. This balance may even be more favourable at higher pH (Periat *et al.* 2013c). While superior performance with AF may in part be related to the deactivating effect of the ammonium ion, it may be that the salt encourages the formation of the water layer on the column surface, giving improved results. The ionic strength of 0.1% FA in water is the least of the three in Table 3.1, but is likely to be considerably reduced in an 85% acetonitrile solution, as indicated by the rise in  $w^s$  pH. The true thermodynamic  $s^s$  pH (which pertains to the pH in the aqueous–organic phase using calibration buffers prepared in the same solution) is related to the  $w^s$  pH by the relationship (3.2):

$$s^s \text{ pH} = s^w \text{ pH} - \delta \quad (3.2)$$

Where  $\delta$  is a term that incorporates both the Gibbs free energy for transference of 1 mol of protons from the standard state in water to the standard state in the hydroorganic solvent at a given temperature, and the residual liquid junction potential (the difference between the liquid junction potential established during calibration in aqueous solutions, and that in the hydroorganic mixture). The value of  $\delta$  is about  $-1.1$  in 85% ACN (Gagliardi *et al.* 2007), implying  $s^s \text{ pH} = 4.0$  and a concentration of formate anions in the mobile phase of only around 0.1 mM/L. While the  $w^s$  pH of PA is lower than that of FA, the concentration of phosphate anions in the same mobile phase is still only around 0.8 mM/L. Still lower ionic strength would be present in solutions containing higher concentrations of ACN; the  $\delta$  value in 90% ACN is about  $-1.6$  (Gagliardi *et al.* 2007). Due (at least) to their low ionic strength, we believe that the degree of ion pairing in these simple acid solutions is likely to be small. In contrast, the ionic strength of the ammonium formate solution is maintained by the presence of the salt. In this case, some degree of ion pairing is possible, no studies are

known that have investigated this possibility in the high concentrations of ACN relevant to HILIC studies. It is possible that some ion-pairing in AF moderates ionic interactions with the stationary phase. Ion pairing would also reduce solute hydrophilicity: both effects may contribute to the reduced retention of bases shown in Fig. 3.3a. As mentioned previously however, all these arguments are complicated by the problem of whether physical parameters in water or in the aqueous–organic mixture should be considered. The ionic strength of the mobile phase may well have influence on the thickness of the water layer which may be beneficial for ionic species. The presence of negatively-charged silanol groups on the stationary phase surface attracts cations, such the buffer cation  $[\text{NH}_4]^+$ . The cation itself is anticipated to be hydrated by some water molecules. Therefore when retaining on the stationary phase in HILIC, it is also possible that AF has specifically favourable properties in the formation of the water layer, in addition to its effect on masking ionised silanols. The observation of apparently strong ionic interactions of the hydride phase was unexpected compared with reports concerning the composition of this material (Boysen *et al.* 2011, Pesek *et al.* 2008). In fact in the present study, the hydride column appeared to behave in a fashion more similar to the bare silica phase, rather than phases like the zwitterionic and amide materials, which demonstrate reduced ionic interactions.

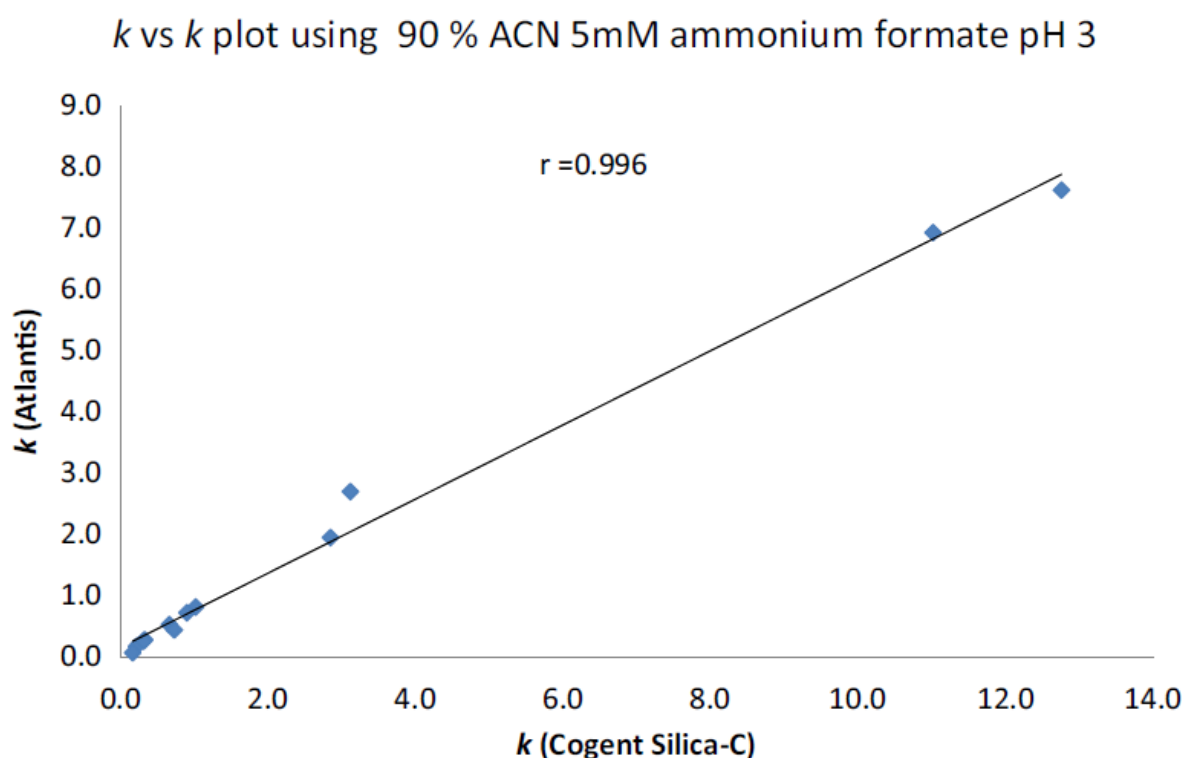


**Fig. 3.5 Comparison of retention ( $k$  vs.  $k$ ) plot for bare silica (Atlantis) vs. hydride silica (Cogent) using 90% ACN containing 5 mM ammonium formate  $w^w$  pH 3.0. Other conditions as Fig. 3.2.**

Fig. 3.5 shows a correlation plot of  $k$  on the bare silica phase vs. the hydride silica phase, showing a high degree of correlation ( $r = 0.996$ ), giving further evidence for their similar properties. In a previous publication (Kumar *et al.* 2013), the average correlation coefficient ( $r$ ) of the retention factors of pairs of six different HILIC columns, again using a set of neutral, cationic and anionic solute and similar mobile phase conditions to the present study, was 0.58. This result emphasises the relative similarity of the hydride and silica phases, compared with the greater differences that typically exist between the selectivity of different HILIC stationary phases.

### **3.3.2. Effect of mobile phase water concentration and buffer on retention and peak shape**

The influence of 5–15% v/v water (95–85% v/v ACN) in mobile phases containing either 0.1% FA or 5 mM AF was studied on the bare silica and the BEH amide stationary phases, in order to investigate any possible variation in findings from the previous section when different water concentrations were used. The bare silica and amide phase were selected for this further study as they are indicated above and in (Kumar *et al.* 2013) to give strong and weak ionic retention, respectively.

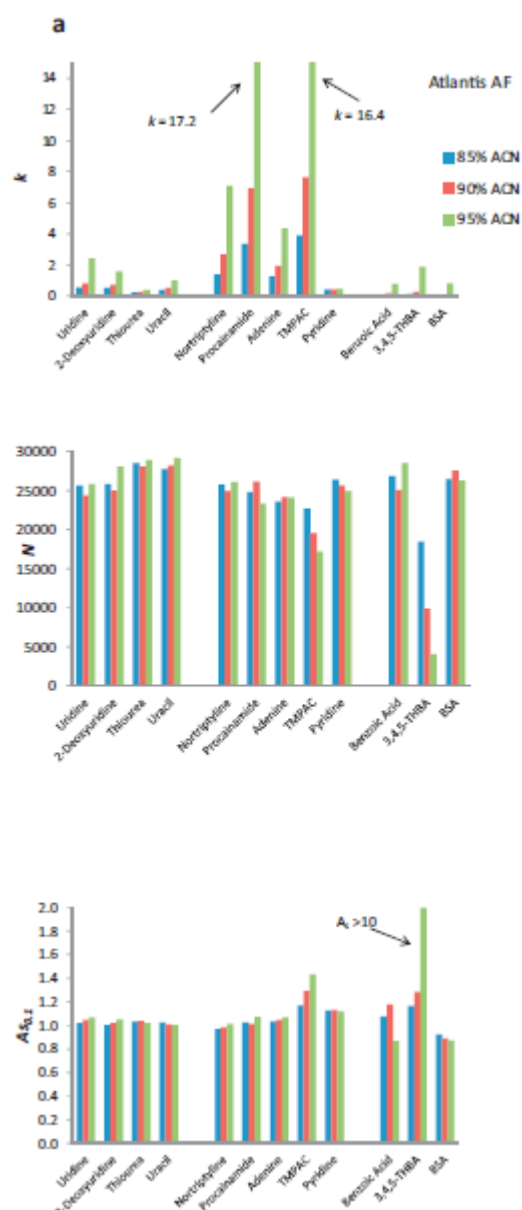


**Fig. 3.6 a**

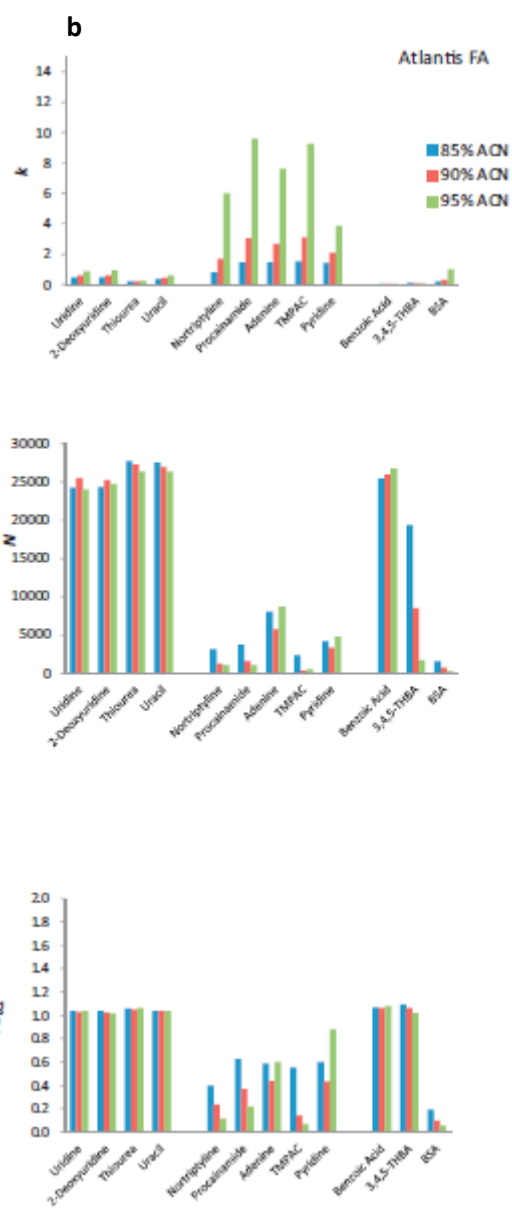


**Fig. 3.6b**

**Fig. 3.6a,b.** Retention factor ( $k$ ), column efficiency ( $N$ ) and asymmetry factor ( $As_{0.1}$ ) measurements for Atlantis silica column using 85–95% ACN containing (a) 5 mM ammonium formate ww pH 3.0 (b) 0.1% formic acid asymmetry data in FA not shown for procainamide as split peaks were obtained. Other conditions see Fig. 3.2.

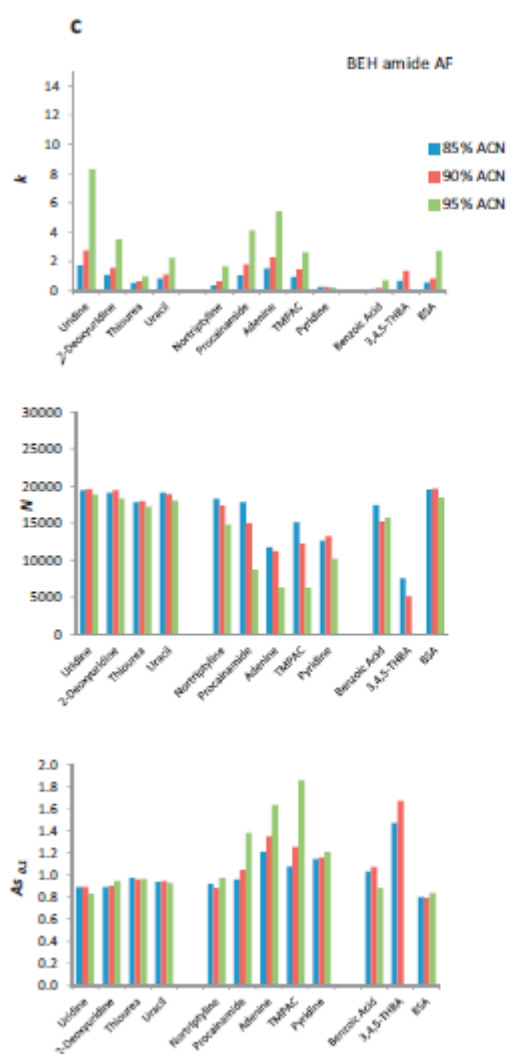


**Fig. 3.6c**

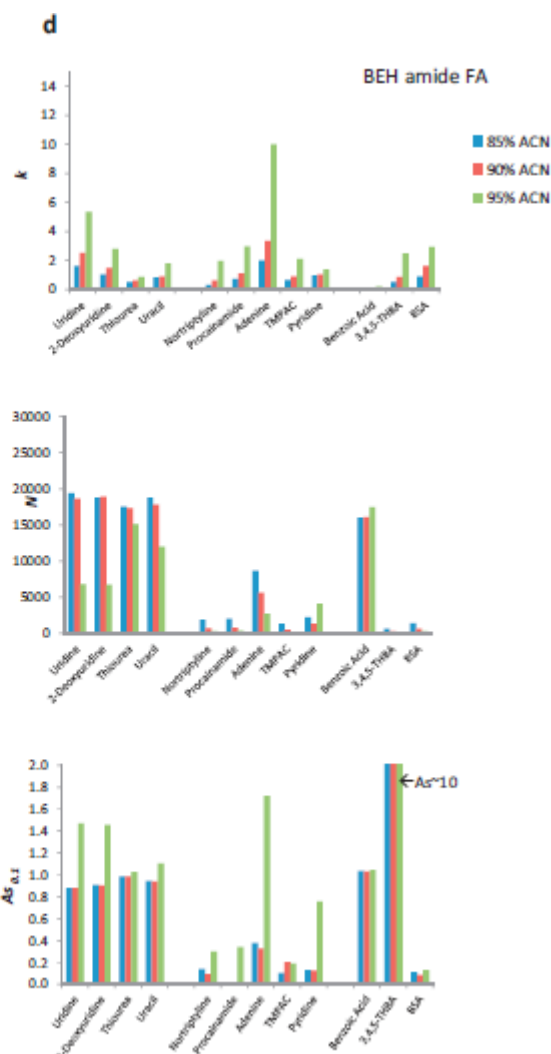


**Fig. 3.6d**

Fig. 3.6c,d. Retention factor ( $k$ ), column efficiency ( $N$ ) and asymmetry factor ( $As_{0.1}$ ) measurements for BEH amide column using 85–95% ACN containing (c) 5 mM ammonium formate  $w^w$  pH 3.0 and (d) 0.1% formic acid; asymmetry data in FA not shown for procainamide as split peaks were obtained. Other conditions see Fig. 3.2.

Fig. 3.6 shows in all cases that retention increases substantially as the ACN content in the mobile phase is increased, which is in accord with increased partition into the stationary phase and/or increased adsorption onto polar surface groups, dependent on the separation mechanism. Considering the results in AF for the silica and amide columns, respectively (Fig. 3.6a and c), the increases in retention with increasing ACN concentration were particularly marked for the cationic solutes when using the silica column, suggesting a possible synergistic effect between hydrophilic and ionic retention. Increases in retention for these solutes using the amide column under the same conditions were considerably smaller. Fig. 3.6a shows that the high efficiency for most solutes in AF found in 3.2 when using 90% ACN was largely maintained over the range 85–95% ACN for the silica column. Average efficiency for the range of solutes in the buffer was again around 25,000 plates ( $h = 2.0$ ). Poorer results were indicated again for 3,4,5-THBA, especially as the concentration of water decreased. The rapid decline of efficiency and increased asymmetry of 3,4,5-THBA in 95% ACN is attributable to the increased retention of this solute, which is very small at lower concentrations of ACN. It is possible that the increased contribution of strong adsorption of solute hydroxyl groups at high ACN concentration contributes to the deterioration in performance. Using the amide column with AF (Fig. 3.6c), decreases in efficiency at the lowest water concentration (95% ACN) were shown for the cationic solutes; 3,4,5-THBA was not eluted under these conditions. The decline in efficiency was accompanied by increased tailing of these solutes in 95% ACN. Using FA, little effect was observed on the efficiency of the neutral solutes on the silica column. However, a decline in efficiency at 95% ACN accompanied by increased tailing, was shown for these neutrals on the amide column (Fig. 3.6d). This decline may be connected with the decrease in the thickness of the water layer on the stationary phase as the concentration of water in the

mobile phase was reduced (McCalley *et al.* 2008b). Remarkable again is the drastic collapse in efficiency on both columns for the anionic and cationic solutes in FA compared with AF, which occurs over the whole range of water concentrations (Fig. 3.6b and d). Again, this drop in efficiency is caused mostly by serious fronting of the peaks in FA. This result once more indicates the necessity for use of buffers in order to achieve acceptable efficiencies for these solutes, even using a stationary phase like BEH amide that possesses reduced ionic interaction characteristics.

### **3.3.3. Causes of poor peak shape for cationic solutes in formic acid**

Fig. 3.7 shows a plot of column efficiency (using the statistical moments method) against sample load over the range 0.05 to 2.5  $\mu\text{g}$  on column for the neutral uridine, the bases adenine and procainamide, and the quaternary compound TMPAC using the silica column and 90% ACN containing 0.1% FA as the mobile phase. It is clear that peak shape for uridine remains approximately constant, with the number of plates deteriorating by only around 13% over this range of sample load. In comparison, the deterioration in efficiency for adenine, procainamide and TMPAC was 61%, 93% and 96%, respectively. The drop in efficiency for these solutes was caused by increased fronting of the peaks as the sample load increased. It is possible that sparse cationic retention sites (ionised silanols) are increasingly overloaded by protonated solutes causing the deterioration in peak shape. As pointed out above, the ionic strength of 0.1% FA in 90% ACN is extremely low, and the concentration of mobile phase counterions (hydroxonium ions) may be insufficient to prevent solute interactions with these column groups. This situation would not arise in AF buffers, as the ionic strength is maintained by the presence of the salt.



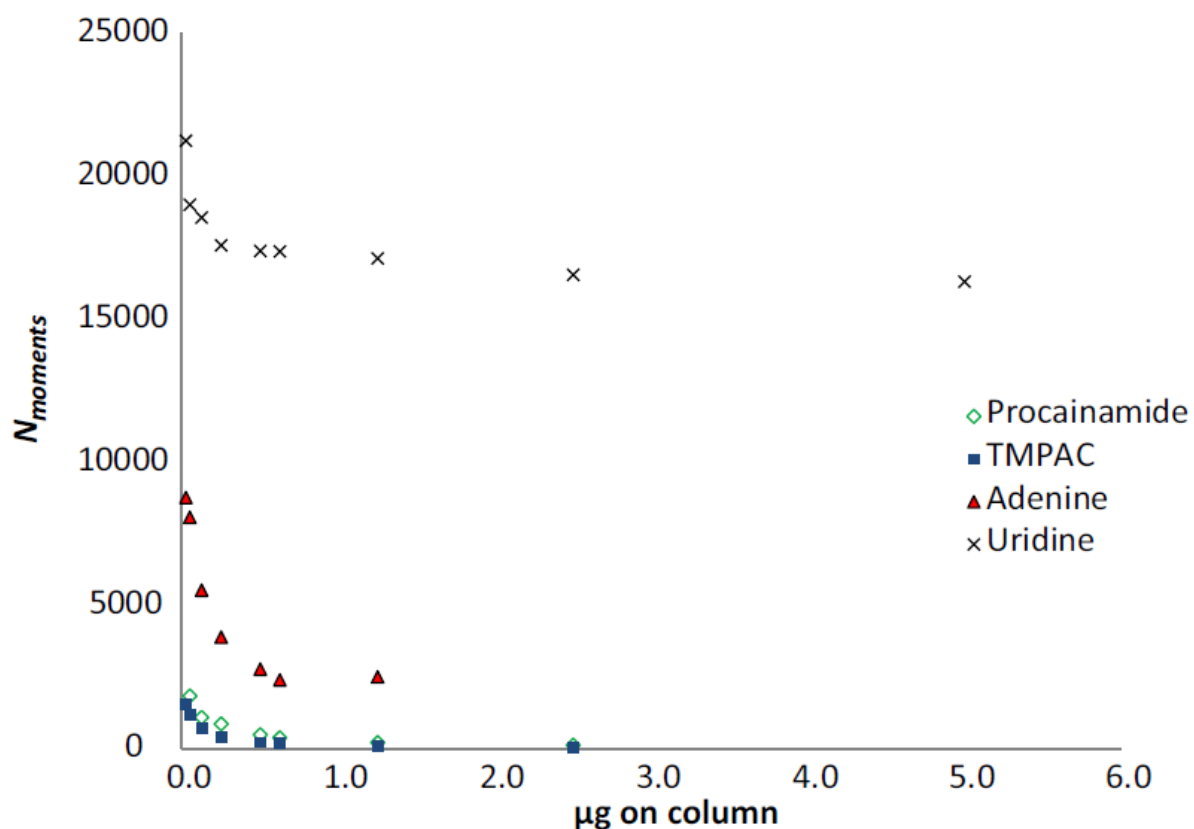


**Fig. 3.7. Effect of sample mass on efficiency of Atlantis silica column using procainamide (strong base), TMPAC (quaternary ammonium salt), adenine (weak base) uridine (neutral). Mobile phase 90% ACN containing 0.1% FA. Other conditions see Section 2.**

### 3.3.4. Effect of buffer salt concentration and salt cation on retention of cationic compounds

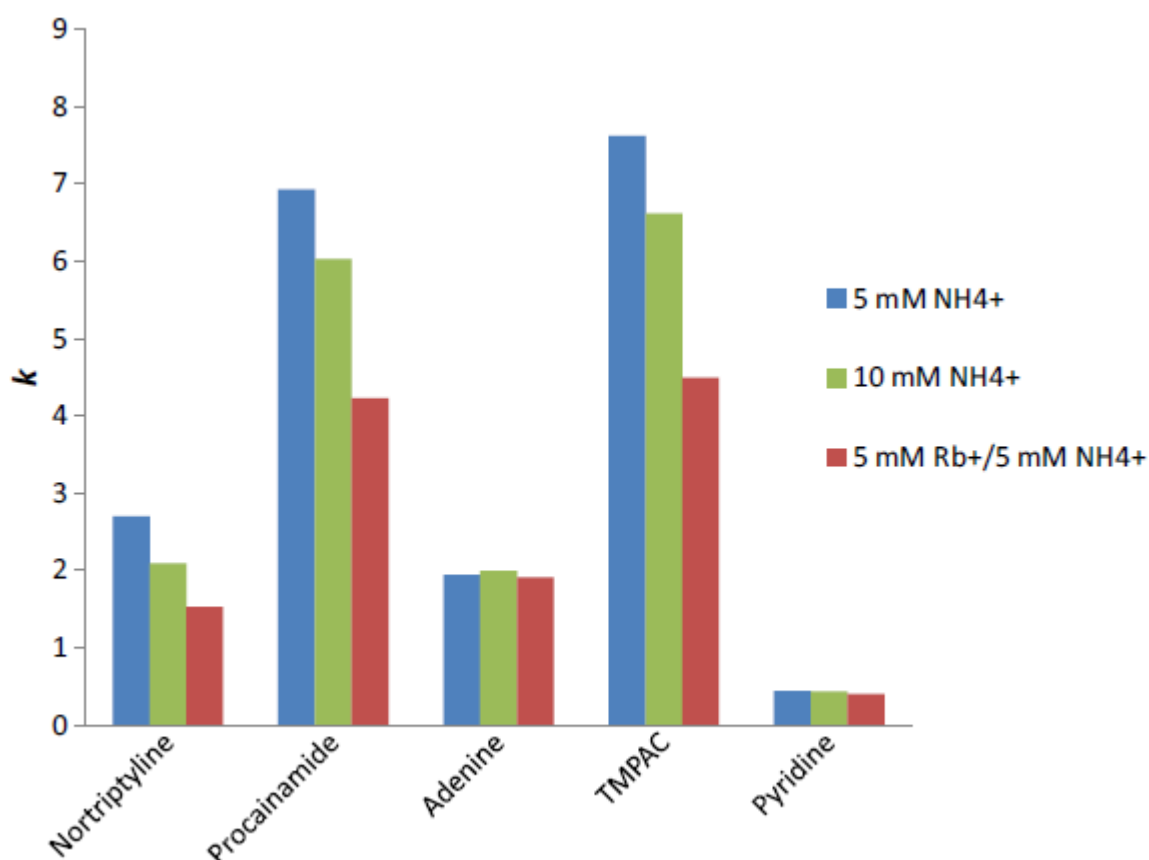


**Fig. 3.8. Effect of buffer salt on retention using Atlantis silica column. Mobile phase 90% ACN containing salt adjusted to  $w^w$  pH 3.0 with FA.**

Fig. 3.7 indicates that increasing the concentration of ammonium formate pH 3.0 from 5–10 mM in 90% ACN decreases retention for the strong bases nortriptyline and procainamide, and the quaternary compound TMPAC, showing the presence of ionic retention for these solutes on the silica column. Maintaining the buffer cation concentration at 10 mM by the substitution of rubidium cations for 5 mM of the AF concentration gave further decreases in the retention of these cationic solutes. It is well known that ion exchangers favour the bonding of ions of higher charge, decreased hydrated radius and

increased polarisability. Thus for the monovalent cations elution strength is generally in the order (Harris 2007):



Ions which are smaller in their non-hydrated state such as  $\text{Li}^+$  have a higher charge density, attracting a larger number of water molecules, resulting in a larger hydrated radius. It is interesting that the weak base pyridine and also adenine show no evidence of ionic retention in Fig. 3.7, suggesting they are not protonated in the mobile phase. Pyridine has a  $\text{pK}_a$  of 5.1 in water, indicating that if pH values in water were applicable, it should be completely protonated in a mobile phase of  $w^w$  pH 3.0. The  $w^s$  pH of a similar mobile phase containing 85% ACN (Table 3.1) is  $\sim 5.1$ , and combined with the effect of the depression of  $\text{pK}_a$  of bases in solutions of high organic solvent composition, would indicate that pyridine is not protonated, explaining the apparent lack of ionic retention and hydrophilic retention of this compound. The increased retention of these weak bases in 90% ACN containing 0.1% FA and PA as shown in Fig. 3.2a and discussed in Section 3.2 above, could be due to protonation of the compounds at the lower  $w^s$  pH of these mobile phases compared with that of AF. These results indicate that  $w^s$  pH should be considered in explaining results in HILIC despite the supposition of a layer of water on the surface of the phase. It is also possible that ionic interactions could occur between solutes situated in the bulk mobile phase and the column, in which case  $w^s$  pH values would also be appropriate.

## Conclusions

The retention and peak shape of some neutral, cationic and anionic solutes was investigated in aqueous acetonitrile mobile phases containing ammonium formate (AF), formic acid (FA)

and phosphoric acid (PA) on four HILIC columns of substantially different properties. Relatively little difference was found between these three mobile phases in terms of retention or column efficiency for the neutral solutes. While peak shapes of ionogenic solutes, particularly cationic compounds, were in general very good using AF, considerable deterioration in peak shape was observed when FA was used. The same result was obtained both on stationary phases with strong ionic retention characteristics (bare silica and hydride silica, which surprisingly showed very similar retention selectivity) and those exhibiting much lower ionic effects (hybrid silica amide and zwitterionic). Peak shape in FA became still worse as the sample load increased. Peak shape is likely to be related to the different pH and ionic strength of the various buffers, as measured in the aqueous or aqueous–organic portion of the mobile phase. For example, the ionic strength of FA solutions in high concentrations of ACN is very low, and thus may adversely affect the formation of the water layer. In contrast, the presence of a reasonable concentration of ammonium ions is likely to encourage formation of the layer as well as masking some of the effects of ionic interactions. Ionic retention of bases was demonstrated by increasing the salt concentration, and by substitution of some of the ammonium for a rubidium salt, which in both cases reduced retention. (Partial) suppression of cationic retention on ionised silanol groups afforded by the use of low pH PA did not improve column efficiency compared with use of AF. Differences in the pH of the various buffers will affect the relative contribution of hydrophilic and ionic mechanisms to retention, which in turn may have an important influence on peak shape. Despite the supposition of a water layer on the column surface, the consideration of  $w^s$  pH values seems important in explaining the retention of weak bases when using mobile phases rich in acetonitrile that are typical for HILIC separations.

## **Chapter 4**

# **Performance of charged aerosol detection with hydrophilic interaction chromatography**

## Abstract

The performance of the charged aerosol detector (CAD) was investigated using a diverse set of 29 solutes, including acids, bases and neutrals, over a range of mobile phase compositions, particularly with regard to its suitability for use in hydrophilic interaction chromatography (HILIC). Flow injection analysis was employed as a rapid method to study detector performance. CAD response was 'quasi-universal', strong signals were observed for compounds that have low volatility at typical operating (room) temperature. For relatively involatile solutes, response was reasonably independent of solute chemistry, giving variation of 12–18% RSD from buffered 95% ACN (HILIC) to 10% ACN (RP). Somewhat higher response was obtained for basic compared with neutral solutes. For cationic basic solutes, use of anionic reagents of increasing size in the mobile phase (formic, trifluoroacetic and heptafluorobutyric acid) produced somewhat increased detector response, suggesting that salt formation with these reagents is contributory. However, the increase was not stoichiometric, pointing to a complex mechanism. In general, CAD response increased as the concentration of acetonitrile in the mobile phase was increased from highly aqueous (10% ACN) to values typical in the HILIC range (80–95% ACN), with signal to noise ratios about four times higher than those for the RP range. The response of the CAD is non-linear. Equations describing aerosol formation cannot entirely explain the shape of the plots. Limits of detection (determined with a column for solutes of low  $k$ ) under HILIC conditions were of the order of 1–3 ng on column, which compares favourably with other universal detectors. CAD response to inorganic anions allows observation of the independent movement through the column of the cationic and anionic constituents of basic drugs, which appear to be accompanied by mobile phase counterions, even at quite high solute concentrations.

# 1. Introduction

An important problem for high performance liquid chromatography (HPLC) is the limited choice of detectors that respond to compounds containing no UV/VIS chromophores. Charged aerosol detection (CAD) is a relatively new type of detector developed for use in HPLC over the last 10 years (Dixon *et al.* 2002). About 100 publications concerning the detector have appeared to date (e.g. (Cohen *et al.* 2012, Gamache *et al.* 2005, Web of Science search topic 'Chromatograph\*' AND TITLE 'Charged Aerosol\*')). The detector seems very suitable for the analysis of some pharmaceuticals and compounds of biomedical significance, at least in the reversed-phase (RP) mode (Vervoort *et al.* 2008), however, more detailed study is necessary to further understand its properties. Its response is dependent on the formation of aerosol particles (see Fig. 4.1), similar to techniques such as evaporative light scattering detection (ELSD) (Mourey *et al.* 1984) and condensation nucleation light scattering detection (CNLSD) (Allen *et al.* 1993). This dependence results in a response which is supposedly independent of solute molecular structure, giving a signal for any compound that is able to form stable aerosol particles. Therefore, CAD is potentially suitable for impurity analysis, particularly in pharmaceutical development where measurement by UV or mass spectrometry (MS) requires the use of standards that maybe unavailable for unknown impurities. In CAD, the aerosol particle becomes charged through collision with positively charged nitrogen gas (Vehovec *et al.* 2010), which differs from MS interfaces which generate molecular ions rather than charged particles (Niessen 2003). The present work aims to study the performance of the CAD, and investigate to what extent it may fulfil the requirements of a universal detector, particularly with regard to its use in hydrophilic interaction chromatography (HILIC). Clearly some factors influencing CAD behaviour are

already understood, although commercial instruments have some differences from the prototype described by Dixon and Peterson (Dixon *et al.* 2002). These differences are sometimes ignored in the literature in discussions of the mechanism of operation of commercial instruments (Almeling *et al.* 2012, Shaodong *et al.* 2010). Nevertheless, the process in both may involve transfer of charge from the sheath gas (e.g. nitrogen) to the solute particles (see Fig. 4.1), which is distinct from the more direct exposure of the corona discharge to the eluent as occurs in atmospheric pressure chemical ionisation (APCI) sources used in mass spectrometry. As CAD response (along with that of all aerosol detectors) depends on the formation of solid particles, it is limited to solutes that have low volatility at the operating temperature. However, few studies have investigated in detail any relationship between volatility and detector signal. The ability to differentiate between solute and mobile phase determines the detection limit, which has been quoted as 0.1–1 ng sample on-column (Hutchinson *et al.* 2012, Cohen *et al.* 2012). Buffers are often critical additives to HPLC mobile phases in any separation mode, but are potentially detrimental to CAD performance. In HILIC, buffers can lead to better peak shape than simple acid solutions (McCalley 2007, Heaton *et al.* 2014c, Pesek *et al.* 2013), thus we wished to investigate their influence on CAD sensitivity. Furthermore, as with other aerosol-based detectors, detector response is dependent on organic solvent content. While changing detector response with organic solvent concentration has been investigated for its detrimental effect on response uniformity in gradient elution (Khandagale *et al.* 2014, Gorecki *et al.* 2006, Hutchinson, Li *et al.* 2010), high organic concentrations as used in HILIC may be advantageous for sensitivity as it should facilitate desolvation of particles in the CAD. Aerosol-based detectors are known to produce non-linear calibration curves (Hutchinson *et al.* 2011), which can arise for different reasons in different detectors. For instance in the ELSD, it is due to both the non-



linearity of aerosol formation and a change in detection mechanism with the size of aerosol particles (Stolywho *et al.* 1983). The mechanism of detection in CAD is more straightforward than ELSD (Vervoort *et al.* 2008), and CAD calibration curves can be close to linear over small concentration ranges (Vehovec *et al.* 2010). The detailed mechanism that causes non-linearity of CAD calibration curves and their profile has not been described to date. Detector response for aerosol-based detectors is believed to be mostly independent of solute chemistry (Vervoort *et al.* 2008). However this factor has also not been investigated in much detail with respect to CAD for a sufficiently broad selection of solute structures. Approximately 50% of drug active pharmaceutical ingredients (API) are salts (Paulekuhn *et al.* 2007), and many salt counter ions do not contain chromophores. An important benefit of CAD is the ability to detect solutes which do not contain chromophores, and thus it should respond to these counterions (Schiesel *et al.* 2012).

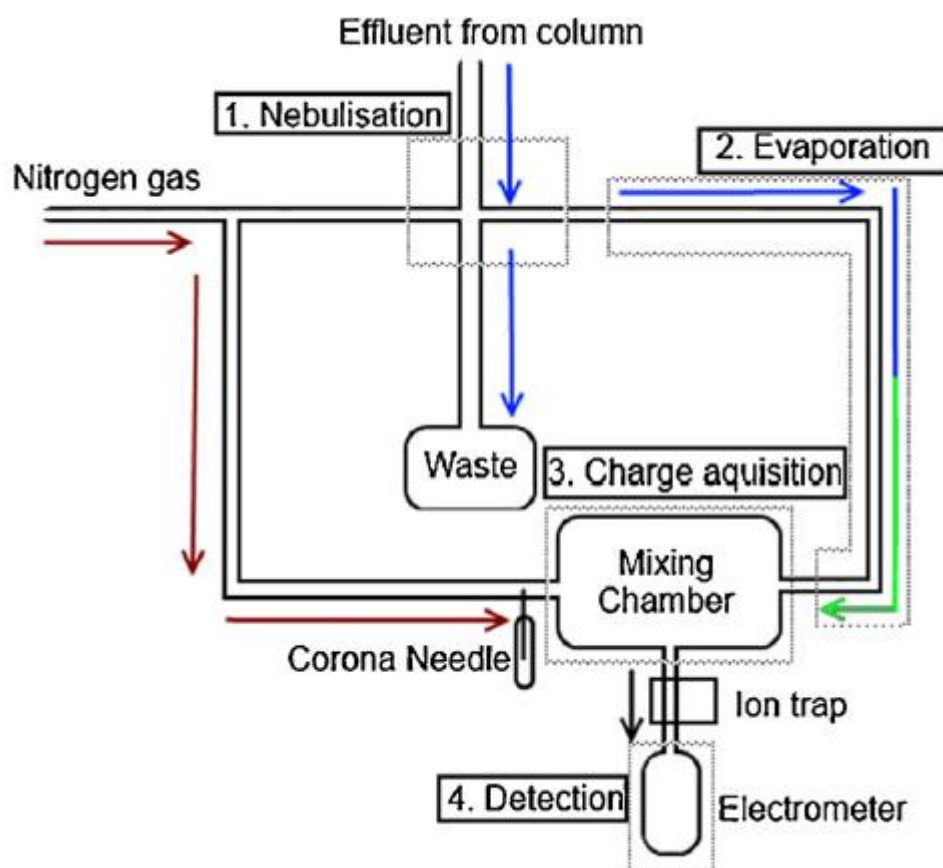


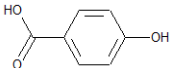
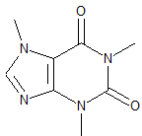
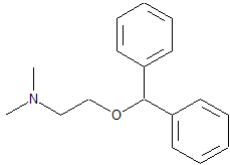
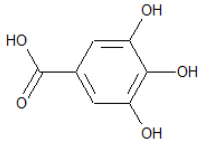
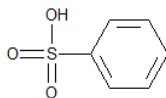
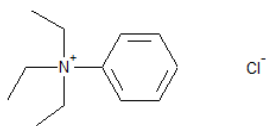
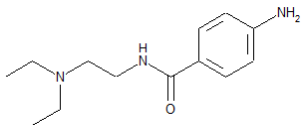

**Fig. 4.1 Simple Schematic of CAD operation**

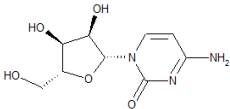
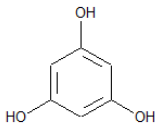
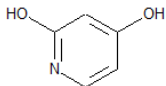
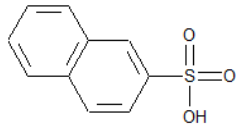
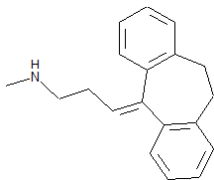
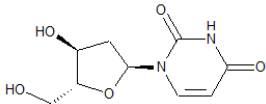
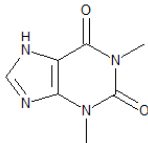
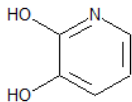
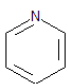
## **2. Experimental**

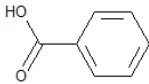
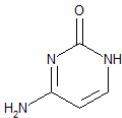
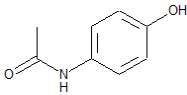
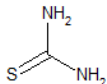
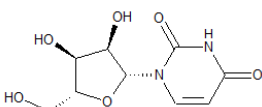
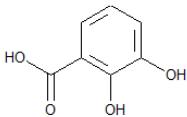
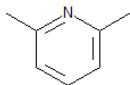
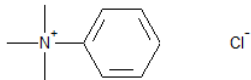
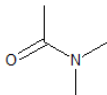
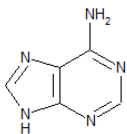
### **2.1 Chemicals and reagents**

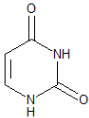
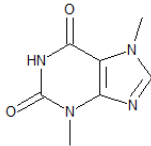
A set of 29 probe compounds comprising acids, bases and neutrals (as used in a previous study (Kumar *et al.* 2013)) was obtained from SigmaAldrich (Poole, UK) and used as probes. Structural and physico-chemical data are provided in Table 4.1. Log D values were calculated as the average from three different software packages: ACD version 12.0 (ACD Labs, Toronto, Canada), Marvin (Chem Axon, Budapest Hungary) and MedChem Designer (Simulations Plus, Lancaster, USA). Standards were diluted in the exact mobile phase from stock solutions typically at 10,000 mg/L made up in 50% ACN containing 0.1% FA. ACN (HPLC gradient grade), ammonium formate (AF), formic acid (FA) (LCMS grade), ammonium acetate (AA) and acetic acid (HPLC grade), were purchased from Fisher Scientific (Loughborough, UK).

**Table 4.1. Identities, structures and physico-chemical characteristics of test compounds.**

Solute	Structure	MW	FW	Log D (pH 3)***	BP / °C	MP / °C
4-hydroxybenzoic acid		138	138	1.46	336*	213.5
Caffeine		194	194	-0.41	178	238
Diphenhydramine		255	292	-0.013	344*	168#
3,4,5–THBA		170	170	0.6	501*	261.5
BSA		158	180	-2.35	319**	65.5
BTEAC		192	228	-1.67	445	191
Procainamide		235	272	-2.38	422*	167#
TMPAC		136	172	-2.01		247

Solute	Structure	MW	FW	Log D (pH 3)***	BP / °C	MP / °C
Cytidine		243	243	-3.51	546*	225
Phluroglucinol		126	126	0.39	331*	204.5
2,4-dihydroxypyridine		111	111	-0.4	510*	274
2-NSA		208	230	-1.09	392**	124.5
Nortriptyline		263	300	1	403*	214\$
2'-deoxyuridine		228	228	-1.49	519**	165
Theophylline		180	180	-0.31	454*	272
2,3-dihydroxypyridine		111	111	-0.62	441*	245
Pyridine		79	79	-0.9	115	-41.6

Solute	Structure	MW	FW	Log D (pH 3)***	BP / °C	MP / °C
Benzoic acid		122	122	1.65	249	122.4
Cytosine		111	111	-2.86	283**	322.5
Paracetamol		151	151	0.58	388*	169.75
Thiourea		76	76	-0.82	187*	177
Uridine		244	244	-2.06	556**	165
2,3-dihydroxybenzoic acid		154	154	0.86	344	205
2,6-dimethylpyridine		107	107	-1.11	144	-5.8
BTMAC		150	186	-2.18		239
N,N-Dimethylacetamide		87	87	-0.48	166	-20
Adenine		135	135	-1.62	554*	220

Solute	Structure	MW	FW	Log D (pH 3)***	BP / °C	MP / °C
Uracil		112	112	-0.97	367**	335
Theobromine		180	180	-0.65	483**	357

\* predicted at 760 mmHg using ACD labs program (see Experimental).

\*\* predicted from (www.chemspider.com)

\*\*\* average log D from three packages (see Experimental)

# value from (www.sigmaaldrich.com)

\$ value from (www.chemicalbook.com)

## 2.2 Equipment and methodology

A Thermo UltiMate 3000 Rapid Separation Liquid Chromatography system was used for all experiments, comprising a quaternary pump, diode array detector (DAD) and either a Corona Ultra or Corona Veo CAD, with Chromeleon 7.2 software (Thermo, Germering, Germany). The CAD is a destructive detector, therefore the DAD and CAD detectors were connected in series in some experiments, with flow first through the DAD. Thermo Viper tubing (0.13 mm ID) was used as connection tubing. Data collection rates were 100 Hz for both DAD and CAD, due to narrow peak widths (typically 1 s at half height in flow injection analysis (FIA)). The Corona Ultra nebuliser (cross flow design similar to that used in atomic

absorption spectrometry) was controlled at 22°C with the evaporator tube at ambient temperature, while the Veo (concentric flow design similar to those used in mass spectrometry) nebuliser was at ambient temperature and the evaporator tube set to 30°C. The Veo had a power function (PF) designed to 'linearise' data, which was set to either 0.67 (this simulates 'off'), 1.00 (the default) or 1.2 (optimised setting using experimental data, see below). An ethylene bridged hybrid (BEH) amide column (150 × 4.6 mm, particle size = 3.5 µm, Waters, Milford, USA) was used for determination of the detection limit, linearity and for the salt separation experiments. An Atlantis bare silica column (250 × 4.6 mm ID, particle size = 5 µm, Waters) was used for some salt composition experiments. The mobile phase was ACN-5 mM ammonium formate or ammonium acetate buffer (80:20, w/w) unless otherwise stated. The pH meter was calibrated in aqueous buffers and formic or acetic acid was used to adjust the aqueous portion to  $w^w$  pH 3 or 5. Solutions at  $w^w$  pH 6.8 were unadjusted 5 mM ammonium acetate. Care is necessary as pH calibration buffers can be a major source of non-volatile contaminants in the mobile phase. In flow injection analysis (FIA), narrow bore tubing (75 µm × 1100 mm) was used in place of the chromatographic column to maintain sufficient backpressure. Samples for FIA were prepared at a concentration of 300 mg/L; injection volumes were 1 µL unless otherwise stated. Flow rate was 1 mL/min. For calculation of retention factors, toluene is generally used as a void volume marker in HILIC with UV detection (Heaton *et al.* 2014b), but is too volatile for use with the CAD. Naphtho [2,3-a] pyrene appeared to be a suitable alternative for CAD.

## 3. Results and discussion

### 3.1.1 Detection limits (HPLC)

When applied to the impurity profiling of amino acid mixtures in nutritional infusion bags, CAD limits of quantitation (LOQ) were reported at 10 ng on-column (1 µg/mL; 10 µL injection) (Schiesel *et al.* 2012). The authors used a signal to noise ratio of 5:1 to determine the LOQ (Schiesel *et al.* 2012), whereas common practice is to use a S:N of 10. Ramos *et al.* reported CAD limits of detection (LOD) 4 times lower than ELSD for analysis of membrane phospholipids by normal phase HPLC (Ramos *et al.* 2008). Hutchinson *et al.* reported that the LOD for 11 solutes was over 5 times smaller using CAD compared with ELSD (Hutchinson *et al.* 2011). Detection limits for an acid, neutral and basic solute in our experiments are shown in Table 4.2 for a typical HILIC mobile phase (5 mM ammonium formate pH 3 in 80% ACN). A signal to noise ratio of 3 was used as LOD and 10 for LOQ. The LOD of 1–3 ng and LOQ of 5–9 ng (both on column, 1 µL injections) compare favourably with other ‘universal’ detectors such as refractive index (LOD ~1 µg on column (Yeung *et al.* 1986)) and ELSD (LOD 1–100 ng on column (Vervoort *et al.* 2008, Shaodong *et al.* 2010)). While the data in Table 4.2 was recorded for the BEH column, using the same mobile phase we did not observe serious noise or bleeding with the Atlantis column, as reported by Jia *et al.* (Jia *et al.* 2011). Table 4.2 (and indeed most of this work) was based on use of an acidic mobile phase, whereas Jia *et al.* used unbuffered ammonium acetate that has approximately neutral pH in aqueous solution. This higher pH might have caused some dissolution of silica and thus noise in the CAD.



**Table 4.2. Detection limits for charged aerosol detection in HILIC conditions. HPLC, mobile phase 80% ACN, 5mM ammonium formate <sub>w</sub><sup>w</sup> pH 3.**

Solute	LOD / mg per L	LOQ / mg per L
BSA	3	9
Uridine	2	6
Nortriptyline	1	5

### 3.1.2 Calibration curves (HPLC)

It has been reported that over wide ranges of analyte concentration, (e.g. 1–1000 ppm) CAD response is non-linear, while over narrow ranges of analyte concentration, it is quasi-linear (Vehovec *et al.* 2010). Using FIA, Hutchinson *et al.* investigated CAD calibration using sucralose, amitriptyline, dibucaine and quinine at concentrations of 1 µg/mL to 1 mg/mL (25 µL injections) (Hutchinson *et al.* 2010). Although not commented on by the authors, their data suggest a low quasi-linear range below approximately 0.05 mg/mL and an upper quasi-linear range between 0.4 and 1.0 mg/mL. Fig. 4.2 shows calibration plots for the acid BSA, the base nortriptyline and the neutral uridine over the range 1–1000 mg/L, using a BEH amide column with the CAD (Fig. 4.2a) and for UV detection (Fig. 4.2b). Hutchinson *et al.* (Hutchinson *et al.* 2010) reported maximum reliable CAD response at 70% ACN, and recommended this concentration for applications requiring maximum sensitivity. Retention is often poor at this ACN concentration in HILIC; a typical range for HILIC is 70–95% ACN. We therefore selected 80% ACN for our study. UV detection shows excellent linearity over the entire range (lowest  $R^2$  0.9995, for Nortriptyline). Our results indicate also a lower quasi-linear range (1–100 mg/L) and an upper quasi-linear range (400–1000 mg/L) for CAD. The calibration curves appear to be sublinear (concave to the x-axis). The consistent general shape of CAD calibration curves (Fig. 4.2a; also (Hutchinson *et al.* 2010)) is perhaps described by some empirical formula, however no such interpretation has been attempted to date.

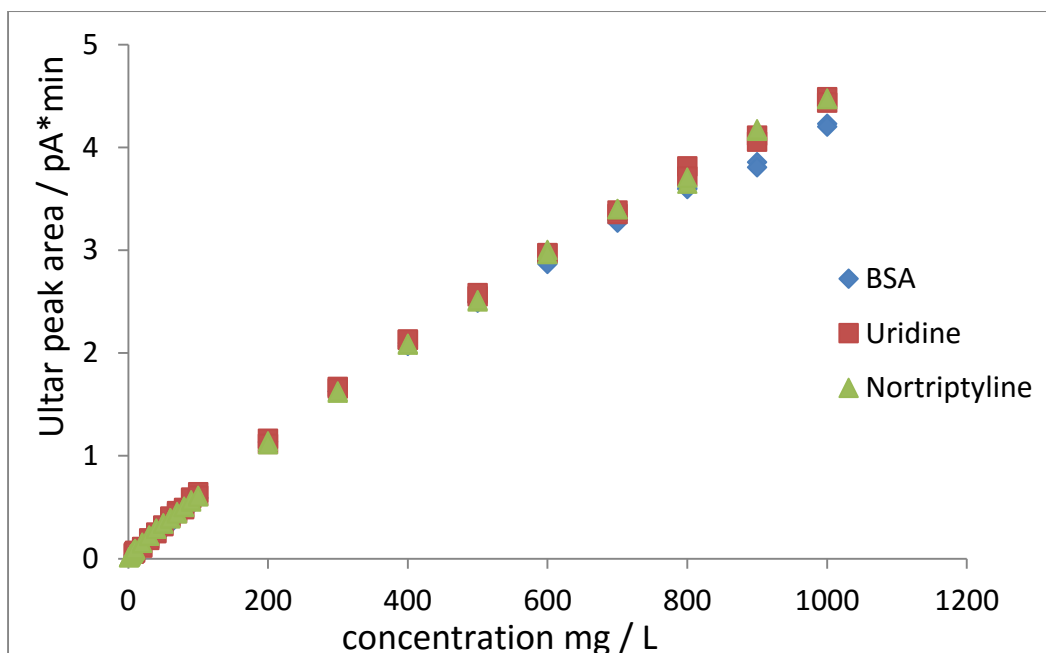


**Fig. 4.2 a. Figure 4.2. Peak area vs. concentration for a neutral (Uridine), acid (BSA) and base (Nortriptyline) (a) CAD Ultra (HPLC, mobile phase 80%ACN, 5 mM ammonium formate pH 3).**

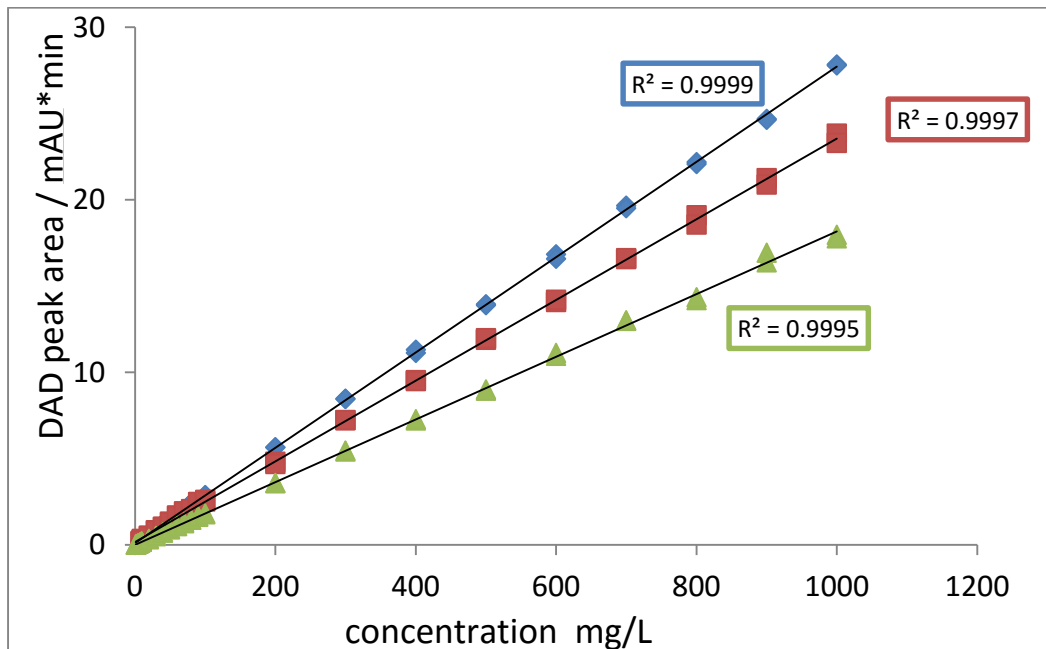


**Fig. 4.2 b Figure 4.2. Peak area vs. concentration for solutes as per Fig. 4.2a, (b) DAD. Conditions as per Fig. 4.2a.**

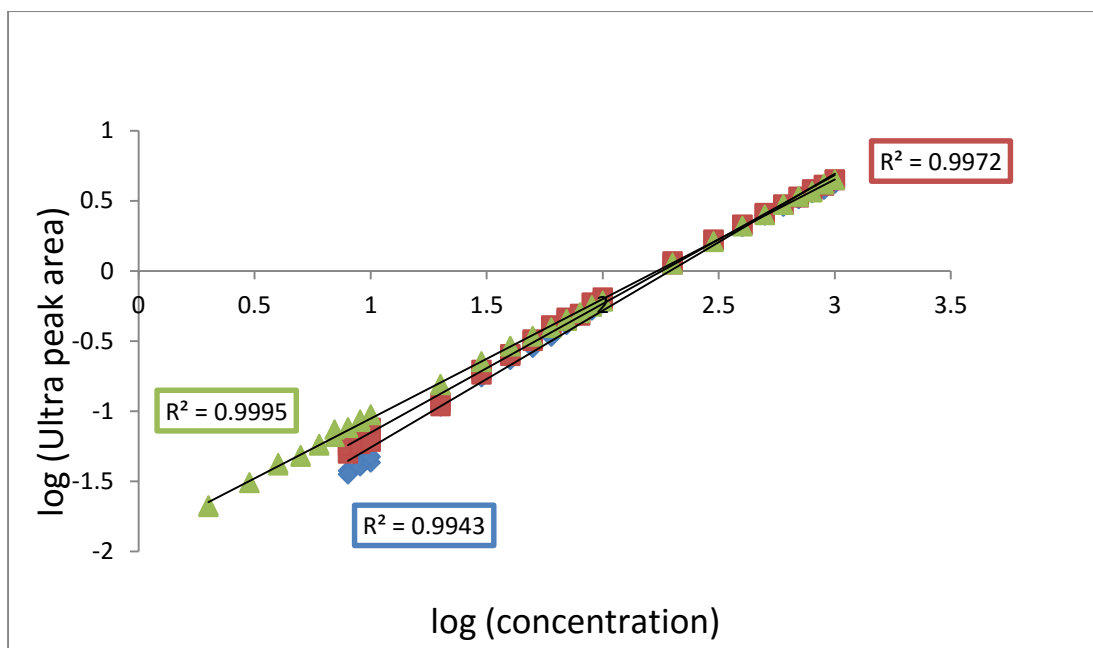


**Fig. 4.2 c. Figure 4.2. Peak area vs. concentration for solutes as per Fig. 4.2a, (c) log/log CAD Ultra. Conditions as per Fig. 4.2a.**

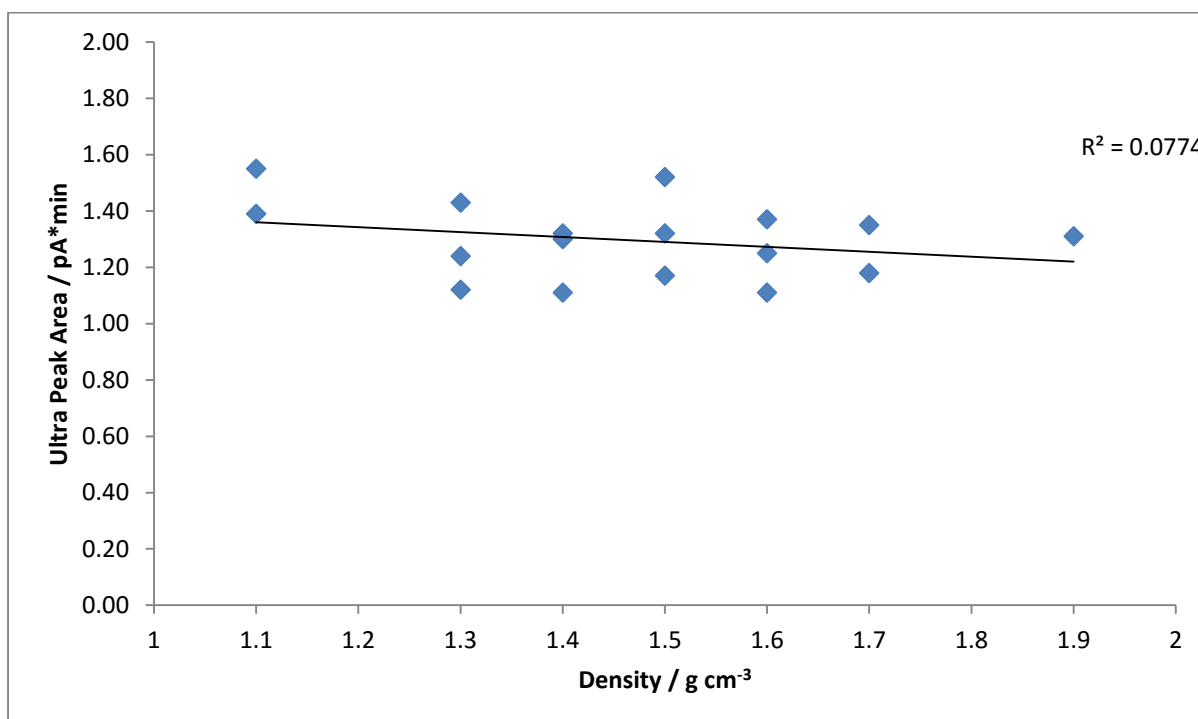


**Fig. 4.2 d. Peak Area vs. Density for 17 non-volatile solutes (FIA, mobile phase 80% ACN with 5mM ammonium formate pH 3).**

**Figure 4.2. Peak area vs. concentration for a neutral (Uridine), acid (BSA) and base (Nortriptyline) (a) CAD Ultra, (b) DAD and (c) log/log CAD Ultra (HPLC, mobile phase 80%ACN, 5 mM ammonium formate pH 3); (d) Peak Area vs. Density for 17 non-volatile solutes (FIA, mobile phase 80% ACN with 5mM ammonium formate pH 3).**

The particle size  $d_p$  as described for ELSD (1) is given by the equation (4.1):

$$d_p = d_D \left( \frac{c}{\rho_p} \right)^{1/3} \quad (4.1)$$

where  $d_D$  is the diameter of the droplet,  $c$  is the analyte concentration and  $\rho_p$  is the density of the particle. The aerosol formation step should be similar in ELSD and CAD. It was assumed by Charlesworth that aerosol particles are approximately spherical for ELSD (Charlesworth 1978), as confirmed by fundamental studies (Reid *et al.* 2011). Dixon and Peterson assumed this for their prototype aerosol detector (Dixon *et al.* 2002). The authors of that study reported that the prototype's detector sensitivity (defined as the gradient of the calibration curve) was lower for solute particles with diameters greater than 10 nm, i.e. the gradient of a plot of response vs. concentration is steep at low concentrations and becomes shallower at higher concentrations. The surface area of a sphere ( $A$ ) is given by (4.2):

$$A = 4\pi r^2 \quad (4.2)$$

It follows that:

$$A_p = d_D^2 \pi \left( \frac{c}{\rho_p} \right)^{2/3} \quad (4.3)$$

Thus, the surface area of the particle ( $A_p$ ) is theoretically proportional to solute concentration via the power equation (4.3). Therefore an increase of solute concentration results in a larger particle surface area and higher detector response. The exponent of (4.3) is not unity. This theory assumes that adsorption of charged nitrogen onto the particles is a linear (Langmuirian) relationship with surface area. Equation (4.4) simplifies the relationship between CAD response and analyte concentration ( $c$ ). Plotting CAD response vs. concentration should yield a non-linear curve with a fractional exponent of 2/3. This relationship is in agreement with work from the manufacturer of the charged aerosol detector (Thomas *et al.* 2014).

$$\text{CAD Response} \propto C^{2/3} \quad (4.4)$$

Taking logs gives (4.5), a simple linear relationship, where log of the coefficient  $a$  becomes the intercept and the slope is 2/3.

$$\log(\text{CAD Response}) = \frac{2}{3} \log C + \log a \quad (4.5)$$

Fig. 4.2c shows log/log calibration plots for Nortriptyline, BSA and Uridine. Linearity was very good, much-improved compared to the raw data (Fig. 4.2a) giving  $R^2$  values of 0.994–1.000; other authors have noted similar good linearity of these log/log plots (Ramos *et al.* 2008, Eom *et al.* 2010). The gradient of these plots ranged from 0.853 to 0.976, (as expected from the sublinear nature of Fig. 4.2a) which clearly is larger than the value of 2/3 expected from equation (4). Chaminade *et al.* reported gradients of CAD log/log calibration plots between 0.79 and 1.11 for membrane phospholipids using normal phase separation (Ramos *et al.* 2008). Nevertheless, log/log plots seem a pragmatic way to calibrate the detector. Newer CAD models such as the Corona Ultra RS and Corona Veo contain an in-built ‘power function’ feature, which is intended to ‘linearise’ data. This function appears to be based

broadly on the arguments presented above, although its operation is proprietary. The use of a user-inputted power function of 1.2 on the Corona Veo gave linearity similar to the log/log plots discussed. Density is also a factor affecting solute particle size in equation (4.3), therefore the possible effect of solute density on detector response was investigated using flow injection analysis data gathered later in this study (see 3.2.3). A plot of detector response vs. solute density is shown in Fig 4.3 d. No apparent relationship was indicated by the coefficient of determination ( $R^2 = 0.0774$ ). However the range of densities in Fig. 4.3d is somewhat small ( $1.11 - 1.9 \text{ gcm}^{-3}$ ). It is speculated that the aerosol particles pack looser at high solute concentrations, leading to a low density which perhaps results in larger than expected particles and a response that is closer to linear than equation (4.3) suggests. To qualify this would perhaps require fundamental studies into measuring aerosol particle density at increasing solute concentration, which is outside the scope of this project.

## **3.2 Response universality and uniformity.**

### **3.2.1 Flow injection analysis**

FIA is a rapid method of determining detector response, avoiding any problems of interference from the column (e.g. irreversible adsorption of part of the injected solute). Problems have been reported of poor reproducibility of peak area at low solute concentrations by FIA (Gorecki *et al.* 2006). It appears that this problem may be related to disturbances shown in blank injections of pure mobile phase. These were minimised by using analyte concentrations of 300 mg/L, which gave blank disturbances that were very small in comparison with the analyte signal.

### **3.2.2 Effect of solute salt composition on response (HPLC; FIA)**

To obtain net neutrality, ionised solutes must be associated with a counterion. This counterion is usually assumed to originate from the mobile phase, although it is conceivable that the counterion from the injected salt is involved, dependent on solute concentrations and mobile phase conditions. To investigate this further, the chloride, bromide and iodide salts of the quaternary ammonium compound benzyltriethylammonium (BTEA) were prepared at 300 mg/L of salt (e.g. 300 mg/L of BTEACl), and individually separated by HPLC using a BEH Amide column (80% ACN, 5 mM AF pH3) (Fig. 4.3a–c). The salts were also analysed by FIA, with identical mobile phase. For analysis by HPLC, peak areas for the same injected mass of each salt decreased for the cationic moiety in the order BTEACl > BTEABr > BTEAI (Table 4.3). This result is in agreement with the cationic part of the salt contributing a decreasing fraction of the total mass as the anion gets larger (chloride to iodide). For HPLC



analysis, the result indicates that the solute cation maybe accompanied by formate anions during passage through the column, as the injected solute cation and anion clearly separate on the column (Fig. 4.3a–c). Note also the different retention times of chloride, bromide and iodide in these Figures. However, the same pattern of detector response was found by FIA, which involves no separation process. The standards were first diluted from the stock solutions (10,000–300 mg/L) with the FIA/HPLC mobile phase and injected into the same solution. This suggested that the large excess of sample diluent formate anions (see Section 2) and mobile phase buffer anions (5 mM AF pH 3) largely replace the solute (halide anions) in solution, which may influence the subsequent formation of aerosol particles. Thus the solute halide ions may have little contribution to the overall response even in FIA. A loading study for nortriptyline hydrochloride was carried out to further investigate the separation of the anion and cation in the HPLC process, up to much higher concentrations than those used in FIA. The salt was dissolved in the exact mobile phase at concentrations from 100 to 10,000 mg/L; separations were carried out on the BEH Amide and also on an Atlantis silica column. Fig. 4.3d and e show distinct peaks for the nortriptylinium cation and the chloride anion at all concentrations on the amide and bare silica column respectively. In the separation of amino acids by electrostatic repulsion-hydrophilic interaction chromatography (ERLIC), Alpert (Alpert 2008) showed a symmetrical peak for arginine when the solute was dissolved in mobile phase –10 mM triethylaminephosphate (TEAP) pH 2 in 70% ACN, using a Polywax LP column. The peak was attributed to arginine phosphate. However, when the solute was dissolved instead in triethylaminemethylphosphonate (TEA-MePO<sub>3</sub>) an additional peak appeared at earlier retention time, with a continuum evident between the peaks. It was suggested that the earlier peak was due to arginine molecules that had retained MePO<sub>3</sub> as the counterion, while some slow counterion exchange takes place with

the mobile phase. Data in Fig. 4.3 show a different behaviour, as they suggest independent migration of the solute anion and cation through the column. Clearly, the result is likely to be influenced by the exact combination of solute, mobile phase buffer (and their concentrations), and stationary phase used. Fig. 4.3d shows detector overload for the modestly-retained nortriptyline ( $k = 1.9$ ) above 20  $\mu\text{g}$  sample load on the BEH amide column, but no evidence of detector overload for the well-retained chloride ( $k = 21$ ) even at 100  $\mu\text{g}$  sample load. The chloride peak continues to increase in size even at the highest sample loads. Fig. 4.3e, using the Atlantis column, shows detector overload for the nortriptylinium cation only above 80  $\mu\text{g}$  sample load and none for the chloride anion, with peaks continuing to behave independently. These data suggest a detector dynamic range of 1 ng to over 20  $\mu\text{g}$ , i.e. over 4 orders of magnitude. The results indicate that even at the highest concentrations studied, a plateau in the chloride response is not attained, suggesting that no association of chloride with nortriptyline occurs. The elution order of solute anion and cation reversed when switching from the BEH Amide (Fig. 4.3d) to the Atlantis bare silica column (Fig. 4.3e), due to much stronger cation exchange retention of nortriptyline on the Atlantis column (Kumar *et al.* 2013).

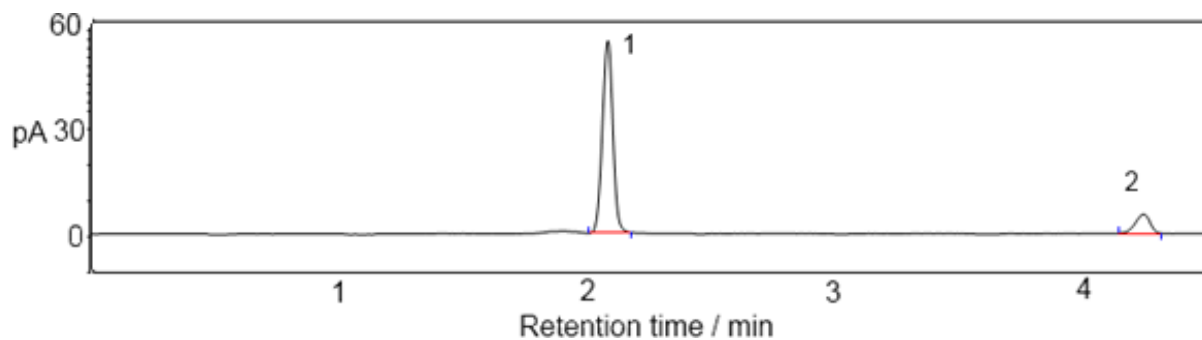


**Fig. 4.3a.** HILIC-CAD separation and detection of the salt (a) benzyltriethylammonium chloride. Peak identities 1 = benzyltriethylammonium, 2 = chloride. HPLC, BEH Amide column, mobile phase 80% ACN with 5 mM ammonium formate pH 3. 300 mg/L, injection volume 1  $\mu$ L.

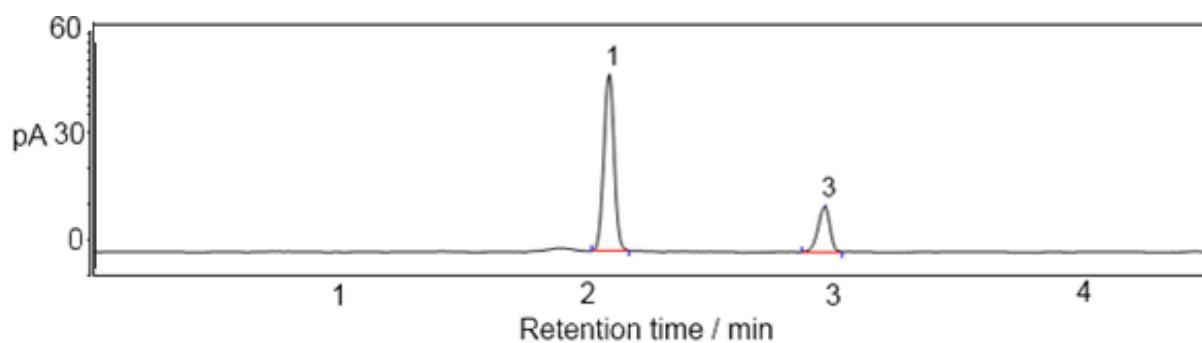


**Fig. 4.3b.** HILIC-CAD separation and detection of the salt (b) benzyltriethylammonium bromide. Peak identities 1 = benzyltriethylammonium, 3 = bromide. HPLC, BEH Amide column, mobile phase 80% ACN with 5 mM ammonium formate pH 3. 300 mg/L, injection volume 1  $\mu$ L.

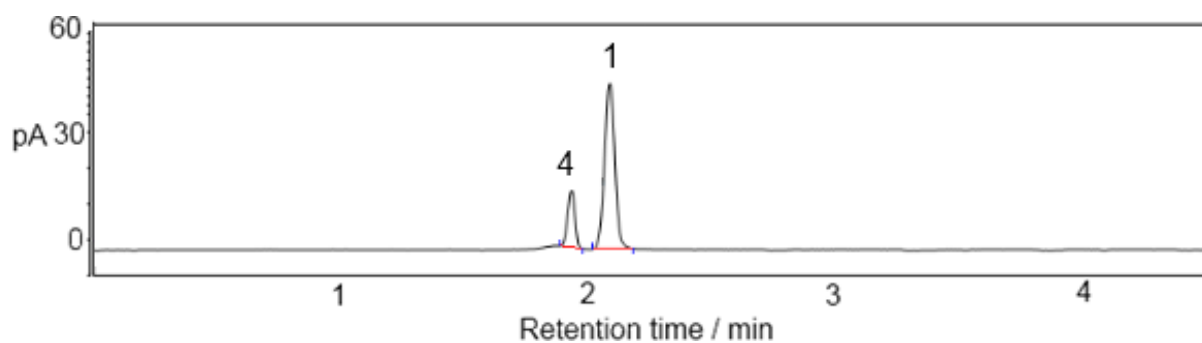


**Fig. 4.3c.** HILIC-CAD separation and detection of the salt (b) benzyltriethylammonium iodide. Peak identities 1 = benzyltriethylammonium, 4 = iodide. HPLC, BEH Amide column, mobile phase 80% ACN with 5 mM ammonium formate pH 3. 300 mg/L, injection volume 1  $\mu$ L.

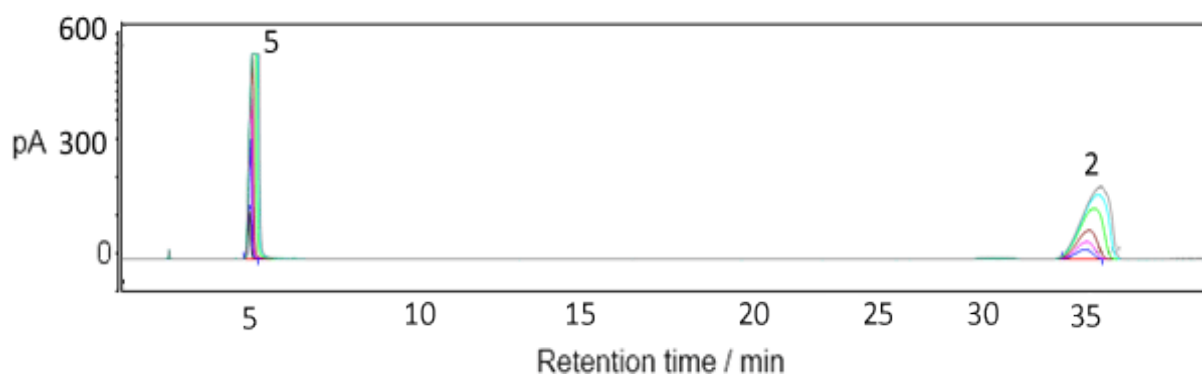


**Fig. 4.3d.** HILIC-CAD separation and detection of the salt (a) nortriptylinium chloride. Peak identities 2 = chloride, 5 = nortriptylinium. HPLC, Atlantis column, mobile phase 95% ACN with 5 mM ammonium formate pH 3. Nortriptyline hydrochloride concentration 100–10,000 mg/L, injection volume 10  $\mu$ L.

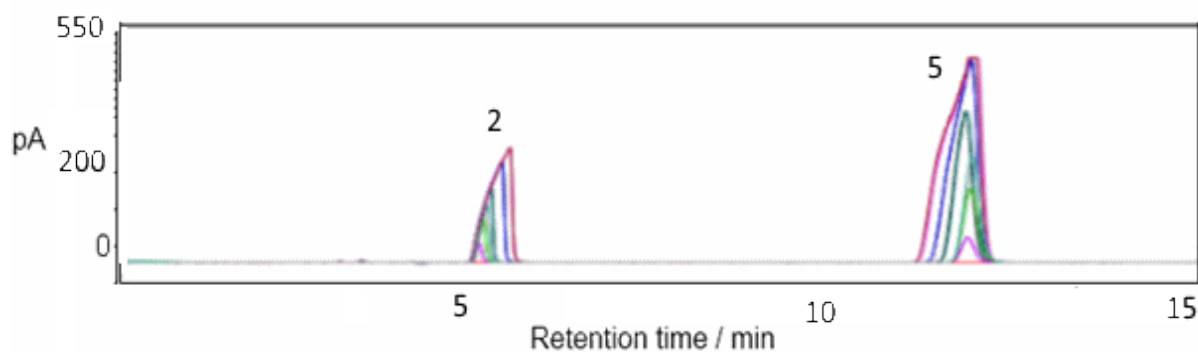


**Fig. 4.3e.** HILIC-CAD separation and detection of the salt (a) nortriptylinium chloride. Peak identities 2 = chloride, 5 = nortriptylinium. HPLC, Atlantis column, mobile phase 95% ACN with 5 mM ammonium formate pH 3. Nortriptyline hydrochloride concentration 100–10,000 mg/L, injection volume 10  $\mu$ L.

**Figure 4.3.** HILIC-CAD separation and detection of the salts (a) benzyltriethylammonium chloride, (b) benzyltriethylammonium bromide, (c) benzyltriethylammonium iodide; (d)–(e) nortriptyline hydrochloride. Peak identities 1 = benzyltriethylammonium, 2 = chloride, 3 = bromide, 4 = iodide, 5 = nortriptylinium. HPLC, mobile phase 80% ACN for (a)–(c), 95% ACN for (d), 90% ACN for (e) all containing 5 mM ammonium formate pH 3, Atlantis column for (e), BEH Amide column for all others. Nortriptyline hydrochloride concentration 100–10,000 mg/L, injection volume 10  $\mu$ L, others 300 mg/L, injection volume 1  $\mu$ L.

**Table 4.3. Peak areas of BTEAC, BTEABr and BTEAI by FIA and HPLC. Mobile phase 80% ACN, 5mM ammonium formate <sub>w</sub> pH 3.**

<b>Compound</b>	<b>Peak area of BTEA+ (FIA)</b>	<b>Peak area of BTEA+ (HPLC)</b>	<b>Proportion of base</b>
<b>BTEAC</b>	1.70	2.89	84%
<b>BTEABr</b>	1.51	2.58	71%
<b>BTEAI</b>	1.39	2.28	60%

### 3.2.3 Response Uniformity (FIA)-dependence on solute and mobile phase buffer

CAD peak areas were measured for injection of 300 ng of the 29 compounds in 80% ACN, 5 mM AF pH 3 using FIA (Fig. 4a). The relative standard deviation (RSD) of the response for 21 compounds (omitting 8 with no or low response N,N-dimethylacetamide to caffeine) was 14% in this mobile phase, which shows reasonable uniformity considering the diverse structures of the compound set. Greater response uniformity for CAD in comparison with UV detection is also seen in Fig. 4.2a and b. Response appeared somewhat higher for basic compounds (shown in blue) than neutrals (green), albeit with some overlap (Fig. 4a). This observation is unexpected and unreported to date, as the production of physical particles by aerosol-based detectors should be independent of solute chemistry. Ionogenic compounds are often available in their salt form (e.g. Nortriptyline 300 mg/L was prepared as 300 mg/L of Nortriptyline HCl salt). While neutral compounds would not be expected to interact strongly with mobile phase buffer constituents in particle formation, this is clearly a possibility for ionogenic compounds, and may be responsible for the differences in response. The mean response for the same 21 compounds was compared for additives commonly used in HILIC in addition to ammonium formate (AF) including formic acid (0.100%, v/v) (FA), ammonium acetate (AA), trifluoroacetic acid (0.200%, v/v) (TFA), and heptafluorobutyric acid (0.345%, v/v) (HFBA) (Table 4.4). The acid solutions were equimolar (26.5 mM). The mean response at 80% ACN concentration did not appear to be greatly affected when changing the pH of the buffer, or simple acid modifiers. However, the spread of response to the individual compounds was greater in mobile phases of equimolar TFA and HFBA (23% and 30% RSD, respectively) than for the other mobile phases. For the particular case of ionised solutes, association with mobile phase counterions of increasing

mass might be expected to produce an increase in CAD response, giving some explanation of these data. Thus for analysis of cationic solutes, the response might increase in the order formate, trifluoroacetate (TFA) and heptafluorobutyrate (HFBA) whose anions have molar mass 45, 113 and 213, respectively. Koupparis and co-workers (Galanakis *et al.* 2006) found that the response for the hydrophilic antibiotic Amikacin using ELSD increased for TFA over FA, further increasing for higher concentrations of TFA. In addition, they evaluated HFBA and nonafluoropentanoic acid (NFPA), claiming that their ELSD responses increased in relation to the mass of the anion of these strong acids. However, the concentration of acid was not kept constant between datasets, either in terms of v/v or molar concentration. If response indeed increases in proportion to the added mass of a heavier anion, the ratio of response for strongly basic solutes, e.g. nortriptyline should be in the order nortriptyline formate: nortriptyline trifluoroacetate: nortriptyline heptafluorobutyrate 1.00:1.22:1.54. To investigate this hypothesis, FIA was performed in FA, TFA and HFBA each at a concentration of 26.5 mM. The compounds used were the stronger base nortriptyline, the weak base cytosine, neutral uridine as a control, the strong acid benzenesulfonic acid and the weak acid 4-HBA. A solute concentration of 600 mg/L was used, which is somewhat higher than used above because of higher baseline disturbances from TFA and HFBA compared to FA. The results (Fig. 4b) show that nortriptyline response did not follow the predicted ratios, with response of 1.00:1.03:1.13 for the FA, TFA and HFBA, respectively. The weak base cytosine followed the same trend, with response increasing in the ratio 1.00:1.09:1.33 for FA, TFA and HFBA but not in line with the predicted increase of 1:1.43:2.07. It is apparent from Fig. 4a that neutral solutes have broadly lower response than ionised basic solutes, although the cause of this is unexplained to date. There have been no published reports of mobile phase pH affecting small molecule solute CAD response, therefore the weak acid 4-



HBA was expected to also be unaffected by choice of acid buffer. However, Fig. 4b shows a decrease in response for 4-HBA in both TFA and HFBA compared with FA (33% decrease in TFA compared to FA). TFA and HFBA are capable of neutralising 4-HBA under the conditions used; decreasing the degree of ionisation of 4-HBA in the stronger acid would result in a predominantly neutral form of the solute reaching the detector. BSA, which is deprotonated at all pH values, was unaffected by the choice of acid buffer. Uridine, which is neutral under these conditions showed small reductions in response in TFA and HFBA (less than 10% reduction in peak area). Khandagale *et al.* described the CAD solute plug as a 'plume' (Khandagale *et al.* 2013), which travels within the detector after nebulisation. The plume has only a finite period of time to undergo all the processes required to produce a peak in the CAD (Fig. 4.1). We estimated the detector residence time at  $\sim 1$  s using an effective detector volume of 14  $\mu\text{L}$  reported by the manufacturer (Gamache *et al.* 2005) and a flow rate of 1 mL/min. The process of forming aerosol particles by evaporation of aerosol droplets is possibly analogous to crystal formation from bulk solution. Ionic solids have much higher melting points than solids of neutral compounds and it is well-known that optimum growth rates for ionic crystals are at least a factor of 10 times greater than for molecular crystals, due to the high strength of coulombic intermolecular interactions relative to weaker van-der-Waals and London dispersion forces (Wright 1989). Perhaps ionogenic solutes are better able to form stable aerosol particles within this short time window, compared to neutrals which are held together by weaker interactions.

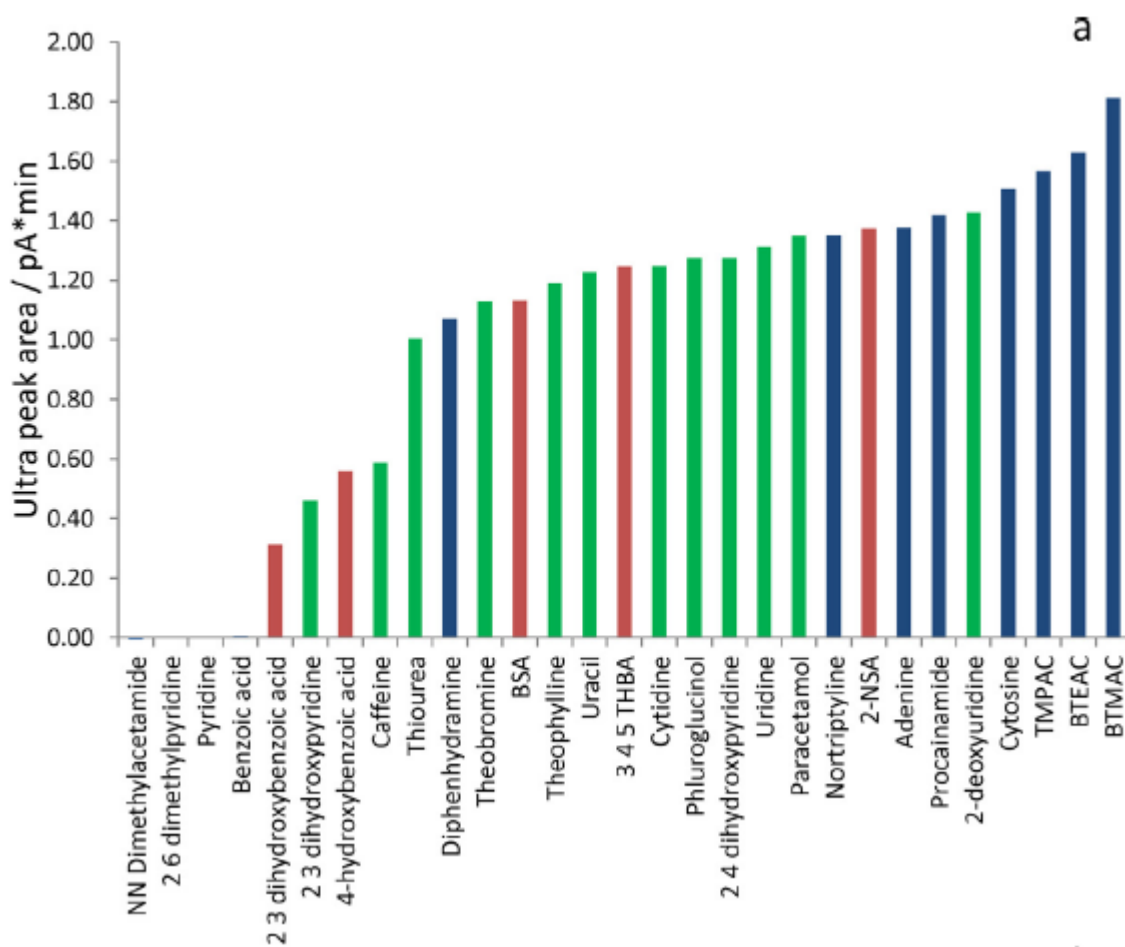


**Fig. 4.4a. CAD response for 29 compounds (FIA, mobile phase 80% ACN, 5 mM ammonium formate pH 3). Blue = bases, red = acids, green = neutrals. 1  $\mu$ L injections**

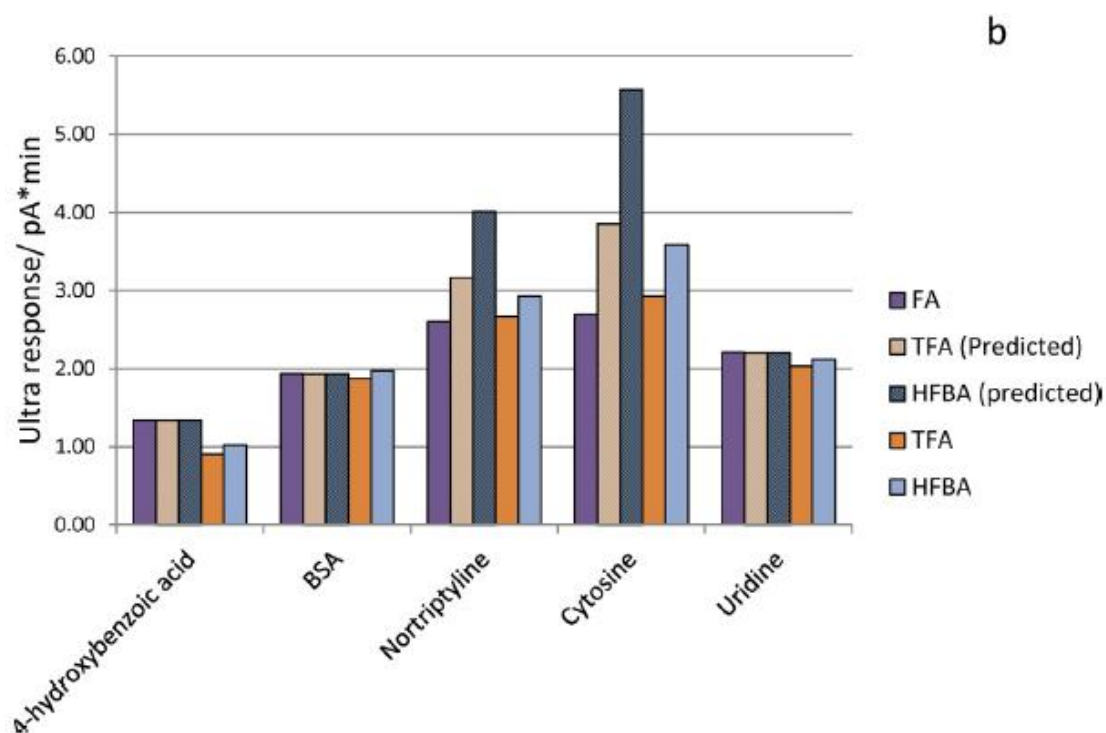


**Fig. 4.4b.** CAD Ultra response in dilute acids for the bases nortriptyline and cytosine, acids BSA and 4-HBA and the neutral Uridine (FIA, 80% ACN, FA (0.1% v/v) vs. TFA (0.2%) vs. HFBA (0.345%)). Predicted values from ratios explained in 3.4.3 in hashed-line bars.

**Figure 4.4.** (a) CAD response for 29 compounds (FIA, mobile phase 80% ACN, 5 mM ammonium formate pH 3). Blue = bases, red = acids, green = neutrals. (b) CAD Ultra response in dilute acids for the bases nortriptyline and cytosine, acids BSA and 4-HBA and the neutral Uridine (FIA, 80% ACN, FA (0.1% v/v) vs. TFA (0.2%) vs. HFBA (0.345%)). Predicted values from ratios explained in 3.4.3 in hashed-line bars.

### 3.2.4 Effect of solute volatility on response

The CAD response using FIA for the set of 29 diverse compounds (Fig. 4a) indicates that eight gave low or no response, three of which were liquids at room temperature (pyridine, 2,6-dimethylpyridine and N,N-dimethylacetamide). Solutes which respond poorly in CAD are too volatile to form stable aerosol particles (Gamache *et al.* 2005). Some relationship between solute volatility and response might be expected. Compounds that respond to CAD in general are those which have higher boiling point, melting point or molecular mass (Fig. 5a–c respectively), which are typical indicators of solute volatility. However, there are clear exceptions. 2,3-dihydroxybenzoic acid (bp 344°C, mp 205°C) gives only a third of the response of diphenhydramine (bp 344°C, mp 168°C). Benzoic acid has an appreciably high boiling point at 249°C and molecular mass of 122 g/mol but gave no response whatsoever; thiourea is smaller with even lower boiling point (bp 187°C, MW 76 g/mol, mp 177°C) but its CAD response was strong. However, benzoic acid has a low mp (122°C) and is known to be volatile, sufficiently so that its analysis by headspace Gas Chromatography (GC)-MS is possible (Pellati *et al.* 2013). The exceptions make a definitive cut-off point for a response difficult to predict purely from physico-chemical indicators of solute volatility. A minority group of four solutes including caffeine and 4-hydroxybenzoic acid (4-HBA) responded in CAD, but with peak areas ca. 40% lower than the strong CAD responders. The bp and mp points of these solutes are diverse. Indeed the data for 4-HBA (bp 336°C, mp 214°C), 2,3-dihydroxypyridine (bp 441°C mp 245°C), and 2,3-dihydroxybenzoic acid (bp 344°C, mp 205°C) overlap with those for strong responders. Caffeine is frequently referred to as 'semi-volatile' (Lauritsen *et al.* 1997). It has a sublimation point (bp Table 4.1) of 178°C, considerably below its melting point of 238°C ( [www.chemicalbook.com](http://www.chemicalbook.com)) which may explain

its behaviour, although its sublimation temperature is still well above the detector settings. The CAD nebuliser is set to room temperature by default, and the evaporation process is also endothermic. Therefore this definition perhaps does not apply to CAD. It seems that experimental measurement (e.g. by FIA) is necessary to confirm response. Fig. 5a–c show clearly that no relationships are apparent between response and melting point, molecular mass, and boiling point, with correlation coefficients close to zero. This result however fits with the claim of reasonably uniform response for non-volatile substances for the CAD. For ELSD, which might be expected to show similar effects, conflicting findings have been published on the effect of MW on detector response (Stolywho *et al.* 1983, Mourey *et al.* 1984).

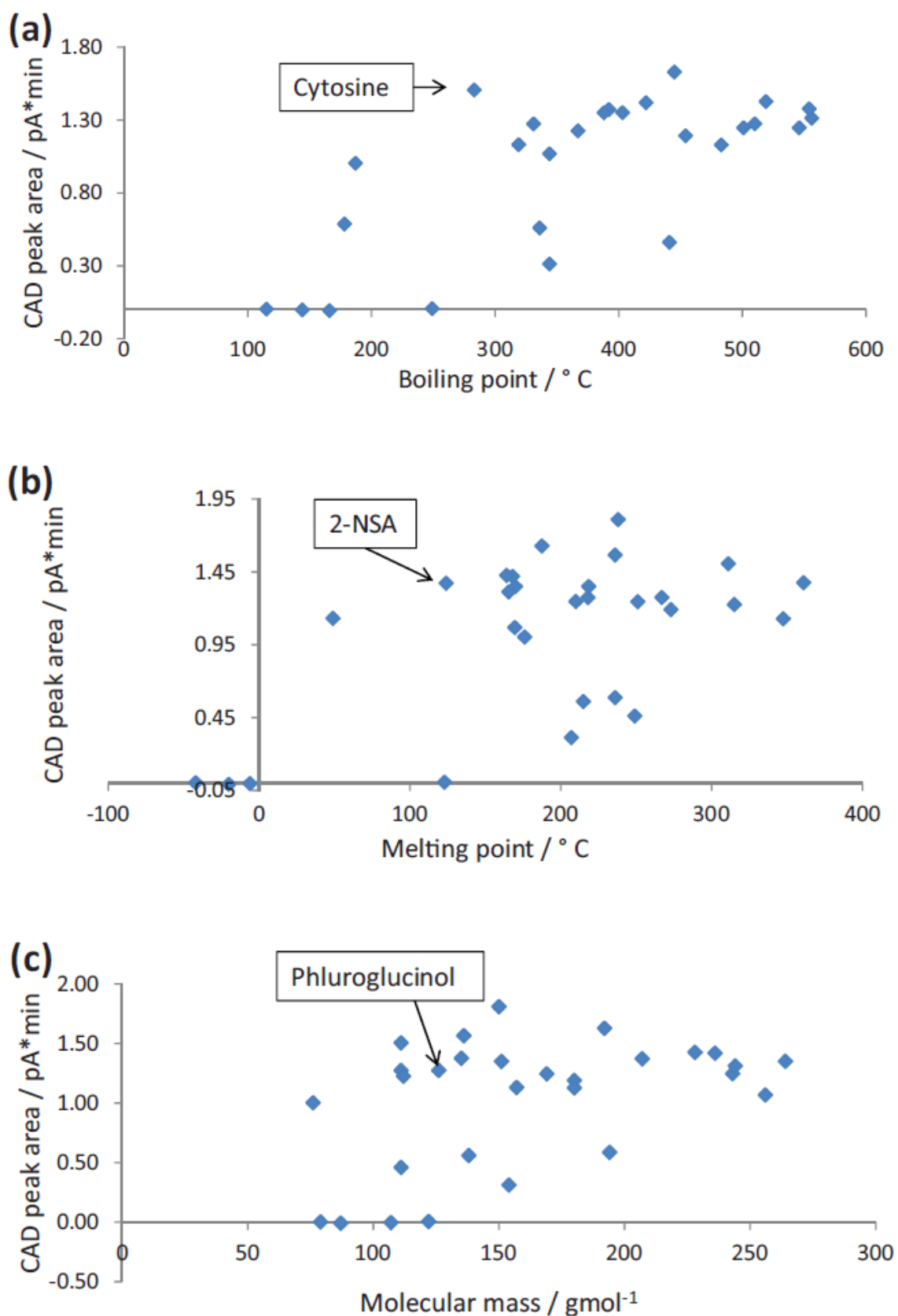


Figure 4.5. CAD response for 29 compounds, plotted against (a) boiling point, and (b) melting point; (c) molecular mass (FIA, conditions as per Fig. 4.2).

### 3.2.5 Effect of organic modifier (FIA)

Haddad and co-workers showed that CAD signal increases in proportion to the organic solvent concentration of the mobile phase for acetonitrile, acetone, isopropyl alcohol and methanol (Hutchinson *et al.* 2012, Hutchinson *et al.* 2010). These previous studies considered only peak areas and not the effect on uniformity of response or signal to noise ratio. Fig. 4.6a shows a plot of peak area vs. organic solvent concentration for 10–95% ACN. CAD response is roughly proportional to ACN concentration, in good agreement with earlier reports (Hutchinson *et al.* 2012, Hutchinson *et al.* 2010). Our data show peak areas under typical HILIC conditions (70–95%ACN) roughly twice that of typical RPLC conditions (10–50% ACN). Excessively large droplets are removed by droplet selection inside the nebuliser (Fig. 4.1). It is possible that highly-aqueous mobile phases produce excessively large droplets by condensation, which are removed in the nebuliser, resulting in reduced CAD response. Smaller droplets in greater numbers are formed with the lower viscosity, density and surface tension of highly organic eluents (Khandagale *et al.* 2014), which perhaps explains the better transport efficiency in these conditions.

Table 4.4 shows that with AF pH 3 as buffer the uniformity of response was slightly improved in HILIC conditions compared with RPLC. Moreau found CAD background current was higher for organic solvents compared to water (Moreau 2006), attributable to their dry residue content (typically 2 ppm); it is therefore conceivable that the high ACN content might also cause high noise with HILIC mobile phases. We measured noise over a 30 min period after system stabilisation (Fig. 4.6b); noise was lower in higher ACN concentrations. As a result, the response of the CAD (measured in terms of S/N) was further improved (Fig. 4.6c) under HILIC conditions compared with the improvements in terms of crude solute

peak area. It is possible that while organic solvents can indeed be a source of particulates, the fine aerosol particles are sufficiently small in organic-rich mobile phases (Khandagale, *et al.* 2014) that they are poorly detected.

**Table 4.4. Peak areas and uniformity of response for 21 compounds in a selection of HILIC mobile phases.**

	Mobile phase									
	95% ACN 5mM AF pH3	80% ACN 5mM AF pH3	50% ACN 5mM AF pH3	10% ACN 5mM AF pH3	80% ACN 5mM AF pH 5	80% ACN 5mM AA pH 5	80% ACN 5mM AA pH 6.8	80% ACN FA (0.1% v/v)*	80% ACN TFA (0.2% v/v)*	80% ACN HFBA (0.345% v/v)*
Mean Ultra response / pA*min	1.83	1.37	1.21	0.37	1.37	1.39	1.37	1.24	1.14	1.38
Uniformity of response (RSD)	12%	14%	15%	18%	13%	12%	14%	13%	23%	30%

\* Acids FA, TFA and HFBA molar concentration each 26.5mM



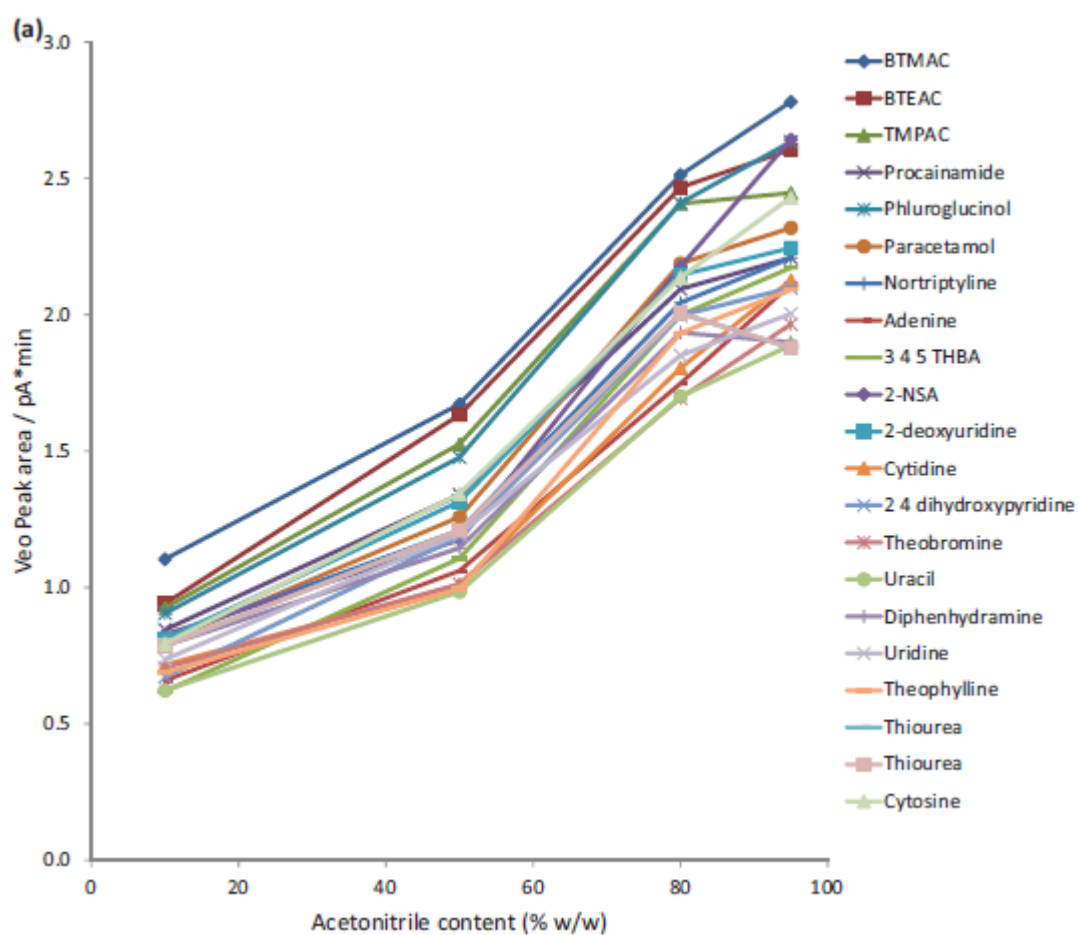


Fig. 4.6a. Effect of organic solvent content on (a) CAD peak area (FIA, mobile phase 10–95% ACN, other conditions as per Fig. 4.2).

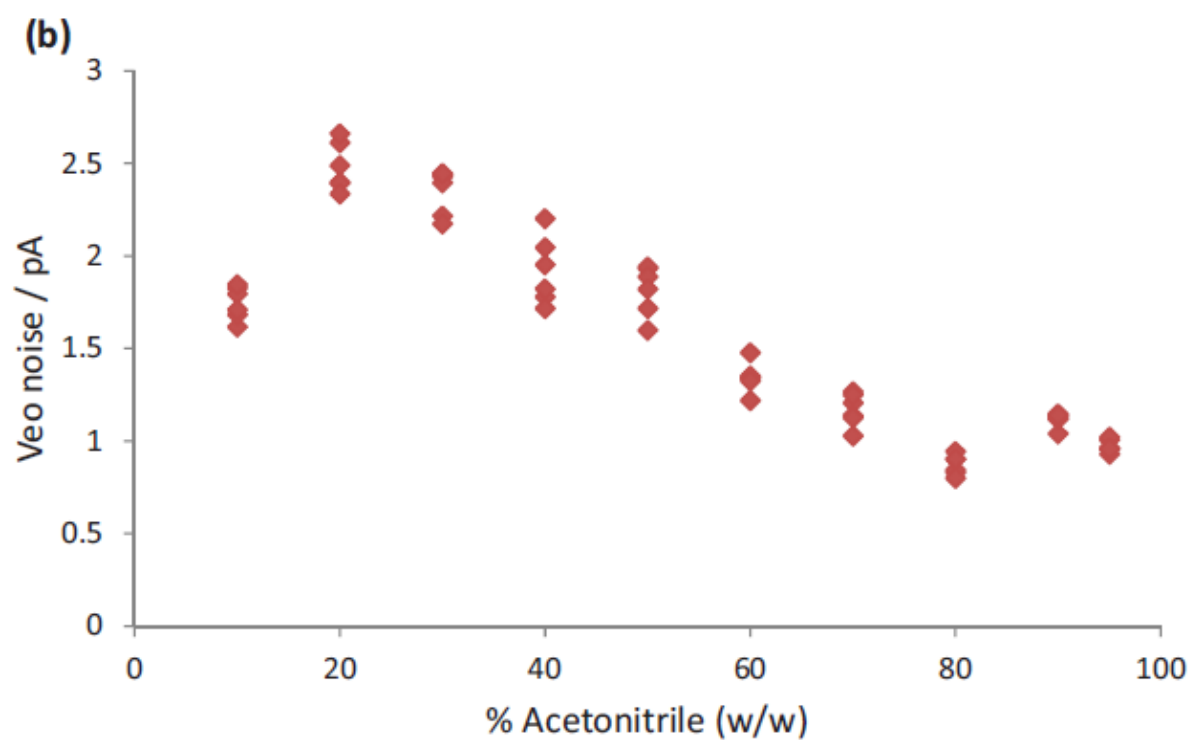


Fig. 4.6b. Effect of organic solvent content on (b) signal to noise ratio (FIA, mobile phase 10–95% ACN, other conditions as per Fig. 4.2).

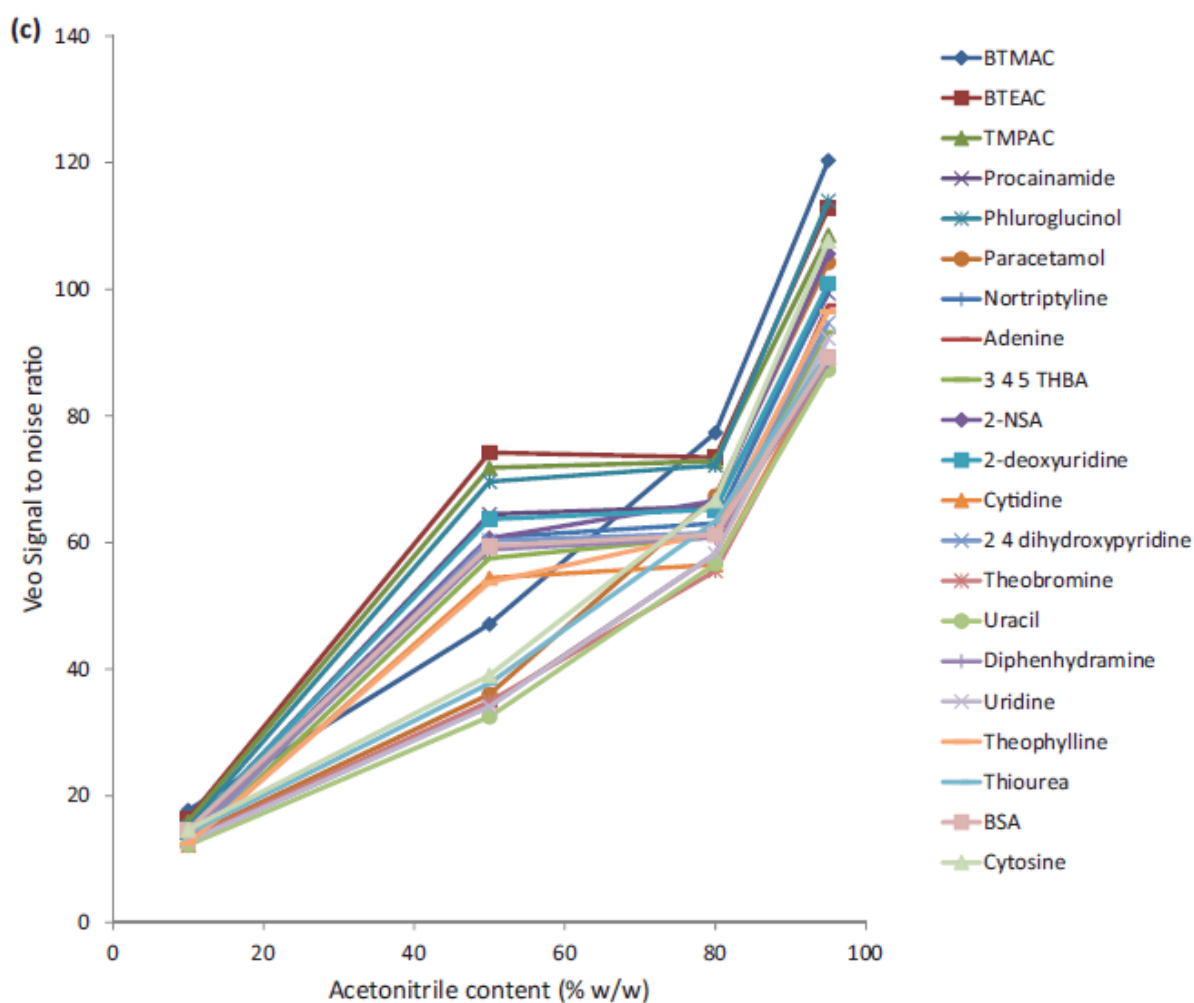


Fig. 4.6c. Figure 4.6. Effect of organic solvent content on (c) noise (FIA, mobile phase 10–95% ACN, other conditions as per Fig. 4.2).

Figure 4.6. Effect of organic solvent content on (a) peak area, (b) signal to noise ratio and (c) noise (FIA, mobile phase 10–95% ACN, other conditions as per Fig. 4.2).

### 3.2.6 Effect of elevated temperature (FIA)

The simpler Corona Ultra design allows thermostating of the nebuliser from 18 to 35°C (with the objective only to prevent freezing when using normal phase solvents); the temperature of the evaporator tube is at ambient. Using HILIC mobile phase, the Veo had a temperature range of 27–88°C for the evaporator tube. Fig. 4.7 shows CAD peak areas for the 29 test compounds at 30, 60 and 80°C at high acetonitrile content (90% ACN). The effect of elevated temperature on the noise was small (not shown). There is clearly no advantage in using high evaporation temperatures for the majority of solutes: signal drops off dramatically in many cases, due to volatilisation of the solute. Nevertheless, evaporation temperature can be a tool for distinguishing analyte from back-ground based on volatility, and it is possible that optimising this temperature in smaller increments (e.g. 5°C) could be beneficial in some cases. Compounds such as caffeine which give moderate CAD response show a dramatic reduction in response at higher temperatures. Xanthine derivatives theobromine and theophylline, which are structurally similar to caffeine, perform well at low temperatures, but also had low CAD response at temperatures of 60°C and above. The base procainamide maintains good CAD peak area at the elevated temperature of 60°C, whereas the base diphenhydramine shows a drop-off comparable to the xanthine derivatives. Procainamide is more hydrophilic than diphenhydramine, and this result suggested a possible relationship with solute log D values. Thus the data were plotted in order of increasing (more positive) log D for hydrophobic solutes from left to right. Solute on the left side of the plot (negative log D values) maintained good CAD peak areas even up to 80°C. Solute on the right side of the plot, (positive log D values), showed drastic reduction in peak area at higher temperatures. It is possible that the hydrophobic solutes

are lost more readily as the ACN evaporates first from the aqueous organic mixture, whereas hydrophilic solutes can be solvated by the remaining aqueous liquid. Fundamental aerosol studies by Reid *et al.* showed that hydrophilic/hydrophobic mixtures in aerosols can form a biphasic droplet (Reid *et al.* 2011). To gain thermodynamic stability, hydrophobic components form surface lenses (partially engulfed structures), due to the relative surface tensions of the two phases (Reid *et al.* 2011). Such a system can perhaps favour migration of hydrophobic components to the surface of aerosol droplets, and at high temperatures lead to their evaporation. The above confirms that low evaporation temperatures are required for optimal CAD performance, as loss of signal can be dramatic for a variety of solutes at higher temperatures. This effect was also observed with the equivalent salt-buffered mobile phase at 10% ACN (data not shown).

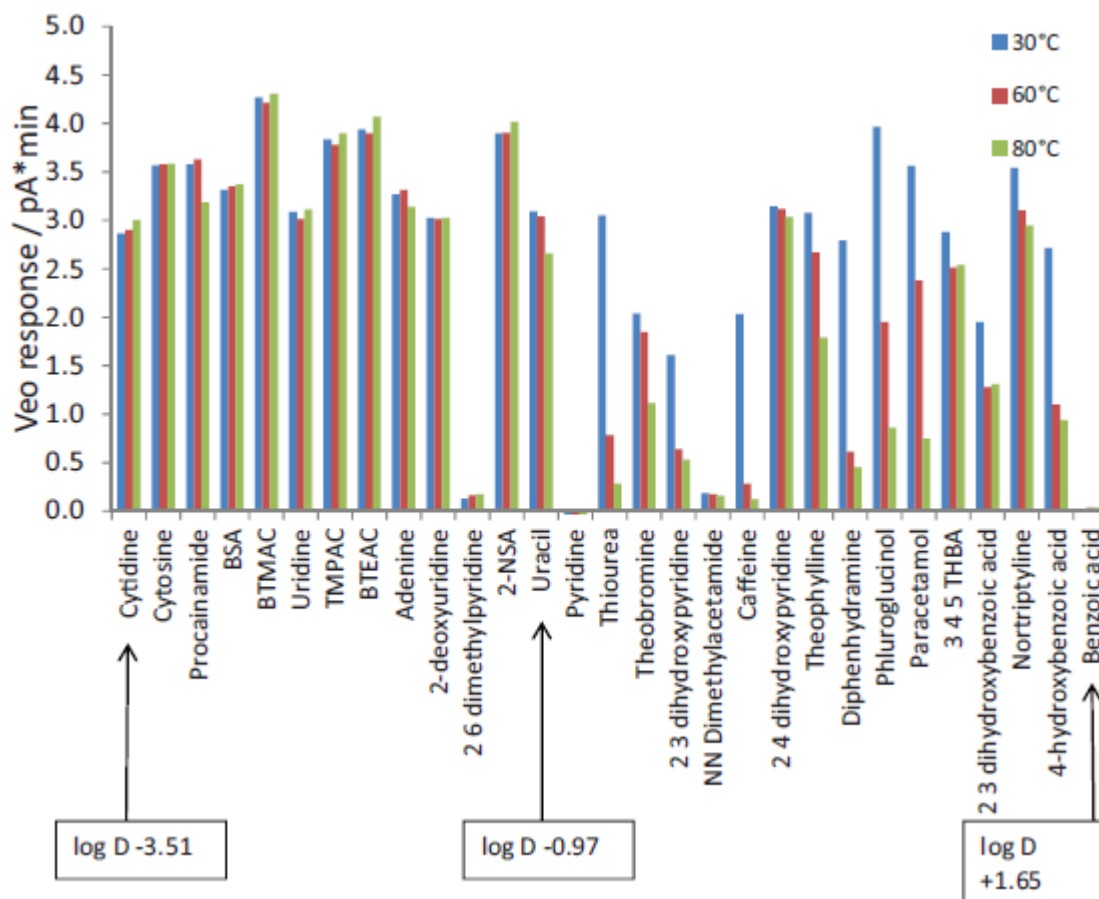
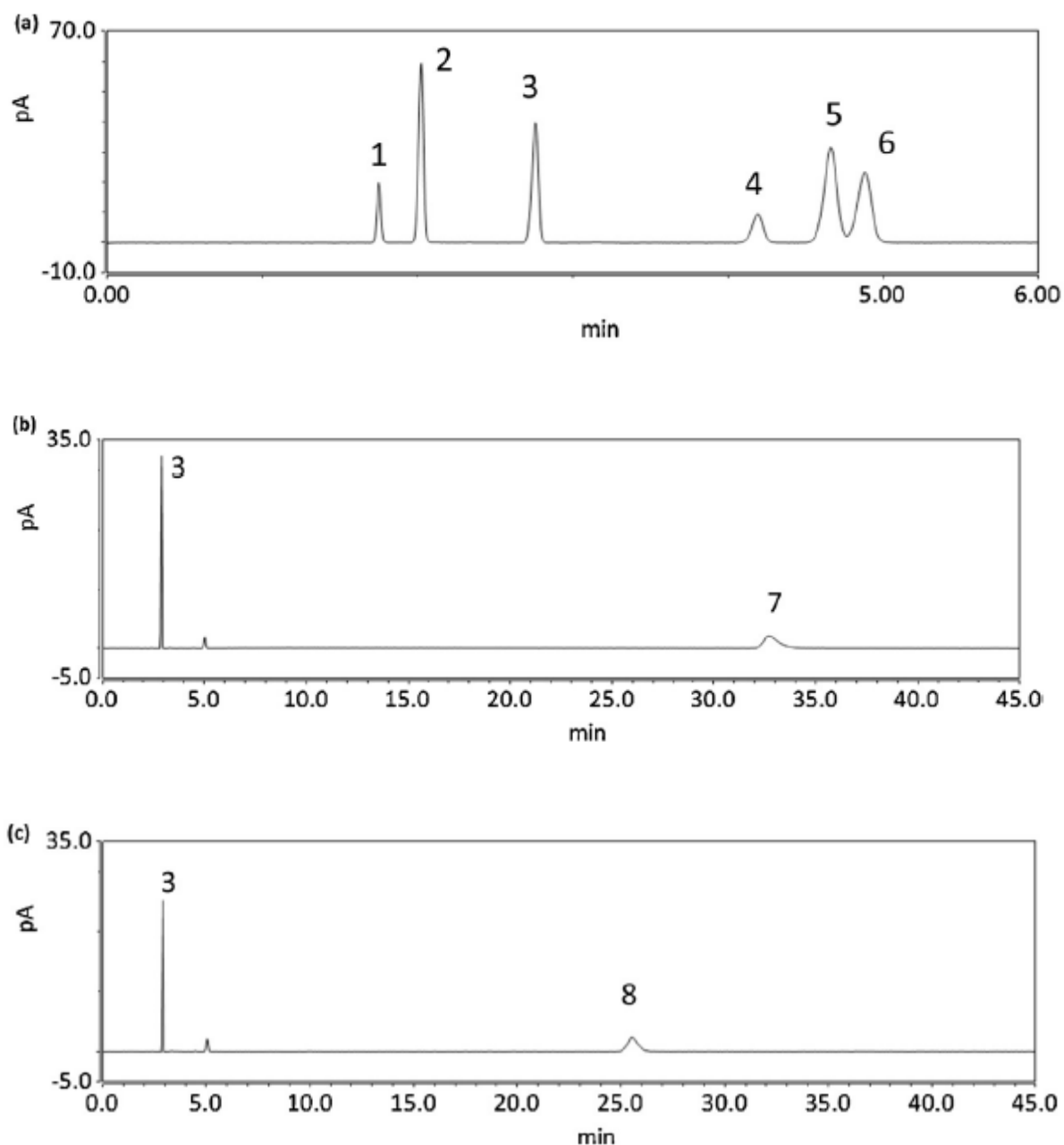


Figure 4.7. Effect of elevated temperatures on Veo response in order of log D (–ve on left, +ve on right) (FIA, mobile phase 90% ACN, other conditions as per Fig. 2). Log D values were the average from three software packages (see Section 2) Blue = 30°C, Red = 60°C, Green = 80°C.

### 3.3 Analysis of salts (HPLC)

Zhang et al. separated and detected 25 typical pharmaceutical salt counter ions by HILIC–CAD (Zhang *et al.* 2010) using gradient elution and a ternary solvent system. The authors reported separation of each ion from each other but did not comment on the separation of anion and cation for single salts. A mixture of inorganic salts was analysed by HILIC-CAD using a BEH Amide column (Fig. 4.8). The CAD was able to detect group (I) and (II) metals, common halides, and nitrate. There was good separation of cations from their corresponding anions. With the exception of chloride and nitrate, these ions are generally UV-transparent. The retention order of these salts is interesting, with cations retaining longer than anions (Fig. 4.8), probably due to ionic retention of cations and repulsion of anions on ionised silanol groups, which exist on all silica based-columns (Kumar *et al.* 2013). HILIC retention for ionogenic solutes is due to a mixture of ion-exchange and partition mechanisms (McCalley 2014, 2014). This application demonstrates the potential application of the CAD in the pharmaceutical industry.



**Figure 4.8.** HILIC separation and CAD detection of (a) a mixture of inorganic salts, (b) calcium chloride, (c) magnesium chloride. Peak identities 1 = iodide, 2 = nitrate, 3 = chloride, 4 = potassium, 5 = sodium, 6 = lithium, 7 = calcium, 8 = magnesium (HPLC, mobile phase 70% ACN, 5 mM ammonium formate pH 3, BEH Amide column).



## 4. Conclusions

The charged aerosol detector (CAD) is a quasi-universal detector for HPLC. Flow injection analysis (FIA) was shown to be a rapid method for assessing the performance of the CAD, as long as baseline disturbances encountered in this method were taken into account. Volatile compounds cannot form stable aerosol particles and give no response. Some compounds (e.g. Caffeine) had response ca. 40% lower than the average, and can be classed as 'semi-volatile' compounds although they were not readily identifiable as such from physico-chemical data (e.g. bp or mp). Response from solute-to-solute was not truly uniform; however over the diverse range of solutes tested the uniformity of response was as low as 12% RSD. The on column detection limit (1–3 ng) and limit of quantitation (5–9 ng) compared favourably to published LOD and LOQ for universal detectors. The detector's dynamic range was over 4 orders of magnitude (1 ng to over 20 µg sample loads) for modestly-retained solutes, which supports data described by the manufacturer. Calibration curves generated by HPLC for three diverse solutes were all non-linear over three orders of magnitude, supporting earlier findings performed by FIA (Gorecki *et al.* 2006, Hutchinson *et al.* 2010). A theoretical explanation based on the findings of the manufacturers of CAD (Thomas *et al.* 2014) was unable to describe the shape of typical CAD calibration curves. Possible solutions are calibration over narrow concentration ranges, plotting log/log calibration curves and use of an inbuilt 'power function'. These were equally effective at producing linear calibration. The precise workings of the 'power function' are proprietary information of the instrument manufacturer, so there may be reticence to its widespread use. HILIC was found to have excellent compatibility with CAD: uniformity of response was improved over RPLC conditions, signal under HILIC conditions was approximately twice as

high and signal to noise around 4 times higher. Interestingly, the CAD signal appeared somewhat higher for basic compounds than neutral compounds. The uniformity of response was less with TFA and HFBA than with AF buffers (23% RSD, 30% RSD and 14%, respectively). Weakly acidic solutes exhibited lower CAD responses in these buffers than for the formate and buffers; conversely weak bases exhibited increased CAD response. It is possible that increasing the mass of buffer counterions may improve the response to solute ions of opposite charge, which was investigated principally using stronger bases (cationic solutes) and different mobile phase acid anions. When maintaining constant molar concentration of the acid, detector response showed some increase, but not in proportion to the weight of the acid anion. Furthermore, the mobile phase pH produced by the different acids can change the degree of ionisation for weakly acidic and basic solutes, which may affect their response. Low evaporation temperatures are recommended for general use. However, hydrophilic solutes gave good response at higher evaporation temperatures (up to 80°C) as they may be retained longer in the aqueous portion of the aerosol particles. The CAD has many potential applications in the pharmaceutical industry, for instance in the monitoring of inorganic anions that can be separated as counterions of basic drugs. It appears that solutes injected as salts dissociate and travel through the column as separate cationic and anionic entities up to high concentrations, presumably accompanied by counterions from the mobile phase.

**The viability of isocratic Hydrophilic Interaction Chromatography with Charged Aerosol Detection for analysis of highly hydrophilic solutes without chromophores; comparison of Ultra and Veo CAD**

## Abstract

The viability of hydrophilic interaction chromatography (HILIC) with Charged Aerosol Detection (CAD) for isocratic HPLC of highly hydrophilic species with no chromophores was established. Using a BEH Amide column, simple sugars (e.g. fructose, glucose, ribose, maltose) were retained and detected; also by an Amino column. Using an Atlantis bare silica column, free amino acids without derivatisation (e.g. glycine, glutamine, aspartic acid and arginine) were retained and detected. All three separations were challenging and resolution was incomplete for combined standards. Sugar analysis using the Corona Veo gave poor signal quality, which was improved using high evaporation tube temperature from below the LOD to above the LOQ (70°C optimal). Like-for-like comparison was performed between the CAD Ultra and Veo detectors, and the Ultra was superior in terms of signal to noise ratio. It is speculated that the use of a concentric flow nebuliser on the Veo delivers excessive impurities which contribute to the higher noise observed on this detector. HILIC-CAD was amenable to these difficult analytes, but further work is necessary to optimise the separations. Development of generic methods is recommended to do this with efficient use of time.

# 1. Introduction

Charged aerosol detection began from the prototype detector of Dixon and Peterson (Dixon et al. 2002). Since then a charged aerosol detector was developed by ESA Biosciences (Gamache *et al.* 2005), which was acquired by ThermoFisher Scientific. The technology has been developed from the prototype to a commercial instrument, most recently as the Corona Ultra, Corona Ultra RS and then Corona Veo models. A significant change was made by the current manufacturers, ThermoFisher Scientific, between the Ultra and Veo: the nebuliser changed from a cross-flow nebuliser to a concentric nebuliser. Additionally, whereas the Ultra had changeable nebuliser needle temperature (to prevent freezing of normal phase solvents), the manufacturer added features in the Veo such as temperature control of the evaporation tube and an in-built 'power function'. As described in Chapter 4, CAD response is non-linear over a wide range of solute concentrations (1-1000 mg / L), and the 'power function' applies a mathematical formula to the Veo signal in order to 'linearise' calibration curves. Like-for-like comparison of the Ultra and Veo detectors has not previously been attempted, therefore prior to potential commitments to the CAD Veo as a generic detector, the Ultra and Veo performance was compared. The fundamental working of the Veo is similar to the Ultra, therefore it is expected that much of the fundamental studies described in Chapter 4 apply to both detectors. However the nebuliser has apparent importance in droplet selection for aerosol detectors: the concentric flow is designed to deliver large quantities of the solute to the detector. However the CAD is a quasi-universal detector which responds reasonably uniformly to non-volatile solutes (Chapter 4), and it is unclear if anticipated improvements in signal are observed with comparable signal quality (in terms of signal to noise ratio). The response of the CAD to solutes which do not contain

chromophores (Chapter 4) suggested other classes of solute such as sugars (Hutchinson *et al.* 2012) and underivatised amino acids may be amenable to charged aerosol detection. An additional problem these solutes pose is their hydrophilicity, which impedes their retention on traditional reversed-phase separations. Reducing sugars such as glucose can be subject to peak splitting by HPLC, which makes quantitative analysis difficult. Glucose poses additional health risks to the alcohol content of beer and cider. Sugars can be derivatised using a fluorescent-active moiety and detected by fluorescence (e.g. (Glowka *et al.* 2007)). This process is time-consuming and the Tanaka group called for alternatives to be found (Kawachi *et al.* 2011). Although applicable HPLC techniques have been established using refractive index (RI) or evaporative light-scattering detection (ELSD) (Nogueira *et al.* 2005), CAD detection limits can be superior to both these detectors (Chapter 4, (Hutchinson *et al.* 2011) and it may offer better performance. Glucose is a health risk due to its link to diabetes, and fructose is subject to increasing health research focus as a possible chronic issue (Lustig 2010). Glucose contains an aldehyde group which undergoes internal nucleophilic addition from its terminal hydroxyl group to form a 6-membered pyranose ring (structure for glucose shown in Fig. 5.1 below). Alternatively the aldehyde can be attacked by the hydroxyl adjacent to the terminal position and form a 5-membered furanose structure, however pyranose is the predominant form in aqueous solution due to reduced strain in the larger ring. This reaction can form either of two isomers, where a hydroxyl group faces upward in the opposite side of the molecule as the  $-\text{CH}_2\text{OH}$  group, or on the same side of the molecule (Fig. 5.1). These are known as the ' $\alpha$ ' and ' $\beta$ ' anomers of the sugar, respectively. Similarly for fructose, its ketone group facilitates formation of an ' $\alpha$ ' or ' $\beta$ ' form.

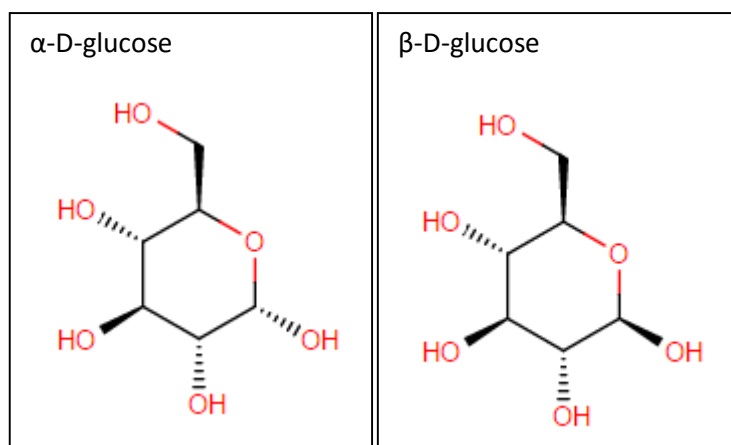


**Fig. 5.1 D-glucose in either ( $\alpha$ ) or ( $\beta$ ) form**

Since reducing sugars such as glucose and fructose can exist as either structure, during HPLC these forms interconvert in a process known as anomerisation which produces split peaks, making quantitation difficult. At high pH hydroxide catalyses this, which is apparently more-rapid than the chromatographic retention and elution processes. Therefore split peaks are avoided using of high-pH mobile phase with small quantities of a strong base e.g. triethylamine (TEA) added (Nogueira *et al.* 2005). However high pH mobile phase dissolves silica column structure by hydrolysing siloxane bonds which hold the structure together (Berthod 1991). Two approaches exist to deal with this: amino-bonded columns use a propylamine ligand as stationary phase, which in contact with water releases hydroxide anions which catalyse the anomerisation as above. Alternatively, hybrid silica such as ethylene bridged hybrid (BEH) has been designed using ethylene bridges in place of siloxane bonds, and mobile phase of high pH ought to be compatible with this stationary phase type. BEH Amide columns, as used in Chapters 3 and 4, have hybrid silica and a hydrophilic amide ligand and ought to be well-suited to these separations, although few reports of this have been published in the scientific literature. Hydrophilic solutes were retained on a range of HILIC columns with excellent peak shape, provided buffers were used in the mobile phase

(Chapter 3). Amino acids are zwitterionic due to their amine and carboxylic acid groups, which enables them to form peptides through condensation reactions. Ionogenic solutes in the form of simple bases and acids require sufficient buffer in mobile phase to chromatograph properly (Chapter 3), therefore buffers are anticipated as necessary for zwitterionic amino acids.

## **2. Experimental**

### **2.1 Chemicals and reagents**

All sugars, amino acids and the 29 probe solutes used for Veo-Ultra comparison were purchased from Sigma Aldrich (Poole, UK).

### **2.2 Equipment and methodology**

A Thermo UltiMate 3000 Rapid Separation Liquid Chromatography system was used for all experiments, comprising a quaternary pump, diode array detector (DAD) and either a Corona Ultra or Corona Veo CAD, with Chromeleon 7.2 software (Thermo, Germering, Germany). The CAD is a destructive detector, therefore the DAD and CAD detectors were connected in series in some experiments, with flow first through the DAD. Thermo Viper tubing (0.13 mm ID) was used as connection tubing. Data collection rates were 100 Hz for both DAD and CAD, due to narrow peak widths (typically 1 s at half height in flow injection analysis (FIA)). The Corona Ultra nebuliser (cross flow design similar to that used in atomic absorption spectrometry) was controlled at 22°C with the evaporator tube at ambient temperature, while the Veo (concentric flow design similar to those used in mass spectrometry) nebuliser was at ambient temperature and the evaporator tube set to 30°C.



The Veo had a power function (PF) designed to 'linearise' data, which was set to either 0.67 (this simulates 'off'), 1.00 (the default) or 1.2 (optimised setting using experimental data, see below). An ethylene bridged hybrid (BEH) amide column (150 × 4.6 mm, particle size = 3.5 µm, Waters, Milford, USA) or a Kromasil NH<sub>2</sub> amino-ligand column (150 × 4.6mm, particle size = 5 µm, Kromasil, LOCATION) were used for sugar separation experiments. An Atlantis bare silica column (250 × 4.6 mm ID, particle size = 5 µm, Waters) was used for amino acid experiments. The mobile phase was ACN with water. For sugar experiments with the Amino column, no buffer was added as the column itself aids can have a high pH in the vicinity of the pore surface (Kawachi *et al.* 2011). Sugar analysis on the BEH Amide column were done using trimethylamine (TEA) as a basic additive to catalyse mutarotation of reducing sugars. Comparative studies between the Veo and Ultra used 5 mM ammonium formate (80:20, w/w) unless otherwise stated, ran isocratically since CAD response sensitive to mobile phase organic solvent content (Russell *et al.* 2015, Hutchinson *et al.* 2012). The pH meter was calibrated in aqueous buffers and formic or acetic acid was used to adjust the aqueous portion to  $w^w$  pH 3 or 5. Solutions at  $w^w$  pH 6.8 were unadjusted 5 mM ammonium acetate. Care is necessary as pH calibration buffers can be a major source of non-volatile contaminants in the mobile phase. In flow injection analysis (FIA), narrow bore tubing (75 µm × 1100 mm) was used in place of the chromatographic column to maintain sufficient backpressure. Samples for FIA were prepared at a concentration of 300 mg/L; injection volumes were 1 µL unless otherwise stated. Flow rate was 1 mL/min.

### 3. Results and discussion

#### 3.1 Viability of sugar analysis using an alternative stationary phase (BEH Amide) and CAD Veo detection

A combined standard of nine sugars (1000 mg / L each) was prepared and run on a BEH Amide column with CAD Veo detection (power function set to 0.67) (Fig. 5.2). Levoglucosan was included, since this sugar is a molecular marker of biomass combustion (Fraser *et al.* 2000) and there is perhaps scope for use of CAD in environmental health studies (Dixon, Baltzell 2006). Fig. 5.2 shows a HILIC-CAD chromatogram of the nine sugars using a BEH Amide column (4.6 x 150mm, 3.5  $\mu$ m) with HILIC mobile phase and TEA additive (70% ACN with 0.1% TEA). Even using this technique and a column specifically designed for sugar separation, this is clearly a challenging problem for complex mixtures of multiple sugars (Fig. 5.2). The signal quality of Figure 5.2 was poorer than expected at this somewhat high solute concentration (1000 mg / L). To characterise the problem of poor signal quality this, some individual sugars were run over the concentration range 100 – 2500 mg / L; Fig. 5.2b-d plot their peak areas and signal to noise ratios. As per Fig. 5.1a, signal to noise ratios were above typical limits of detection ( $S:N > 3$ ) at solute concentrations of 100 mg / L, although these were below limits of quantitation ( $S:N < 10$ ). This is inferior to the LOQ reported in chapter 4, with LOD of 5-9 mg / L (also 1  $\mu$ L injections). It is possible the TEA used to prepare alkaline mobile phase contributed to this poor signal quality, although the data in chapter 4 used the same type of column with appreciable salt content as mobile phase buffer, which can itself contribute to reduction of signal quality (Vervoort *et al.* 2008). As discussed in chapter 4, the Veo evaporation tube temperature can be increased up to around 90°C, which may aid signal quality. Figure 5.2e-f show the effect of increasing the evaporation tube temperature

from 30-80°C in 10°C increments. At 30°C, signal quality was so poor for galactose that even at 1000 mg / L the S:N was below the LOD (S:N 1.2). However increasing the evaporation temperature to 70°C moved the same experiment to above the LOQ (S:N 15). Glucose showed similar improvements in signal quality at higher evaporation temperatures, with optimum performance also at 70°C. The improvement in S:N at higher evaporation temperature is interesting, as in chapter 4 it was shown that many solutes exhibit dramatic reductions in signal at higher evaporation temperatures. However those that lost signal were predominantly hydrophobic solutes ( $\log D > 0$ ). Glucose and galactose are highly hydrophilic and perhaps when inside the CAD retain in the aqueous portion of the aerosol droplet. The higher evaporation temperature also resulted in higher peak areas for both sugars, therefore perhaps at lower temperatures it is difficult to evaporate water from droplets containing these solutes. At higher temperatures (e.g. 70°C), it is possible that their droplets desolvate more efficiently to then form aerosol particles for detection. It is perhaps worthy of note that even with optimised evaporation temperature, the signal quality is somewhat low at the concentration of 1000 mg / L (Fig. 5.2 e-f). The TEA used to modify the mobile phase to high pH was perhaps responsible for the high noise, therefore a 10-fold decrease of TEA (0.01% cf. 0.1% TEA) was attempted, however peak broadening occurred for both glucose and galactose, with no obvious improvements in signal quality (data not shown). It was unclear if the Veo was perhaps responsible, and therefore like-for-like comparison of the Ultra and Veo was considered necessary.

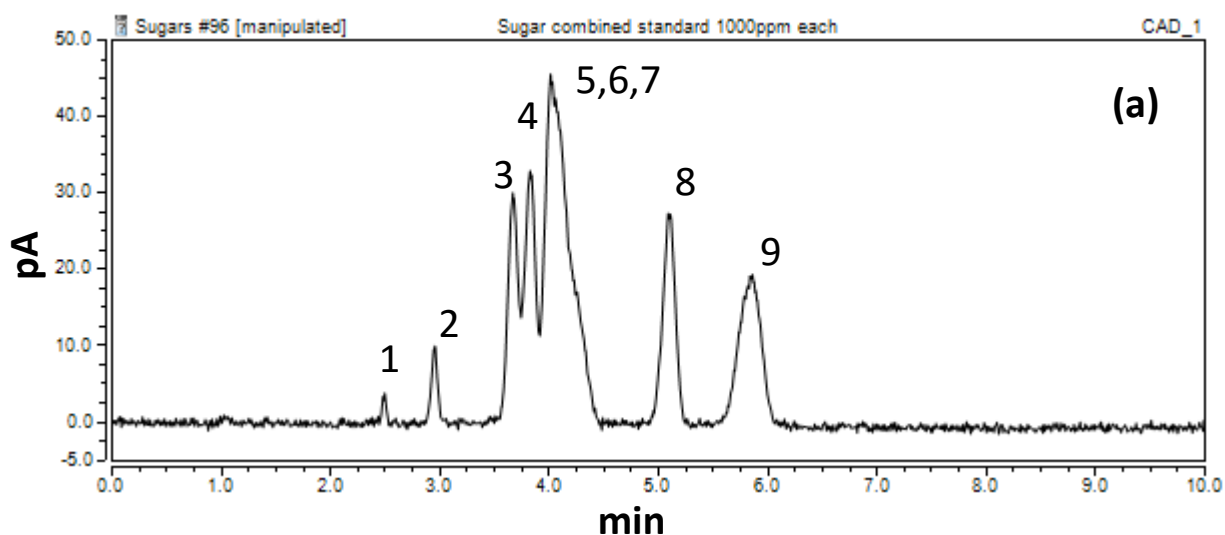


**Fig. 5.2 (a)** Nine sugars on BEH Amide column. Mobile phase 70% ACN with 0.1% TEA, CAD Veo detection (1) Levoglucosan, (2) Ribose, (3) Fructose, (4) Mannose, (5) Maltose, (6) Glucose, (7) Galactose, (8) Sucrose, (9) Sorbitol. 1000mg/L each, 1  $\mu$ L injections.

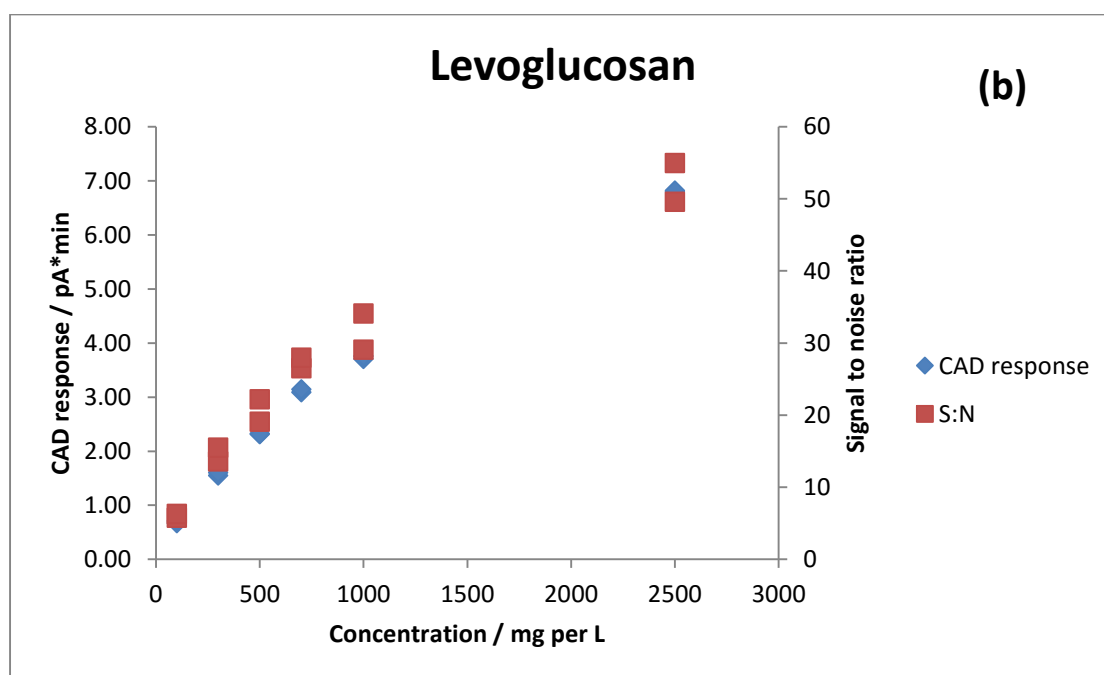


**Fig. 5.2 (b)** Levoglucosan CAD Veo peak area and Signal to Noise ratios 100 – 2500 mg / L

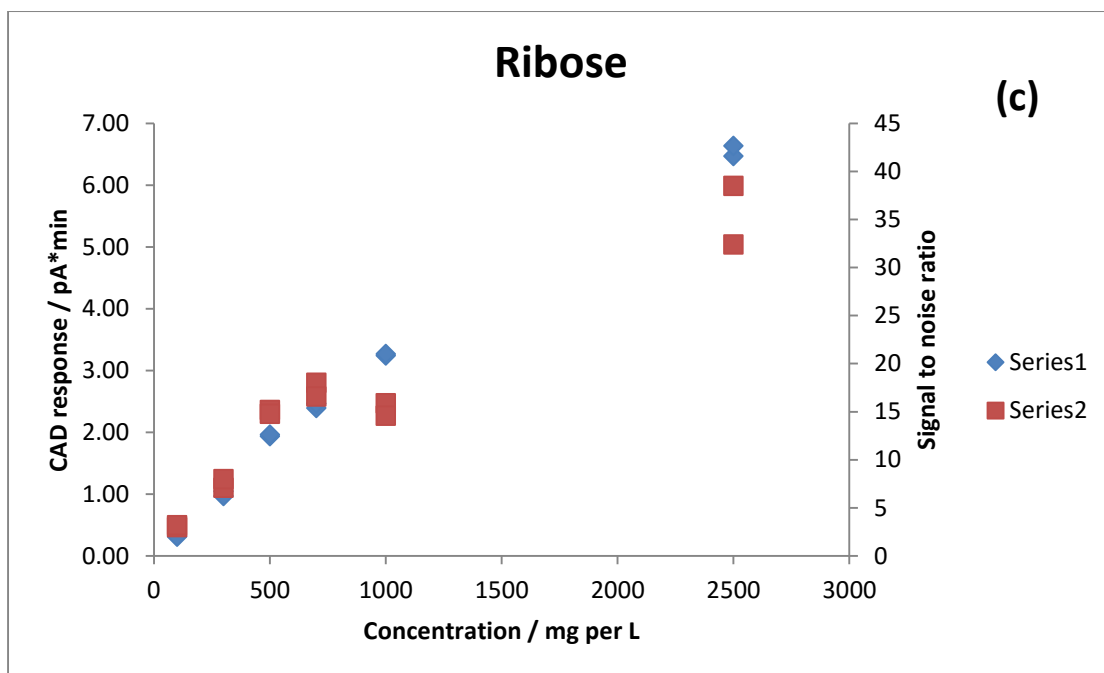


Fig. 5.2 (c) Ribose CAD Veo peak area and Signal to Noise ratios 100 – 2500 mg / L

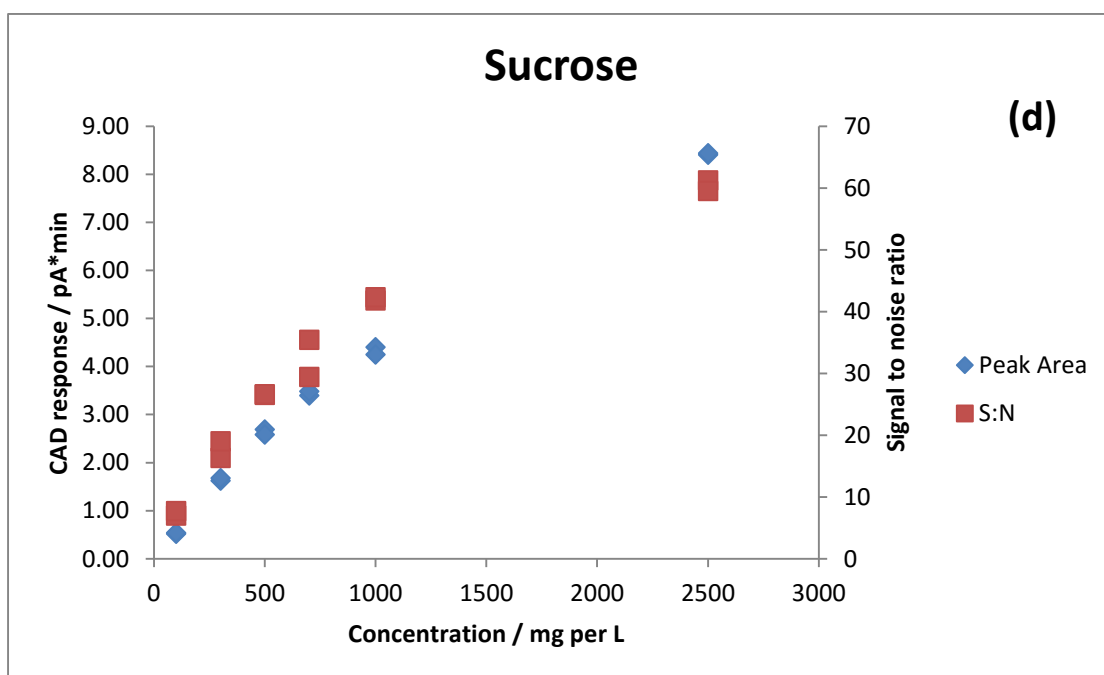


Fig. 5.2 (d) Sucrose CAD Veo peak area and Signal to Noise ratios 100 – 2500 mg / L

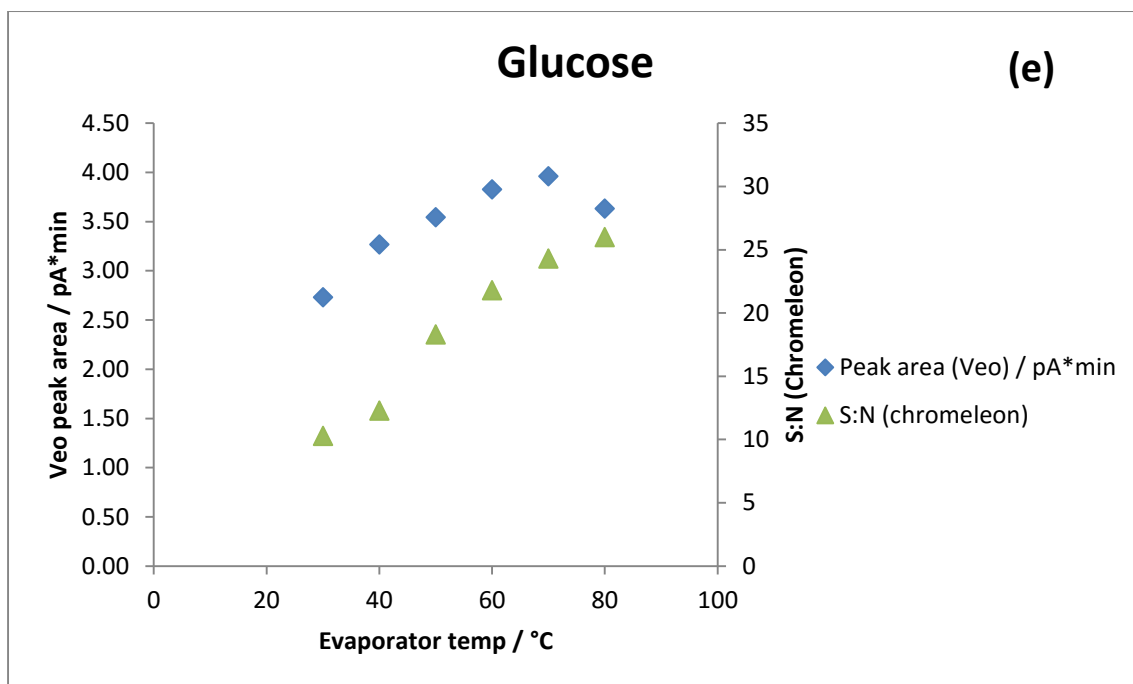


Fig. 5.2 (e) Glucose CAD Veo peak area and S:N at 1000 mg / L, 1  $\mu$ L injection, mobile phase 75% ACN with 0.1% TEA.

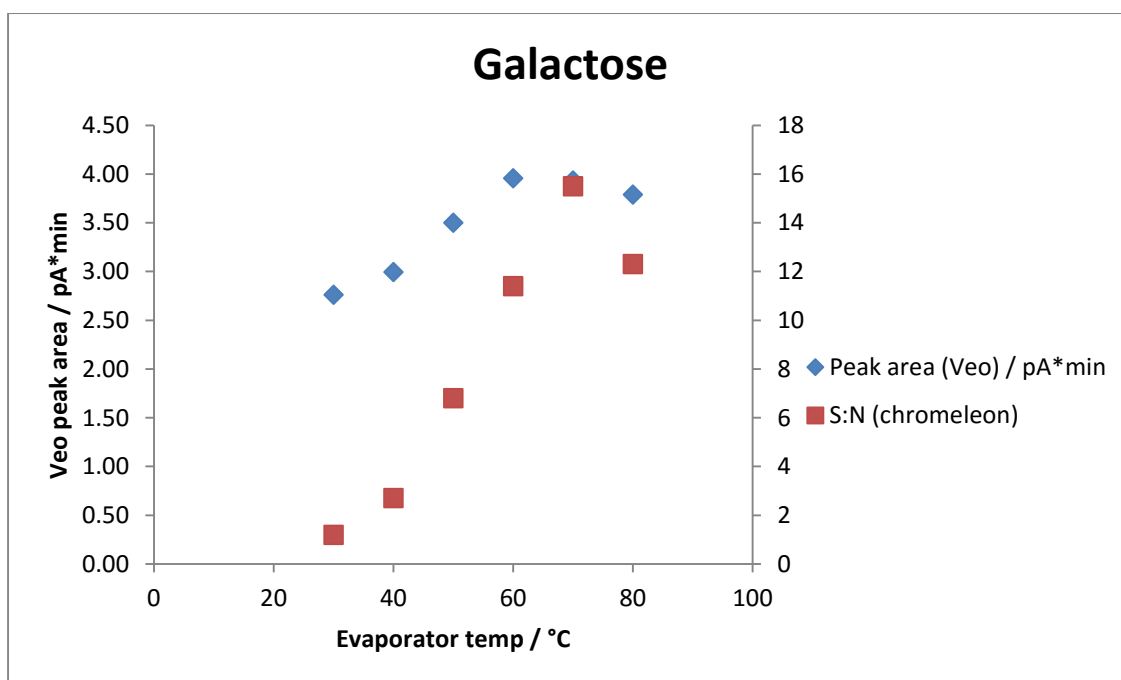


Fig 5.2 (f) Galactose CAD Veo peak area and S:N at 1000 mg / L, 1  $\mu$ L injection, mobile phase 75% ACN with 0.1% TEA.

## 3.2 Comparison of Ultra and Veo CAD

The unusual results with sugars suggested a more detailed investigation of the sensitivity of the two detectors, using a much wider range of solutes, was necessary. Therefore this was investigated in some detail by flow injection analysis (FIA) using 29 diverse solutes including acids, bases and neutrals, performed as described in Chapter 4 at 300 mg / L, flow rate 1mL / min and 1 µL injection volume. The concentric-flow nebuliser used in the Veo supposedly delivers more solute to the detector than the cross-flow nebuliser used in the Ultra. Figure 5.3a compares peak areas of the Ultra and Veo detectors for identical solutes and identical mobile phases (LCMS grade buffers used). Peak areas were around 50% larger with the Veo than the Ultra, as expected (Fig. 5.3a). However this does not take noise into account and signal quality (in terms of signal to noise ratio) perhaps better describes detector performance when comparing the two models. Using equation (5.1), signal to noise ratios were calculated for these data.

$$\text{Signal : Noise} = \frac{\text{Peak height (pA)}}{\text{RMS noise (pA)}} \quad (5.1)$$

Noise was manually collected as per chapter 4 (30 minute collection, RMS noise measured by Chromeleon software over 5 min period) and signal to noise calculated using Microsoft Excel. In contrast to the raw peak area results of Fig. 5.3a, the S:N data (Fig. 5.3b) show signal to noise ratios (thus signal quality) was superior using the Ultra compared to the Veo, by a factor of around 9. Considering signal and noise separately, the noise values for the Veo are 9 times higher than the Ultra (Fig. 5.3c). Unexpectedly, with the exception of a few semi-volatile solutes, the peak heights (Fig. 5.3d) were somewhat lower for the Veo. The net

effect is the superior signal quality using the CAD Ultra. These data were communicated to the manufacturer and the industrial collaborator for further reflection (Appendix II).

### **3.2.1 Noise in buffered and unbuffered mobile phase**

It may be possible that the mobile phase buffers were responsible for the detector noise, therefore noise was measured for different mobile phases containing either no buffer at all, just acid, just salt, or acid and salt. The pH meter used to check the  $w^w$  pH of mobile phase leaks a small amount of potassium chloride into the mobile phase in order to measure conductivity, therefore this was a possible source of contamination which perhaps can cause detector noise (note in Chapter 4 the CAD was sensitive to inorganic salts). Noise was collected using the Veo (power function 0.67) in each of these mobile phases and the results are shown in Fig. 5.3 e. In the absence of any buffer (red bar in Fig. 5.3 e), the noise was less than half of that observed in salt-acid buffers (light blue and orange bars). Therefore the solvents themselves perhaps contributed some of the noise and the remainder are due to the buffers used. The green and purple bars show noise levels in acid-only and salt-only mobile phase respectively (Fig. 5.3 e) suggesting the salt and acid both contribute to detector noise. For both the salt-acid buffers (light blue and orange bars in Fig. 5.3 e), noise levels were comparable. Therefore it is unlikely that the pH probe was responsible for the high noise observed in the Veo detector (note: LCMS grade buffers were used in all experiments). A pragmatic approach to continue this study of highly hydrophilic solutes with no chromophore was to instead use the CAD Ultra.



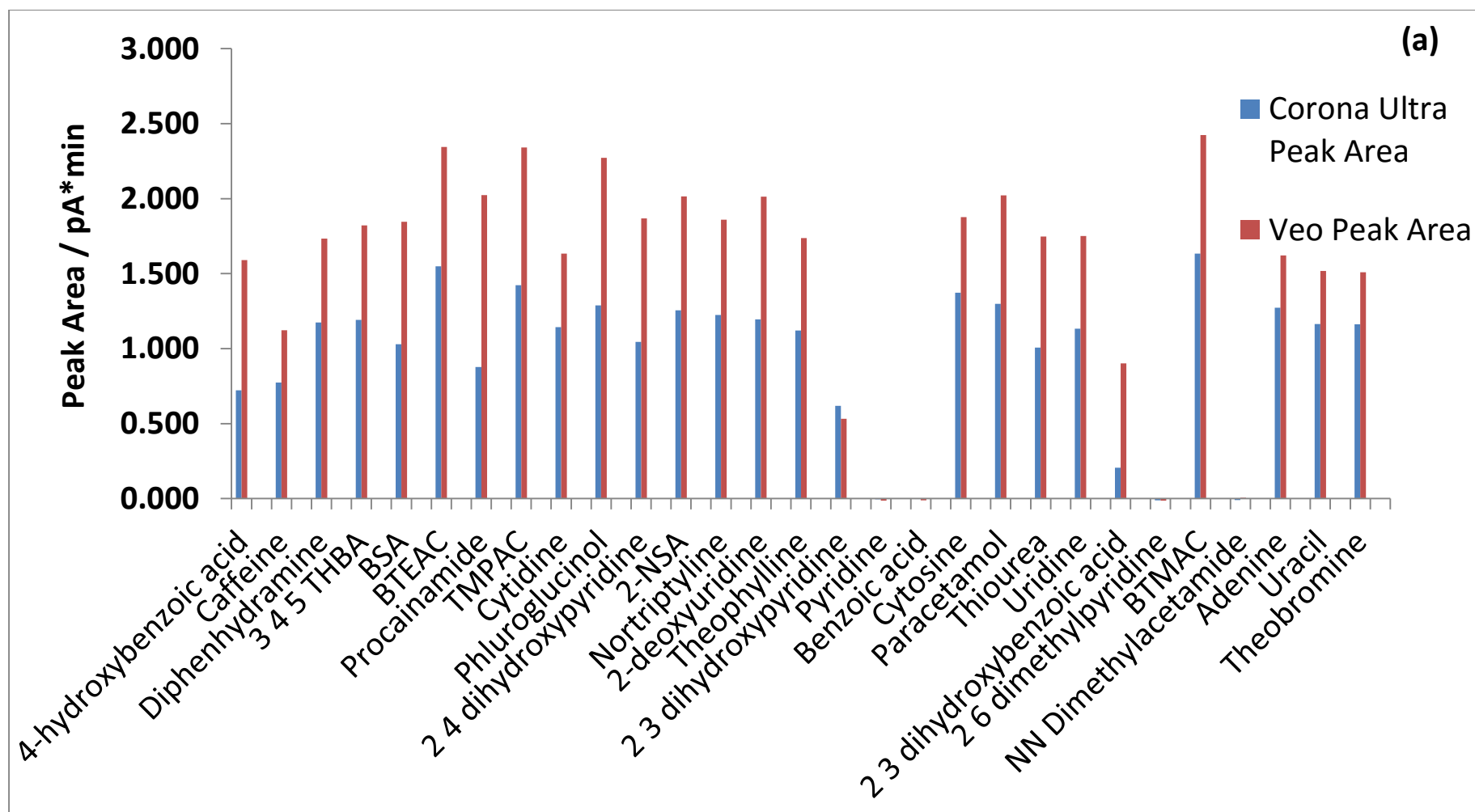


Figure 5.3a. Peak areas by flow injection analysis for 29 solutes for two CAD models. Blue = Ultra, Red = Veo

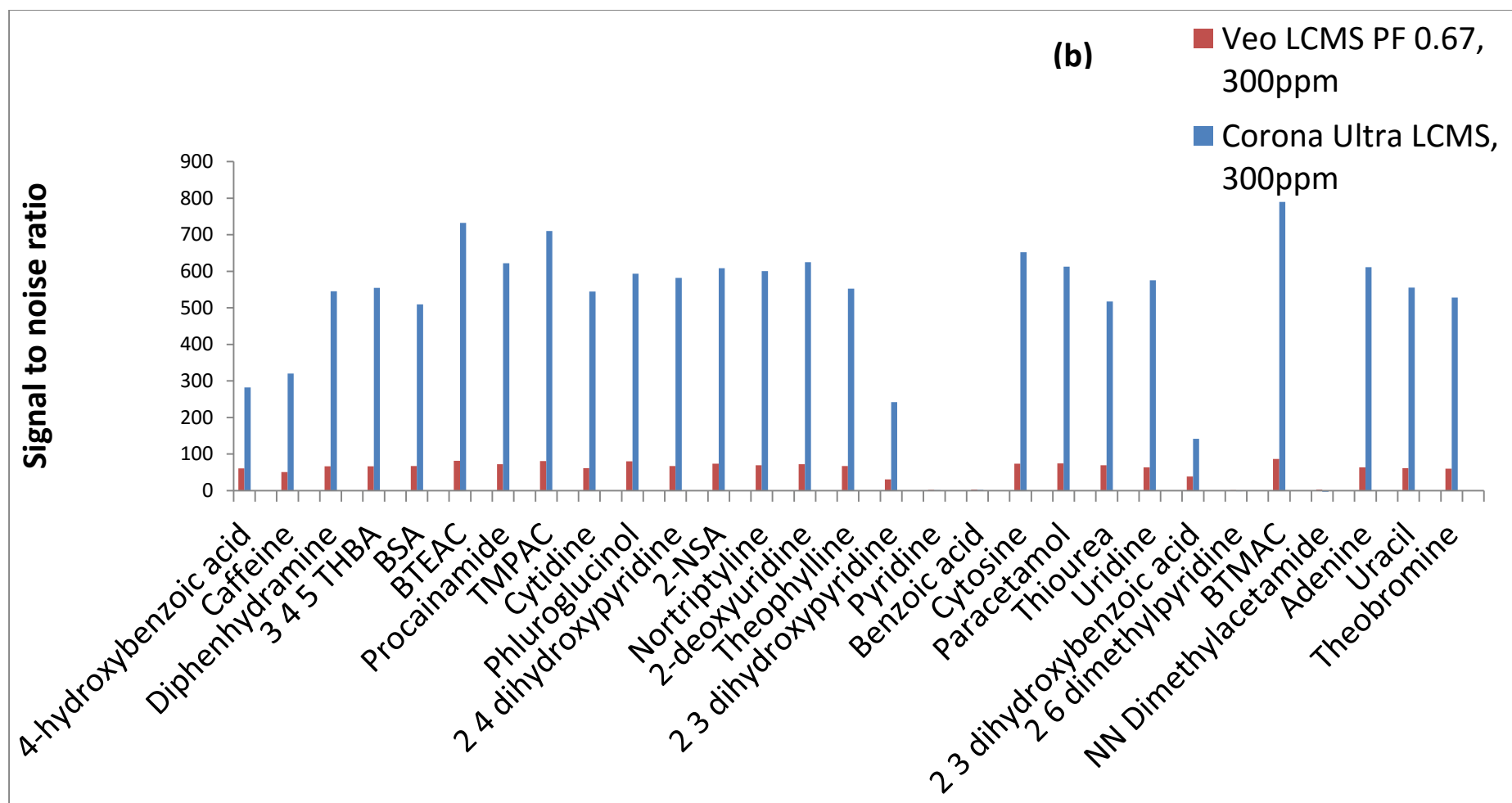
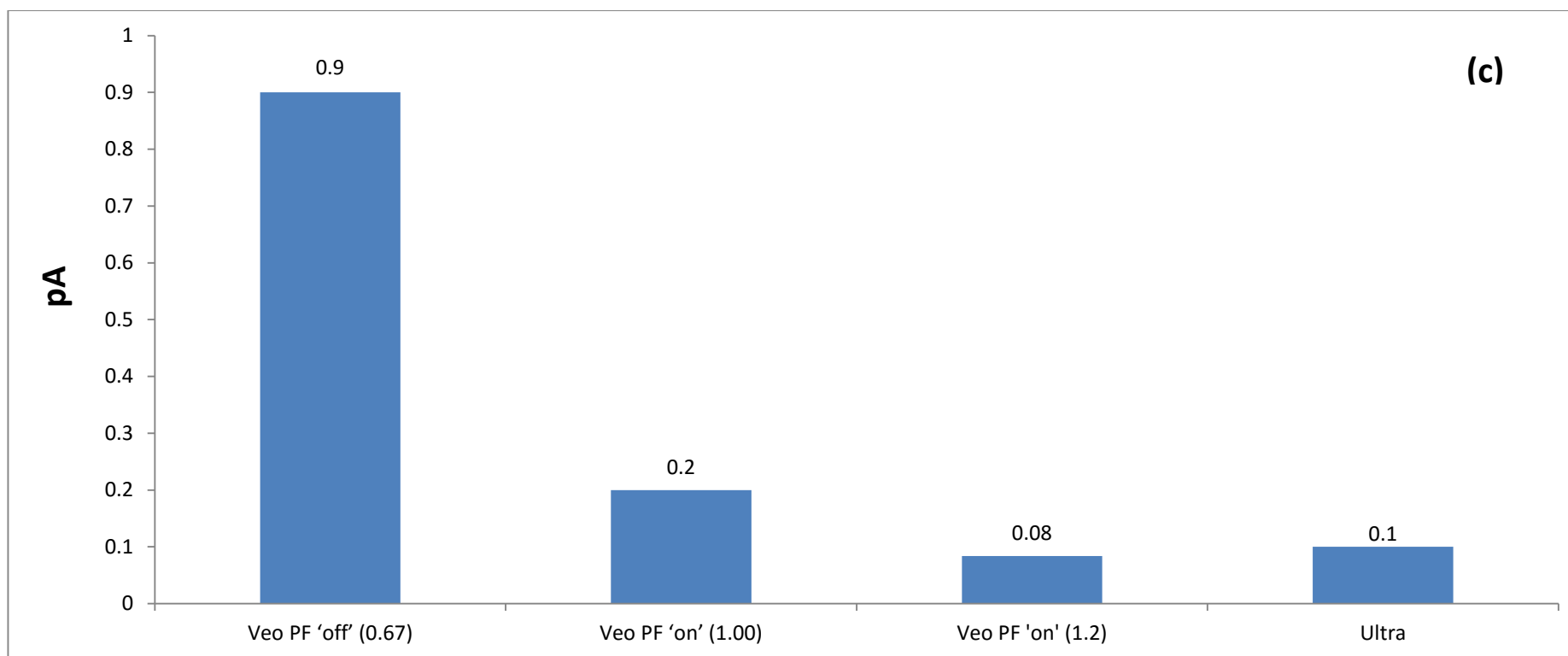


Fig. 5.3b Signal to noise ratios by flow injection analysis for 29 solutes for two CAD models. Blue = Ultra, Red = Veo. Noise manually calculated, peak heights. Veo power function set to 0.67 to simulate 'off'.



**Fig. 5.3c CAD noise levels, mobile phase 80% ACN with 5mM AF pH 3. Veo with power function 'off', 'on' default setting 1.00 and 'on' optimised setting 1.2, Ultra.**

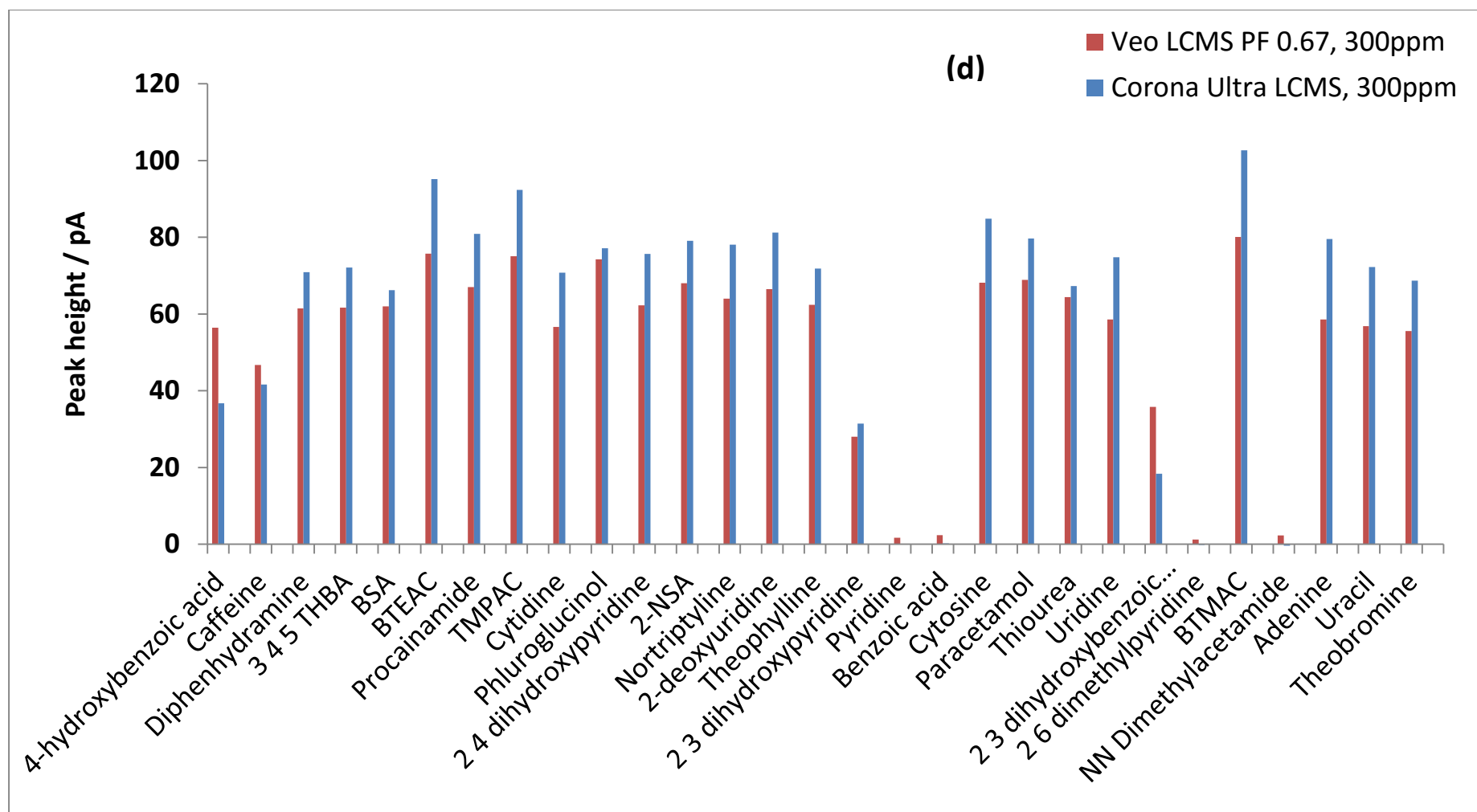
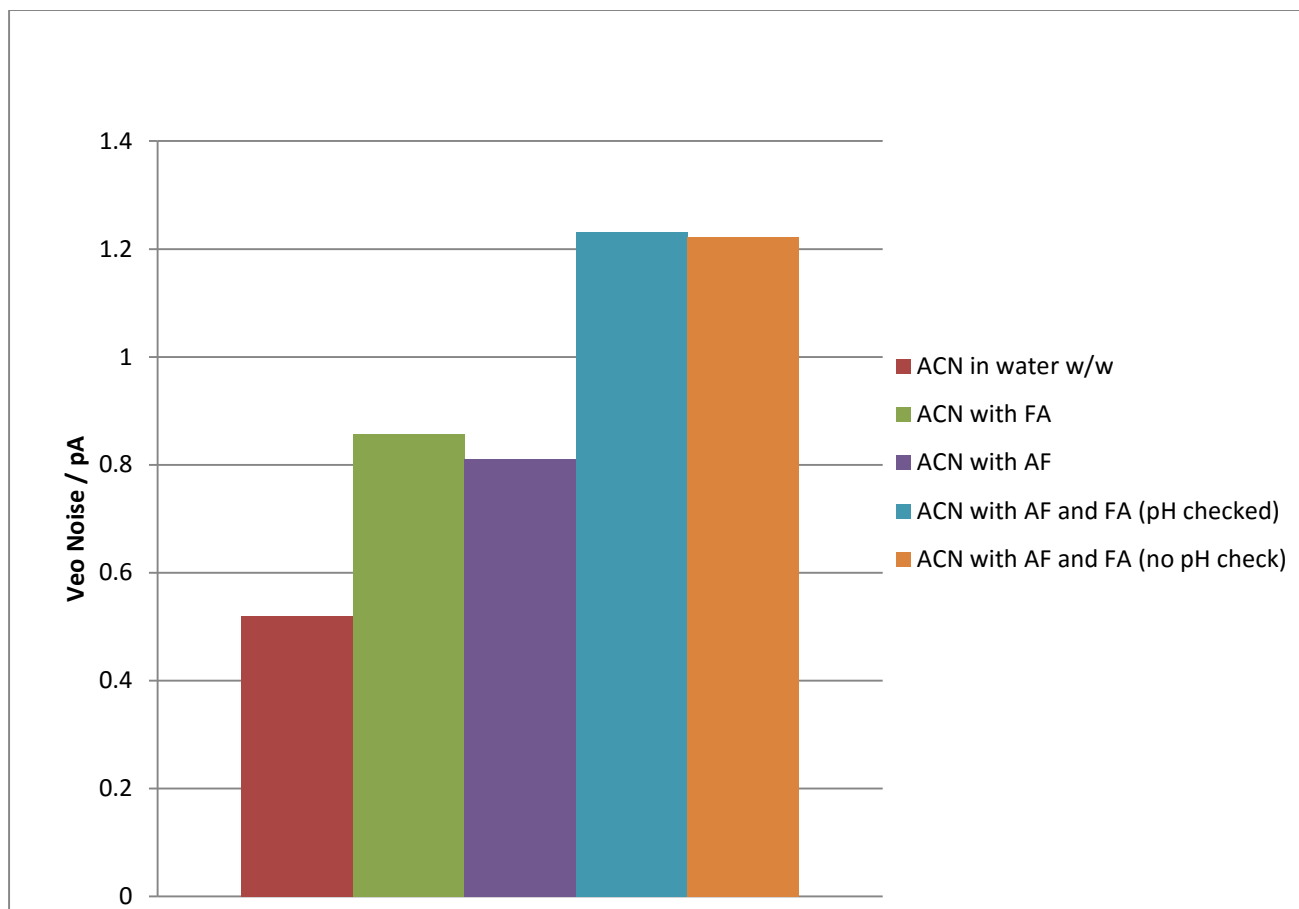


Fig. 5.3 d Peak height (as CAD signal) by flow injection analysis for 29 solutes for two CAD models. Blue = Ultra, Red = Veo. Veo power function set to 0.67 to simulate 'off'.

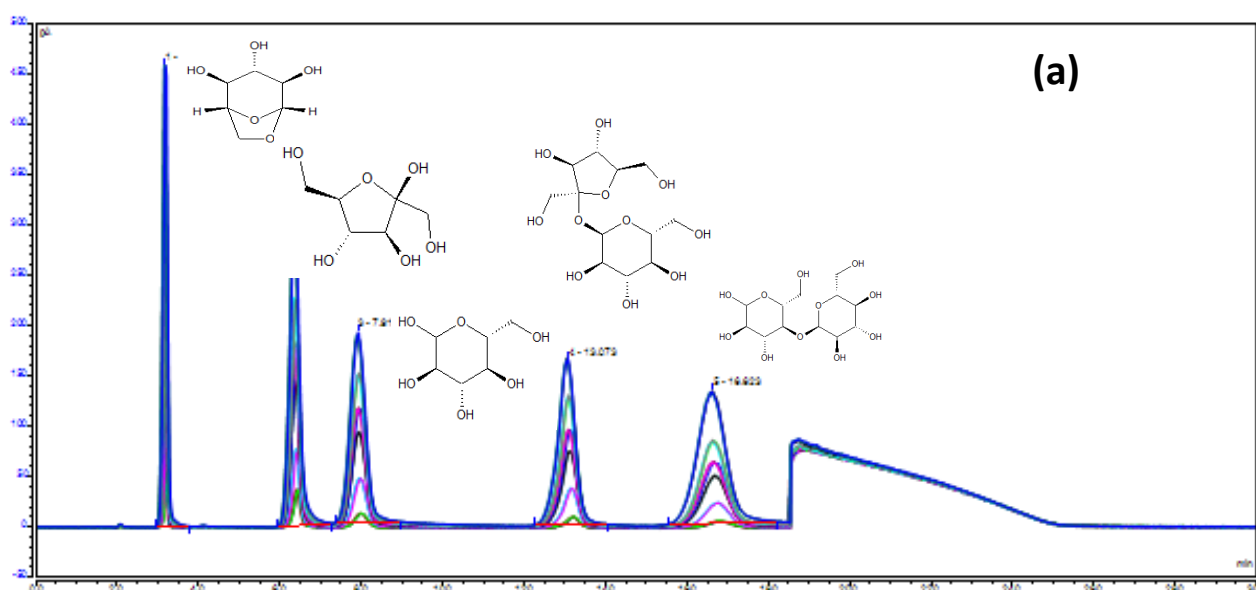


**Fig. 5.3 e Noise measurements to ascertain which mobile phase components contributed (FIA using Veo, Mobile phase 80% ACN with either no buffer, formic acid (0.1% v/v), ammonium formate (5 mM) with no acid, ammonium formate with formic acid pH measured in aqueous buffers (5mM AF,  $w^w$  pH 3) or ammonium formate with formic acid added but no pH measurement made (5mM with FA).**

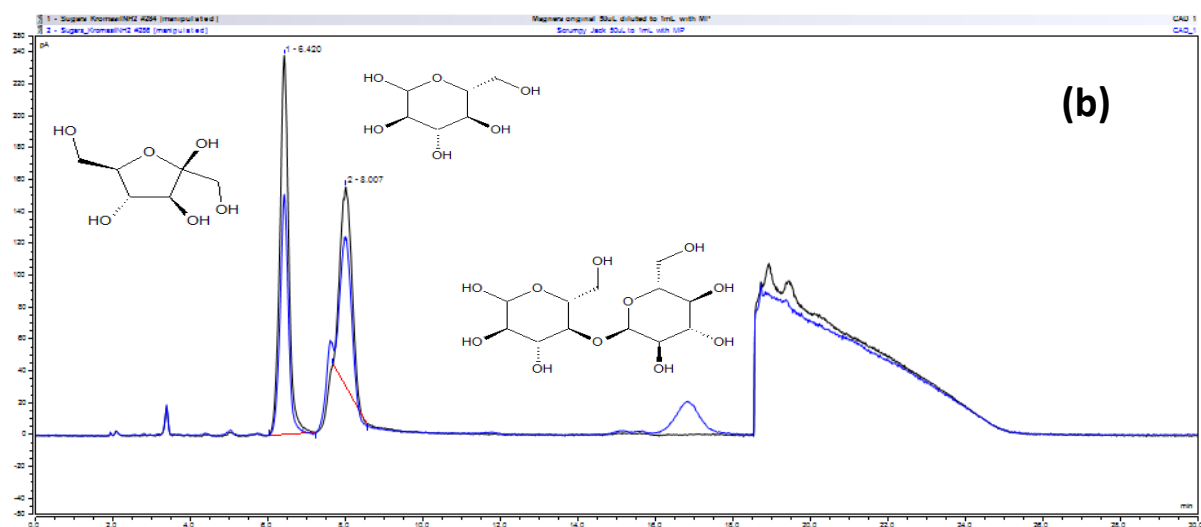
### 3.3 Analysis of Simple Sugars in Beer and Cider

Figure 5.4 shows overlaid chromatograms for calibration standards (Fig. 5.4a) and real samples of ciders (Fig. 5.4b) and beer (Fig. 5.4c), using an Amino column with HILIC mobile phase (Kromasil NH<sub>2</sub>, 4.6 x 150 mm, 5 µm, mobile phase 80% ACN with water) and CAD Ultra detection. Real samples were filtered using a 0.22 µm hydrophobic filter, which was tested for losses with fructose solution. Losses were around 10% which was deemed acceptable for this proof-of-concept study. As expected from other reports (Hutchinson *et al.* 2012), the CAD was able to detect all five sugars used. However peak shape was poor for glucose in the cider samples, therefore reliable quantitation was impossible. Calibration curves were plotted to quantify levels of sugar detected. Over a wide concentration range (50 – 2000 mg / L of the respective sugar), linearity was more poor than over a narrow concentration range (50 – 500 mg / L), which was suggested by Vehovec and Obreza in a review of CAD operation (Vehovec *et al.* 2010). The results are shown in Table 5.1. Ciders contained high levels of simple sugars, 10 mg / mL fructose and at least 7 mg / mL glucose, although further work is necessary to accurately quantify glucose due to peak shape issues. These are however, at approximately typical levels: a previous study by Gomis *et al.* using derivatisation and RPLC with UV detection found ciders contained 6.5 mg/mL fructose and 17 mg/mL glucose (Gomis *et al.* 2001). It is possible that the cider samples were sufficiently acidic that the glucose did not experience a high enough pH for rapid mutarotation. It is possible that addition of extra base to those samples would preclude the peak distortion from occurring. An alternative approach is to use a BEH Amide column and alkaline mobile phase. Whereas the beers contained low levels of simple sugars (1 mg / mL maltose), the CAD detected large peaks during the column wash stage. It is possible these are more-

complex sugars such as maltooligosaccharides which can be present in beer (Nogueira *et al.* 2005), however CAD is a quasi-universal detector (Chapter 4) and use of reference standards is necessary to identify those peaks in the beer matrix. In the context of this project, this proof-of-concept study was not completed, in order to focus on core aims of the project, namely loadability and preparative HILIC (chapter 6), and achieve publication of Chapter 4 findings (Russell *et al.* 2015).



**Fig. 5.4a** Sugar analysis performed using an 'Amino' HPLC column (Kromasil NH2, 4.6 x 150mm, 5 $\mu$ m) calibration using (1) Levogluconan, (2) Fructose, (3) Glucose, (4) Sucrose, (5) Maltose.



**Fig. 5.4 b HILIC separation of sugars in Ciders with Charged Aerosol Detection.**

**(1) Fructose, (2) Glucose, (3) Maltose.**

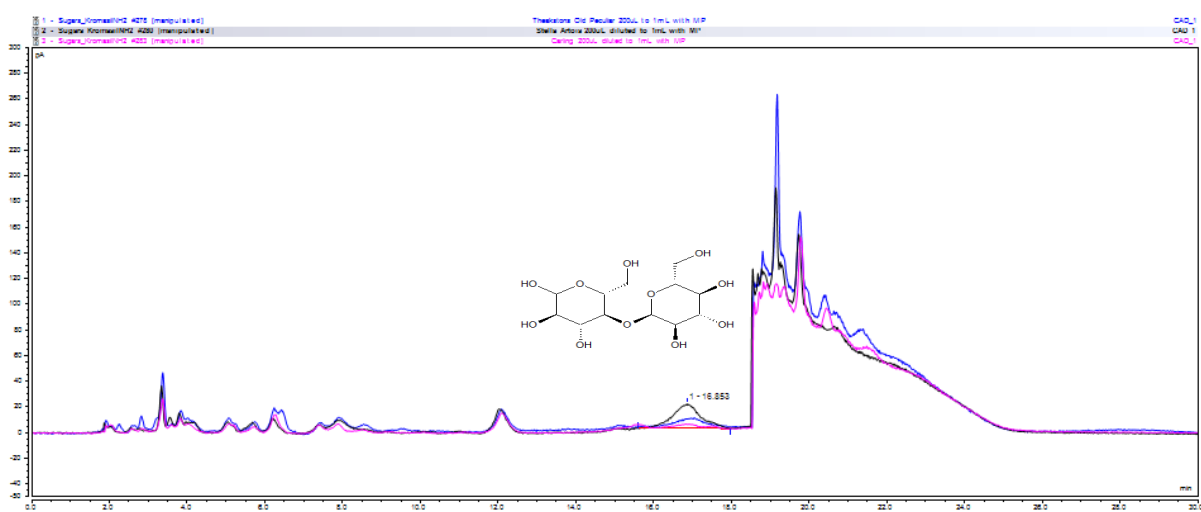


**Fig. 5.4 c HILIC separation of sugars in Beers with Charged Aerosol Detection. (1) Maltose.**



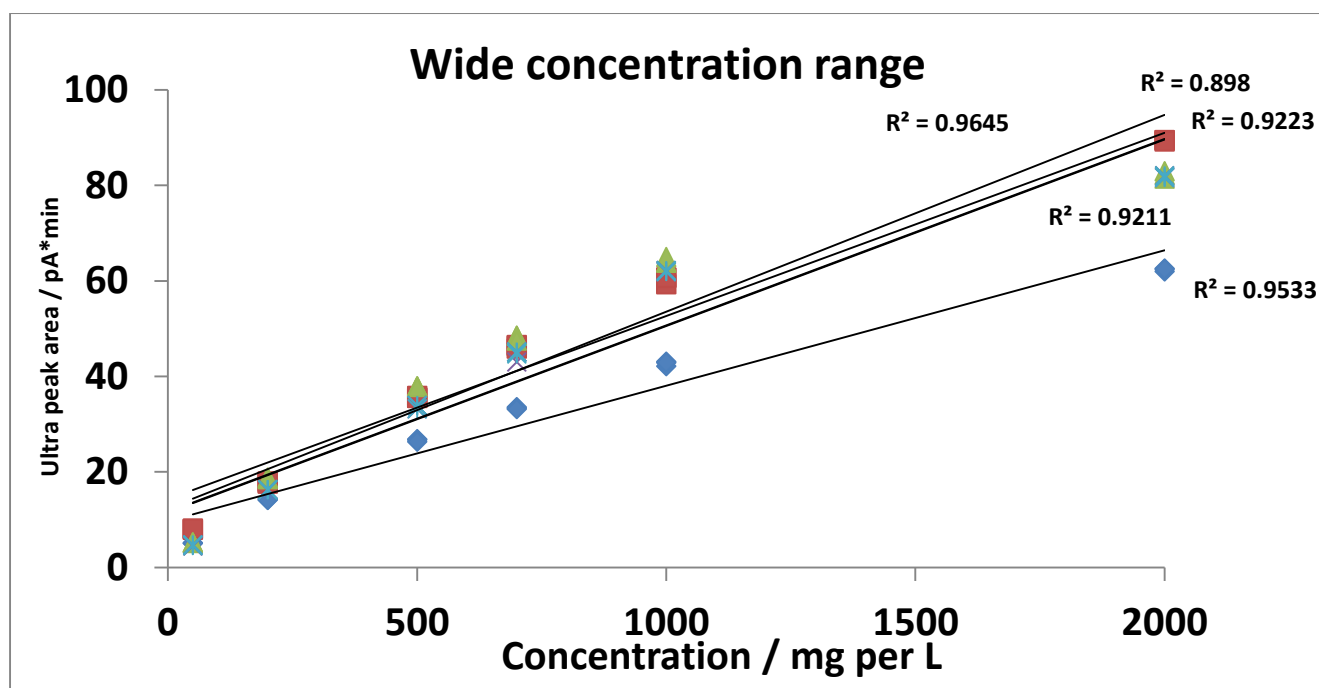


Fig. 5.4 d Calibration curves of five sugars over a wide concentration range (50 – 2000 mg / mL)

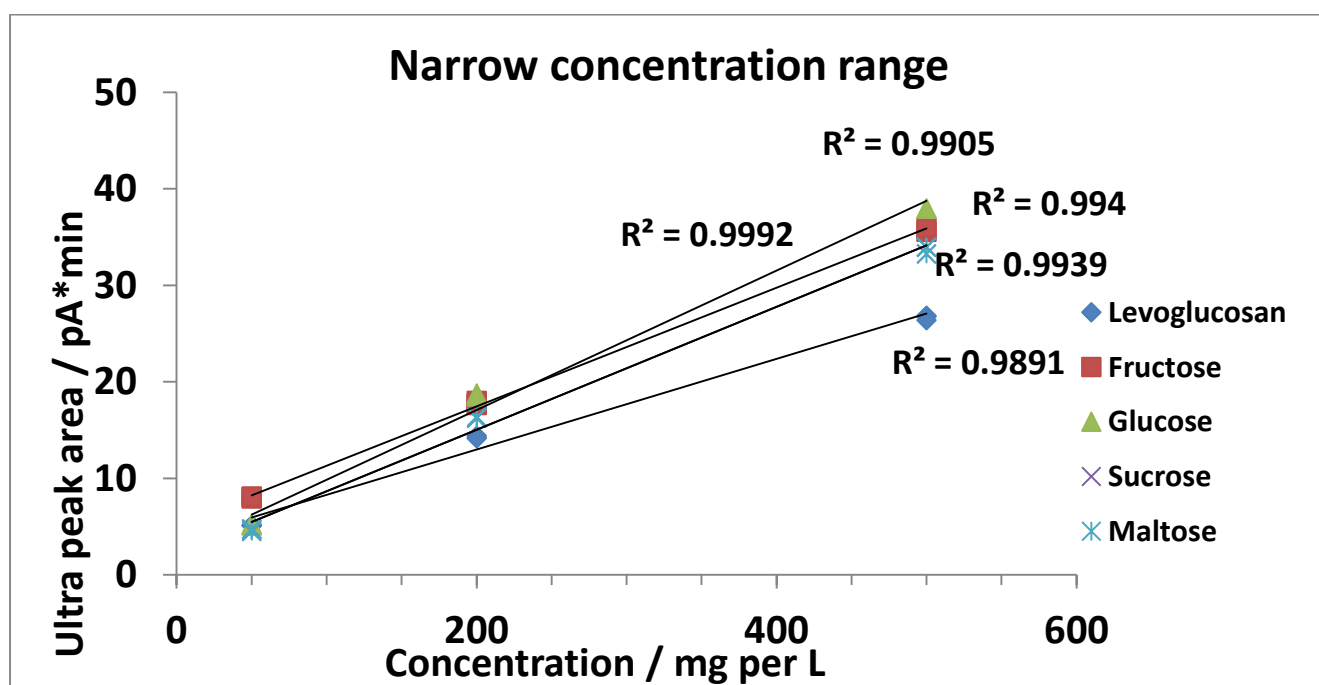


Fig. 5.4 e Calibration curves of five sugars over a narrow concentration range (50 – 500 mg / mL)

**Table 5.1. Sugar concentrations found in ciders and beer**

Sample	Concentration / mg per mL		
	Fructose	Glucose	Maltose
Ciders			
Magner's Original	23	12-30	-
Scrumpy Jack	10	7-22	3.6
Beers			
Theakston's Old Peculiar	-	-	*
Stella Artois	1	-	*
Carling Black Label	-	-	*

\* Peaks detected during column wash possibly complex sugars such as maltooligosaccharides (Nogueira *et al.* 2005)

### 3.4 Analysis of underivitisied Amino Acids

Amino acids are highly hydrophilic, which can be further affected by the functional groups on a particular amino acid side chain. Most underivatised amino acids do not contain strong chromophores for UV detection, therefore these are derivatised with reagents such as o-phthaldialdehyde (OPA) which react with primary amines to produce a product that is

sufficiently hydrophobic to retain by RPLC and able to absorb either fluorescent light (Roth 1971) . Using HILIC, amino acids have been analysed in their phosphorylated form, since the phosphate functionality absorbs UV adequately (Alpert 1990). Since the CAD responds to any non-volatile solute (Chapter 4), and HILIC retains hydrophilic species with good efficiency (Chapter 4), it may be possible to directly separate these by HILIC and detect by CAD. This was attempted using an Atlantis bare silica column (Fig. 5.5) which shows all four amino acids were retained by the column and detected by the CAD. However resolution was poor for the amino acids with neutral side-chains (glycine, glutamine) and peak shape was poor for aspartic acid. It may be possible to successfully separate these and even larger numbers of amino acids by HILIC with further method development, in particular use of a polar-ligand HILIC column such as BEH Amide or ZIC-HILIC which have complementary selectivity to the bare silica column used in Fig. 5.5. Due to time constraints that was not possible within the scope of this project.

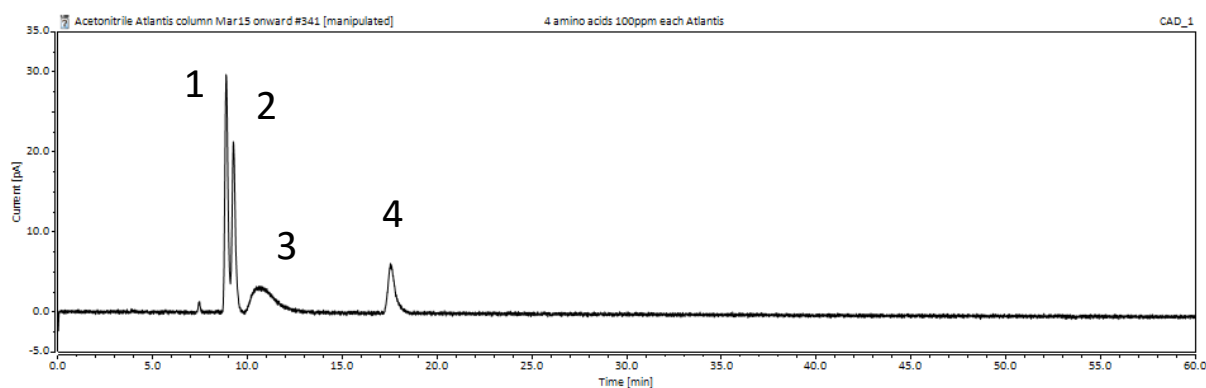


**Fig. 5.5 HILIC chromatogram of four underivatised amino acids: (1) Glycine, (2) Glutamine, (3) Aspartic Acid), (4) Arginine. Atlantis bare silica column (4.6 x 250 mm, 5  $\mu$ m), mobile phase 75% ACN with 5mM AF pH 3 with FA.**



## 4. Conclusions

Some highly hydrophilic solutes that have no chromophore were retained by HILIC and detected by CAD, namely simple sugars and amino acids. Signal quality was poor when a high pH HILIC mobile phase was used with the newer Veo model CAD. Further investigation showed signal quality was relatively poor for the Veo also in salt-buffered HILIC mobile phase. Like for like comparison of the older Ultra and newer Veo models showed the Ultra outperformed the Veo in terms of signal to noise ratio at a modest solute concentration (300 mg / L). Further investigation showed the signal (measured as peak height) was lower for the Veo and noise was higher, which combined made for the superior performance of the Ultra model. These results were fed back to the manufacturer and the industrial partner of this project, and it remains to be seen what the fate will be of the charged aerosol detector in light of reduced performance with this recent model. Levels of simple sugars were measured by CAD with HILIC separations on an Amino column for real samples of beer and cider. The beers had low levels of maltose (1mg / mL), and the ciders high levels of glucose and fructose (>7 and >10 mg / mL, respectively), equivalent to around 0.5 and 10 g per British pint. The current health guidelines advise a recommended limit of 30 g of sugar consumption per day for adults. Similar levels have been previously reported (Gomis *et al.* 2001). Therefore in addition to recommended guidelines for alcohol consumption, these data suggest consumption of excess of 1 pint of sweet cider daily could have health implications for potential chronic conditions such as diabetes. Further work is necessary to clarify this, as the glucose levels studied are only estimates due to issues with glucose peak shape. Some amino acids were successfully retained by HILIC on an Atlantis bare silica column and detected by CAD, however there were issues with peak resolution and shape for one solute. There is scope for serious productivity gains in amino acid analysis through further method development by HILIC-CAD, compared to existing derivatisation methods. Development of generic HILIC methods can simplify this (Chapter 6), and future work integrating generic methods with inverse gradients to compensate for the sensitivity of CAD to mobile phase organic solvent content (Gorecki *et al.* 2006).

## **Chapter 6**

# **Some pragmatic methods to purify polar pharmaceuticals for fragment-based drug discovery**

## Abstract

Some approaches to separate hydrophilic 'building block' compounds in analysis and purification by HPLC, useful for fragment-based drug discovery were investigated. Eight probe compounds were used including two weak base structural isomers, two zwitterions, two additional weak bases, a hydrophilic strong base and a hydrophilic neutral solute. Low pH RPLC was ineffective with no resolution of these compounds, and high pH separated just three out of the eight solutes. Hydrophilic interaction chromatography (HILIC) was instead considered. Substituting acetone for the more-common acetonitrile as mobile phase organic modifier, retention orthogonality was not found, with good agreement between  $k$  vs.  $k'$  plots for the same column (Atlantis) and 29 diverse probe solutes. Retention was lower in acetone than acetonitrile, perhaps due to acetone's stronger hydrogen-bonding basicity disrupting the HILIC water layer. Generic and focused HILIC methods were developed which separated all eight probe compounds on Atlantis and BEH Amide columns, with alternate retention order as expected from HILIC column comparison studies. Transferring these methods to preparative systems successfully separated simulated crudes on both columns. Productivity was usable on both columns, and moving to an At-Column-Dilution (ACD) system, up to 223 mg of crude purified per hour, due to the large injection volumes an ACD system can deliver (4mL cf. 1mL standard prep). Diluents were considered, as low solubility can limit prep loading. DMSO had good apparent solubility, and addition of small quantities of TFA (1%) improved this further (15 and 22 mg / mL possible, respectively). However DMSO was incompatible with HILIC-Prep-ACD. Removing the DMSO and adding TFA (1%) to HILIC mobile phase as diluent was successful in terms of apparent solubility and chromatographic performance. Overall, HILIC was a viable technique for analysis and purification of 'building block' solutes and is anticipated to be complementary to other techniques (e.g. supercritical fluid chromatography, SFC).

# 1. Introduction

Fragment-based drug discovery requires analysis and purification of small molecules as potential new drugs. These can be hydrophilic, and weakly basic or zwitterionic chemical functional groups provide potential biological activity and capacity for formation of C-X bonds in further synthesis (Scott *et al.* 2012). Hydrophilic species retain poorly in RPLC, and sample overload is severe for ionogenic solutes in RPLC, many of which are hydrophilic (McCalley 2010b, Gritti *et al.* 2015). Both these problems can be overcome for strongly basic drug molecules (e.g. nortriptyline), as these can be retained by high-pH RPLC by neutralising the solute and promote hydrophobic retention on octadecylsilane (ODS) stationary phases (Davies *et al.* 2008). Retention and loadability of hydrophilic neutral solutes and zwitterions cannot be satiated by high pH RPLC approaches as they remain hydrophilic at high pH and retain poorly. Hydrophilic interaction chromatography (HILIC) (Alpert 1990) is an attractive solution to that. HILIC retention mechanisms are complex (McCalley 2010b, Hemstrom 2006) and have received intense focus in recent studies (Kawachi *et al.* 2011, Dinh *et al.* 2011, Kumar *et al.* 2013, Heaton *et al.* 2014c, Gritti *et al.* 2013c). The exact mechanism depends on which solute, column and mobile phase pH are used (Kumar *et al.* 2013), and in a broad sense hydrophilic species retain by a mixture of partition, ion-exchange and hydrogen-bonding interactions (Kawachi *et al.* 2011, Dinh *et al.* 2011, Kumar *et al.* 2013). Purification is a necessary application of HILIC, however studies of this are scarce in the scientific literature. Purification by HPLC commonly employs sample loads far above the column capacity, and separation performance is degraded as a result of shifts in retention and broad peaks with low efficiency. McCalley reported in 2007 that bare silica HILIC column(s) have loading capacity around ten times higher than RPLC for bases (McCalley 2007), which are particularly problematic in RPLC (McCalley 2010a). Gritti and Guichon studied the overloading of strong bases propranolol and amitriptyline hydrochloride using a bridged ethylene hybrid (BEH) silica in HILIC, reporting similar improvements over RPLC and even a CSH-C18 RPLC column which contained positive charges to control solute repulsion, which is thought to be responsible for the tailing overload of charged bases even at low solute concentration on RPLC (Gritti *et al.* 2015). Bonded phase columns are available with diverse chemistries in HILIC, which provide substantial changes in selectivity (Kawachi *et al.* 2011, McCalley 2013, 2014, Dinh *et al.* 2011). However as far as can be determined, none of



these columns have featured in HILIC purification or loadability studies. The principle interest of this project is the analysis and purification of hydrophilic pharmaceuticals and polar “building block” molecules. The present study evaluates HILIC in a generic method setup. However a basic understanding of solubility in HILIC has not been established in the literature. One study by Ruta *et al.* reported the water content of diluents used in sample preparation must be kept to a minimum for HILIC separations (Ruta *et al.* 2010) and alternative solvents may be possible diluents for HILIC (Ruta *et al.* 2010). More recently Heaton and McCalley also reported efficiency losses at high diluent water content, using UPLC columns (Heaton *et al.* 2016). Further work in this area is crucial if HILIC can be employed to purify polar solutes on the scale (e.g. in excess of 100 mg on-column) required by the pharmaceutical industry.

## 2. Theory

### 2.1 Loadability

Loadability indicates preparative performance, as purifications are done under conditions of mass overload, where large samples are loaded onto the column to purify crudes productively. Loadability studies are typically performed on analytical scale columns and can inform choices of stationary phase chemistry for scale-up preparative studies. Loadability can be empirically measured as  $\omega_{0.5}$  (sample load in mg, at which the column efficiency is reduced by half) as established by Snyder as a robust method to compare loading performance in terms of peak efficiency (Snyder *et al.* 1987). As a rule of thumb, loadability for neutral solutes in RPLC is proportional to approximately 0.4 times the surface area of stationary phase (Eble *et al.* 1987, Dai *et al.* 2009). Loadability of bases has attracted the majority of research focus (McCalley 2007, Gritti *et al.* 2015) and acids also (Hägglund *et al.* 1997). Loadability has been measured by McCalley on a bare silica column in HILIC for the bases procainamide and nortriptyline (McCalley 2007); loadability was superior in HILIC by an order of magnitude (10  $\mu$ g HILIC; 1  $\mu$ g RPLC). Adsorption of solutes to the stationary phase is a mixture of linear, Langmuirian processes and kinetic contributions at higher sample loads (Gritti *et al.* 2015). At low loads, kinetic processes dominate and peaks are

Gaussian, at higher loads thermodynamic contributions contribute and peak shape is distorted. The underlying cause of kinetic processes for charged solutes, described by Hägglund and Stahlberg for strong acid solutes (Hägglund *et al.* 1997), has been scrutinised extensively by Guiochon and Gritti using frontal analysis (Gritti *et al.* 2009, 2009) and McCalley and co-workers using mass overload (McCalley 2007, 2008a, 2010b, 2012). Two principle theories explain this, that a small number of high-energy adsorption sites with slow kinetics which have limited loading capacity (Gritti *et al.* 2004), or mutual repulsion of ionic solutes (Hägglund *et al.* 1997) distorts the solute plug. A recent paper by Guiochon and Gritti on mass transfer in HILIC concluded that long-range eddy dispersion persists in HILIC compared to RPLC (Gritti *et al.* 2013c), possibly due to slow movement of solutes through the relatively viscous water layer inside the stationary phase pores (Gritti *et al.* 2013c). This is possibly due to the resistance to solid-liquid mass transfer caused by the relatively high microviscosity of the water layer (Gritti *et al.* 2013c, Heaton *et al.* 2014c), and for some solutes possibly multi-point hydrogen-bonding with the stationary phase silanols (Heaton *et al.* 2014c). In theory, extrapolation of analytical-level loadability to preparative separations is possible and this can inform a choice of suitable stationary phase for preparative separations. However, mass overload is just one component of the challenge in scaling-up separations to preparative separations. In practise loadability is not seen as sufficient proof that a separation can be useful in purification. Injection volumes can be scaled from analytical to preparative columns according to the ratio of the squares of the column diameters, but in practise this allows for highly limited preparative loads (e.g. acceptable efficiencies on 4.6mm i.d. columns require injections no larger than around 16  $\mu\text{L}$  (Dolan 2014), which scale to  $441 / 21 \times 16 = 336 \mu\text{L}$ ). For a typical sample at 10 mg / mL, this corresponds to 3.36  $\mu\text{g}$  per injection, which is unacceptable in terms of productivity (see 2.4). Although loading studies using analytical columns can be used to troubleshoot problems of poor peak shape and demonstrate clear benefits of HILIC, these benefits have not been sufficiently demonstrated on preparative systems. There is therefore demand for an empirical study to apply HILIC in an industrial setting on preparative systems with wider-bore columns to assess the viability of HILIC purifications.

## 2.2 Peak shape

In RPLC, strong bases overload in a so-called 'sharks tail' peak shape (for examples and thorough discussion on the challenges of HPLC separations of basic compounds the reader is directed to this review (McCalley 2010a)). A HILIC study of overload using partially-porous bare silica particles reported fronting for the hydrophilic strong base procainamide and some tailing for the hydrophobic base nortriptyline (McCalley 2008a). A comparison of RPLC on C18 and HILIC on bare silica reported excellent peak shape in the latter, provided buffer or trifluoroacetic acid (TFA) was used in the mobile phase (McCalley 2007). The detailed study of peak shape in HILIC (chapter 3) found efficiency and asymmetry is excellent for neutrals, acids and bases for all HILIC columns studied, again provided buffered mobile phase was used. However peak shape in preparative HILIC separations has not been sufficiently characterised and this was a consideration of this study.

## 2.3 Solubility

Although on-column loadability is important in preparative separations, solubility is also an important problem. Analytical separations can be scaled-up using wide bore columns, theoretically with no change in separation performance. The larger injection volumes obviously result in larger loads of compound deposited on-column, but if sample solubility is not properly addressed, very large volumes or multiple injections are necessary, which is inefficient and time-consuming (Forssén *et al.* 2014).

$$\log S_{\text{mix}} = \log S_{\text{W}} + (s \log K_{\text{OW}} + t)f_{\text{c}} \quad (6.1)$$

To preclude laborious trial-and-error experiments, the equation of Yalkowsky and co-workers can estimate the solubility of a compound in a given solvent, and those authors determined that solubility in a water-cosolvent system is proportional to the log of solute partition coefficient ( $\log K_{\text{OW}} = \log P$ ) when the solute is in the neutral form (Millard *et al.* 2002) (equation 6.1).  $S_{\text{mix}}$  and  $S_{\text{W}}$  are the total solubilities of the cosolvent system and in water, respectively.  $s$  and  $t$  are the cosolvent constants that are solute independent, and are linear regression terms for slope and intercept, respectively;  $f_{\text{c}}$  is the volume fraction of

the cosolvent in the aqueous mixture. This is useful in pharmaceutical formulation development and also RPLC, where in both cases the primary solvent is water with a small concentration of organic modifier used to aid solubility. Equation 6.1 is an excellent predictor of solubility in the case of rather hydrophobic solutes in highly aqueous diluents. However HILIC mobile phase is somewhat different to these systems, typically comprised of less than 30% water content, and the solute is hydrophilic. Additionally, it is preferable for solutes to be in their ionised form in HILIC, since in this state they are more hydrophilic and able to retain on these columns, therefore equation 6.1 can be useful for neutral solutes. Although the use of water in sample diluents ought to aid solubility, this can be detrimental to peak shape (Ruta *et al.* 2010, Heaton *et al.* 2016) and should be kept to a minimum. Those authors suggested alternative solvents such as DMSO or IPA can be explored to achieve appreciable solubility when preparing samples for HILIC analysis. In this study, solubility is termed ‘apparent solubility’, simply described by Alsenz and Kansy as ‘the amount of a substance that dissolves in a given volume of solvent at a specified temperature’ (Alsenz *et al.* 2007). Here the apparent solubility is used to describe dissolving the sample in the minimum possible volume of solvent. In this study, solute concentrations are typically quoted in mg per mL, as this reflects the current practise in the field.

## 2.4 Productivity

In preparative chromatography, the objective is production of pure compound using minimal resources within a reasonable time frame. This can be measured as productivity (equation 6.2).

$$P_{R,i} = \frac{n_{\text{coll}}}{t_c V_{\text{col}}} \quad (6.2)$$

Fornstedt’s group showed the amount collected ( $n_{\text{coll}}$ ), divided by the product of the cycle time ( $t_c$ ) and column volume ( $V_{\text{col}}$ ) can be used as an indicator of productivity ( $P_{R,i}$ ) (Forssén *et al.* 2014), (6.2). In a generic setup, cycle time ( $t_c$ ) and column volumes ( $V_{\text{col}}$ ) are kept constant, and the amount collected is directly proportional to the mass of crude purified in a cycle. Therefore a simple relationship can be measured according to equation 6.3, whereby productivity ( $P_R$ ) is measured as mass purified ( $m_{\text{purif}}$ ) per unit time ( $t$ ), in mg / hr. This can

be used as a simple means to quantify the usefulness of purification, provided chromatograms can qualify sufficient purity has been achieved.

$$P_R \propto \frac{m_{\text{purif}}}{t} \quad (6.3)$$

## 3. Experimental

### 3.1 Chemicals and reagents

Probe compounds were purchased from Sigma Aldrich (Poole, UK). Eight solutes including strong and weak bases, neutrals and zwitterions were used develop generic analytical and preparative methods (Table 6.1). These were chosen from the Sigma ‘building block’ catalogue according to the following criteria: a Log D vs. pH plot suggesting hydrophilic behaviour unlikely to be made hydrophobic by use of low or high pH modifier, and acceptable price of ordering small quantities (1-25 g for under around £100). For ease of reference, the five compounds with no obvious trivial name have been arbitrarily assigned four letter acronyms, described in Table 6.1 (e.g. 2-Aminopyridine-3-carboxylic acid was referred to as ‘APCA’). Additionally procainamide hydrochloride and cytidine were chosen as strongly-retained markers for the Atlantis and BEH Amide columns respectively, based on their behaviour in an earlier HILIC study on these column chemistries (Kumar *et al.* 2013). A diverse set of 29 solutes including acids, bases and neutrals was used to compare retention orthogonality of acetone and acetonitrile as mobile phase modifiers, as used in Chapter 4.

**Table 6.1. Probe solutes used in generic and scale-up studies**

Solute	Structure	Log D vs. pH plot (chemicalize)
2-Aminopyridine-3-carboxylic acid (APCA)		
Adenine		
2-Amino-3-hydroxypyridine (AHPY)		
2-Aminopyridin-4-ol (APOL)		
Procainamide Hydrochloride		
Cytidine		
6-Aminoindazole (AIAZ)		
2,5-Diaminobenzenesulfonic acid (DABS)		

## 3.2 Apparatus and methodology

A Thermo U3000 system was used in initial diluent experiments, with quaternary pump, diode array detection (DAD) and either a Corona Ultra or Corona Veo CAD, with Chromeleon 7.2 software. The CAD is a destructive detector, therefore the DAD and CAD detectors were connected in series, with flow first through the DAD. 0.13 mm ID Viper tubing (Thermo, Munich, Germany) was used to minimise system dead volume.

An Agilent 1100 system (Agilent, Waldbronn, Germany) was used to prepare generic and focused gradient analytical methods, with a binary pump and DAD for detection, with Chemstation software. Columns were used at ambient temperature.

A bespoke Waters Purification system was used in preparative separations using a 2525 inlet pump, 2767 Sample Manager with in-built injection system and post-fraction UV detection, custom-made timing loops connecting the injection system to the Waters QDa Mass Spectrometer and Waters 2996 DAD for detection. A Waters 515 pump was used as make-up flow to the MS. Masslynx software controlled the preparative system, with the fraction trigger set to discard all eluates to waste in this proof-of-concept study. A second bespoke Waters Purification system was used with At-Column Dilution installed, with 2 x 2525 inlet pumps such that the one delivered the sample and the second made up flow with mobile phase.

An Atlantis bare silica column (150 × 4.6 mm ID, particle size = 3 µm, Waters) and an ethylene bridged hybrid (BEH) amide column (150 × 4.6 mm, particle size = 3.5 µm, Waters, Milford, USA) were used for analytical methods. Columns with wider-bore (21 mm prep, 4.6 mm i.d. analytical) but identical stationary phase chemistry and identical length were used in preparative separations, from the same manufacturer (Waters, Milford, USA).

The mobile phase was ACN-5 mM ammonium formate buffer unless otherwise stated. The pH meter was calibrated in aqueous buffers and formic acid was used to adjust the aqueous portion to  $w^w$  pH 3. Thus the strongly-eluting mobile phase was a solution of 70% v/v acetonitrile; 30% v/v pH3, 16.7mM aqueous ammonium formate (pH adjusted with formic acid) and the weakly-eluting mobile phase 95% v/v acetonitrile; 5% v/v pH3, 16.7mM aqueous ammonium formate (pH adjusted with formic acid).



Analytical samples were prepared as 0.5 mg /mL combined standards in 50-50 Acetonitrile-water with 0.1% formic acid (v/v) unless otherwise stated. Alternative diluents were investigated at higher concentrations, including DMSO, DMF-DMSO, DMSO with TFA (1%) and mobile phase taken from the weakly-eluting mobile phase reservoir then TFA added (1%). Note: TFA was not added into the mobile phase, as this can result in exclusion of bases in HILIC (McCalley 2015). Sample solubility was assessed as the weighed amount dissolved in the minimal quantity of the appropriate solvent, termed apparent solubility as per Alsenz and Kansy (Alsenz et al. 2007).

## **4. Results and discussion**

### **4.1 Choosing separation conditions with alternate selectivity**

#### **4.1.1 Changing the selectivity using the organic solvent**

It has been reported that there are selectivity differences between acetone and acetonitrile mobile phases in HILIC (Heaton *et al.* 2011), which is beneficial for developing methods with alternative selectivity. However this has not been studied with a sufficiently broad range of solutes. Figure 6.2a shows the retention of 29 probe solutes using acetonitrile or acetone as organic modifier, using the 85% organic solvent and identical buffer preparation in both methods. Correlating retention in different conditions has been used to find alternate selectivity in HILIC methods (Kumar *et al.* 2013) and comparing columns (Heaton *et al.* 2014b). The correlation coefficient (R) was calculated between retention factor in acetone and retention factor in ACN. This was  $R=0.93$  which is much higher than expected. This which suggests that alternate selectivity can be shown for some solutes (Heaton *et al.* 2011) but is not observed for a broad range of solutes. Figure 6.1b compares the magnitude of retention between Acetonitrile and Acetone for neutrals and weak bases; Fig 6.1c for acids. For some weak bases (e.g. cytosine) and neutrals (e.g. uridine), retention was around half in acetone (Fig 6.1b); retention factors for all acids were zero or the acids eluted before the void (Fig 6.1c). The much lower retention of neutral and weak bases which contain large numbers of hydrogen-bonding groups is interesting (Table 6.1). There was good correlation

between the number of hydrogen bonding groups per solute and retention factor ratio (ACN/Acetone) ( $R^2 = 0.86$ , see Fig. 6.1d). It is possible that hydrogen-bonding capability of acetone is greater than that of acetonitrile. The so-called  $\beta$  term which represents hydrogen-bond basicity is 0.38 for acetone, compared to 0.25 for acetonitrile (Snyder *et al.* 2010). It is possible that solutes with hydrogen-bonding character interact favourably with acetone and reduce the hydrophilicity of these solutes. In HILIC, a fine layer of water is held to the stationary phase (Alpert 1990, McCalley *et al.* 2008b). In acetonitrile, there are relatively weak interactions between solute and solvent and it is possible that the solutes can displace water from the stationary phase surface. In acetone, however, solutes with hydrogen-bonding character are associated with the relatively hydrophobic solvent molecules and it is possible these are less able to displace water from the stationary phase, thus retention is lower in acetone rather than acetonitrile mobile phase. Alternatively, as described above, acetone has stronger hydrogen-bond basicity than acetonitrile and it is conceivable that it hydrogen bonds with water, which is present both in the HILIC mobile phase and forms the water layer on the stationary phase. Acids should retain only by partition into the water layer on this silica column, due to negatively-charged silanols not offering ion-exchange to these solutes. However the absence of retention of acids in acetone mobile phase suggests they are unable to partition by a HILIC-like mechanism. It is possible that acetone scavenges water from the mobile phase through hydrogen-bonding and even possibly the water layer itself, thus reducing retention of hydrogen-bond rich solutes and eliminating retention of acids. It was considered possible that there may be some difference between the hydroorganic pH between the two solvents, which can affect retention for ionogenic solutes. Using a pH meter calibrated in aqueous solvent, the  $w^S$  pH was measured as 0.4 units lower in the acetone mobile phase compared to the acetonitrile mobile phase. This was considered a small variation, which in any case would not account for the reduction in retention for neutral solutes in acetone. Nevertheless acetone mobile phase can perhaps be useful for excessively-retained solutes which are strongly hydrophilic. However in a pragmatic approach, acetone does not offer alternate selectivity compared to acetonitrile and was not used for generic polar methods. Alternatively, stationary phases with alternate selectivity were investigated (see below).

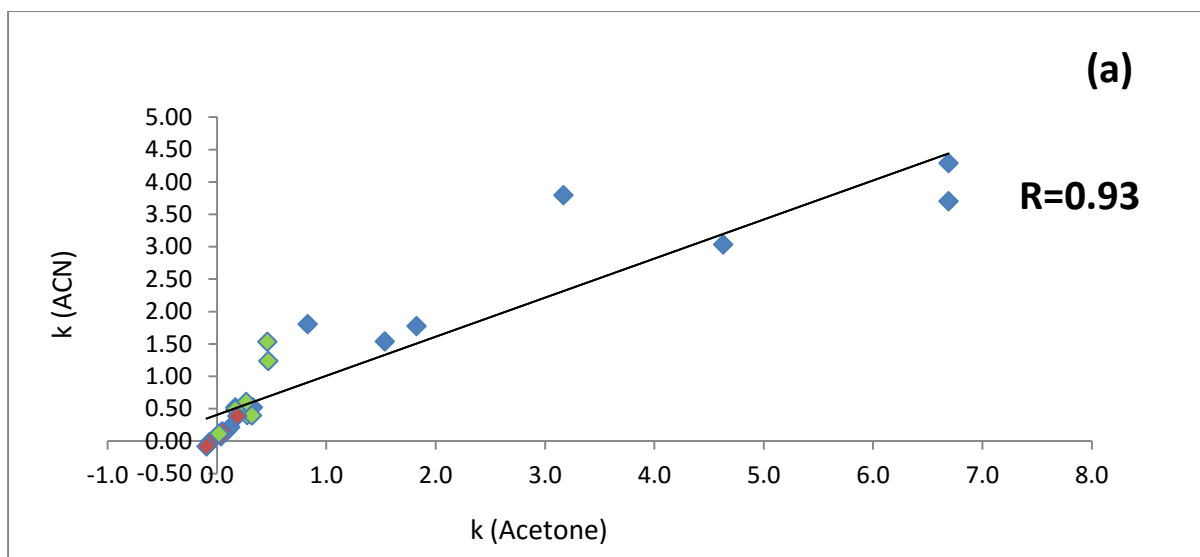


**Fig. 6.1a.**  $k$  (Acetonitrile) vs.  $k$ (Acetone); Atlantis (4.6x250mm, 5 $\mu$ m). Mobile phase 85% organic solvent with 5mM ammonium formate  $w^w$  pH 3 with FA

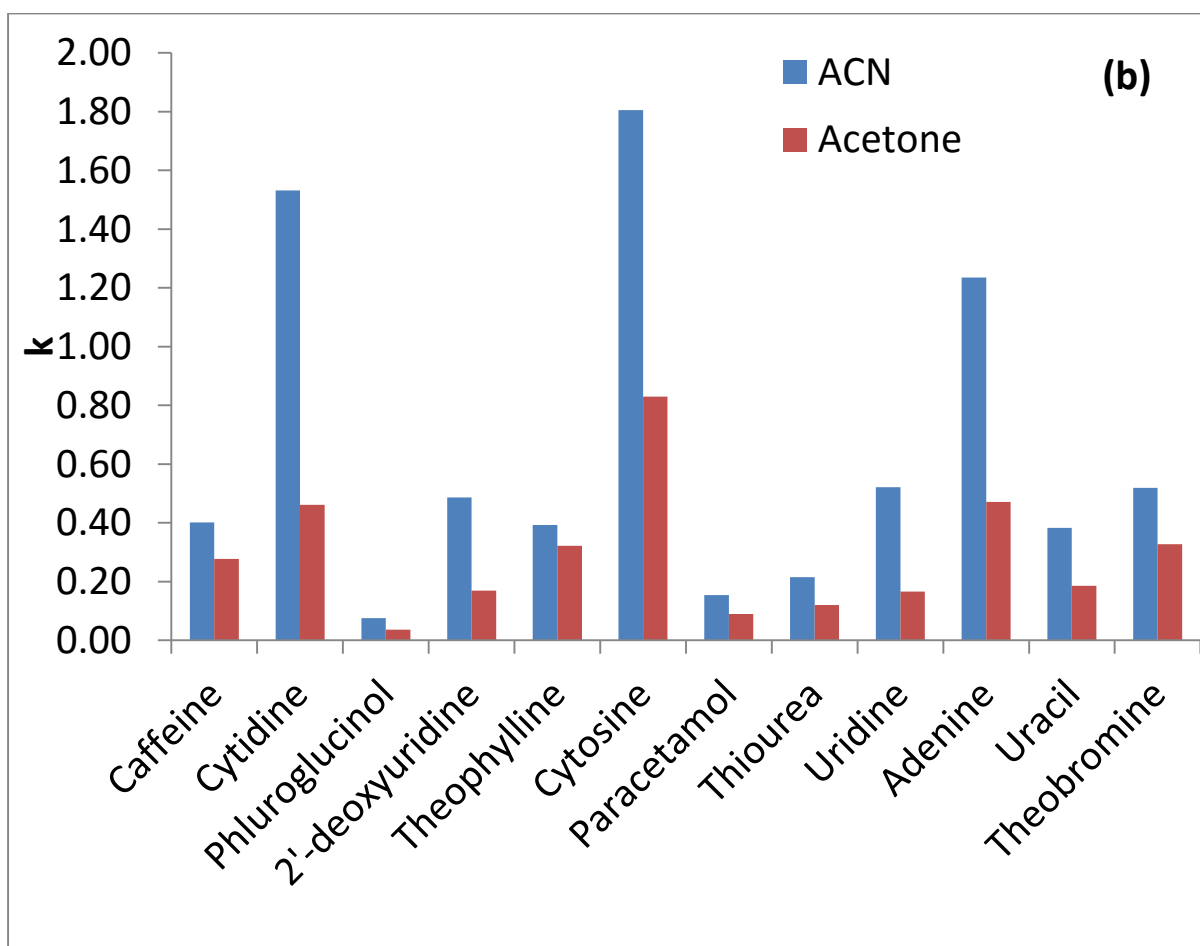


**Fig. 6.1b.** Retention of neutrals and weak bases; Atlantis (4.6x250mm, 5 $\mu$ m). Mobile phase 85% organic solvent with 5mM ammonium formate  $w^w$  pH 3 with FA

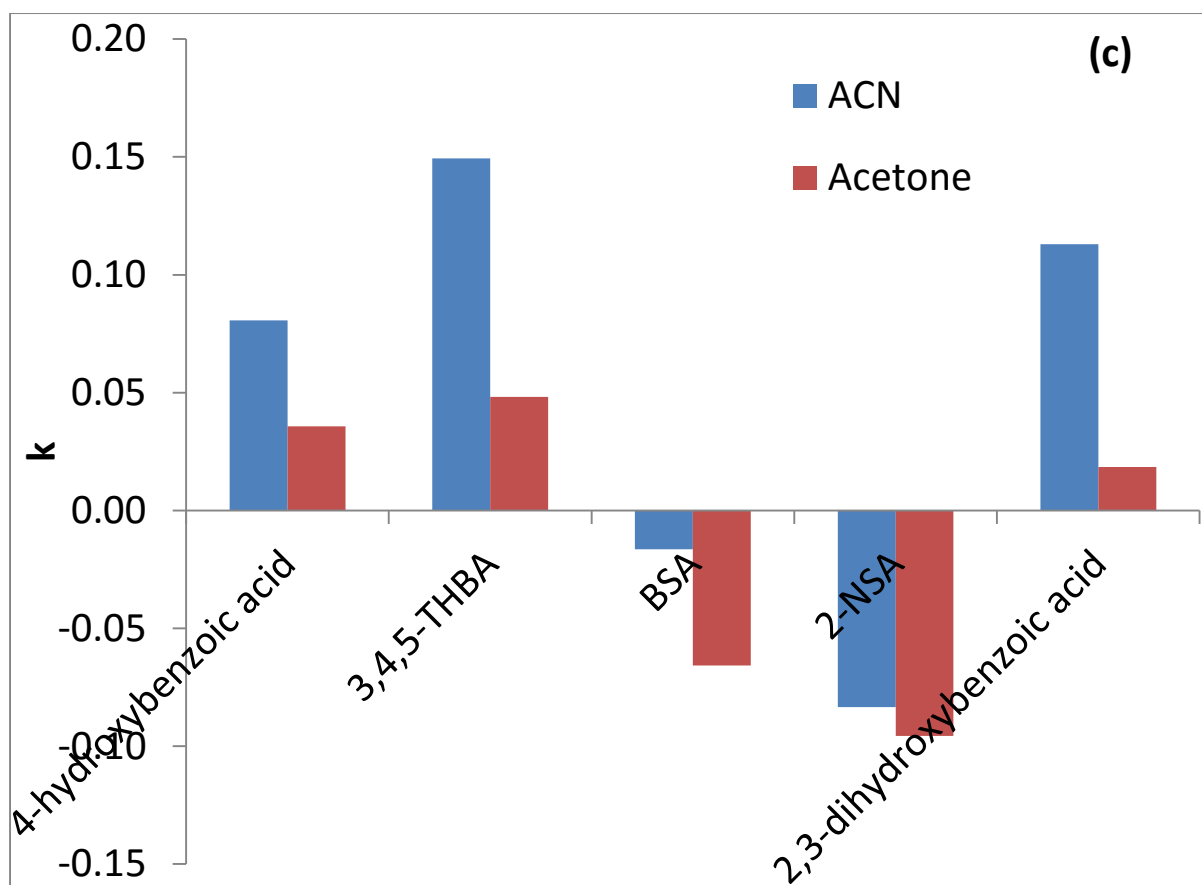


Fig. 6.1c. Retention of acids; Atlantis (4.6x250mm, 5 $\mu$ m). Mobile phase 85% organic solvent with 5mM ammonium formate  $w^w$  pH 3 with FA

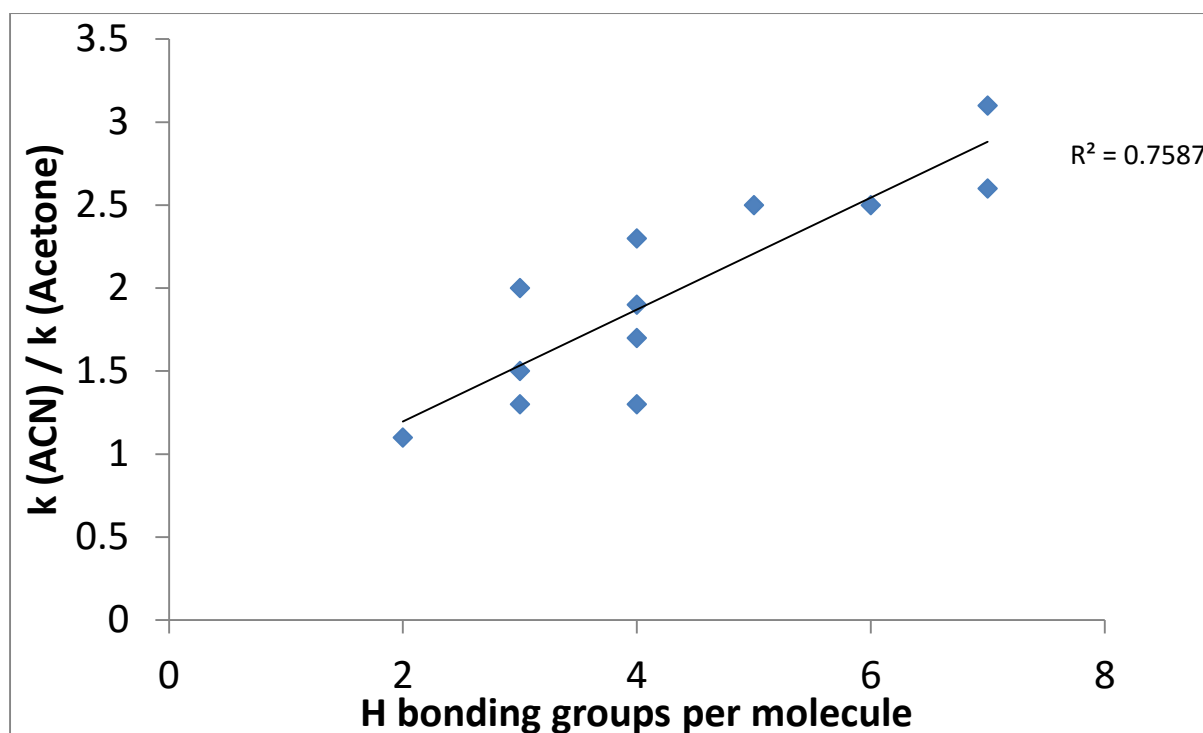


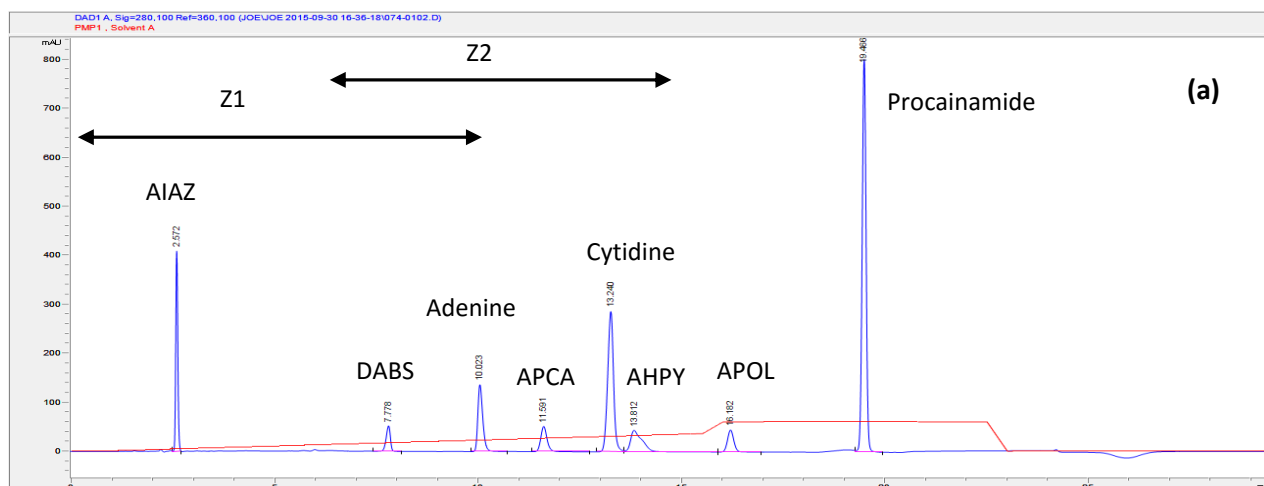
Fig. 6.1d. Relationship between retention ratio in ACN vs. Acetone and number of hydrogen bonding groups per molecule

Figure 6.1. (a)  $k(\text{Acetonitrile})$  vs.  $k(\text{Acetone})$ ; Atlantis (4.6x250mm, 5 $\mu\text{m}$ ); (b) Retention of neutrals and weak bases; (c) retention of acids. 85% Acetonitrile or Acetone with 5mM Ammonium Formate pH3, LCMS grade buffers; (d) relationship between retention ratio in ACN vs. Acetone and number of hydrogen bonding groups per molecule.

#### 4.1.2 Changing the selectivity by changing the stationary phase in generic HILIC methods

Bare silica and BEH Amide stationary phases were used, since these have been reported to have alternate selectivity with respect to each other (Kumar *et al.* 2013). Generic gradient methods were developed for each column. The generic gradient methods started with a brief (30s) isocratic hold at 100% solvent 'B' (95% ACN with 5mM ammonium formate  $w^w$  pH 3 with FA) to provide retention for the early-eluting solutes, then solutes were eluted by increasing the mobile phase water content using a gradient increase of solvent 'A' (70% ACN with 5mM ammonium formate  $w^w$  pH 3 with FA). Thus for the Atlantis column (4.6 x 150mm, 3  $\mu\text{m}$ ) the generic gradient method was 0% solvent 'A' isocratic hold for 30s, gradient to 36% solvent 'A' over 15 min, wash at 60% 'A' in 30s held for 6.5 min, gradient

reset to 0% 'A' in 30s then equilibration held for 6.5 min to give a 29.5 min method. For the BEH Amide column (4.6 x 150mm, 3  $\mu$ m), the generic gradient method was an isocratic hold for 30s, gradient to 24% solvent 'A' in 15.5 min, held for 6.5 min then gradient reset in 30s to 0% 'A' and equilibration held for 6.5 min, to give also give a 29.5 min method. Shorter equilibration and wash stages were attempted but the retention times were irreproducible (data not shown). Fig. 6.3a and 6.3d show generic HILIC gradient methods separating all eight solutes on both columns. There was alternate retention order between the Atlantis (Fig. 6.3a) and BEH Amide (6.3d) columns. These data therefore suggested the columns were indeed suitable for inclusion in a polar 'tool-box'. However for both columns there was a somewhat narrow elution window for most solutes within the centre of the gradient (Fig. 6.3a,d). Therefore to improve upon the separation between solutes that eluted in the start or middle of the gradient, focused methods were developed which expand designated areas of the gradient and were expected to improve separation (see 4.1.3). Fig. 6.3 b-c and e-f show focused isocratic methods on the Atlantis and BEH Amide column respectively, which are discussed below in 4.1.3.



**Fig. 6.2a.** Separation of eight probe solutes using a generic gradient method on the Atlantis column (4.6 x 150mm, 3  $\mu$ m). Solvent 'A' = 70% ACN with 5mM Ammonium Formate  $w^w$  pH 3 with formic acid; 'B' = 95% ACN with 5mM Ammonium Formate  $w^w$  pH 3 with formic acid. 0% solvent 'A' 30s isocratic hold, then 0-36% 'A' in 15 min, wash at 60% 'A' in 30s held for 6.5 min, gradient reset in 30s to 0% 'A' then equilibration held for 6.5 min to give 29.5 min method. Probe solutes 6-Aminoindazole (AIAZ), 2,5-Diaminobenzenesulfonic acid (DABS), Adenine, 2-Aminopyridine-3-carboxylic acid (APCA), Cytidine, 2-Amino-3-hydroxypyridine (AHPY), 2-Aminopyridin-4-ol (APOL), Procainamide Hydrochloride. Full structures shown in Table 6.1 above.

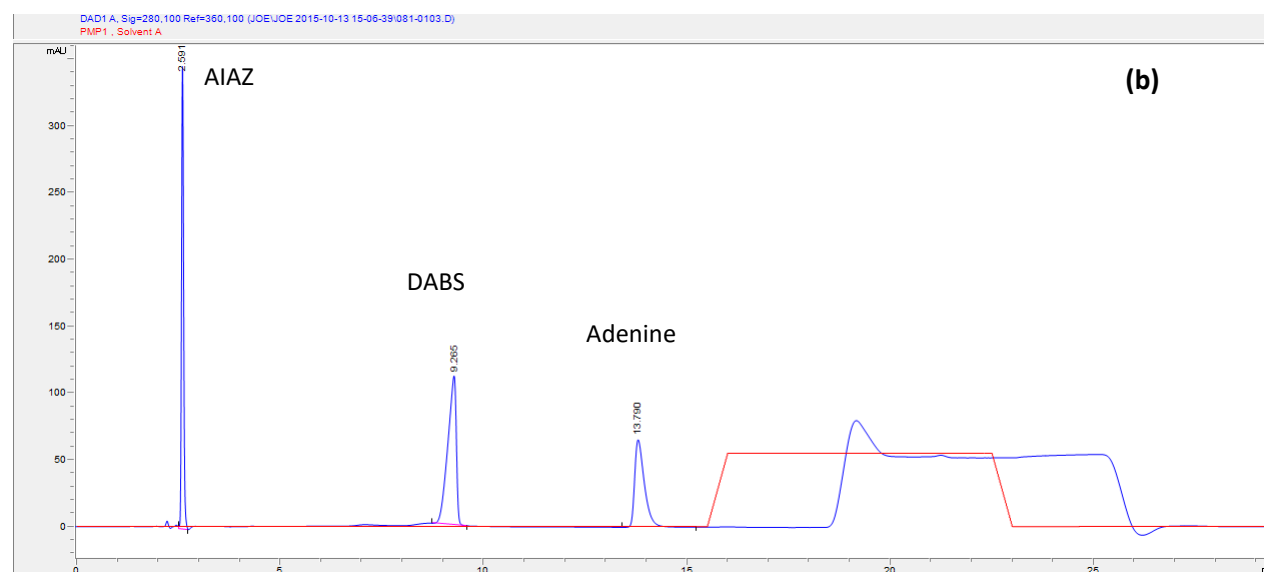


**Fig. 6.2b** Separation of three probe solutes, Atlantis column elution 'Zone 1' (zone, column and solvents as per Fig. 6.2a) using a focused isocratic method. Method 0% solvent 'A' hold for 15.5 min then wash at 60% 'A' in 30s held for 6.5 min, gradient reset to 0% 'A' in 30s then held for 6.5 min to give 29.5 min method. For solute descriptions see Fig. 6.2a.

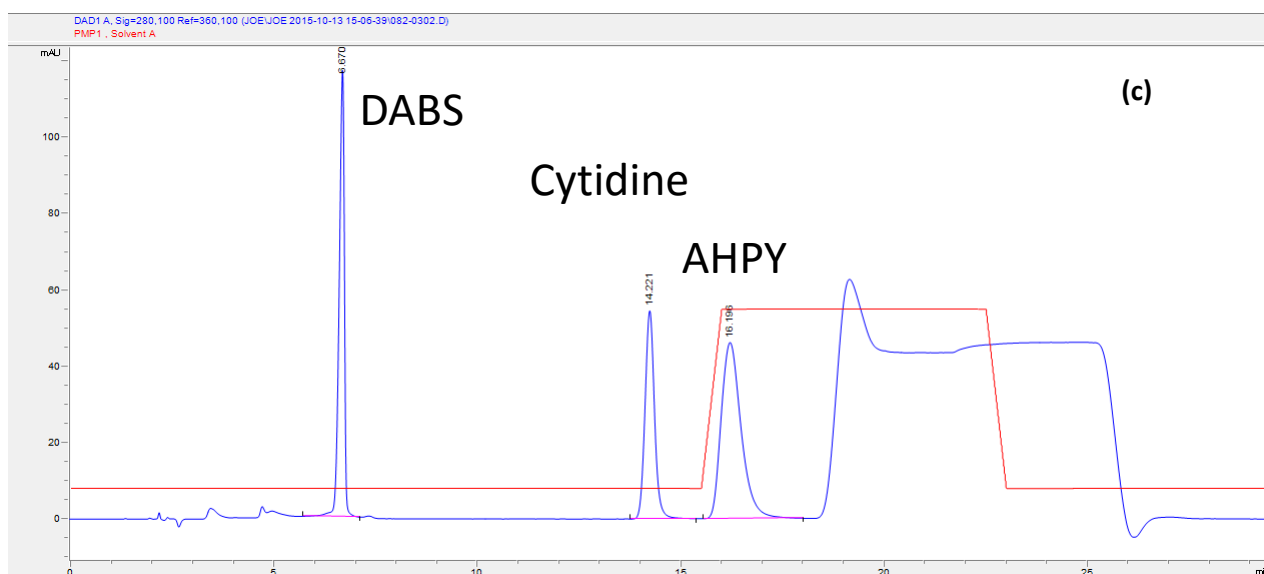


**Fig. 6.2c.** Separation of three probe solutes, Atlantis column elution 'Zone 2' (zone, column and solvents as per Fig. 6.2a) using a focused isocratic method. Method 8% solvent 'A' hold for 15.5 min then wash at 60% 'A' in 30s held for 6.5 min, gradient reset to 0% 'A' in 30s then held for 6.5 min to give 29.5 min method. For solute descriptions see Fig. 6.2a

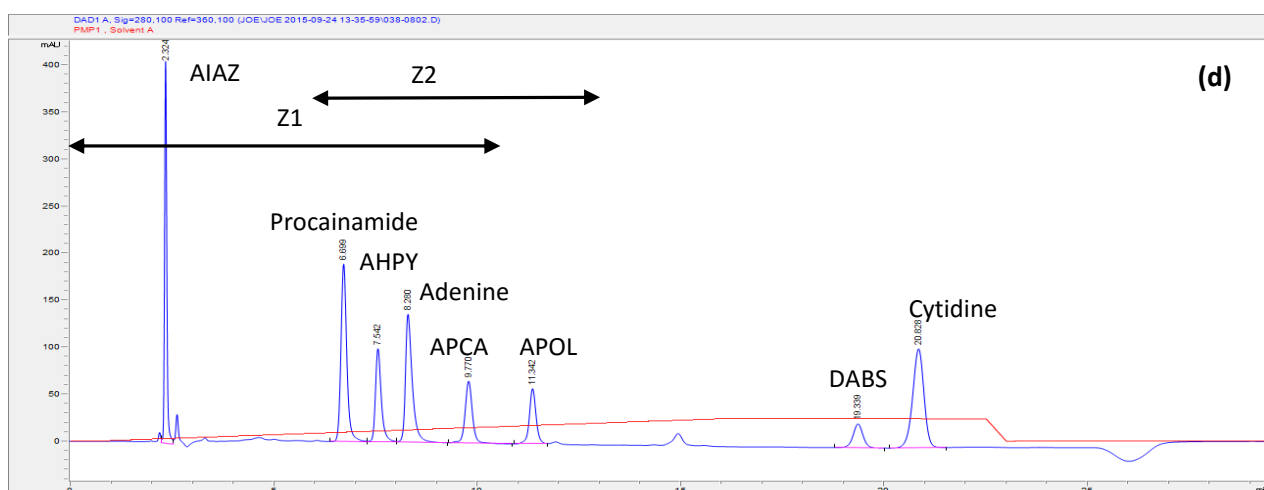


**Fig. 6.2d.** Separation of eight probe solutes using a generic gradient method on the BEH Amide column (4.6 x 150mm, 3.5  $\mu$ m). Solvents as per Fig. 6.2a. Method 0% solvent 'A' 30s isocratic hold, then 0-24% 'A' in 15.5 min, held at 24% 'A' for 6.5 min, gradient reset in 30s to 0% 'A' then equilibration held for 6.5 min to give 29.5 min method. For solute descriptions see Fig. 6.2a.



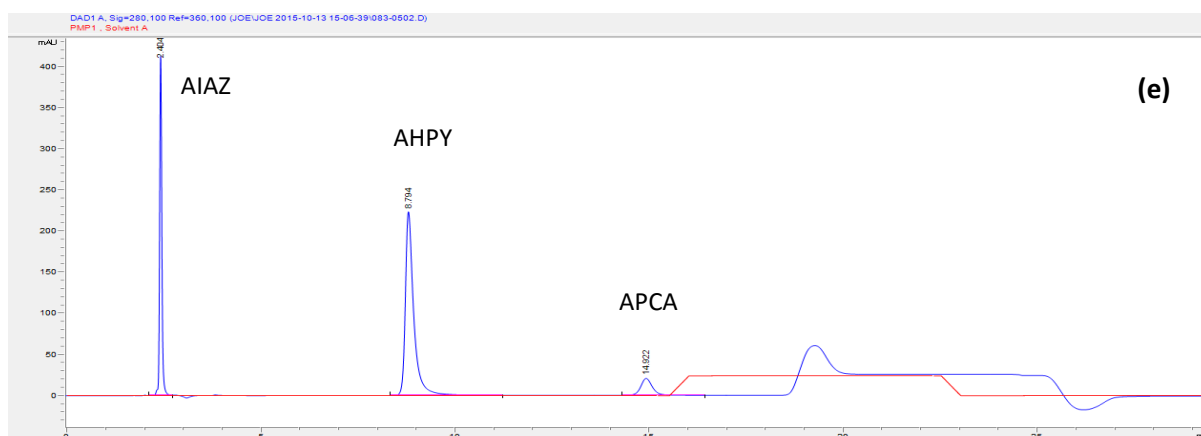


**Fig. 6.2e.** Separation of three probe solutes, BEH Amide column elution 'Zone 1' (zone and column as per Fig 6.2d, solvents as per Fig. 6.2a) using a focused isocratic method. Method 0% solvent 'A' held for 15.5 min then wash at 24% 'A' in 30s held for 6.5 min, gradient reset to 0% 'A' in 30s then held for 6.5 min to give 29.5 min method. For solute descriptions see Fig. 6.2a

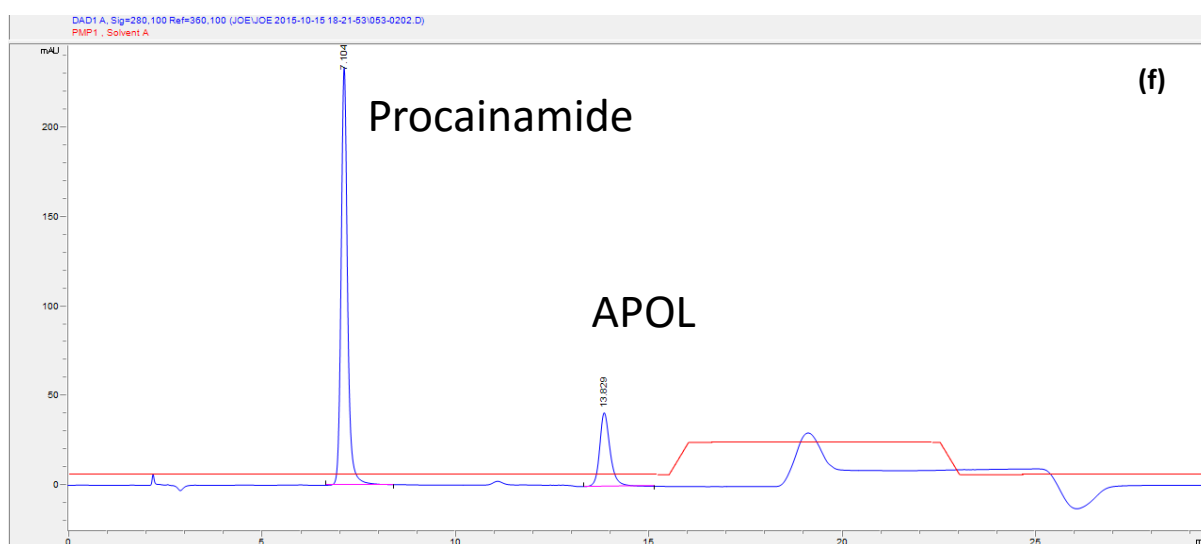


**Fig. 6.2f.** Separation of two probe solutes, BEH Amide column elution 'Zone 2' (zone, column as per 6.2d, solvents as per Fig. 6.2a above) using a focused isocratic method. Method 0% solvent 'A' held for 15.5 min, then wash at 24% 'A' in 30s held for 6.5 min, gradient reset to 6% 'A' in 30s then held for 6.5 min to give 29.5 min method. For solute descriptions see Fig. 6.2a.

**Figure 6.2.** Separation of probe solutes using generic and zone analytical methods, using (a) Atlantis column with generic gradient for eight solutes, (b) early-eluting solutes with zone 1 isocratic method, (c) middle-eluting solutes with zone 2 isocratic method, (d) BEH Amide column Generic method for eight solutes, (e) early-eluting solutes with zone 1 isocratic method, (f) middle-eluting solutes with zone 2 isocratic method. (a) – (c) Atlantis column, (d) – (f) BEH Amide column. Solute identities as per Table 6.1

### 4.1.3 Focused analytical 'zone' methods

The chromatograms in Fig. 6.2 a,d (discussed in 4.1.2 above) show separation of all eight polar probe solutes by generic gradient methods on the Atlantis and BEH Amide columns respectively, however there is a somewhat narrow elution window for the majority of the probes which can perhaps be improved upon. The focused gradient approach enhances the separation of a compound of interest from closely-eluting impurities, and this can possibly be applied to improve upon the generic gradient separations. This technique is well-established in industry as a pragmatic means to achieve separation, although its coverage in the literature is limited to a few application notes, e.g. (Tei *et al.* 2013). This approach has yet to be attempted with HILIC, as far as can be determined in this project. Rather than using the full gradient, elution zones are chosen arbitrarily across the gradient, with appropriate probe compounds used as markers to describe the start and end of each zone. 'Zone 1' describes early-eluting solutes, 'Zone 2' middle-eluting solutes and 'Zone 3' are late-eluting solutes. In this study, on the Atlantis column 'Zone 1' was between AIAZ and Adenine (Fig. 6.2a-c), and 'Zone 2' between DABS and AHPY; on the BEH Amide column 'Zone 1' was between AHPY and APCA, and 'Zone 2' between Procainamide and APOL (Fig. 6.2d-f; see Fig 6.2a for solute identities). Initially, focused gradient methods were attempted on the Atlantis and BEH Amide columns, where a gradient was applied to the elution zones shown in Figs. 6.2a and 6.2d for each column, respectively. Focused gradients are somewhat shallow, for example an attempted 'Zone 2' focused gradient on the Atlantis column was 30s isocratic hold at 17% 'A' then 17-19% 'A' in 15 min, wash in 30s at 26% A held for 6.5 min, gradient reset to 17% 'A' in 30s and equilibration for 6.5 min, solvents as per Fig 6.2a. Unexpectedly the focused gradients had very limited effect on improving selectivity of probe compounds on either column (data not shown). There was an apparent resistance of the probe compounds to manipulation of their retention using focused gradients, even those with quite different functionality. This is a phenomenon not reported to date and it is possible that solute retention is resistant to small changes in water content of the mobile phase. This perhaps relates to the water layer which is partly responsible for solute retention in HILIC (Alpert 1990, Irgum 2007, McCalley 2010b). It has been reported that more water was held on a bare silica HILIC stationary phase at higher water concentration (McCalley *et al.* 2008b). It is therefore perhaps possible that small increases in mobile phase

water concentration in a shallow gradient result in accumulation of that water inside the stationary phase pores. This perhaps counteracts the elution power of the mobile phase. This phenomenon was not observed in generic gradients, which change the water content to a greater extent and more rapidly during the method (e.g. the Atlantis generic gradient changed from 0-36% 'A' in 15 min compared to 17-19% 'A' in 15 min, and the BEH Amide generic gradient changed 0-24% 'A' in 15.5 min, solvents as per Fig. 6.2a). Therefore focused isocratic methods were developed instead, where the water held to the stationary phase ought not to change during the isocratic portion of the method. Fig. 6.2b shows a focused isocratic method on the Atlantis column (4.6 x 150mm, 3  $\mu$ m) for elution 'Zone 1', corresponding to early-eluting solutes (Fig. 6.2b). Fig. 6.2c shows a focused isocratic method on the same Atlantis column for elution 'Zone 2' for medium-eluting solutes (Fig. 6.2c). Fig. 6.2 e-f show the corresponding 'Zone 1' and 'Zone 2' focused isocratic methods on the BEH Amide column (4.6 x 150mm, 3.5  $\mu$ m). To compare the separation of probe solutes by focused isocratic and generic gradient methods on both columns, the retention times of critical pairs from Fig. 6.2a-f are shown in Table 6.2. The difference of retention time between the critical pair was used to determine if any improvement was found between generic gradient and focused isocratic methods. Further study may consider peak capacity as a more robust indicator of chromatographic performance (Neue 2005) as retention time difference does not take peak width into account, however for this study retention time difference provides a simple and pragmatic means to measure separation. The elution 'Zone 1' focused isocratic method on the Atlantis column (Fig. 6.2b) was particularly effective at improving separation of early-eluting probes: the retention time difference ( $\Delta t_R$ ) between DABS and Adenine ( $\Delta t_R$  4.6 min 'Zone 1' focused isocratic, 2.2 min generic gradient methods) improved in the focused isocratic method compared to the generic gradient method (Table 6.2). Likewise for the BEH Amide column, Fig. 6.2e and Table 6.2 show the focused isocratic method for elution 'Zone 1' on this column was also more effective than the generic gradient method at separating early-eluting probes, in this case AHPY and APCA ( $\Delta t_R$  6.1 min focused isocratic, 2.3 min generic gradient). The focused isocratic method on the Atlantis column for elution 'Zone 2' also improved upon the corresponding generic gradient method (method described above) for that column (e.g. Cytidine and AHPY  $\Delta t_R$  2.0 min focused isocratic 'Zone 2' method compared to 0.6 min by generic gradient method, both on the Atlantis column) but to a lesser extent than the 'Zone 1' method ( $\Delta t_R$  4.6 min

between DABS and Adenine by 'Zone 1' focused isocratic method described above). On the BEH Amide column the respective elution 'Zone 2' focused isocratic method was appreciably more effective at separating Procainamide and APOL than the generic gradient on that column ( $\Delta t_R$  6.7 min focused isocratic method, 4.6 min generic gradient method as described above). Focused methods were developed as an elution Zone 3 methods for late-eluting solutes but not used as these offered no improvements over generic gradients on either column (data not shown). The pragmatic focus of this study, however, required that the methods be reasonably straightforward to implement. Open Access systems were already well-established in GSK laboratories for day-to-day use by RP and could possibly be a convenient method for some polar solutes. Therefore the set of eight solutes were injected onto the Open Access RP system (see 4.1.3 below).

**Table 6.2. Retention times of critical pairs in elution ‘Zone 1’ and ‘Zone 2’ by generic and focused isocratic methods on Atlantis and BEH Amide columns. Solvents as per Fig. 6.2a.**

Solute	Generic Atlantis 0-36% ‘A’ with wash at 60% ‘A’	Zone 1 Atlantis 0% ‘A’ with wash at 60% ‘A’
	Retention time / min	
DABS	7.778	9.205
Adenine	10.023	13.790
$\Delta t_R$	2.2	4.6
	Generic Atlantis 0-36% ‘A’ with wash at 60% ‘A’	Zone 2 Atlantis 8% ‘A’ with wash at 60% ‘A’
	Retention time / min	
Cytidine	13.240	14.221
AHPY	13.812	16.196
$\Delta t_R$	0.6	2.0
	Generic BEH Amide 0-24% solvent ‘A’ with wash at 24% ‘A’	Zone 1 BEH Amide 0% solvent ‘A’ then wash at 24% ‘A’
	Retention time / min	
AHPY	7.542	8.794
APCA	9.770	14.922
$\Delta t_R$	2.3	6.1
	Generic BEH Amide 0-24% solvent ‘A’ with wash at 24% ‘A’	Zone 2 BEH Amide 6% solvent ‘A’ then wash at 24% ‘A’
	Retention time / min	
Procainamide	6.699	7.104
APOL	11.342	13.829
$\Delta t_R$	4.6	6.7

### 4.1.3 Changing the selectivity using RPLC toolbox methods at low pH and high pH

While RPLC is not generally a good technique for the retention of polar compounds, it might be possible to retain and resolve some polar solutes using variations on this mechanism, therefore separations were attempted on existing Open Access systems at GSK at low pH with Formic Acid (Fig. 6.3a), TFA (Fig. 6.3b) and high pH (Ammonium Bicarbonate adjusted to pH 10 with Ammonia solution) (Fig. 6.3c). Eight polar test probes were used as per Table 6.1. The low pH method did not resolve the probe solutes (Fig. 6.3a-b). Interestingly, the base Procainamide did retain in RP by the high pH method (Fig. 6.3c), presumably by neutralisation above its pKa of 9.04, which promotes hydrophobic interactions with RPLC columns (Davies *et al.* 2008). However the high pH method resolved only three out of eight solutes, all three of which were all basic (Fig. 6.3c). Therefore the RP approach was abandoned in favour of the generic gradient methods (4.1.2) and the focused isocratic methods (4.1.3), which were transferred to a preparative system to then evaluate HILIC purifications (4.2.1).

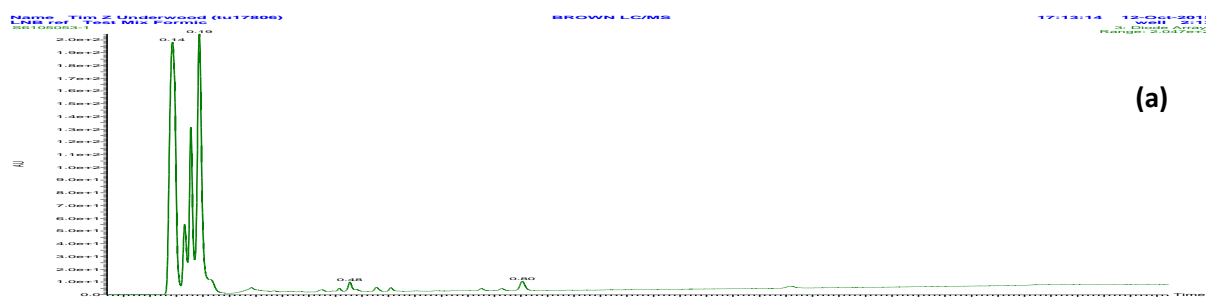
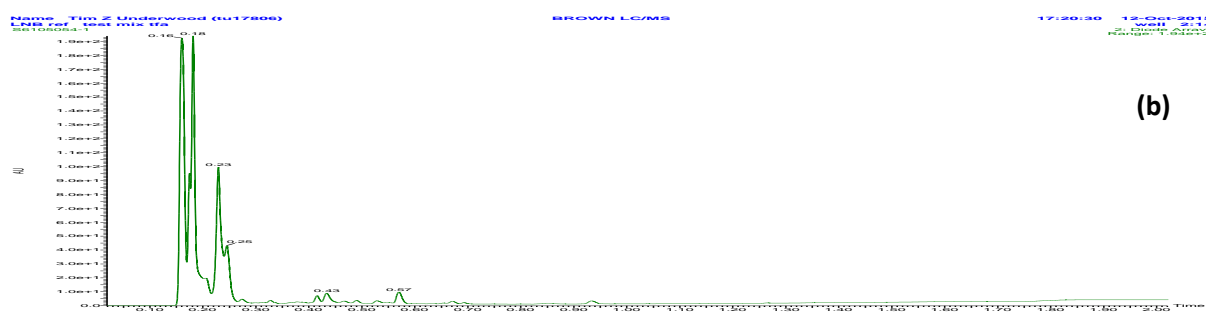
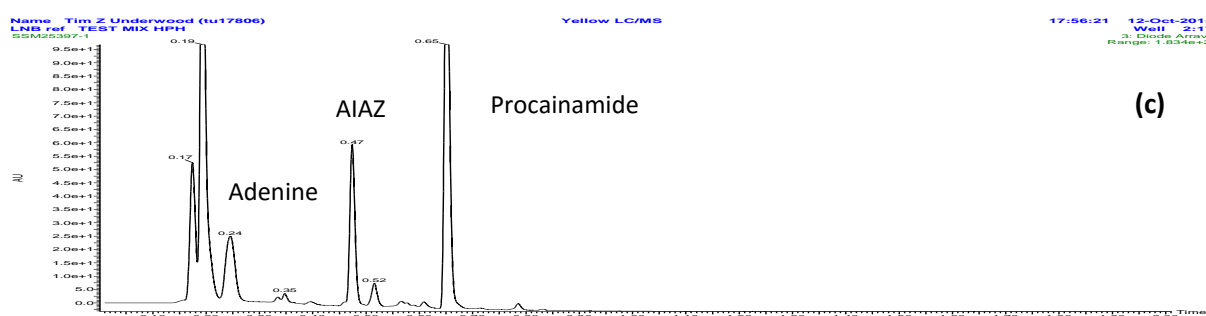


**Fig. 6.3a. Injection of eight probe solutes on RP Open Access system: Formic Acid method. Acquity UPLC CSH C18 column (2.1mm x 50mm, 1.7 $\mu$ m) column compartment at 40 °C. Solvent 'A' 0.1% v/v solution of Formic Acid in Water, 'B' 0.1% v/v solution of Formic Acid in Acetonitrile. Gradient 97% 'A' to 5% 'A' in 1.5 min then held for 0.4 min, reset to 97% 'A' in 0.1 min to give 2 min method. 0.5  $\mu$ L injection.**



(b)

**Fig. 6.3b** Injection of eight probe solutes on RP Open Access system: TFA method. Acquity UPLC CSH C18 column (2.1mm x 50mm, 1.7 $\mu$ m) column compartment at 40 °C. Solvent 'A' 0.1% v/v solution of Trifluoroacetic Acid in Water, 'B' 0.1% v/v solution of Trifluoroacetic Acid in Acetonitrile. Gradient 95% 'A' to 5% 'A' in 1.5 min then held for 0.4 min, reset to 95% 'A' in 0.1 min to give 2 min method. 0.5  $\mu$ L injection.



(c)

**Fig. 6.3c.** Injection of eight probe solutes on RP Open Access system: high pH method. Acquity UPLC CSH C18 column (2.1mm x 50mm, 1.7 $\mu$ m) column compartment at 40 °C. Solvent 'A' 10 mM Ammonium Bicarbonate in water adjusted to pH 10 with Ammonia solution, 'B' Acetonitrile. Gradient 97% 'A' held for 0.05 min, then to 5% 'A' in 1.45 min then held for 0.4 min, reset to 97% 'A' in 0.1 min to give 2 min method. 0.3  $\mu$ L injection.

Figure 6.3. Chromatograms of Eight probe solutes by RPLC Open Access system (a) Formic Acid (b) TFA and (c) high pH; solute identities as per Table 6.1, conditions provided in legend for each chromatogram.

## 4.2 Sample preparation using different injection solvents to improve analyte solubility

To establish if a generic HILIC-prep solvent system was possible, diluent experiments run at analytical-scale showed good solubility in DMSO diluent (data not shown). To prepare the highest concentration in the minimum solvent volume, a range of typical solvents were prepared, using a simulated 'crude' comprising of the weak base adenine and the zwitterionic 'APCA' in the ratio 1: 9 (w/w) to simulate product of 90% purity. Apparent

solubility data are shown in Table 6.3. Apparent solubility in acetonitrile and acetone diluents containing formic acid were low at 6.4 mg /mL (Table 6.3). In preparative LC even stronger acids such as TFA are added, which enhance solubility. Therefore a small proportion (1%) of TFA was added to DMSO and an apparent solubility was observed 50% higher than neat DMSO (23 mg / mL). It is unclear why this is the case, and perhaps relates to the ion-pairing properties of this strong acid. To investigate alternative diluents to cover broad ranges of solute polarity, half the DMSO was substituted for dimethylformamide (DMF) which is an aprotic polar organic solvent commonly used in RPLC-prep to solubilise samples (Neue *et al.* 2003), again with TFA (1%). This achieved an apparent solubility of 13 mg /mL, which was unfavourable compared to DMSO-TFA and thus not usable as a generic solvent system in HILIC-prep. Mixtures of DMSO-Water-TFA were attempted (1:1 with 1% v/v, respectively), since theory described by Yalkosky and co-workers (Millard *et al.* 2002) suggested polar solutes are best solvated by water-cosolvent mixtures. This showed promise, with apparent solubility around double that of neat DMSO 32 mg / mL (Table 6.3). Higher concentrations of water with DMSO were then considered combined with a higher TFA content (75% water with 10% TFA added, respectively), to establish if even higher solubility was possible, and in fact this was no better than lower water content (30 mg/mL 75% water-25% DMSO with 10% TFA, cf. 32 mg / mL 50% water-50% DMSO with 1% TFA). It is possible that such high water content in the diluents would destroy chromatographic performance (Heaton *et al.* 2016) but this has not been evaluated on preparative or At-Column Dilution systems for HILIC (see 4.3 below).



**Table 6.3. Apparent solubility of HILIC-prep simulated crudes for some solvent systems**

Sample	Solvent	Apparent solubility/ mg/mL
APCA/Adenine 9:1 (w/w)	ACN-water (50-50 v/v) with FA (0.1% v/v)	6.4
APCA/Adenine 9:1 (w/w)	Acetone-water (50-50 v/v) with FA (0.1% v/v)	6.4
APCA/Adenine 9:1 (w/w)	DMSO	15
APCA/Adenine 9:1 (w/w)	DMSO with TFA (1% v/v)	23
APCA/Adenine 9:1 (w/w)	DMF-DMSO (50-50 v/v) with 1% TFA (v/v)	13
APCA/Adenine 9:1 (w/w)	DMSO-Water (50-50 v/v) with 1% TFA (v/v)	32
APCA/Adenine 9:1 (w/w)	DMSO-Water (25-75 v/v) with 10% TFA (v/v)	30

## 4.3 Purification by HILIC

### 4.3.1 Generic vs. focused methods on an Atlantis column

Analytical methods (see 4.1.2-4.1.3) were transferred to a prep-scale system to evaluate their suitability to purify polar solutes. All the preparative methods used a generic volumetric flow rate of 20 mL / min and run time of 30 min on the Atlantis and BEH Amide columns (21 x 150mm, 5 µm) using a standard preparative system. 1% TFA in DMSO (v/v) chosen as a generic diluent due to its good apparent solubility (4.2.1.2 above). Chromatograms are shown for the Atlantis in Fig. 6.4a – c using the simulated crude

'APCA/AHPY' prepared at a concentration of 22 mg / mL. The generic gradient preparative method is shown in Fig. 6.4a and 'Zone 2' focused isocratic method in Fig. 6.4b. On the Atlantis column, the generic gradient method was as effective as a focused isocratic method for purification of this simulated crude (Fig. 6.4a-b). The poor separation by 'Zone 2' focused isocratic method is consistent with the only modest improvements in separation afforded by the 'Zone 2' isocratic method analytically (4.1.3, Fig. 6.3a,c). A focused gradient method was developed for this column (Fig. 6.4c) and the resulting preparative chromatogram is shown in Fig. 6.4c. In this case, the focused gradient outperformed the focused isocratic and generic gradient methods in terms of achieving baseline resolution at increasing sample injection volumes (Fig. 6.4). It would seem that for the gradient methods the relatively rapid increases in mobile phase water content favours the benefit of gradient methods where after initial isocratic separation, the solute band is accelerated to the mobile phase velocity and the band is somewhat narrower (Fig. 6.4 a,c compared to Fig. 6.4 b).

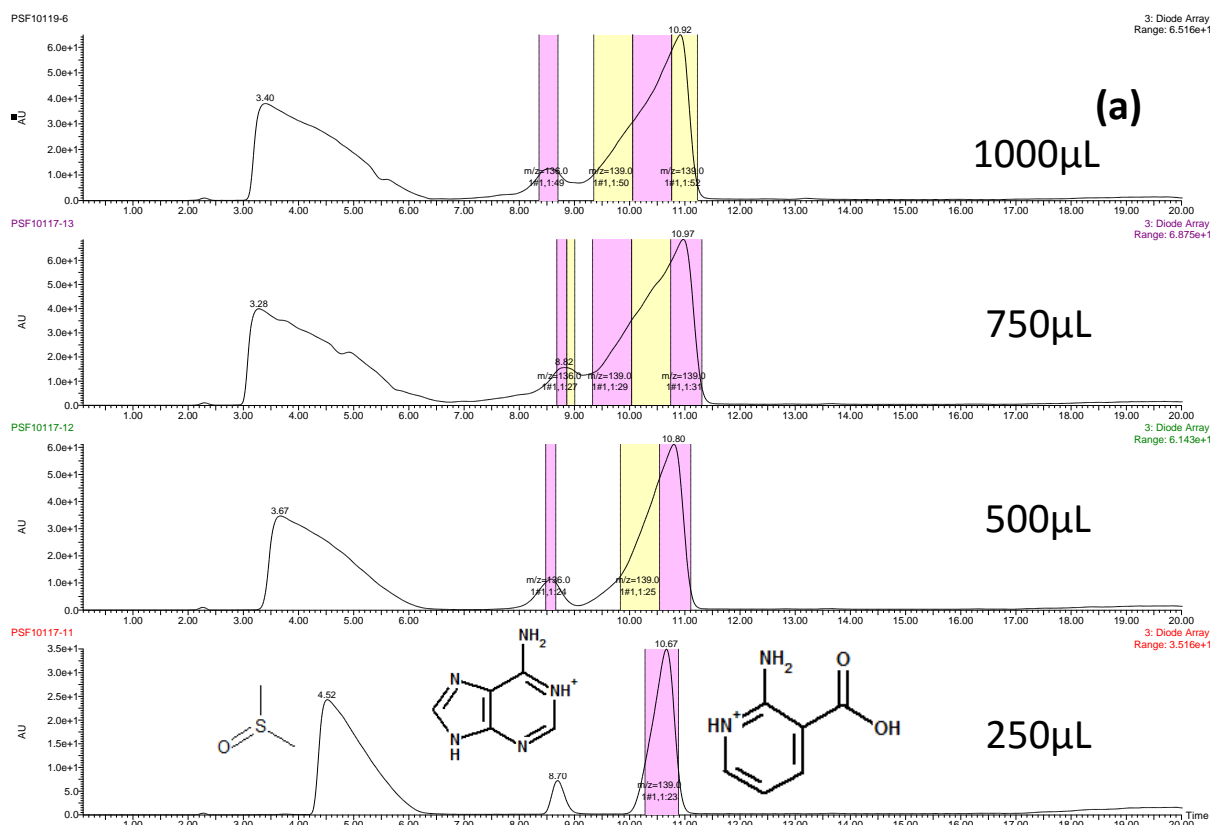


**Fig. 6.4a.** HILIC-prep chromatograms of simulated crudes with increasing injection volumes, Atlantis column (21mm x 150 mm, 5 μm); generic gradient method. Solutes are simulated crude 'APCA/Adenine' 9:1 (w/w), diluent 1% TFA (v/v) in DMSO. Solvents as per Fig. 6.3a, flow rate 20mL / min. Gradient 0% 'A' isocratic hold (30s) then 0-36% 'A' in 15 min, wash stage at 60% 'A' in 30s held for 6.5 min, gradient reset to 0% 'A' in 30s then equilibration for 7 min to give a 30 minute method.

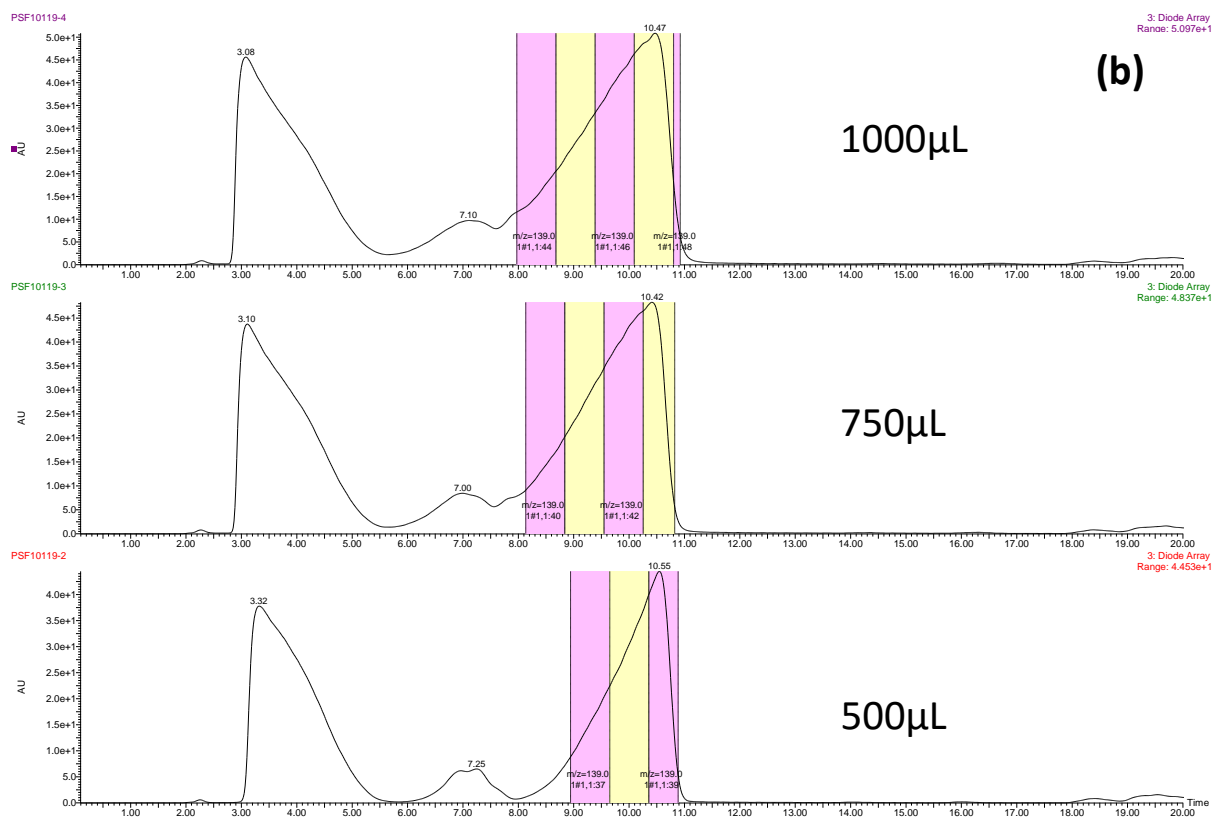


**Fig. 6.4b.** HILIC-prep chromatograms of simulated crudes with increasing injection volumes, Atlantis column (21mm x 150 mm, 5 $\mu\text{m}$ ); zone 2 focused isocratic method. Solutes are simulated crude 'APCA/Adenine' 9:1 (w/w), diluent 1% TFA (v/v) in DMSO, flow rate 20mL / min. Method 8% 'A' isocratic held for 15.5 min, wash stage at 60% 'A' in 30s, reset to 0% 'A' in 30s then equilibration held for 7 min to also give a 30 minute method.

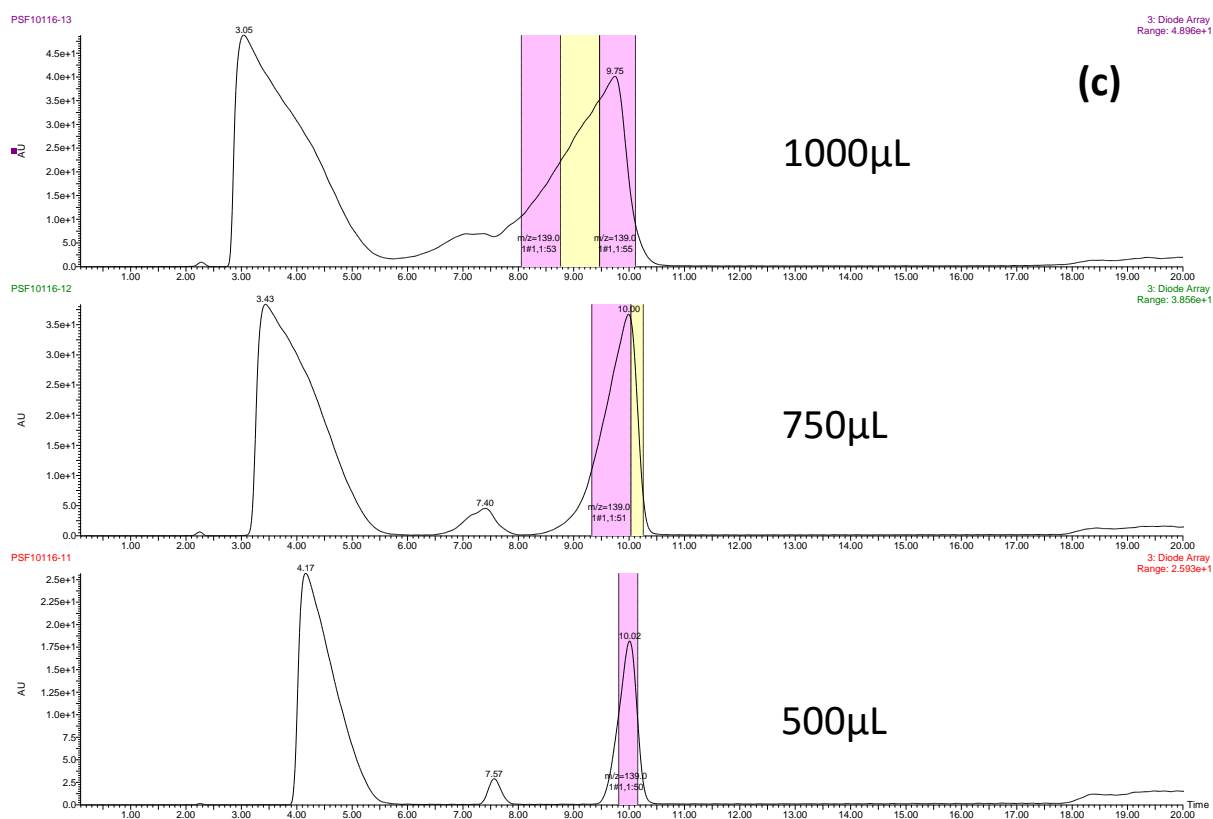


**Fig. 6.4c. HILIC-prep chromatograms of simulated crudes with increasing injection volumes, Atlantis column (21mm x 150 mm, 5 μm); zone 2 focused gradient method. Solutes are simulated crude 'APCA/Adenine' 9:1 (w/w), diluent 1% TFA (v/v) in DMSO, flow rate 20mL / min, solvents as per Fig. 6.2a. Method 5-18% solvent 'A' in 15.5 min , wash at 60% 'A' in 30s held for 6.5 min, reset to 5% 'A' in 30s held for 7 min to give a 30 min method.**

**Fig. 6.4. HILIC-prep chromatograms of simulated crudes with increasing injection volumes, Atlantis column (21mm x 150 mm, 5 μm); (a) generic gradient method; (b) zone 2 focused isocratic method, (c) zone 2 focused gradient method. Solute is simulated crude 'APCA/Adenine' 9:1 (w/w), diluent 1% TFA (v/v) in DMSO, flow rate 20mL / min.**

### 4.3.2 Generic vs. focused methods on a BEH Amide column

Simulated crudes of 'Procainamide/AHPY' were prepared in DMSO-TFA (1% v/v) at a concentration of 22 mg / mL and injected onto the BEH Amide column using a generic gradient method (Fig. 6.5a) and focused isocratic method (Fig. 6.5b). On this column, baseline resolution by focused method was facile and scalable, whereas for the generic gradient the two components co-eluted and resolution was impossible (Fig. 6.5). Overall

Fig. 6.4-6.5 show that generic or focused gradient methods can separate hydrophilic solute mixtures at preparative levels. The two columns have alternate retention order, therefore in practise a challenging purification on one column can be overcome by switching to the other column or using a focused method on the same column. It is interesting that although Procainamide/AHPY were close-eluting on the BEH Amide by preparative methods, these are well-separated at analytical scale on the Atlantis column, where AHPY is within zone 2 but procainamide elutes later than elution zone 2 (Fig. 6.3a). In this case it is anticipated that solutes which behave similar to Procainamide and AHPY can also be resolved by switching columns. In contrast AHPY/Adenine were close-eluting on both the Atlantis and BEH Amide columns at analytical scale, and on both columns these are eluted in 'zone 2' (Fig. 6.3a, Fig. 6.3d), therefore switching columns is unlikely to be effective at improving the separation of these solutes and indeed those that eluted in the 'zone 2' area of the chromatogram. Perhaps generic gradient or focused gradient methods can be more effective at preparative separation of such medium-eluting solutes (Fig. 6.4a-c). It is unclear, however if the loss of separation performance at large injection volumes is due to volume overload or mass overload of the stationary phase. The preparative peaks typically fronted on both columns, which is normally observed for mass overload of basic solutes in HILIC (e.g. McCalley 2007).

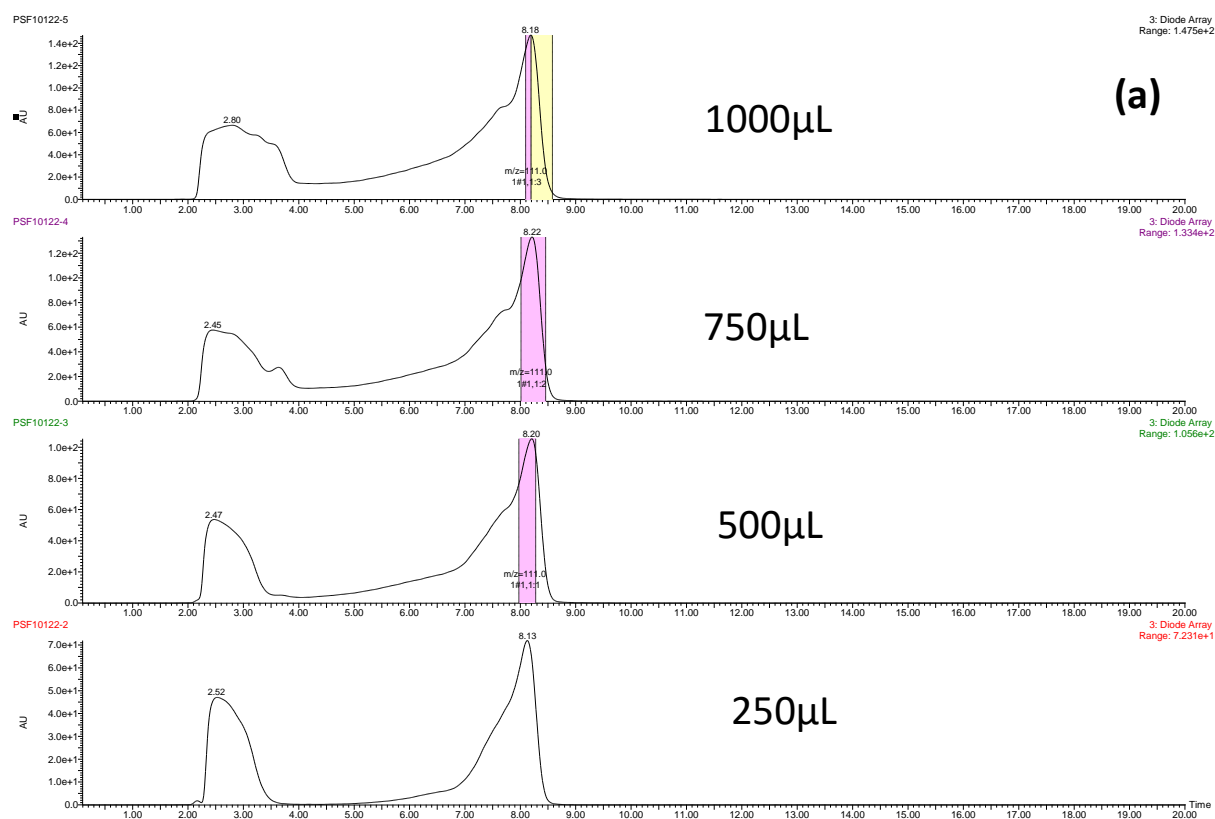


**Fig. 6.5a. HILIC-prep chromatograms of simulated crudes with increasing injection volumes BEH Amide column (21mm x 150mm, 5µm) (a) generic gradient method for 'Procainamide/AHPY'. Gradient 0-24% solvent 'A' over 15 min with wash at 60% 'A' for 6.5 min, gradient reset to 0% 'A' then equilibration for 7 min to give 30 min method. Diluent 1% TFA in DMSO (v/v).**

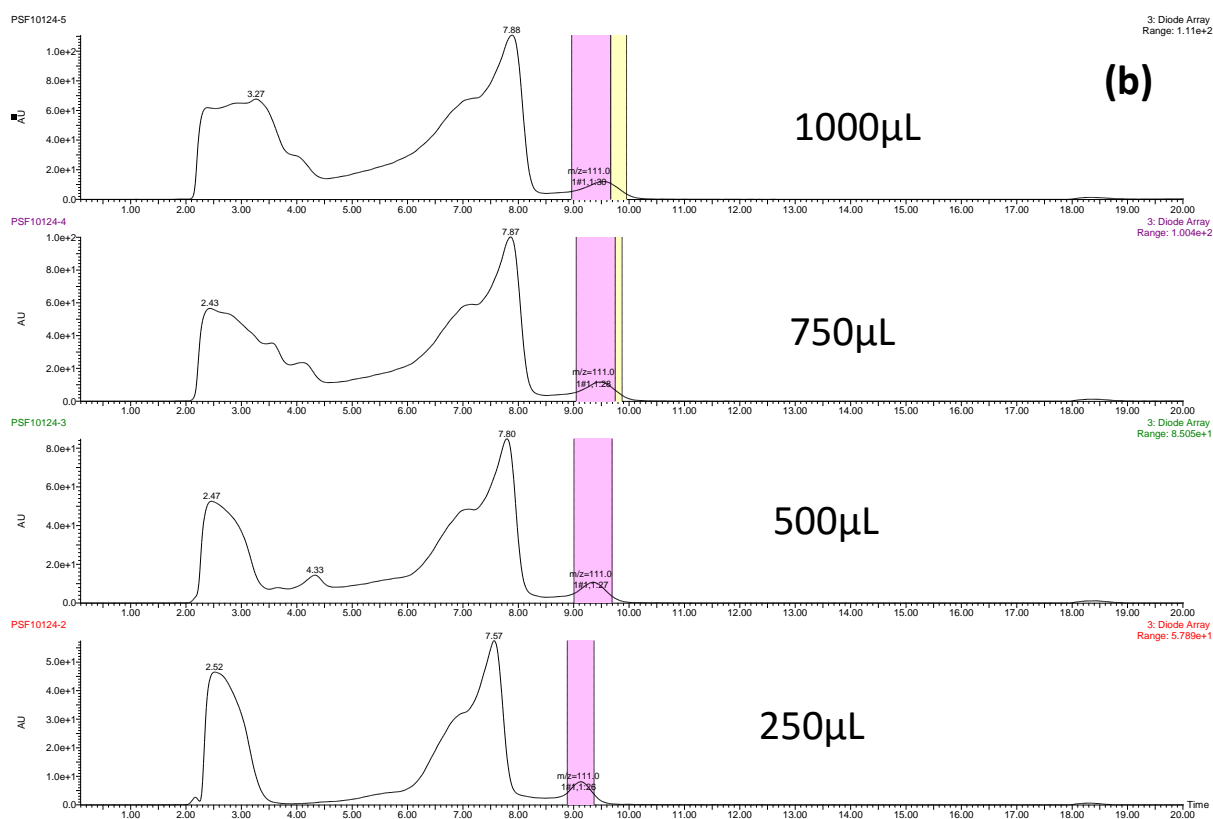


**Fig. 6.5b.** HILIC-prep chromatograms of simulated crudes with increasing injection volumes BEH Amide column (21mm x 150mm, 5µm), (b) elution zone 1 focused isocratic method for 'Procainamide/AHPY', flow rate 20mL / min. Method 0% solvent 'A' held for 15.5 min, wash at 60% 'A' in 30s held for 7 min, reset to 0% 'A' equilibration held for 7 min to give 30 min method.

**Fig. 6.5** HILIC-prep chromatograms of simulated crudes with increasing injection volumes BEH Amide column (21mm x 150mm, 5µm) (a) generic gradient method on for 'Procainamide/AHPY', (b) focused zone 1 isocratic method for 'Procainamide/AHPY', flow rate 20mL / min

### 4.3.3 Purification by HILIC using an At-Column Dilution (ACD) system

At-Column Dilution (ACD) is designed for purifying large quantities of compound to overcome poor solubility, as described by Neue *et al.* (Neue *et al.* 2003). The sample can be injected by ACD in a solvent with good solubility and this is diluted with mobile phase of weak elution power to avoid distortion in peak shape from the sample diluent. The key benefit of ACD is the ability to inject large volumes of crude solutions for purification, from a



limit of 1 mL on a standard prep system used in this study to 4 mL on the ACD system, respectively. Here the sample is introduced via a pump in the diluent as prepared (e.g. for HILIC 1% TFA (v/v) in DMSO) in a slow-moving stream, and a splitter dilutes the sample plug before it reached the head of the column with mobile phase of low elution power (typically highly aqueous in RPLC). Thus a low volumetric flow rate (3 mL / min) is directed through the sample introduction pump to deposit the injection on the head of the column over the first 4 minutes of the method. A second pump is used (17 mL / min) to make-up an overall flow rate of 20 mL / min through the column, with a stream solely of mobile phase reservoir 'B' (95% ACN with 5mM AF pH 3 with FA). A method was developed using the Atlantis column (21 x 150mm, 5  $\mu$ m) using a version of the generic gradient used on the standard preparative system (4.3.1 above). Initially, 1% TFA (v/v) in DMSO was used as diluent but the peaks were smeared across the chromatogram and the separation was not usable (data not shown). In RPLC-ACD, it is common practise to use DMSO as a diluent, due to good generic solubility and also its polarity ensures it is unretained, depositing the solute onto the column head. Neue *et al.* investigated the use of DMSO diluent on standard preparative and ACD systems, reporting peak distortions on the standard system attributable to viscous fingering due to a viscosity mismatch between DMSO and aqueous mobile phase at the start of their RP gradient (Neue *et al.* 2003). However in ACD there should be efficient mixing of DMSO with the mobile phase to negate such effects and indeed those authors reported good performance in DMSO diluent when ACD was used, attributable to dilution of the DMSO (Neue *et al.* 2003). This is given further consideration in 4.4.1 below. Therefore although the diluents shown in Table 6.3 were clearly useful on a standard preparative system (Fig. 6.4, 6.5), an alternative approach was necessary for HILIC-Prep-ACD. The diluent was instead prepared to match the mobile phase (95% ACN with 5mM AF pH 3). It was anticipated that solubility would be compromised by using mobile phase rather than DMSO therefore TFA was added at concentrations of 1, 5 or 10% to ensure solubility was adequate. Careful application of heat and the addition of TFA resulted in apparent solubility of 23.4 mg / mL (APCA/Adenine 9:1 w/w) and 31.7 mg / mL (Cytidine/Adenine 9:1 w/w) (both 1% TFA v/v). The resulting chromatograms on the ACD system using the Atlantis column a generic method are shown in Fig. 6.6a. At 1% TFA, baseline resolution of the simulated crude Cytidine/Adenine (31.7 mg / mL) was possible, however the peaks became distorted at 5% TFA and retention of both solutes collapsed at 10% TFA content (Fig. 6.6a). This suggests

that TFA in the diluent alters the selectivity of the mobile phase, which was unexpected when using HILIC on an ACD system. This is discussed further in 4.4.3 below. Nevertheless, limiting the TFA content to 1% (v/v) for ACD removes this issue altogether (Fig. 6.6a). Fig. 6.6b shows injections of simulated crude 'Cytidine/Adenine' on the ACD system. Whereas to the standard preparative system which was able to purify crudes up to 1 mL injection per cycle (Fig. 6.4), the ACD system can easily improve on that to 4mL injections per cycle (Fig. 6.5b), which represents 127 mg in a single cycle. Interestingly, there was comparable separation performance for a 1mL injection of Cytidine/Adenine (9:1 w/w) on both the ACD and standard preparative systems (data not shown). Both the standard preparative injections and ACD injections gave overloaded peaks which fronted with increasing retention time as the sample size increased, which could be due to volume or mass overload. On the ACD system, however, when the sample fills the loop its volume is made up to 4mL from a dedicated reservoir (in this study mobile phase solvent 'B' was used, to match the low elution strength of mobile phase at the start of the gradient), such that 4mL solution is always injected onto the column. Thus the 'sample volume' on the ACD is the volume drawn from the vial into the injection loop, for example a 1mL sample is drawn into the loop together with 3mL of solvent 'B' (described above) and 4mL is injected on column, the composition of which broadly matches the mobile phase at the start of the gradient. Therefore volume overload is perhaps unlikely by ACD since the sample is injected at a low flow rate and mixed with mobile phase to minimise losses in separation performance from the diluent. The overloaded peaks by ACD therefore probably were due to mass overload, which is normal in the high loadings of preparative LC (Neue 2005). In contrast, there was no such countermeasure to volume overload on the standard preparative system, therefore it is possible those samples not injected by ACD experienced some volume overload in addition to mass overload. There are no reports of ACD being attempted with HILIC purification, and these results clearly show applicability of Prep-HILIC-ACD to purify polar 'building block' compounds in useful quantities.

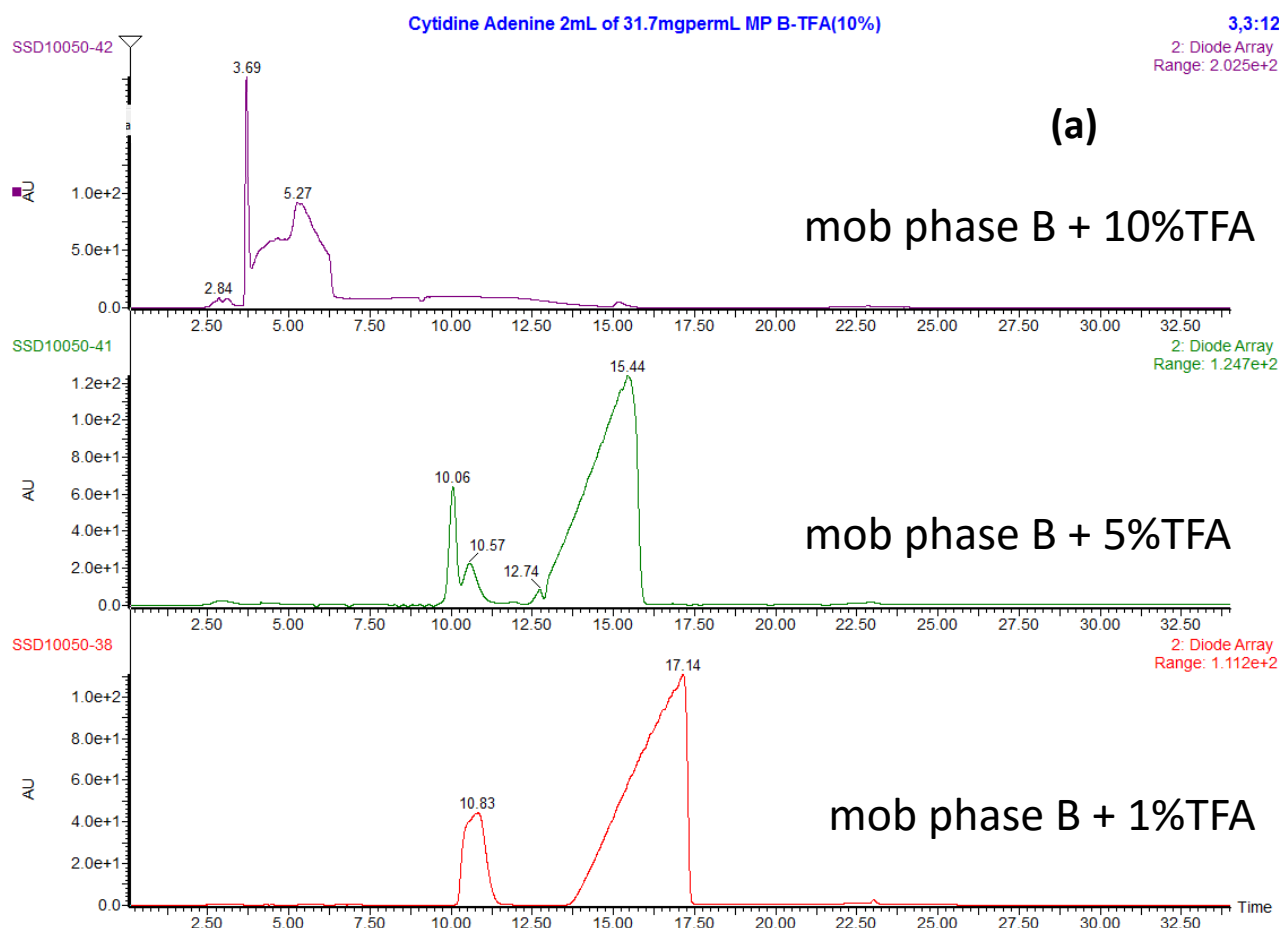
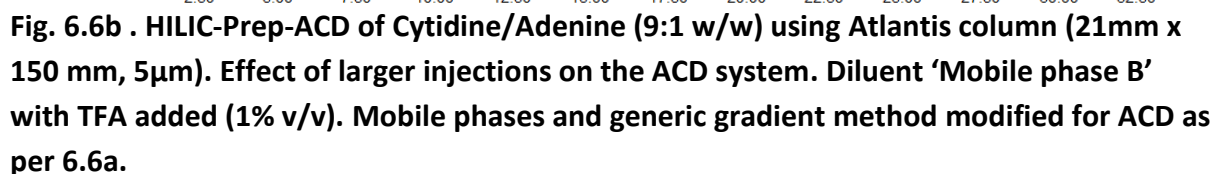


**Fig. 6.6a. HILIC-Prep-ACD of Cytidine/Adenine (9:1 w/w) using Atlantis column (21mm x 150 mm, 5 $\mu$ m); effect of diluent TFA content. Diluent 'Mobile phase B' with TFA added (1, 5 or 10% v/v). Mobile phase 'A' = 70% ACN with 5mM Ammonium Formate w<sup>w</sup> pH 3 with formic acid; 'B' = 95% ACN with 5mM Ammonium Formate ww pH 3 with formic acid. Generic gradient method adapted to ACD: 0% 'A' isocratic for 30s then 0-36% 'A' gradient over 15 min, wash at 60% 'A' for 6.5 min, gradient reset to 0% 'A' then equilibration for 7 min to give 34 min method.**



#### 4.3.4 Preparative productivity

Page 188 of 246

equation simplifies to a straightforward measure of amount purified per unit time (equation 6.3). The generic methods developed in this study are 30 minutes long, which allows for a simple measurement of productivity in terms of mass of crude (in mg) purified per hour. Note the ACD methods are 34 min, which includes a 4min sample introduction at the start of the method. Thus the data of 4.3.1 – 4.3.3 can be evaluated in terms of productivity. In daily operation, a 'yardstick' of greater than 30 mg crude purified in a reasonable time frame is used to discriminate useful preparative methods ('scalable'). However in the field of drug development some chemists require only a few milligrams of novel compound to be purified. Thus a lower, but on occasion acceptable, limit shows possible preparative methods to fall-back on ('small-scale'). Figure 6.7 plots the data for three simulated crudes of 4.3.1 – 4.3.3 using these limits, designating 60 mg of crude purified per hour a 'scalable' limit and 20 mg crude per hour a 'small-scale' lower limit. ACD methods on the Atlantis column gave the best performance, at 223 mg per hour using 4mL injections for the crude 'Cytidine/Adenine'. Productivity of generic gradient methods (Fig. 6.4-6.5) was somewhat similar between the standard prep and ACD system (63 mg/hr standard system, 55 mg/hr ACD) for the same 1mL injection volume of identical crude but the ACD is 4 min longer. These are both around 'scalable' limit, but for other crudes the standard prep system was limited to small-scale purifications, which are acceptable in some cases. Keeping the diluent constant (DMSO with TFA 1%), the focused elution 'Zone 2' gradient method (5-18% 'A' in 15 min, by wash at 60% 'A' in 30s held for 6.5 min, gradient reset to 5% 'A' in 30s then equilibration held for 7 min to give a 30 min method, solvents as per Fig. 6.2a) outperformed the generic and 'Zone 2' isocratic (productivity 33, 22 and 22 mg / hour, respectively), due to improvements in peak shape (Fig. 6.5). Using the same diluent, for the BEH Amide column productivity was even higher at 44 mg / hour for the crude shown in red (Procainamide/AHPY). Further improvements are perhaps possible through minimising the DMSO content of the diluent. Removing the DMSO altogether and applying careful heat spiking with a small amount of TFA (as described in 4.3.3), crudes in diluent taken directly from solvent 'B' with added TFA (1% TFA v/v in 95% ACN with 5mM AF pH 3 with FA), productivities of 46.8 and 63.4 mg / hour were observed by generic methods on the standard prep system (crudes APCA/Adenine and Cytidine/Adenine, respectively). The productivity plots of Figure 6.7 indicate that HILIC can purify hydrophilic solutes in useful

quantities within a reasonable timeframe. Data for all usable preparative separations are provided in Table 6.4, for information.

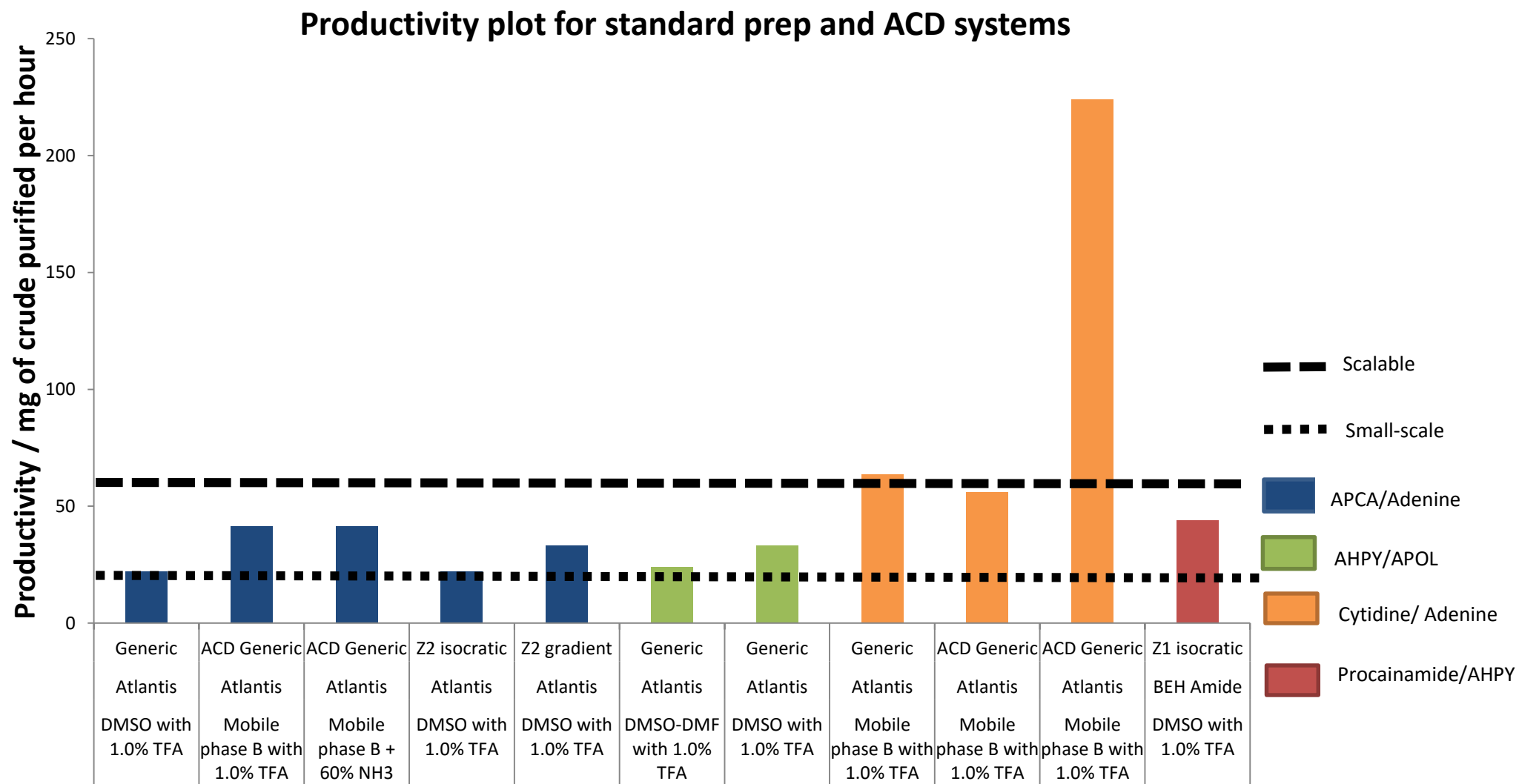


**Fig. 6.7. Productivity plot for preparative methods on standard and ACD systems. Arbitrary cut-offs of 20 mg / hr for small-scale purifications (dotted line) and 60 mg / hr for large-scale shown (dashed line).**

**Table 6.4 HILIC-Prep data for information**

Method	Solutes	Concentration mg / mL	Volume injected μL	Productivity mg / hr
<b>Standard Prep</b>				
<b>Atlantis</b>				
<b>Generic</b>	APCA/Adenine	6.4 <sup>a</sup>	250	3.2
	APCA/Adenine	6.4 <sup>b</sup>	250	3.2
	APCA/Adenine	12 <sup>c</sup>	750	18
	APCA/Adenine	22 <sup>d</sup>	500	22
	Cytidine/Adenine	31.7 <sup>e</sup>	1000	63.4
	AHPY/APOL	12 <sup>c</sup>	1000	24
	AHPY/APOL	22 <sup>d</sup>	750	33
<b>Z2 isocratic</b>	APCA/Adenine	22 <sup>d</sup>	500	22
<b>Z2 gradient</b>	APCA/Adenine	22 <sup>d</sup>	750	33
<b>BEH Amide</b>				
<b>Generic</b>	Procainamide/AHPY	22 <sup>d</sup>	-	-
	APCA/APOL	22 <sup>d</sup>	250	11
	APCA/Adenine	22 <sup>d</sup>	<250	<11
<b>Z1 isocratic</b>	Procainamide/AHPY	22 <sup>d</sup>	1000	44
<b>Z2 isocratic</b>	APCA/APOL	22 <sup>d</sup>	<250	<11
	APCA/Adenine	22	<250	<11
<b>ACD</b>				
<b>Atlantis Generic</b>	APCA/Adenine	23.4 <sup>e</sup>	1000	46.8*
	APCA/Adenine	39 <sup>d</sup>	-	-
	APCA/Adenine	23.4 <sup>f</sup>	1000	46.8
	Cytidine/Adenine	31.7 <sup>e</sup>	1000	63.4
	Cytidine/Adenine	31.7 <sup>e</sup>	2000	126.8
	Cytidine/Adenine	31.7 <sup>e</sup>	3000	190.2
	Cytidine/Adenine	31.7 <sup>e</sup>	4000	253.6

**a = 30% ACN in Water with 0.1% Formic Acid**

**b = 30% Acetone in Water with 0.1% Formic Acid**

**c = DMSO-DMF with 1.0% TFA**

**d = DMSO with 1.0% TFA**

**e = Mobile phase B with 1.0% TFA**

**f = Mobile phase B + 60% NH3**

**\* distorted peak shape for zwitterionic APCA**



### 4.3.5 Purification of zwitterion(s)

The zwitterions used in this study (APCA, DABS) were unretained by Open Access RPLC methods (Figure 6.3). Classical ion-exchange methods can purify zwitterionic amino acids such as threonine, serine, proline and glycine, and this technique has been established since at least the 1950's (Hirs *et al.* 1952). In a generic approach, however, use of the same equipment and ideally the same stationary phase for the majority of separations is an attractive prospect. The crude 'APCA/Adenine', where the zwitterion APCA was in excess of 9:1 by mass to the weak base adenine, was analysed using the bare silica Atlantis column on a generic gradient method (Figure 6.8). To simplify the zwitterion to a basic or acid form, a strong acid (TFA) or strong base (ammonia) was added to the diluent, respectively. Due to possible chromatographic interference from the DMSO (4.4.4), this was substituted for 'Mobile phase B' (95% ACN with 5mM AF pH 3 with FA). The separation using TFA (Fig. 6.8 bottom) was useable, shown by the resolution of the two components (confirmed by extracted ion chromatograms, not shown). However APCA peak shape was severely distorted, as essentially two peaks with apexes at 12.37 and 19.99 min and a connecting bridge. The TFA added to the diluent is a strong acid and APCA ought to be injected as a single form, a positively-charged base. Fig. 6.8 middle and upper chromatograms show the separation of the two solutes with added ammonia (20% and 60% v/v respectively), with improved peak shape of APCA compared to when TFA was used (Fig. 6.8 lower chromatogram). At 60% ammonia, the severe distortion of APCA peak shape eliminated (Fig. 6.8 upper), and it is anticipated that this separation can scale even higher on the ACD system if necessary (see Figure 6.6b for comparison). Ammonia was added with caution, as high pH mobile phase damages silica-based stationary phases due to dissolution of the silica. However the ammonia was used in the diluent only, which is expected to elute from the column within the method cycle (which contains a wash stage), as opposed to ammonia used in the mobile phase, which constantly flows through the column. Nevertheless, it is recommended that further studies consider the use of BEH silica in as an alternative to the 'type B' silica used in this study: BEH uses ethylene bridges to replace silanols and the stationary phase is better resistant to use of high pH mobile phase. The severely distorted peak shape of APCA suggests its retention is more complex than simple hydrophilic cation-exchange which occurs on this column for simple bases (Kumar *et al.* 2013). It is interesting

that this distorted peak shape with TFA was not observed for the neutral solute cytidine using TFA diluent by ACD (Fig. 6.6a shown in 4.3.3 above). Therefore APCA was probably not present as neutral in TFA diluent, also this is unlikely given its pI is around 4.75 ([www.chemicalize.org](http://www.chemicalize.org)). At the presumed high pH afforded by ammonia ACPA is an acid, which should not retain on this bare silica column, however it was well retained under these conditions (Fig. 6.6a). Due to project time constraints, this could not be investigated further. Comparison with basic, neutral and acid solutes under equivalent conditions would be of interest as further study. The data of Fig. 6.8 show HILIC can be a viable option for purification of hydrophilic zwitterionic compounds.

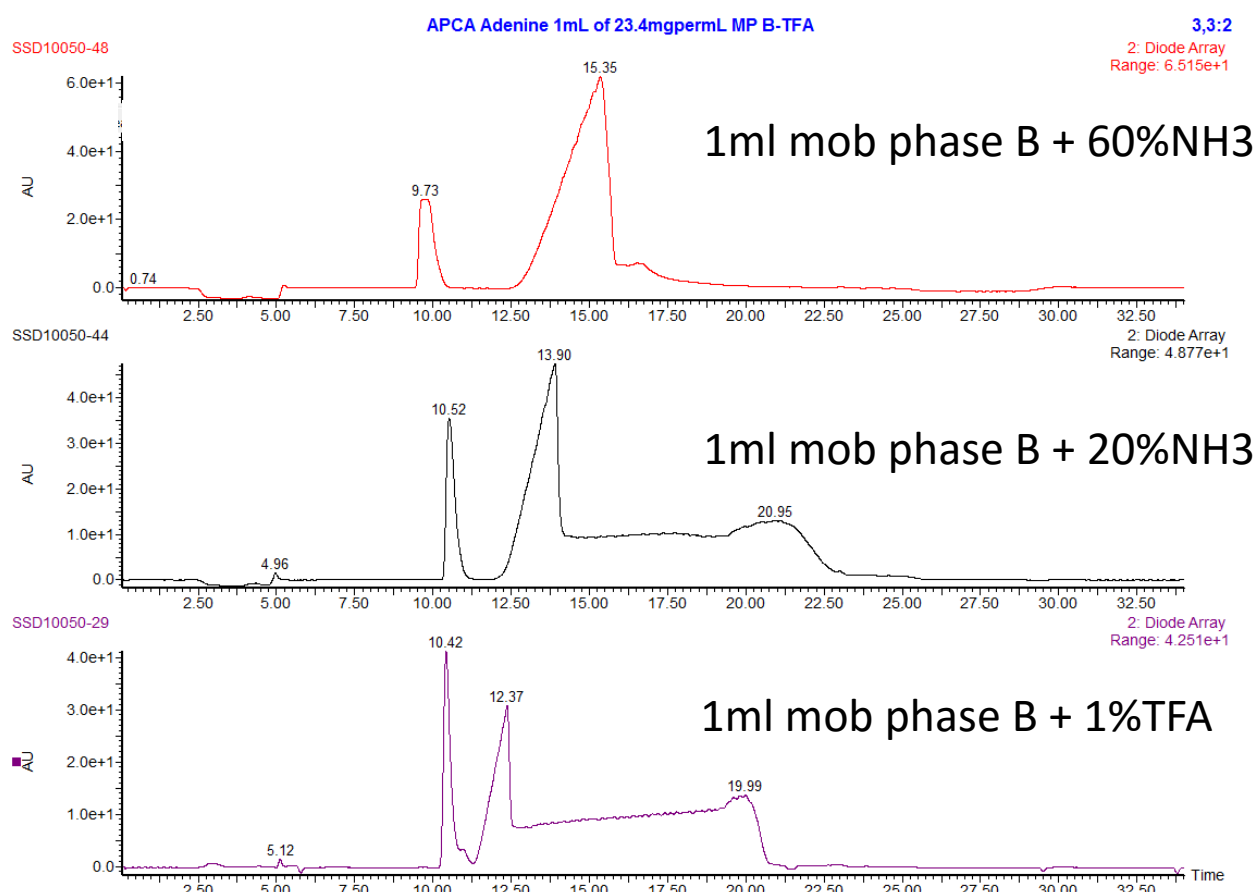


**Fig. 6.8. HILIC-Prep-ACD chromatograms investigating any benefit of adding acid (TFA) or base (NH<sub>3</sub>) to the diluent for a crude containing a zwitterionic solute (APCA) and a weak base (Adenine) (23.4 mg / mL). Atlantis column with generic ACD method, 1 mL injections.**

## 4.4 Possible explanations for poor ACD performance using DMSO or TFA

### 4.4.1 Characterising of the effect of DMSO on peak shape using an analytical system

It became apparent during prep ACD work (4.3.3) that DMSO present in the diluent possibly caused distorted peaks. To characterise this further, analyses were performed on a Thermo UHPLC system using an isocratic method on an Atlantis column (4.6mm i.d. x 250mm, dp 5µm) with a typical HILIC mobile phase (85% or 95% ACN, 5mM AF pH 3 with FA). To establish if DMSO had affinity for this HILIC stationary phase, samples were prepared as a combined standard in neat DMSO (Fig. 6.9a) (DABS/APCA/AHPY at 1mg / mL each), also in 50% ACN with 0.1% FA (v/v) with no DMSO present (Fig. 6.9b). The UV diode array detector was set to a somewhat low wavelength (240 nm) to detect DMSO. Fig. 6.9a shows an injection of a combined standard of DABS, APCA and AHPY on an Atlantis column (4.6 x 250mm, 5µm) with 85% ACN mobile phase, buffered with 5mM AF pH 3, sample prepared in neat DMSO. Fig. 9a shows a large peak with a retention time around 5-6 min which is possibly either some impurity or DMSO itself. However Fig. 9b shows the same sample prepared in diluent containing no DMSO (50% ACN in water with 0.1% FA (v/v)), with the same separation conditions as Fig 9.a. Fig. 9b does not show this peak, therefore it is possible that DMSO retained on the Atlantis column with a broad, overloaded peak with severe tailing, apex approximately 5.2 min ( $k \approx 0.7$ ) (Fig. 9a). This suggests that DMSO does have some affinity for that stationary phase in HILIC. Solute peak distortion occurred for both AHPY and APCA when this was present in the diluent (Fig. 6.9a) in agreement with an earlier study (Ruta *et al.* 2010). The presence of DMSO prevented the loss of efficiency from being accurately measured due to distortion of the AHPY peak (Fig. 6.9a). To characterise any relationship between DMSO content in the diluent and peak efficiency, which has not been reported for HILIC, Fig. 6.9c shows injections made on the same column under more-retentive conditions (95% ACN, 5mM AF pH 3 with FA). Samples were again prepared as combined standards, but at higher concentration (DABS/APCA/AHPY at 5mg / mL each in neat DMSO) to allow for further dilution of the DMSO. Each sample was diluted further with

either neat DMSO or solution from mobile phase reservoir 'B' (95% ACN with 5mM AF pH 3 with FA) to give an overall concentration of 1mg / mL for each sample, with decreasing DMSO content from neat DMSO down to 20% DMSO. Measurement using 0% DMSO content was not possible at this solute concentration, due to insufficient solubility at 95% ACN. Fig. 6.9c shows some peaks are distorted even at low DMSO content. Figure 9d plots the data of Fig 6.9c as peak efficiency vs. DMSO content of the diluent. There was some tolerance of DMSO content for the well-retained zwitterion APCA ( $k=8.8$ ), with only 16% loss of efficiency (16,699 plates at 100% DMSO, 19,812 plates at 20% DMSO) (Fig. 6.9d). However peaks of both the moderately-retained zwitterion DABS ( $k=4.8$ ) and weakly-retained weak base AHPY ( $k=3.1$ ) were highly sensitive to DMSO content: above 30% DMSO, AHPY was severely distorted with peak splitting. DABS exhibited shifts in retention for all incremental increases in DMSO content and efficiency loss was high at 64% (Fig. 6.9d: 5,764 plates at 100% DMSO, 16,587 plates at 20% DMSO) (data provided in Table 6.5, for information). It is apparent from the peak shape DMSO in Fig. 6.9a that the DMSO overloads the column, which may be due to volume overload or mass overload. However the injection volume (5  $\mu$ L) is not excessively large for the standard HPLC column used in this part of the study (4.6 x 250mm, 5  $\mu$ m) and this is perhaps unlikely. To closer examine the DMSO peak, Fig. 6.9e shows a zoomed in chromatogram of the 100% DMSO injection from Fig. 6.9c, with a low wavelength UV channel displayed (215nm in 6.9e, 330nm in 6.9c) and highly retentive conditions on the Atlantis column (95% ACN mobile phase buffered with 5mM AF pH 3). Given that DMSO has some affinity for the stationary phase (Fig. 6.9a), mass overload is possible. In the neat DMSO injection (Fig. 6.9a,e), 5 mg of DMSO is injected which is large for an analytical column, around 1000 times larger than the sample mass injected for the individual solutes (5  $\mu$ g). Closer inspection of Fig. 6.9e shows that although the majority of the DMSO retains until around 7-8 min, the DMSO remains on the column until around 15 min into the run, under these isocratic, highly-retentive conditions. It is interesting that DMSO has a hydrogen bond basicity of 0.43, which is somewhat higher than acetone (0.38) and acetonitrile (0.25) (Snyder *et al.* 2010). In the case of acetone as a mobile phase modifier (4.2.1), it is possible this solvent interacts with hydrogen bonding solutes resulting loss of retention. The similarly strong hydrogen bonding basicity of DMSO, when used in high diluent content, perhaps similarly interacts strongly with these solutes, all three of which contain hydrogen bonding groups (3 on AHPY, 4 on APCA, 5 on DABS). In contrast,

when acetone was used as diluent (4.3), its effect on retention or peak shape was negligible (Fig. 6.4a), presumably because it is sufficiently hydrophobic ( $\log D > 0$  (www.chemicalize.org)) to be unretained (Fig. 6.4a) and eluted from the column before it could interfere with retention. DMSO, however was retained (Fig. 6.9a) and perhaps mediated between solute and stationary phase in a disruptive manner such that peaks were distorted. A recent study in a series by Dolan, Snyder *et al.* investigating causes of retention in RPLC speculated that in RPLC, solutes capable of hydrogen-bond acidity interact with hydrogen-bond basic silanols on the silica surface of those columns (Carr *et al.* 2015). Additionally, Heaton *et al.* reported that ephedrines able to internally hydrogen-bond were less retentive on a bare silica column than those with available hydrogen-bonding groups (Heaton *et al.* 2012). Perhaps DMSO and acetone are able to accept solute acidic hydrogen bonds from solutes which would otherwise interact with the water layer or silica surface. It is interesting to note the tailing peak shape of DMSO, in contrast to the fronting typically observed for charged bases in HILIC under conditions of mass overload. Nevertheless it is therefore preferable to minimise the quantity of DMSO used to prepare samples in HILIC, for both analysis and purification by ACD (4.4).

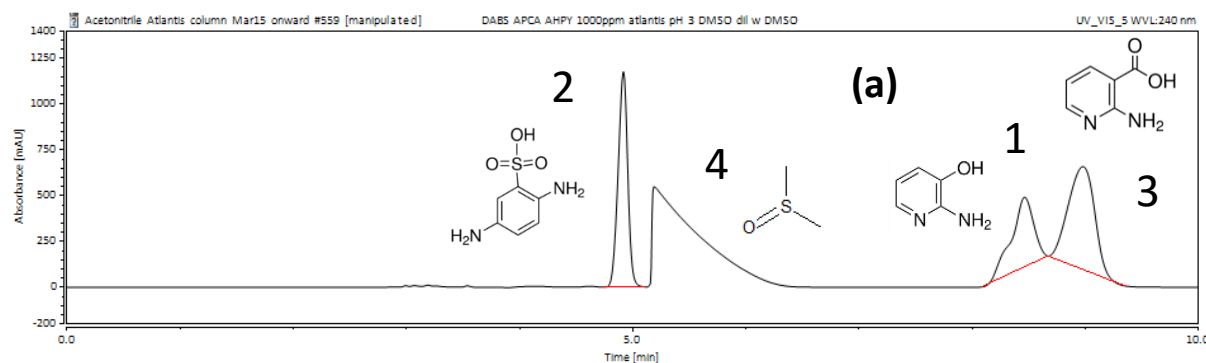


**Fig. 6.9a.** Chromatograms for combined standards of DABS, APCA and AHPY. Diluent neat DMSO. DAD detection at 240nm, mobile phase 85% ACN 5mM AF pH 3 with FA. Atlantis column (4.6 x 250mm, 5  $\mu$ m). Peak identities (1) AHPY, (2) DABS, (3) APCA, (4) DMSO. 5  $\mu$ L injections

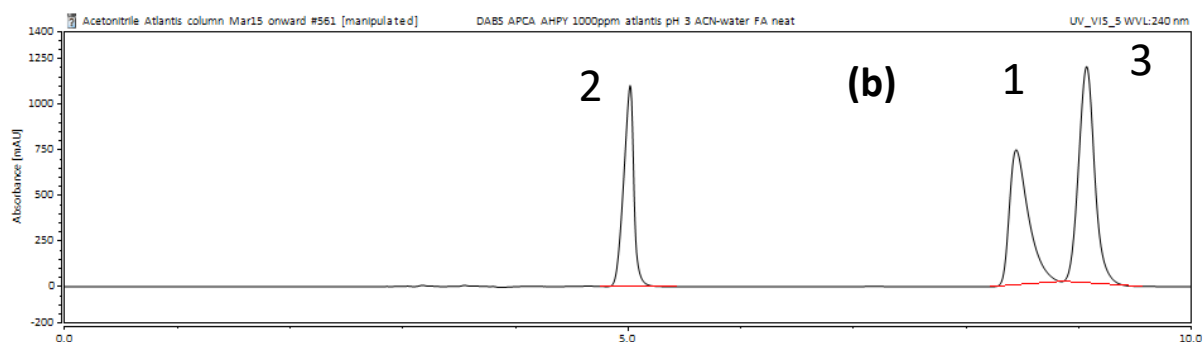


**Fig. 6.9b.** Chromatograms for combined standards of DABS, APCA and AHPY. Diluent ACN-water-FA (50-50, 0.1% acid v/v). DAD detection at 240nm, Mobile phase 85% ACN 5mM AF pH 3 with FA. Atlantis column (4.6 x 250mm, 5  $\mu$ m). Peak identities (1) AHPY, (2) DABS, (3) APCA. 5  $\mu$ L injections

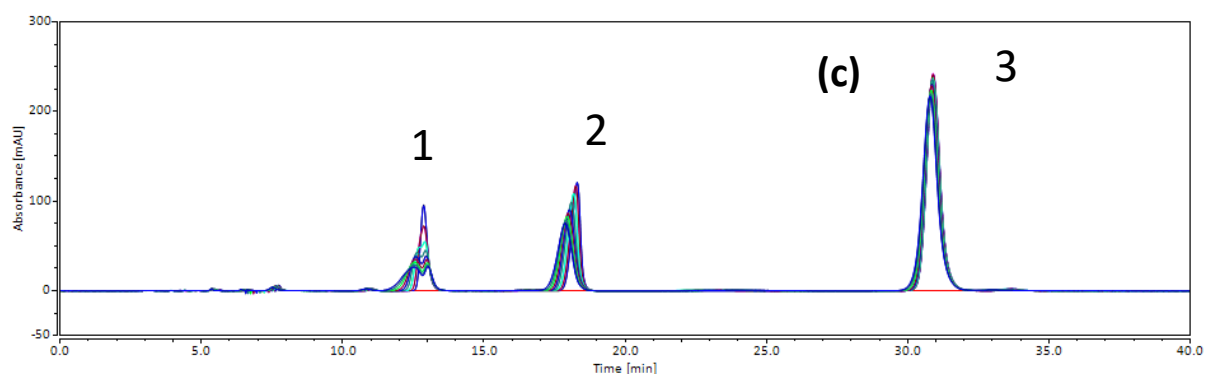


**Fig. 6.9c.** Overlaid chromatograms combined standard prepared in diluent with increasing DMSO content (20-100% DMSO in mobile phase) (Atlantis column, mobile phase 95% ACN 5mM AF pH 3 with FA, UV 330nm). Peak identities (1) AHPY, (2) DABS, (3) APCA. 5  $\mu$ L injections

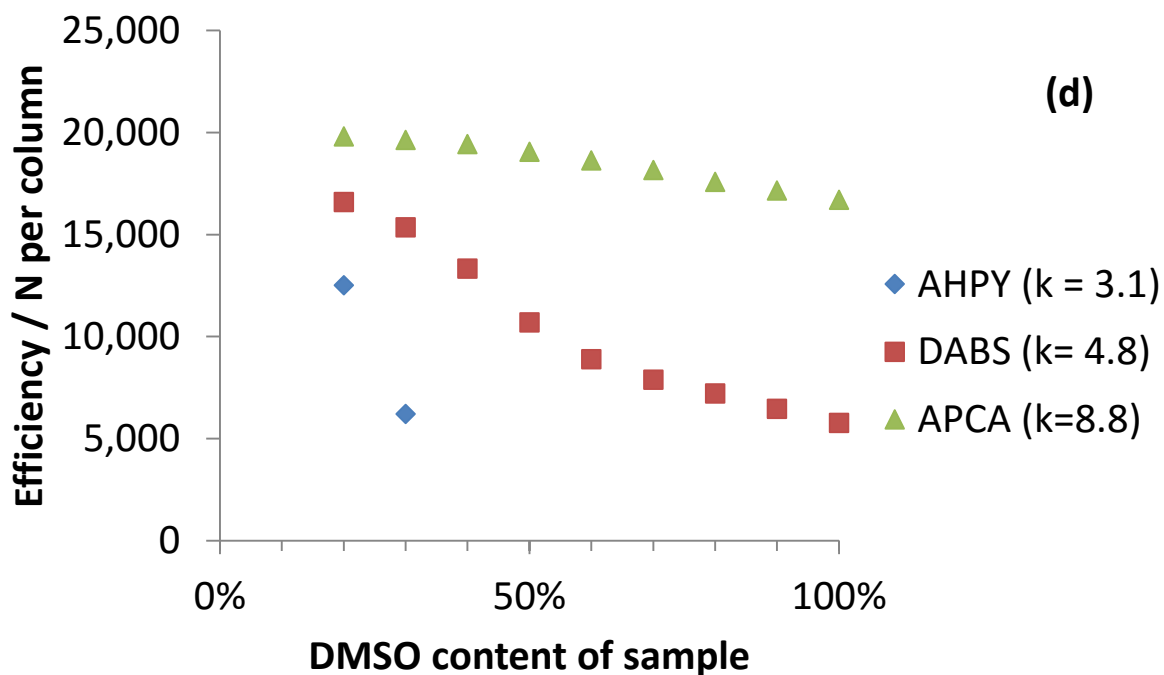


Fig. 6.9d. Plot of efficiency ( $N_{0.5}$ ) vs. DMSO content using data from 6.9c

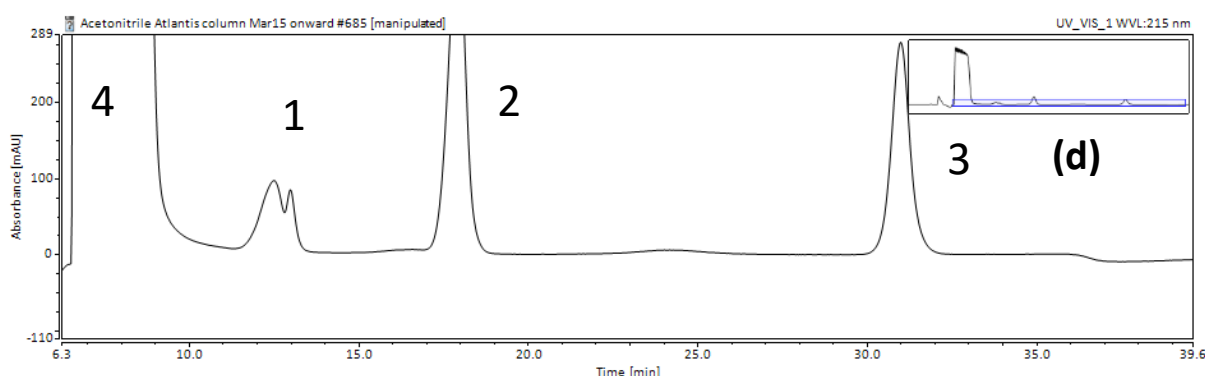


Fig. 6.9e. Zoomed chromatogram using 100% DMSO diluent, UV 215nm. Other conditions as per Fig. 6.9c. Full chromatogram shown inset. 5  $\mu$ L injection

Figure 6.9. Effect of DMSO on isocratic analytical separations (a) chromatograms for combined standards of DABS, APCA and AHPY prepared in neat DMSO showing extra peak observed at low wavelength UV (240nm, 85% ACN 5mM AF pH 3 with FA) (b) combined standard prepared with ACN-water-FA (50-50, 0.1% acid v/v), (c) overlaid chromatograms combined standard prepared in increasing DMSO content (20-100% DMSO) (Atlantis column, 95% ACN 5mM AF pH 3 with FA) (d) plot of efficiency vs. DMSO content. Peak identities (1) AHPY, (2) DABS, (3) APCA, (4) DMSO.

**Table 6.5 Effect of diluent DMSO content on analytical peak efficiency, for information**

DMSO content in 1mL sample	N / plates per column		
	AHPY (k = 3.1)*	DABS (k= 4.8)*	APCA (k=8.8)*
20%	12,515	16,587	19,812
30%	6,208 <sup>δ</sup>	15,348	19,644
40%	I	13,335	19,428
50%	I	10,689	19,060
60%	I	8,899	18,628
70%	I	7,896	18,164
80%	I	7,215	17,588
90%	I	6,455	17,152
100%	I	5,764	16,699
* t <sub>0</sub> (toluene) = 3.145 min; <sup>δ</sup> peak shouldering; I peak splitting; UV 330nm			



### 4.4.3 Loss of resolution in ACD with 10% TFA diluent

To maximise the mass loaded on column by ACD (4.3.3), TFA was added to sample diluents (1, 5 and 10% TFA v/v in 95% ACN with 5mM AF pH 3, i.e. mobile phase from reservoir B spiked with the respective amount of TFA), with a view to enhance apparent solubility. However as noted in 4.3.3, this was disastrous above 1% TFA with complete loss of retention at 10% TFA (v/v). The conditions used in ACD, where the diluent is slowly injected onto the column to maximise loadability, is perhaps analogous to the use of TFA as a mobile phase buffer on analytical systems. McCalley recently reported that use of TFA in HILIC mobile phases can result in repulsion of bases from bare silica stationary phases, with a possible explanation being the accumulation of positive charges in the column pores. These are perhaps hydroxonium ions that balance the negative charge of trifluoroacetate (McCalley 2015). In ACD the sample is slowly introduced in this technique (3mL / min with make-up from weak-eluting solvent at 17mL / min) in a similar fashion to use of TFA as a mobile phase buffer. It is possible that the excessive TFA (10%) used in some Prep-HILIC-ACD samples (Fig. 6.6a) resulted in a similar phenomenon to that reported on analytical columns when TFA was used as a mobile phase buffer in HILIC (McCalley 2015).

## 5. Conclusion

This study found some generic approaches for analysis and purification of polar 'building block' compounds by HILIC-HPLC, HILIC-Prep and HILIC-Prep-ACD. Attempts at separating a mixture of eight polar probe solutes low pH using formic acid or trifluoroacetic acid were unsuccessful. A high pH method separated only three out of the eight probe solutes, interestingly including the strong base procainamide and the weak bases 6-Aminoindazole and adenine. HILIC methods were developed with alternate selectivity. Following earlier reports of selectivity differences between acetone and acetonitrile (Heaton *et al.* 2011), acetone was substituted for acetonitrile, however there was good correlation between retention of 29 probe solutes including acids, bases and neutrals in acetone and acetonitrile mobile phases. Retention in acetone was lower for equivalent organic content mobile phase on the same column compared to ACN. It is possible that acetone's somewhat stronger hydrogen-bonding basicity contributes to this, perhaps through acetone-solute interactions or acetone-water interactions, the latter of which would preclude an appreciable water layer from forming on the stationary phase. Drawing on the conclusions of HILIC column evaluation studies (Kumar *et al.* 2013, Dinh *et al.* 2011, Kawachi *et al.* 2011), an Atlantis bare silica and BEH Amide column were chosen due to expected alternate selectivity. Generic HILIC methods on both the Atlantis bare silica and BEH Amide column successfully separated all eight test probes, which included weak bases which were structural isomers (2-Amino-3-hydroxypyridine and 2-Aminopyridin-4-ol), two zwitterions (2,5-Diaminobenzenesulfonic acid and 2-Aminopyridine-3-carboxylic acid), two other weak bases (Adenine and 6-Aminoindazole) one strong hydrophilic base (procainamide hydrochloride) and a neutral solute (cytidine). Retention order on these columns was alternative, suggesting in practise switching from one column to the other is a possible option to achieve separation of challenging hydrophilic solutes. Focused isocratic methods were developed using these probe solutes as markers dividing up the full gradient into elution zones, to enhance selectivity in areas where a compound of interest may elute. These methods were transferred to a standard prep system, where separations were possible with injection volumes up to 1 mL. Useful concentrations of simulated crude were achieved using DMSO with a small TFA content (1% v/v) and this was viable for preparative separation of up to 16.5 mg crude on column in a single injection (Atlantis) to 22mg (BEH Amide). Moving the

generic method to an At Column Dilution preparative system, where the sample is introduced slowly onto the head of the column and a make-up flow delivers weakly-eluting mobile phase (95% ACN with 5mM AF pH 3, diluent of mobile phase with 1% TFA added v/v) improved this dramatically to 4 mL injections of similar concentrations. However the ACD system was somehow incompatible with the use of DMSO in the diluent, which was somewhat unexpected. The effect of DMSO diluent on peak shape was characterised on an analytical system using an Atlantis column of identical column chemistry. It was found that DMSO has some affinity for HILIC stationary phase, in addition to the affinity solutes have for DMSO implied by their good solubility in this solvent. DMSO content above 20% analytically resulted in peak splitting for a weakly-retained solute and loss of theoretical plates for better-retained solutes. However the performance of DMSO as a diluent on standard preparative systems was acceptable in many cases. On the ACD system, even at injection volumes comparable to the standard prep system (1mL), separation was impossible. It is unclear how ACD is incompatible with DMSO for that technique, and the large injection volumes used in ACD are perhaps a contributory factor. However a possible explanation is that the slow sample introduction, which is purposefully used in ACD, enables the DMSO to percolate through the column and overload adsorption sites which disrupts solute retention. It is advised that DMSO is used with caution in HILIC, to preserve acceptable chromatographic performance analytically and preparatively when ACD is used. Low levels of TFA, however, gave improvements in apparent solubility, and provided its content was limited to 1 % (v/v), there was no obvious deleterious effect on chromatography. Use of TFA even afforded good apparent solubility in acetonitrile-rich diluent with careful warming of samples (31.7 mg / mL). Productivity plots adapted from (Forssén *et al.* 2014) to a generic measurement of crude purified per hour showed clear viability of HILIC-Prep and HILIC-Prep-ACD to purify useful quantities of hydrophilic 'building block' compounds (63 mg / h and 223 mg /h, respectively). Overall it is concluded that HILIC is viable as a technique to analyse and purify compounds in fragment-based drug design. Further work is necessary to evaluate both columns in ACD and apply conclusions from this study to broader projects. Other techniques such as supercritical fluid chromatography (SFC) (Lesellier *et al.* 2015), which uses carbon dioxide as an organic mobile phase under high pressure, can also separate polar solutes. Both techniques have mobile phase that is easily removed in work up following purification although CO<sub>2</sub> sublimates to gas once the pressure

is removed. It is anticipated that HILIC and SFC are complementary options in achieving these aims.

## **Chapter 7**

# **Overall Conclusion and Further Work**

## 1. Overall Conclusion

Generic methods for analysis and purification of polar pharmaceuticals were developed using the technique hydrophilic interaction chromatography (HILIC). The mobile phase was chosen based on a detailed study of possible buffers, including simple acids and buffers on a range of stationary phases. Formic acid as a mobile phase buffer was disastrous in terms of peak efficiency for ionisable compounds, and resulted in retention shifts. It is believed that the reasons for this are the low ionic strength of formic acid, which is poorly able to shield ionogenic solutes from solute-solute and solute-stationary phase repulsion, thus resulting in poor efficiency. Ammonium formate buffer, 5mM  $w^w$  pH 3, was chosen as a generic mobile phase buffer, which gave good to excellent peak efficiency for most solutes on all columns studied. Measurement of pH where the electrode is first calibrated in aqueous buffers then the hydroorganic solvent (acetonitrile/water with buffer) showed the  $w^s$  pH of the buffer when measured in high concentrations of acetonitrile is more-neutral than expected from the  $w^w$  pH 3 (measured in aqueous solution).

The performance of the Charged Aerosol Detector with Hydrophilic Interaction Chromatography (HILIC) was evaluated with a broad range of solutes, using two HILIC columns and by flow injection analysis (FIA). It was anticipated that CAD response would be excellent in HILIC due to facile evaporation of these acetonitrile-rich mobile phases. This was the case: peak areas doubled in HILIC compared to RPLC conditions by FIA, and signal to noise ratios roughly quadrupled which was even better than expected. On further investigation, the noise decreased in HILIC compared to RPLC conditions, again possibly due to facile evaporation. The CAD was found to have quasi-universal response, with no response for volatile solutes that are liquid at room temperature and reduced response for so-called

semi-volatile solutes such as caffeine. Response was reasonably uniform for 21 non-volatile solutes (14% RSD with HILIC mobile phase), and a previously unreported observation was made that bases gave higher responses than neutral compounds. It was considered possible that this was due to salt formation, and the increased CAD response was possibly due to added mass from a salt counter-ion. Studies of response for a range of solute chemistries using mobile phase acid buffers with increasing acid anion mass (FA, TFA and HFBA respectively) showed basic solutes exhibited somewhat increased response in the heavier-acid anions. However this did not increase stoichiometrically with the increased mass of acid anion, suggesting a complex mechanism. Unexpectedly, response for weak acids decreased when TFA and HFBA were used relative to the response in FA. TFA and HFBA are stronger acids and it is possible that weak acids were neutralised. In accordance with earlier observations, the neutral form of a solute can give lower CAD response than when charged, and it was suggested it is possible the short time available to undergo all detector processes ( $\sim 1\text{s}$ ) favours rapid formation of stable aerosol particles, which is conceivably easier for ionogenic solutes due to stronger intermolecular forces. Detector linearity was investigated by HPLC for an acid, a hydrophobic base and a hydrophilic neutral solute, and found to be non-linear over 1-1000 mg / L (three orders of magnitude). It was attempted to fit experimental data to an equation derived from aerosol formation in ELSD, but the CAD plots were more-linear than expected over this scale. It is speculated that particle density does not increase in proportion to increases in solute concentration, which could explain the shape of the CAD calibration curves. Non-chromophoric solutes were successfully detected by CAD, including inorganic salts (combined standard including ions  $\text{Na}^+$ ,  $\text{Cl}^-$ ,  $\text{K}^+$ ,  $\text{NO}_3^-$ ,  $\text{Li}^+$ ,  $\text{Br}^-$ ,  $\text{I}^-$ ) which were separated isocratically on a BEH Amide column. Loading large amounts of the salt nortriptyline hydrochloride on a BEH Amide and bare silica Atlantis column revealed

that chloride signal did not level off at higher concentrations. This suggested that cations and anions migrate separately down the column at all observed concentrations, forming independent solute bands. Using these data, a dynamic range over four orders of magnitude was observed (1 – 10,000 mg / L). A new version of the CAD, the Corona Veo, was compared to the previous Corona Ultra model. The Veo nebuliser was a concentric design, comparable to an MS interface, as opposed to the cross-flow design of the Ultra, comparable to atomic adsorption spectroscopy. At moderate sample concentrations, the signal to noise ratio was superior on the Ultra model, which was unexpected. It is speculated that the change in nebuliser design is a possible cause of this, since concentric nebulisers are designed to deliver the majority of the effluent, whereas cross-flow nebulisers send the majority of effluent to waste. Although more solute is delivered to the detector in the Veo, more noise is also transported and the signal quality suffers. A feature of the Veo was the ability to increase the evaporation tube temperature up to 90°C, to manipulate volatility and improve signal quality. This feature was used in a study on the viability of HILIC-CAD to retain and detect highly hydrophilic species with no chromophore: simple sugars and amino acids. Use of an optimised evaporation temperature at 70°C improved signal and signal quality for the sugars glucose and galactose from below the limit of detection to above the limit of quantitation. However we observed disastrous losses of signal for hydrophobic solutes at temperature increases (30°C to 60°C and 80°C). It is possible this was due to evaporation of hydrophobic species from the aerosol droplet at elevated temperatures. It was therefore recommended that evaporation temperature kept low as a generic detector setting. Using the Ultra CAD and an amino column with HILIC mobile phase, real samples of cider and beer were analysed for content of simple sugars. High levels of fructose (4 g per British pint) and glucose (~30 g per British pint) were found in the cider, though glucose peak shape was



distorted and quantitation of that sugar can only be roughly estimated. A possible cause was the acidity of the cider sample slowing down the speed of mutarotation and this analysis requires further method development. A combined standard of four underivatised amino acids was retained by HILIC on an Atlantis bare silica column and detected by CAD, although baseline resolution was not achieved. Separation of these highly hydrophilic species remains challenging even by HILIC and generic method development is preferable to optimise time spent on these separations.

A selection of polar building block solutes was chosen to evaluate the viability of HILIC as purification technique: eight solutes containing zwitterions, weak bases, a strong base and a hydrophilic neutral species. Some approaches to develop methods with alternate selectivity, which can then be used in a 'tool box' of methods. Using analytical columns, separation of this mixture was impossible by RPLC at low pH, and at high pH only three out of eight were resolved. HILIC separations were therefore investigated. To achieve alternate selectivity, the possibility of changing mobile phase organic solvent was investigated using a bare silica HILIC column. Acetone was substituted for acetonitrile, as ACN is expensive and toxic and has been reported to show alternate selectivity (Heaton *et al.* 2011). However, to compare selectivity between the two mobile phases, the correlation coefficients of separations for 29 solutes on an Atlantis column using acetone or ACN were found to be near one. This suggests the retention order is relatively unchanged between acetone and ACN and this alternative solvent probably offers little selectivity advantages. Interestingly, retention of acids was lost completely in acetone. Additionally, solutes with strong hydrogen-bonding character lost retention to a greater extent than those with lower hydrogen-bonding character. Acetone is a relatively strong hydrogen-bonding base, and it is possible this is

able to hydrogen-bond to the solute, and thus reduce solute-stationary phase interactions. Alternatively, acetone may hydrogen-bond with the stationary phase and block solute retention: retention for all species was lower in acetone than ACN. Instead, achieving alternate selectivity by changing the column was considered, as reports suggested this can be effective in HILIC (e.g. Kumar *et al.* 2013). Generic HILIC gradient methods were developed on bare silica and BEH Amide analytical columns and these could resolve a mixture of all eight solutes. Focused isocratic methods were then developed to further improve upon these separations for solutes eluted in early and central zones of the gradient. These methods were transferred to a preparative system using wider-bore columns with identical chemistry and length (21 vs. 4.6 mm i.d., 15 cm length, 5  $\mu$ m particle size). A generic measure of productivity was used, measured in mg of 'crude' purified per hour, was used to evaluate performance for three simulated crudes using generic and focused methods. The generic method was then transferred to an At-Column Dilution preparative system, where the separation scaled up to 4,000  $\mu$ L injections and resulted in productivity in excess of 250 mg of crude purified per hour. The conclusion was that HILIC is indeed a viable purification technique for polar pharmaceuticals. Solvents used in the sample diluent had some deleterious effects on the separations, namely dimethylsulfoxide (DMSO) and water, both of which can dissolve hydrophilic solutes. Investigation on an analytical system with an Atlantis bare silica column showed DMSO destroyed peak shape at greater than 20% v/v concentration (the rest being ACN) in the injection solvent, although it did improve apparent solubility for hydrophilic solutes. On balance, minimising DMSO content was advised in a generic setup.

## 2. Further Work

Similarities in retention behaviour between the bare silica and type C silica were intriguing, similarly for reports by the Watson group (Bawazeer *et al.* 2012). It is unclear what the specific cause of this is. Further study including analysis of stationary phase emptied from columns and examined with a suitable technique such as FT-IR or NMR may elucidate this further. It is anticipated a possible cause is the silica hydride bond itself is unstable. An alternative interpretation is the crosslink siloxanes in the 'silanised' layer of silica hydride are not in fact connected, providing a layer of silanol groups. This would mean a highly hydrophilic environment in the pores of 'type C' silica. This would be somewhat different to the environment of 'type B' silica which contains siloxane bonds which are reasonably lipophilic and silanols which are hydrophilic. However, a study by Santali *et al.* showed the retention of quaternary basic solutes increased at low ACN content on both 'type B' and 'type C' silica columns when a quaternary salt-buffered mobile phase was used. Although not commented on by those authors, this suggests that siloxane crosslinks were in fact intact. Therefore the stability of the silica hydride bond is perhaps a cause.

The HILIC-CAD applications (Chapter 5) of sugar and amino acid analysis require further method optimisation. It is anticipated that use of the Ultra CAD with a BEH Amide column and high pH mobile phase can perform this analysis. Given that sugar consumption has health implications, and current labelling on sweetened beverages only states the overall sugar content, a generic HILIC-CAD sugar analysis would be useful to determine levels of individual sugars. Therefore collaboration with a healthcare researcher would perhaps be appropriate. Integration of a generic method similar to those in chapter 6 with inverse gradient equipment (Gorecki *et al.* 2006) is perhaps a promising strategy for that. It is *a*.

*priori* known that beers and ciders contain sugar based on their apparent sweetness, but not which individual sugar and at what levels those are. Based on anecdotal evidence the general population are unfamiliar with HPLC or indeed any separation science beyond separating dyes on filter paper as taught in school. It may therefore be an interesting public engagement exercise to educate people about HPLC, CAD and sugar content of drinks to collect samples of alcoholic drinks from volunteers in an evening, for example from a Student's Union, analyse those using a pre-prepared generic HILIC-CAD method and send those to the volunteer for their information. Perhaps even a smartphone app could be developed for this purpose.

A pragmatic study of purification by HILIC showed performance in terms of productivity for HILIC in prep was excellent, particularly when At-Column dilution was used (chapter 6). However the precise reason for improved stationary phase loadability in HILIC compared to RPLC for polar pharmaceuticals remains elusive. Though not shown here, a brief study was undertaken in this project comparing bare silica, BEH amide and BEH-C18 columns for some bases. The Atlantis outperformed the BEH Amide and both HILIC columns outperformed BEH-C18. This may be due to the partition mechanism of HILIC involving the water layer, rather than a possible surface interaction mechanism in RP, although partition is also a component of RP retention. However bare silica columns in HILIC show better loadability of bases than RP (McCalley 2007, Gritti *et al.* 2015), and for example the base procainamide had distorted peak shape on the BEH Amide column in chapter 6. It is speculated that bare silica columns such as the Atlantis are optimal for purification of basic solutes by HILIC, due to an abundance of cation exchange sites in the form of silanols. Bonded phase columns such as the BEH Amide do not have such availability of cation exchange sites, as shown by

their weak cation exchange behaviour in terms of retention (Kawachi *et al.* 2011, Dinh *et al.* 2011, Kumar *et al.* 2013). Likewise perhaps neutral solutes are perhaps better suited to a polar bonded phase column such as BEH Amide, as those columns are thought to hold more water for solute partitioning (Dinh *et al.* 2013). A study comparing loadability of HILIC column chemistries other than bare silica (e.g. BEH Amide, ZIC-HILIC, pentadiol) may show good performance for neutral and zwitterionic solutes. Additionally, alternative non-silica stationary phases such as porous graphitic carbon (PGC, Hypercarb) may have alternative selectivity in HILIC mobile phase. However their loadability in HILIC mobile phase is uncharacterised and is interesting for further study.

The full adoption of HILIC-Prep and HILIC-Prep-ACD is desirable given the promising results in chapter 6. This is outside of the scope of this study, which instead has been disseminated to the industrial collaborator of this project to inform decisions with regards to these techniques. In particular, comparison to an evaluation of SFC would inform the optimum choice of technique for polar pharmaceuticals.

A possible explanation for reduced retention in acetone compared to acetonitrile HILIC mobile phase is possibly a disruption of hydrogen bonding between the solute and stationary phase (chapter 6). However the main focus of that study was on developing generic methods for analysis and purification, and limited time could be spent investigating this issue. A report by Carr *et al.* suggested 'type III' hydrogen bonding columns in RPLC, i.e. those which contain a polar group as a ligand, had strong hydrogen-bonding with solutes (Carr *et al.* 2015). A more in-depth study comparing retention in acetone and ACN on a BEH Amide column in HILIC may show less-pronounced reduction in retention compared to the bare silica column used in chapter 6, as BEH Amide columns have hydrogen bonding

character shown by retention increasing greatly in 95% compared to 85% ACN for certain solutes. e.g. uridine (Kumar *et al.* 2013). The weak retention afforded by acetone mobile phase may be a useful attribute for highly hydrophilic species such as sugars and amino acids, where the UV absorbance of acetone isn't a problem.

## References

Allen, L.B. and Koropchak, J.A., 1993. Condensation Nucleation Light-Scattering - a New Approach to Development of High-Sensitivity, Universal Detectors for Separations. *Analytical Chemistry*, **65**(6), pp. 841-844.

Almeling, S., Ilko, D. and Holzgrabe, U., 2012. Charged aerosol detection in pharmaceutical analysis. *Journal of pharmaceutical and biomedical analysis*, **69**, pp. 50-63.

Alpert, A., 1990. Hydrophilic-Interaction Chromatography for the Separation of Peptides, Nucleic-Acids and Other Polar Compounds. *Journal of chromatography*, **499**, pp. 177-196.

Alsenz, J. and Kansy, M., 2007. High throughput solubility measurement in drug discovery and development. *Advanced Drug Delivery Reviews*, **59**(7), pp. 546-567.

Bawazeer, S., Sutcliffe, O.B., Euerby, M.R., Bawazeer, S. and Watson, D.G., 2012. A comparison of the chromatographic properties of silica gel and silicon hydride modified silica gels. *Journal of Chromatography a*, **1263**, pp. 61-67.

Berthod, A., 1991. Silica: backbone material of liquid chromatographic column packings. *Journal of Chromatography A*, **549**(0), pp. 1-28.

Bicker, W., WU, J., Laemmerhofer, M. and Lindner, W., 2008. Hydrophilic interaction chromatography in nonaqueous elution mode for separation of hydrophilic analytes on silica-based packings with noncharged polar bondings. *Journal of Separation Science*, **31**(16-17), pp. 2971-2987.

Blanco Gomis, D., Muro Tamayo, D. and Mangas Alonso, J., 2001. Determination of monosaccharides in cider by reversed-phase liquid chromatography. *Analytica Chimica Acta*, **436**(1), pp. 173-180.

Boysen, R.I., Yang, Y., Chowdhury, J., Matyska, M.T., Pesek, J.J. and Hearn, M.T.W., 2011. Simultaneous separation of hydrophobic and hydrophilic peptides with a silica hydride stationary phase using aqueous normal phase conditions. *Journal of Chromatography A*, **1218**(44), pp. 8021-8026.

Buckenmaier, S.M.C., McCalley, D.V. and Euerby, M.R., 2004. Rationalisation of unusual changes in efficiency and retention with temperature shown for bases in reversed-phase high-performance liquid chromatography at intermediate pH. *Journal of Chromatography A*, **1060**(1-2), pp. 117-126.

Camenzuli, M., Ritchie, H.J., Ladine, J.R. and Shalliker, R.A., 2012. Enhanced separation performance using a new column technology: Parallel segmented outlet flow. *Journal of Chromatography a*, **1232**, pp. 47-51.

Carr, P.W., Dolan, J.W., Dorsey, J.G., Snyder, L.R. and Kirkland, J.J., 2015. Contributions to reversed-phase column selectivity: III. Column hydrogen-bond basicity. *Journal of Chromatography A*, **1395**(0), pp. 57-64.

Carr, P.W., Dolan, J.W., Neue, U.D. and Snyder, L.R., 2011. Contributions to reversed-phase column selectivity. I. Steric interaction. *Journal of Chromatography a*, **1218**(13), pp. 1724-1742.

Charlesworth, J., 1978. Evaporative Analyzer as a Mass Detector for Liquid-Chromatography. *Analytical Chemistry*, **50**(11), pp. 1414-1420.



- Cohen, R.D., Liu, Y. and Gong, X., 2012. Analysis of volatile bases by high performance liquid chromatography with aerosol-based detection. *Journal of Chromatography a*, **1229**, pp. 172-179.
- Dai, J., Carr, P.W. and MCCalley, D.V., 2009. A new approach to the determination of column overload characteristics in reversed-phase liquid chromatography. *Journal of Chromatography A*, **1216**(12), pp. 2474-2482.
- Dai, J., Mendonsa, S.D., Bowser, M.T., Lucy, C.A. and Carr, P.W., 2005. Effect of anionic additive type on ion pair formation constants of basic pharmaceuticals. *Journal of Chromatography A*, **1069**(2), pp. 225-234.
- Davies, N.H., Euerby, M.R. and MCCalley, D.V., 2008. Analysis of basic compounds by reversed-phase high-performance liquid chromatography using hybrid inorganic/organic phases at high pH. *Journal of Chromatography a*, **1178**(1-2), pp. 71-78.
- Dinh, N.P., Jonsson, T. and Irgum, K., 2013. Water uptake on polar stationary phases under conditions for hydrophilic interaction chromatography and its relation to solute retention. *Journal of Chromatography A*, **1320**(0), pp. 33-47.
- Dinh N.P., Jonsson, T. and Irgum, K., 2011. Probing the interaction mode in hydrophilic interaction chromatography. *Journal of Chromatography A*, **1218**(35), pp. 5880-5891.
- Dixon, R.W. and Baltzell, G., 2006. Determination of levoglucosan in atmospheric aerosols using high performance liquid chromatography with aerosol charge detection. *Journal of Chromatography A*, **1109**(2), pp. 214-221.
- Dixon, R. and Peterson, D., 2002. Development and testing of a detection method for liquid chromatography based on aerosol charging. *Analytical Chemistry*, **74**(13), pp. 2930-2937.
- Dolan, J.W., 2014. How Much Can I Inject? Part I: Injecting in Mobile Phase. *Lc Gc North America*, **32**(10), pp. 780-+.
- Dunn, A., April 2013. *Experiences in automating System Suitability* April 2013, 2013 Chromatographic Society Spring Meeting.
- Eble, J.E., Grob, R.L., Antle, P.E. and Snyder, L.R., 1987. Simplified description of high-performance liquid chromatographic separation under overload conditions, based on the Craig distribution model: II. Effect of isotherm type, and experimental verification of computer simulations for a single band. *Journal of Chromatography A*, **384**, pp. 45-79.
- Eom, H.Y., Park, S., Kim, M.K., Suh, J.H., Yeom, H., Min, J.W., Kim, U., Lee, J., Youm, J. and Han, S.B., 2010. Comparison between evaporative light scattering detection and charged aerosol detection for the analysis of saikosaponins. *Journal of Chromatography A*, **1217**(26), pp. 4347-4354.
- Espada, A., Molina-Martin, M., Dage, J. and Kuo, M., 2008. Application of LC/MS and related techniques to high-throughput drug discovery. *Drug discovery today*, **13**(9-10), pp. 417-423.
- Fallas, M.M., Buckenmaier, S.M.C. and MCCalley, D.V., 2012. A comparison of overload behaviour for some sub 2  $\mu$  m totally porous and sub 3  $\mu$  m shell particle columns with ionised solutes. *Journal of Chromatography a*, **1235**, pp. 49-59.
- Forssén, P., Samuelsson, J. and Fornstedt, T., 2014. Relative importance of column and adsorption parameters on the productivity in preparative liquid chromatography II: Investigation of separation

systems with competitive Langmuir adsorption isotherms. *Journal of Chromatography A*, **1347**(0), pp. 72-79.

Fraser, M. and Lakshmanan, K., 2000. Using levoglucosan as a molecular marker for the long-range transport of biomass combustion aerosols. *Environmental science & technology*, **34**(21), pp. 4560-4564.

Gagliardi, L.G., Castells, C.B., Rafols, C., Roses, M. and Bosch, E., 2007. delta Conversion parameter between pH scales ((s)(w)pH and (s)(s)pH) in acetonitrile/water mixtures at various compositions and temperatures. *Analytical Chemistry*, **79**(8), pp. 3180-3187.

Galanakis, E.G., Megoulas, N.C., Solich, P. and Koupparis, M.A., 2006. Development and validation of a novel LC non-derivatization method for the determination of amikacin in pharmaceuticals based on evaporative light scattering detection. *Journal of pharmaceutical and biomedical analysis*, **40**(5), pp. 1114-1120.

Gamache, P., McCarthy, R., Freeto, S., Asa, D., Woodcock, M., Laws, K. and Cole, R., 2005. HPLC analysis of non-volatile analytes using charged aerosol detection. *Lc Gc Europe*, **18**(6), pp. 345-+.

Glowka, F.K. and Karazniewicz-Lada, M., 2007. Determination of roxithromycin in human plasma by HPLC with fluorescence and UV absorbance detection: Application to a pharmacokinetic study. *Journal of Chromatography B-Analytical Technologies in the Biomedical and Life Sciences*, **852**(1-2), pp. 669-673.

Gorecki, T., Lynen, F., Szucs, R. and Sandra, P., 2006. Universal response in liquid chromatography using charged aerosol detection. *Analytical Chemistry*, **78**(9), pp. 3186-3192.

Gritti, F. and Guiochon, G., 2015. Hydrophilic interaction chromatography: A promising alternative to reversed-phase liquid chromatography systems for the purification of small protonated bases. *Journal of Separation Science*, **38**(10), pp. 1633-1641.

Gritti, F. and Guiochon, G., 2013a. Effect of parallel segmented flow chromatography on the height equivalent to a theoretical plate. I—Performance of 4.6 mm × 30 mm columns packed with 3.0 μm Hypurity-C18 fully porous particles. *Journal of Chromatography A*, **1297**(0), pp. 64-76.

Gritti, F. and Guiochon, G., 2013b. Comparison between the intra-particle diffusivity in the hydrophilic interaction chromatography and reversed phase liquid chromatography modes. Impact on the column efficiency. *Journal of Chromatography a*, **1297**, pp. 85-95.

Gritti, F. and Guiochon, G., 2013c. Mass transfer mechanism in hydrophilic interaction chromatography. *Journal of Chromatography a*, **1302**, pp. 55-64.

Gritti, F. and Guiochon, G., 2009. Adsorption mechanism of acids and bases in reversed-phase liquid chromatography in weak buffered mobile phases designed for liquid chromatography/mass spectrometry. *Journal of Chromatography A*, **1216**(10), pp. 1776-1788.

Gritti, F. and Guiochon, G., 2009. Band profiles of reacting acido-basic compounds with water–methanol eluents at different and ionic strengths in reversed-phase liquid chromatography. *Journal of Chromatography A*, **1216**(15), pp. 3175-3184.

Gritti, F. and Guiochon, G., 2004. Retention of Ionizable Compounds in Reversed-Phase Liquid Chromatography. Effect of the Ionic Strength of the Mobile Phase and the Nature of the Salts Used on the Overloading Behavior. *Analytical Chemistry*, **76**(16), pp. 4779-4789.

Gritti, F., Hölzel, A., Tallarek, U. and Guiochon, G., 2015. The relative importance of the adsorption and partitioning mechanisms in hydrophilic interaction liquid chromatography. *Journal of Chromatography A*, **1376**(0), pp. 112-125.

Guiochon, G., Moysan, A. and Holley, C., 1988. Influence of various Parameters on the Response Factors of the Evaporative Light-Scattering Detector for a Number of Non-Volatile Compounds. *Journal of Liquid Chromatography*, **11**(12), pp. 2547-2570.

Guiochon, G. and Trapp, O., 2013. Basic Principles of Chromatography. *Ullmann's Encyclopedia of Industrial Chemistry*. Wiley-VCH Verlag GmbH & Co. KGaA, .

Guo, Y. and Gaiki, S., 2005. Retention behavior of small polar compounds on polar stationary phases in hydrophilic interaction chromatography. *Journal of Chromatography a*, **1074**(1-2), pp. 71-80.

Hägglund, I. and Ståhlberg, J., 1997. Ideal model of chromatography applied to charged solutes in reversed-phase liquid chromatography. *Journal of Chromatography A*, **761**(1-2), pp. 3-11.

*Halo Penta-HILIC brochure*. 2014.

Harris, D.C., 2007. *Quantitative Chemical Analysis, Seventh edition*. NY: Freeman, New York.

Heaton, J.C. and MCalley, D.V., 2016. Some factors that can lead to poor peak shape in hydrophilic interaction chromatography, and possibilities for their remediation. *Journal of Chromatography A*, **1427**, pp. 37-44.

Heaton, J.C. and MCalley, D.V., 2014a. Comparison of the kinetic performance and retentivity of sub-2  $\mu\text{m}$  core-shell, hybrid and conventional bare silica phases in hydrophilic interaction chromatography. *Journal of Chromatography A*, **1371**(0), pp. 106-116.

Heaton, J.C., Russell, J.J., Underwood, T., Boughtflower, R. and MCalley, D.V., 2014b. Comparison of peak shape in hydrophilic interaction chromatography using acidic buffers and simple acid solutions. *Journal of chromatography.A*, **1347**, pp. 39-48.

Heaton, J.C., Wang, X., Barber, W.E., Buckenmaier, S.M.C. and MCalley, D.V., 2014c. Practical observations on the performance of bare silica in hydrophilic interaction compared with C18 reversed-phase liquid chromatography. *Journal of Chromatography A*, **1328**(0), pp. 7-15.

Heaton, J., Jones, M.D., Legido-Quigley, C., Plumb, R.S. and Smith, N.W., 2011. Systematic evaluation of acetone and acetonitrile for use in hydrophilic interaction liquid chromatography coupled with electrospray ionization mass spectrometry of basic small molecules. *Rapid Communications in Mass Spectrometry*, **25**(24), pp. 3666-3674.

Hirs, C.H.W., Moore, S. and Stein, W.H., 1952. Isolation of amino acids by chromatography on ion exchange columns; use of volatile buffers. *The Journal of biological chemistry*, **195**(2), pp. 669-696.

Hemstrom, P. and Irgum, K., 2006. Hydrophilic interaction chromatography. *Journal of Separation Science*, **29**(12), pp. 1784-1821.

Hoelke, B., Gieringer, S., Arlt, M. and Saal, C., 2009. Comparison of Nephelometric, UV-Spectroscopic, and HPLC Methods for High-Throughput Determination of Aqueous Drug Solubility in Microtiter Plates. *Analytical Chemistry*, **81**(8), pp. 3165-3172.

Hutchinson, J.P., Li, J., Farrell, W., Groeber, E., Szucs, R., Dicinoski, G. and Haddad, P.R., 2011. Comparison of the response of four aerosol detectors used with ultra high pressure liquid chromatography. *Journal of Chromatography a*, **1218**(12), pp. 1646-1655.

Hutchinson, J.P., Li, J., Farrell, W., Groeber, E., Szucs, R., Dicinoski, G. and Haddad, P.R., 2010. Universal response model for a corona charged aerosol detector. *Journal of Chromatography a*, **1217**(47), pp. 7418-7427.

Hutchinson, J.P., Remenyi, T., Nesterenko, P., Farrell, W., Groeber, E., Szucs, R., Dicinoski, G. and Haddad, P.R., 2012. Investigation of polar organic solvents compatible with Corona Charged Aerosol Detection and their use for the determination of sugars by hydrophilic interaction liquid chromatography. *Analytica Chimica Acta*, **750**, pp. 199-206.

Jia, S., Park, J.H., Lee, J. and Kwon, S.W., 2011. Comparison of two aerosol-based detectors for the analysis of gabapentin in pharmaceutical formulations by hydrophilic interaction chromatography. *Talanta*, **85**(5), pp. 2301-2306.

Jencks, W., 1981. On the Attribution and Additivity of Binding-Energies. *Proceedings of the National Academy of Sciences of the United States of America-Biological Sciences*, **78**(7), pp. 4046-4050.

Karatapanis, A.E., Flamegos, Y.C. and Stalikas, C.D., 2009. HILIC separation and quantitation of water-soluble vitamins using diol column. *Journal of Separation Science*, **32**(7), pp. 909-917.

Kawachi, Y., Ikegami, T., Takubo, H., Ikegami, Y., Miyamoto, M. and Tanaka, N., 2011. Chromatographic characterization of hydrophilic interaction liquid chromatography stationary phases: Hydrophilicity, charge effects, structural selectivity, and separation efficiency. *Journal of Chromatography a*, **1218**(35), pp. 5903-5919.

Khandagale, M.M., Hilder, E.F., Shellie, R.A. and Haddad, P.R., 2014. Assessment of the complementarity of temperature and flow-rate for response normalisation of aerosol-based detectors. *Journal of Chromatography A*, **1356**(0), pp. 180-187.

Khandagale, M.M., Hutchinson, J.P., Dicinoski, G.W. and Haddad, P.R., 2013. Effects of eluent temperature and elution bandwidth on detection response for aerosol-based detectors. *Journal of Chromatography A*, **1308**(0), pp. 96-103.

Kirkland, J.J. and Destefano, J.J., 2006. The art and science of forming packed analytical high-performance liquid chromatography columns. *Journal of Chromatography a*, **1126**(1-2), pp. 50-57.

Kirkland, J.J., 1968. High-performance ultraviolet photometric detector for use with efficient liquid chromatographic columns. *Analytical Chemistry*, **40**(2), pp. 391-396.

Korfmacher, W.A., 2005. Foundation review: Principles and applications of LC-MS in new drug discovery. *Drug discovery today*, **10**(20), pp. 1357-1367.

Kostiainen, R. and KAUPPILA, T.J., 2009. Effect of eluent on the ionization process in liquid chromatography-mass spectrometry. *Journal of Chromatography A*, **1216**(4), pp. 685-699.

Kumar, A., Heaton, J.C. and MCCalley, D.V., 2013. Practical investigation of the factors that affect the selectivity in hydrophilic interaction chromatography. *Journal of Chromatography A*, **1276**, pp. 33-46.

Laemmerhofer, M., Richter, M., Wu, J., Nogueira, R., Bicker, W. and Lindner, W., 2008. Mixed-mode ion-exchangers and their comparative chromatographic characterization in reversed-phase and hydrophilic interaction chromatography elution modes. *Journal of Separation Science*, **31**(14), pp. 2572-2588.

Lane, S.J., Eggleston, D.S., Brinded, K.A., Hollerton, J.C., Taylor, N.L. and Readshaw, S.A., 2006. Defining and maintaining a high quality screening collection: the GSK experience. *Drug discovery today*, **11**(5-6), pp. 267-272.

Lauritsen, F. and Ketola, R., 1997. Quantitative determination of semivolatile organic compounds in solution using trap-and-release membrane inlet mass spectrometry. *Analytical Chemistry*, **69**(23), pp. 4917-4922.

Law, B. and Temesi, D., 2000. Factors to consider in the development of generic bioanalytical high-performance liquid chromatographic-mass spectrometric methods to support drug discovery. *Journal of Chromatography B*, **748**(1), pp. 21-30.

Lesellier, E. and West, C., 2015. The many faces of packed column supercritical fluid chromatography – A critical review. *Journal of Chromatography A*, **1382**, pp. 2-46.

Lustig, R.H., 2010. Fructose: Metabolic, Hedonic, and Societal Parallels with Ethanol. *Journal of the American Dietetic Association*, **110**(9), pp. 1307-1321.

Mallet, C., Lu, Z. and Mazzeo, J., 2004. A study of ion suppression effects in electrospray ionization from mobile phase additives and solid-phase extracts. *Rapid Communications in Mass Spectrometry*, **18**(1), pp. 49-58.

Mallis, L.M., Sarkahian, A.B., Kulishoff, J.M. and Watts, W.L., 2002. Open-access liquid chromatography/mass spectrometry in a drug discovery environment. *Journal of Mass Spectrometry*, **37**(9), pp. 889-896.

Mant, C.T. and Hodges, R.S., 2008. Mixed-mode hydrophilic interaction/cation-exchange chromatography (HILIC/CEX) of peptides and proteins. *Journal of Separation Science*, **31**(15), pp. 2754-2773.

Marchand, D.H., Carr, P.W., MCCalley, D.V., Neue, U.D., Dolan, J.W. and Snyder, L.R., 2011. Contributions to reversed-phase column selectivity. II. Cation exchange. *Journal of Chromatography A*, **1218**(40), pp. 7110-7129.

Martin, A.J. and Synge, R.L., 1941. *Biochem. J.*, **35**, pp. 1358.

MCCalley, D.V., 2015. Study of retention and peak shape in hydrophilic interaction chromatography over a wide pH range. *Journal of Chromatography A*, **1411**, pp. 41-49.

MCCalley, D.V., 2010a. The challenges of the analysis of basic compounds by high performance liquid chromatography: Some possible approaches for improved separations. *Journal of Chromatography A*, **1217**(6), pp. 858-880.

MCCalley, D.V., 2010b. Study of the selectivity, retention mechanisms and performance of alternative silica-based stationary phases for separation of ionised solutes in hydrophilic interaction chromatography. *Journal of Chromatography a*, **1217**(20), pp. 3408-3417.

MCCalley, D.V., 2008a. Evaluation of the properties of a superficially porous silica stationary phase in hydrophilic interaction chromatography. *Journal of Chromatography A*, **1193**(1–2), pp. 85-91.

MCCalley, D.V., 2007. Is hydrophilic interaction chromatography with silica columns a viable alternative to reversed-phase liquid chromatography for the analysis of ionisable compounds? *Journal of Chromatography a*, **1171**(1-2), pp. 46-55.

MCCalley, D.V. and Neue, U.D., 2008b. Estimation of the extent of the water-rich layer associated with the silica surface in hydrophilic interaction chromatography. *Journal of Chromatography a*, **1192**(2), pp. 225-229.

Melnikov, S.M., Hoeltzel, A., Seidel-Morgenstern, A. and Tallarek, U., 2012. A Molecular Dynamics Study on the Partitioning Mechanism in Hydrophilic Interaction Chromatography. *Angewandte Chemie-International Edition*, **51**(25), pp. 6251-6254.

Melnikov, S.M., Hoeltzel, A., Seidel-Morgenstern, A. and Tallarek, U., 2011. Composition, Structure, and Mobility of Water-Acetonitrile Mixtures in a Silica Nanopore Studied by Molecular Dynamics Simulations. *Analytical Chemistry*, **83**(7), pp. 2569-2575.

Millard, J.W., Alvarez-Núñez, F.A. and Yalkowsky, S.H., 2002. Solubilization by cosolvents: Establishing useful constants for the log–linear model. *International journal of pharmaceuticals*, **245**(1–2), pp. 153-166.

Moreau, R.A., 2006. The analysis of lipids via HPLC with a charged aerosol detector. *Lipids*, **41**(7), pp. 727-734.

Mourey, T.H. and Oppenheimer, L.E., 1984. Principles of Operation of an Evaporative Light-Scattering Detector for Liquid-Chromatography. *Analytical Chemistry*, **56**(13), pp. 2427-2434.

Neue, U.D., 2005. Theory of peak capacity in gradient elution. *Journal of Chromatography A*, **1079**(1–2), pp. 153-161.

Neue, U.D., Mazza, C.B., Cavanaugh, J.Y., Lu, Z. and Wheat, T.E., 2003. At-column dilution for improved loading in preparative chromatography. *Chromatographia*, **57**(1), pp. S121-S127.

Niessen, W.M.A., 2003. Progress in liquid chromatography–mass spectrometry instrumentation and its impact on high-throughput screening. *Journal of Chromatography A*, **1000**(1–2), pp. 413-436.

Nogueira, L.C., Silva, F., Ferreira, I.M.P.L.V.O. and Trugo, L.C., 2005. Separation and quantification of beer carbohydrates by high-performance liquid chromatography with evaporative light scattering detection. *Journal of Chromatography A*, **1065**(2), pp. 207-210.

Olsen, B., 2001. Hydrophilic interaction chromatography using amino and silica columns for the determination of polar pharmaceuticals and impurities. *Journal of Chromatography a*, **913**(1-2), pp. 113-122.

Paulekuhn, G.S., Dressman, J.B. and Saal, C., 2007. Trends in active pharmaceutical ingredient salt selection based on analysis of the Orange Book Database. *Journal of medicinal chemistry*, **50**(26), pp. 6665-6672.

Pellati, F., Prencipe, F.P. and Benvenuti, S., 2013. Headspace solid-phase microextraction-gas chromatography–mass spectrometry characterization of propolis volatile compounds. *Journal of pharmaceutical and biomedical analysis*, **84**(0), pp. 103-111.

Periat, A., Debrus, B., Rudaz, S. and Guillarme, D., 2013a. Screening of the most relevant parameters for method development in ultra-high performance hydrophilic interaction chromatography. *Journal of Chromatography a*, **1282**, pp. 72-83.

Periat, A., Boccard, J., Veuthey, J., Rudaz, S. and Guillarme, D., 2013b. Systematic comparison of sensitivity between hydrophilic interaction liquid chromatography and reversed phase liquid chromatography coupled with mass spectrometry. *Journal of Chromatography a*, **1312**, pp. 49-57.

Periat, A., Grand-Guillaume Perrenoud, A. and Guillarme, D., 2013c. Evaluation of various chromatographic approaches for the retention of hydrophilic compounds and MS compatibility. *Journal of Separation Science*, **36**(19), pp. 3141-3151.

Pesek, J.J., Matyska, M.T. and Kim, A.M., 2013. Evaluation of stationary phases based on silica hydride for the analysis of drugs of abuse. *Journal of Separation Science*, **36**(17), pp. 2760-2766.

Pesek, J.J., Matyska, M.T., Fischer, S.M. and Sana, T.R., 2008. *J. Chromatogr. A*, **1204**, pp. 48.

Poole, C.F. and Poole, S.K., 2009. Foundations of retention in partition chromatography. *Journal of Chromatography a*, **1216**(10), pp. 1530-1550.

Ramos, R.G., Libong, D., Rakotomanga, M., Gaudin, K., Loiseau, P.M. and Chaminade, P., 2008. Comparison between charged aerosol detection and light scattering detection for the analysis of Leishmania membrane phospholipids. *Journal of Chromatography a*, **1209**(1-2), pp. 88-94.

Reid, J.P., Dennis-Smith, B., Kwamena, N.A., Miles, R.E.H., Hanford, K.L. and Homer, C.J., 2011. The morphology of aerosol particles consisting of hydrophobic and hydrophilic phases: hydrocarbons, alcohols and fatty acids as the hydrophobic component. *Physical Chemistry Chemical Physics*, **13**(34), pp. 15559-15572.

Rivera, C.A., Bender, J.S., Manfred, K. and Fourkas, J.T., 2013. Persistence of Acetonitrile Bilayers at the Interface of Acetonitrile/Water Mixtures with Silica. *Journal of Physical Chemistry a*, **117**(46), pp. 12060-12066.

Roth, M., 1971. Fluorescence reaction for amino acids. *Analytical Chemistry*, **43**(7), pp. 880-882.

Russell, J.J., Heaton, J.C., Underwood, T., Boughtflower, R. and MCalley, D.V., 2015. Performance of charged aerosol detection with hydrophilic interaction chromatography. *Journal of Chromatography A*, **1405**, pp. 72-84.

Ruta, J., Rudaz, S., MCalley, D.V., Veuthey, J. and Guillarme, D., 2010. A systematic investigation of the effect of sample diluent on peak shape in hydrophilic interaction liquid chromatography. *Journal of Chromatography A*, **1217**(52), pp. 8230-8240.

Santali, E.Y., Edwards, D., Sutcliffe, O., Bailes S., Euerby M., Watson D.G., 2014. A Comparison of Silica C and Silica Gel in HILIC Mode: The Effect of Stationary Phase Surface Area. *Chromatographia*, **77**, pp. 873-881.

Scott, D.E., Coyne, A.G., Hudson, S.A. and Abell, C., 2012. Fragment-Based Approaches in Drug Discovery and Chemical Biology. *Biochemistry*, **51**(25), pp. 4990-5003.

Schiesel, S., Laemmerhofer, M. and Lindner, W., 2012. Comprehensive impurity profiling of nutritional infusion solutions by multidimensional off-line reversed-phase liquid chromatography x hydrophilic interaction chromatography-ion trap mass-spectrometry and charged aerosol detection with universal calibration. *Journal of Chromatography a*, **1259**, pp. 100-110.

Shaodong, J., Lee, W.J., EE, J.W., Park, J.H., Kwon, S.W. and LEE, J., 2010. Comparison of ultraviolet detection, evaporative light scattering detection and charged aerosol detection methods for liquid-chromatographic determination of anti-diabetic drugs. *Journal of pharmaceutical and biomedical analysis*, **51**(4), pp. 973-978.

Snyder, L.R., Kirkland, J.J. and Dolan, J.W., 2010. *Introduction to Modern Liquid Chromatography*. Hoboken, New Jersey, USA: John Wiley & Sons Inc.

Snyder, L.R., Cox, G.B. and Antle, P.E., 1987. A simplified description of HPLC separation under overload conditions. A synthesis and extension of two recent approaches. *Chromatographia*, **24**(1), pp. 82-96.

Stolyhwo, A., Colin, H. and Guiochon, G., 1983. Use of Light-Scattering as a Detector Principle in Liquid-Chromatography. *Journal of chromatography*, **265**(1), pp. 1-18.

Tei, A., Penduff, P., Guilliet, R. and Schulenberg-Schell, H., 2013. Using Focused Gradients on a Combined Analytical/Preparative HPLC System to Optimize the Scale-up Process from 4.6 to 50 mm Columns. *Lc Gc Europe*, **26**(6), pp. 315-+.

Thomas, D., Bailey, B., Plante, M. and Acworth, I., 2014. *Charged Aerosol Detection and Evaporative Light Scattering Detection – Fundamental Differences Affecting Analytical Performance - Poster presented at HPLC 2014* 2014, Thermo Scientific.

Tyteca, E., Périat, A., Rudaz, S., Desmet, G. and Guillarme, D., 2014. Retention modeling and method development in hydrophilic interaction chromatography. *Journal of Chromatography A*, **1337**(0), pp. 116-127.

Underwood, T., May 2014. *Generic Approaches to the Analysis and Purification of Small, Highly Polar Molecules* May 2014, 2014 Chromatographic Society Spring Meeting.

Van Deemter, J.J., Zuiderweg, F.J. and Klinkenberg, A., 1956. Longitudinal diffusion and resistance to mass transfer as causes of nonideality in chromatography. *Chemical Engineering Science*, **5**(6), pp. 271-289.

Vehovec, T. and Obreza, A., 2010. Review of operating principle and applications of the charged aerosol detector. *Journal of Chromatography a*, **1217**(10), pp. 1549-1556.



Vervoort, N., Daemen, D. and Toeroek, G., 2008. Performance evaluation of evaporative light scattering detection and charged aerosol detection in reversed phase liquid chromatography. *Journal of Chromatography a*, **1189**(1-2), pp. 92-100.

Web Of Science, 2013.

Wright, J.D., 1989. *Molecular Crystals*. Cambridge, UK: Cambridge University Press.

[www.chemicalbook.com](http://www.chemicalbook.com), 2015.

[www.chemspider.com](http://www.chemspider.com), 2015.

[www.sigmaaldrich.com](http://www.sigmaaldrich.com), 2015.

Yang, Y., Matyska, M.T., Boysen, R.I., Pesek, J.J. and Hearn, M.T.W., 2013. Simultaneous separation of hydrophobic and polar bases using a silica hydride stationary phase. *Journal of Separation Science*, **36**(7), pp. 1209-1216.

Yeung, E. and Synovec, R., 1986. Detectors for Liquid-Chromatography. *Analytical Chemistry*, **58**(12), p. 1237.

Zhang, K., Dai, L. and Chetwyn, N.P., 2010. Simultaneous determination of positive and negative pharmaceutical counterions using mixed-mode chromatography coupled with charged aerosol detector. *Journal of Chromatography A*, **1217**(37), pp. 5776-5784.

Zhang, T., Watson, D.G., 2015. A short review of applications of chromatography mass spectrometry based metabolomics techniques to the analysis of human urine. *Analyst*, **140**, p.2907

Zhou, T. and Lucy, C.A., 2008. Hydrophilic interaction chromatography of nucleotides and their pathway intermediates on titania. *Journal of Chromatography A*, **1187**(1-2), pp. 87-93.

## **Appendix I**

### **Figures, Tables, Equations, Symbols and Abbreviations**

## I.1 List of Figures

**Fig 1.1: bonding a ligand to silica using a condensation reaction**

**Fig 1.2: Simple scheme of HILIC retention with neutral (X), basic (X+) and acidic (Y-) solutes**

**Fig. 1.3: The Charged Aerosol Detector**

**Figure 1.4. At Column Dilution**

**Fig 3.1: Structures, pKa, log P/D and charge at ww pH 3 and ww pH 5 for the probe solutes**

**Fig. 3.2. Initial results for eleven probe compounds, (a) Atlantis (b) BEH Amide, (c) Cogent, (d) ZIC-HILIC columns. Vertical scale is peak efficiency at half-height in plates per column; peak asymmetry at 10% height shown in purple boxes above efficiency bar plots. Stationary phase BEH Amide (4.6 x 150mm, 3.5 $\mu$ m) mobile phase 89.425% ACN with respective buffer. Blue = Ammonium Formate 5mM; Red = Formic Acid 0.1% v/v.**

**Fig. 3.3 ZIC-HILIC column (a) nortriptyline with mobile phase 90% ACN, 5 mM overall AF pH 3; (b) nortriptyline with 90% ACN containing 0.1% FA; (c) BSA with AF; (d) BSA with FA; (e) pyridine with AF; (f) pyridine with FA. Flow rate 0.5 cm<sup>3</sup>/min.**

**Fig. 3.4 Comparison of retention (k vs. k') plot for bare silica (Atlantis) vs. hydride silica (Cogent) using 90% ACN containing 5 mM ammonium formate ww pH 3.0. Other conditions as Fig. 2.**

**Fig. 3.5 Retention factor (k), column efficiency (N) and asymmetry factor (As<sub>0.1</sub>) measurements for Atlantis silica column using 85–95% ACN containing (a) 5 mM ammonium formate ww pH 3.0 (b) 0.1% formic acid; for BEH amide column using (c) 5 mM ammonium formate ww pH 3.0 and (d) 0.1% formic acid; asymmetry data in FA not shown for procainamide as split peaks were obtained. Other conditions see Fig. 2.**

**Fig. 3.6. Effect of sample mass on efficiency of Atlantis silica column using procainamide (strong base), TMPAC (quaternary ammonium salt), adenine (weak base) uridine (neutral). Mobile phase 90% ACN containing 0.1% FA. Other conditions see Section 2.**

**Fig. 3.7. Effect of buffer salt on retention using Atlantis silica column. Mobile phase 90% ACN containing salt adjusted to ww pH 3.0 with FA.**

**Fig. 4.1 Simple Schematic of CAD operation**

**Figure 4.2. Peak area vs. concentration for a neutral (Uridine), acid (BSA) and base (Nortriptyline) (a) CAD Ultra, (b) DAD and (c) log/log CAD Ultra (HPLC, mobile phase 80%ACN, 5 mM ammonium formate pH 3).**

Figure 4.3. HILIC-CAD separation and detection of the salts (a) benzyltriethylammonium chloride, (b) benzyltriethylammonium bromide, (c) benzyltriethylammonium iodide; (d)–(e) nortriptyline hydrochloride. Peak identities 1 = benzyltriethylammonium, 2 = chloride, 3 = bromide, 4 = iodide, 5 = nortriptylinium. HPLC, mobile phase 80% ACN for (a)–(c), 95% ACN for (d), 90% ACN for (e) all containing 5 mM ammonium formate pH 3, Atlantis column for (e), BEH Amide column for all others. Nortriptyline hydrochloride concentration 100–10,000 mg/L, injection volume 10 L, others 300 mg/L, injection volume 1 µL.

Figure 4.4. (a) CAD response for 29 compounds (FIA, mobile phase 80% ACN, 5 mM ammonium formate pH 3). Blue = bases, red = acids, green = neutrals. (b) CAD Ultra data indilute acids for the bases nortriptyline and cytosine, acids BSA and 4-HBA and the neutral Uridine (FIA, 80% ACN, FA (0.1% v/v) vs. TFA (0.2%) vs. HFBA (0.345%)). Predicted values from ratios explained in 3.4.3 in hashed-line bars.

Figure 4.5. CAD response for 29 compounds, plotted against (a) boiling point, and (b) melting point; (c) molecular mass (FIA, conditions as per Fig. 4.2).

Figure 4.6. Effect of organic solvent content on (a) peak area, (b) signal to noise ratio and (c) noise (FIA, mobile phase 10–95% ACN, other conditions as per Fig. 4.2).

Figure 4.7. Effect of elevated temperatures on Veo response in order of log D (–ve on left, +ve on right) (FIA, mobile phase 90% ACN, other conditions as per Fig. 2). Log D values were the average from three software packages (see Section 2) Blue = 30°C, Red = 60°C, Green = 80°C.

Figure 4.8. HILIC separation and CAD detection of (a) a mixture of inorganic salts, (b) calcium chloride, (c) magnesium chloride. Peak identities 1 = iodide, 2 = nitrate, 3 = chloride, 4 = potassium, 5 = sodium, 6 = lithium, 7 = calcium, 8 = magnesium (HPLC, mobile phase 70% ACN, 5 mM ammonium formate pH 3, BEH Amide column).

Fig. 5.1 D-glucose in either (α) or (β) form

Fig. 5.2 (a) Nine sugars on BEH Amide column. Mobile phase 70% ACN with 0.1% TEA, CAD Veo detection (1) Levoglucosan, (2) Ribose, (3) Fructose, (4) Mannose, (5) Maltose, (6) Glucose, (7) Galactose, (8) Sucrose, (9) Sorbitol. 1 µL injections; (b) Levoglucosan CAD Veo peak area and Signal to Noise ratios 100 – 2500 mg / L; (c) Ribose CAD Veo peak area and Signal to Noise ratios 100 – 2500 mg / L; (d) Sucrose CAD Veo peak area and Signal to Noise ratios 100 – 2500 mg / L; (e) Glucose CAD Veo peak area and S:N at 1000 mg / L, 1 µL injection, mobile phase 75% ACN with 0.1% TEA; (f) Galactose CAD Veo peak area and S:N at 1000 mg / L, 1 µL injection, mobile phase 75% ACN with 0.1% TEA.

Figure 5.3 (a) Peak areas by flow injection analysis for 29 solutes for two CAD models. Blue = Ultra, Red = Veo; (b) Signal to noise ratios by flow injection analysis for 29 solutes for two CAD models. Blue = Ultra, Red = Veo. Noise manually calculated, peak heights. Veo power function set to 0.67 to simulate 'off'; (c) CAD noise levels, mobile phase 80% ACN with 5mM AF pH 3. Veo with power function 'off', 'on' default setting 1.00 and 'on' optimised setting 1.2, Ultra; d Peak height (as CAD signal) by flow injection analysis for 29 solutes for two CAD models. Blue = Ultra, Red = Veo. Veo power function set to 0.67 to simulate 'off'.

Fig. 5.4 (a) Sugar analysis performed using an 'Amino' HPLC column (Kromasil NH<sub>2</sub>, 4.6 x 150mm, 5µm) calibration using (1) Levoglucosan, (2) Fructose, (3) Glucose, (4) Sucrose, (5) Maltose; (b) HILIC separation of sugars in Ciders with Charged Aerosol Detection (1) Fructose, (2) Glucose, (3) Maltose; (c) HILIC separation of sugars in Beers with Charged Aerosol Detection. (1) Maltose; (d) Calibration curves of five sugars over a wide concentration range (50 – 2000 mg / mL); (e) Calibration curves of five sugars over a narrow concentration range (50 – 500 mg / mL).

Fig. 5.5 HILIC chromatogram of four underivatised amino acids: (1) Glycine, (2) Glutamine, (3) Aspartic Acid, (4) Arginine. Atlantis bare silica column (4.6 x 250 mm, 5 µm), mobile phase 75% ACN with 5mM AF pH 3 with FA.

Figure 6.1. Comparison of (a)  $k'$  (Acetonitrile) vs.  $k'$ (Acetone); Atlantis (4.6x250mm, 5µm); (b) Retention of neutrals and weak bases; (c) retention of acids. 85% Acetonitrile or Acetone with 5mM Ammonium Formate pH3, LCMS grade buffers; (d) relationship between retention ratio in ACN vs. Acetone and number of hydrogen bonding groups per molecule.

Figure 6.2. Separation of probe solutes using generic and zone analytical methods, using (a) Atlantis column with generic gradient for eight solutes, (b) early-eluting solutes with zone 1 isocratic method, (c) middle-eluting solutes with zone 2 isocratic method, (d) BEH Amide column Generic method for eight solutes, (e) early-eluting solutes with zone 1 isocratic method, (f) middle-eluting solutes with zone 2 isocratic method. (a) – (c) Atlantis column, (d) – (f) BEH Amide column. Solute identities as per Table 6.1

Figure 6.3. Chromatograms of Eight probe solutes by RPLC Open Access system (a) Formic Acid (b) TFA and (c) high pH; solute identities as per Table 6.1, conditions provided in legend for each chromatogram.

Fig. 6.4. HILIC-prep chromatograms of simulated crudes with increasing injection volumes, Atlantis column (21mm x 150 mm, 5µm); (a) generic gradient method; (b) zone 2 focused isocratic method, (c) zone 2 focused gradient method. Solute are simulated crude 'APCA/Adenine' 9:1 (w/w), diluent 1% TFA (v/v) in DMSO, flow rate 20mL / min.

Fig. 6.5 HILIC-prep chromatograms of simulated crudes with increasing injection volumes BEH Amide column (21mm x 150mm, 5µm) (a) generic gradient method on for 'Procainamide/AHPY', (b) focused zone 1 isocratic method for 'Procainamide/AHPY', flow rate 20mL / min

Figure 6.6. HILIC-Prep-ACD of Cytidine/Adenine (9:1 w/w) using Atlantis column (a) effect of diluent TFA content (b) effect of larger injections on the ACD system. Mobile phase 'A' = 70% ACN with 5mM Ammonium Formate w<sup>w</sup> pH 3 with formic acid; 'B' = 95% ACN with 5mM Ammonium Formate ww pH 3 with formic acid. Generic gradient method adapted to ACD: 0% 'A' isocratic for 30s then 0-36% 'A' gradient over 15 min, wash at 60% 'A' for 6.5 min, gradient reset to 0% 'A' then equilibration for 7 min to give 34 min method.

**Fig. 6.7. Productivity plot for preparative methods on standard and ACD systems. Arbitrary cut-offs of 20 mg / hr for small-scale purifications (dotted line) and 60 mg / hr for large-scale shown (dashed line).**

**Fig. 6.8. HILIC-Prep-ACD chromatograms investigating any benefit of adding acid (TFA) or base (NH<sub>3</sub>) to the diluent for a crude containing a zwitterionic solute (APCA) and a weak base (Adenine) (23.4 mg / mL). Atlantis column with generic ACD method, 1 mL injections.**

**Fig. 6.9. Effect of DMSO on isocratic analytical separations (a) chromatograms for combined standards of DABS, APCA and AHPY prepared in neat DMSO showing extra peak observed at low wavelength UV (240nm, 85% ACN 5mM AF pH 3 with FA) (b) combined standard prepared with ACN-water-FA (50-50, 0.1% acid v/v), (c) overlaid chromatograms combined standard prepared in increasing DMSO content (20-100% DMSO) (Atlantis column, 95% ACN 5mM AF pH 3 with FA) (d) plot of efficiency vs. DMSO content. Peak identities (1) AHPY, (2) DABS, (3) APCA, (4) DMSO.**

## I.2 List of Tables

3.1. pH, ionic strength and buffer capacity of aqueous buffer solutions;  $w^s$  pH measured in 85% ACN. \*This was used as 0.1% of an 85% solution (14.6 mM/L).

Table 4.1. Identities and physico-chemical characteristics of test compounds.

Table 4.2. Detection limits for charged aerosol detection in HILIC conditions. HPLC, mobile phase 80% ACN, 5mM ammonium formate  $w^w$  pH 3.

Table 4.3. Peak areas of BTEAC, BTEABr and BTEAI by FIA and HPLC. Mobile phase 80% ACN, 5mM ammonium formate  $w^w$  pH 3.

Table 4.4. Peak areas and uniformity of response for 21 compounds in a selection of HILIC mobile phases.

Table 5.1. Sugar concentrations found in ciders and beer

Table 6.1. Probe solutes used in generic and scale-up studies

Table 6.2. Retention times of critical pairs in elution 'Zone 1' and 'Zone 2' by generic and focused isocratic methods on Atlantis and BEH Amide columns. Solvents as per Fig. 6.2a.

Table 6.3. Apparent solubility of HILIC-prep simulated crudes for some solvent systems

Table 6.4 HILIC-Prep data for information

Table 6.5 Effect of diluent DMSO content on analytical peak efficiency, for information

## **I.3 List of Equations**

**1.1 column volume ( $V_m$ )**

**1.2 retention volume ( $V_r$ )**

**1.3 retention factor ( $k$ )**

**1.4 selectivity factor ( $\alpha$ )**

**1.5 Peak efficiency at half-height ( $N_{0.5}$ )**

**1.6 Height equivalent to one theoretical plate ( $H$ )**

**1.7 Average velocity of the mobile phase ( $u$ )**

**1.8 van Deemter equation:  $H$ , described by three processes: axial diffusion (A), longitudinal diffusion (B) and mass transfer (C)**

**1.9 Reduced plate height ( $h$ )**

**1.10 Reduced co-ordinate van Deemter equation**

**1.11 System backpressure ( $\Delta P$ )**

**1.12 Chromatographic resolution ( $R_s$ )**

**1.13 Retention ( $\log k$ ) as a function of the Hydrophobic-Subtraction model**

**1.14 Partitioning between an aqueous and non-aqueous phase**

**1.15 Partition coefficient ( $P$ )**

**1.16  $\log P$**

**1.17 Dissociation of an acid ( $HA$ ) to hydroxonium ( $H_3O^+$ ) and its anion ( $A^-$ ) in the presence of water**

**1.18 Acid dissociation constant ( $K_a$ )**

**1.19 Henderson-Hasselbach equation**

**1.20  $\log D$**

**1.21 Preparative scale-up factor**

**3.1 Column efficiency ( $N$ ) measured from the first ( $M_1$ ) and second statistical moments ( $M_2$ )**

**3.2 True thermodynamic  $s^s$  pH**

**4.1 The diameter of the particle in ELSD ( $d_D$ )**

**4.2 surface area of a sphere ( $A$ )**



**4.3 Surface area of an aerosol particle ( $A$ ) in relation to solute concentration ( $C$ )**

**4.4 Relationship between CAD response and analyte concentration ( $C$ )**

**4.5 Relationship between  $\log$  (CAD response) and  $\log$  (analyte concentration) ( $C$ )**

**5.1 Signal to noise ratio ( $S:N$ )**

**6.1 Solubility in a cosolvent mixture ( $S_{\text{mix}}$ )**

**6.2 Preparative productivity ( $P_{R,i}$ )**

**6.3 Generic expression for preparative productivity ( $P_R$ )**

## I.4 List of Symbols

<b>&gt;</b>	<b>greater than</b>
<b>%</b>	<b>percent</b>
<b>£</b>	<b>pound sterling</b>
<b>Å</b>	<b>angstrom</b>
<b><math>\alpha</math></b>	<b>selectivity factor</b>
<b><math>\alpha'</math></b>	<b>solute hydrogen bonding interactions of an acidic solute to a basic stationary phase</b>
<b>a</b>	<b>intercept</b>
<b>A</b>	<b>axial diffusion coefficient (van Deemter 'A term')</b>
<b>A</b>	<b>column hydrogen bonding interactions of a basic solute to an acidic stationary phase</b>
<b>A<sup>-</sup></b>	<b>deprotonated acid A</b>
<b>A</b>	<b>Surface area of a sphere</b>
<b>A<sub>p</sub></b>	<b>Surface area of a(n aerosol) particle</b>
<b>As<sub>0.1</sub></b>	<b>peak asymmetry at 10% height</b>
<b><math>\beta</math></b>	<b>hydrogen bond basicity</b>
<b><math>\beta'</math></b>	<b>solute hydrogen bonding interactions of a basic solute to an acidic stationary phase</b>
<b>B</b>	<b>longitudinal diffusion coefficient (van Deemter 'B term')</b>
<b>B</b>	<b>column hydrogen bonding interactions of an acidic solute to a basic stationary phase</b>
<b>c</b>	<b>solute concentration</b>
<b>C</b>	<b>column interactions between an ionic solute and charge-bearing column</b>
<b>C</b>	<b>mass transfer coefficient (van Deemter 'C term')</b>
<b>C</b>	<b>celcius</b>
<b>cm</b>	<b>centimetre(s)</b>
<b>cm<sup>3</sup></b>	<b>cubic centimetre(s)</b>

$C_{(aq)}$	solute concentration in aqueous solvent phase
$C_{(org)}$	solute concentration in organic solvent phase
Cs	caesium
$\delta$	correction of $w^s$ pH to $s^s$ pH
D	Distribution coefficient
$d_D$	droplet diameter
dp	particle diameter
°	degree
C18	octadecylsilyl stationary phase
$\eta'$	solute hydrophobic interactions
EB	retention of ethylbenzene
F	volumetric flow rate
fc	volume fraction of cosolvent in an aqueous mixture
g	gram(s)
h	reduced plate height
H	height equivalent to a theoretical plate
H	column hydrophobic interactions
H	hydrogen
Hg	mercury
$H_3O^+$	hydroxonium ion
HA	protonated acid
HZ	hertz
$\kappa'$	solute ion-exchange between an ionic solute and charge-bearing column
k	retention factor
K	potassium
Ka	acid dissociation constant
$K_{ow}$	octanol-water partition coefficient

<b>k<sub>1</sub></b>	<b>retention factor of weakly-retained peak (see k, α)</b>
<b>k<sub>2</sub></b>	<b>retention factor of strongly-retained peak (see k, α)</b>
<b>ρ<sub>p</sub></b>	<b>particle density</b>
<b>L</b>	<b>column length</b>
<b>L</b>	<b>litre(s)</b>
<b>Li</b>	<b>lithium</b>
<b>Log D</b>	<b>log of distribution coefficient (see D)</b>
<b>μg</b>	<b>microgram(s)</b>
<b>μL</b>	<b>microliter(s)</b>
<b>μm</b>	<b>micrometre(s)</b>
<b>M<sub>1</sub></b>	<b>first statistical moment</b>
<b>M<sub>2</sub></b>	<b>second statistical moment</b>
<b>m<sup>2</sup></b>	<b>square metres</b>
<b>mAU</b>	<b>milliabsorbance units</b>
<b>min</b>	<b>minute(s)</b>
<b>mg</b>	<b>milligram(s)</b>
<b>mL</b>	<b>millilitre(s)</b>
<b>mm</b>	<b>millimetre(s)</b>
<b>mM</b>	<b>millimolar</b>
<b>mmol</b>	<b>millimole(s)</b>
<b>ng</b>	<b>nanogram(s)</b>
<b>nm</b>	<b>nanometre(s)</b>
<b>N</b>	<b>plate number</b>
<b>N<sub>0.5</sub></b>	<b>peak efficiency at half-height (plate number)</b>
<b>Na</b>	<b>sodium</b>
<b>n<sub>coll</sub></b>	<b>amount collected during preparative fractionation</b>
<b>NH<sub>2</sub></b>	<b>amino functional group</b>

<b><math>\text{NH}_4^+</math></b>	<b>ammonium</b>
<b><math>N_{\text{moments}}</math></b>	<b>peak efficiency by moments method</b>
<b>P</b>	<b>partition coefficient</b>
<b>pA</b>	<b>picoamps</b>
<b>pH</b>	<b>scale of acidity</b>
<b>pKa</b>	<b>logarithmic acid dissociation constant</b>
<b>ppm</b>	<b>parts per million</b>
<b><math>P_R</math></b>	<b>productivity of a generic preparative separation</b>
<b><math>P_{R,i}</math></b>	<b>productivity of a preparative separation for solute i</b>
<b>Rb</b>	<b>rubidium</b>
<b><math>t_0</math></b>	<b>retention time of an unretained solute</b>
<b><math>t_R</math></b>	<b>retention time of retained solute</b>
<b>r</b>	<b>correlation coefficient</b>
<b><math>R^2</math></b>	<b>coefficient of determination</b>
<b><math>R_s</math></b>	<b>Chromatographic Resolution</b>
<b><math>\sigma</math></b>	<b>solute steric interactions</b>
<b>s</b>	<b>second(s)</b>
<b>s</b>	<b>cosolvent constant (slope)</b>
<b><math>S^*</math></b>	<b>column steric interactions</b>
<b>Si-H</b>	<b>silica hydride bond</b>
<b><math>S_{\text{mix}}</math></b>	<b>solubility in a cosolvent mixture</b>
<b>S:N</b>	<b>Signal to Noise ratio</b>
<b><math>S_w</math></b>	<b>solubility in water</b>
<b>t</b>	<b>cosolvent constant (intercept)</b>
<b>t</b>	<b>time</b>
<b><math>t_c</math></b>	<b>cycle time</b>
<b><math>V_{\text{col}}</math></b>	<b>column volume</b>

<b><math>V_m</math></b>	<b>column volume</b>
<b><math>V_r</math></b>	<b>retention volume</b>
<b><math>v/v</math></b>	<b>volume by volume</b>
<b><math>w/w</math></b>	<b>weight by weight</b>
<b><math>W_{0.5}</math></b>	<b>peak width at half-height</b>
<b><math>w^w</math> pH</b>	<b>pH calibrated in aqueous buffers and measured in aqueous solution</b>
<b><math>w^s</math> pH</b>	<b>pH calibrated in aqueous buffers and measured in hydroorganic solution</b>
<b><math>X_{(aq)}</math></b>	<b>solute partitioned into aqueous solvent</b>
<b><math>X_{(non-aq)}</math></b>	<b>solute partitioned into organic solvent</b>
<b>Z1</b>	<b>zone 1</b>
<b>Z2</b>	<b>zone 2</b>

### 3. I.5 List of abbreviations

<b>AA</b>	<b>Ammonium Acetate</b>
<b>ACD</b>	<b>At Column Dilution</b>
<b>ACN</b>	<b>Acetonitrile</b>
<b>AF</b>	<b>Ammonium Formate</b>
<b>AHPY</b>	<b>2-Amino-3-hydroxypyridine</b>
<b>AIAZ</b>	<b>6-Aminoindazole</b>
<b>ANP</b>	<b>Aqueous Normal Phase</b>
<b>APCA</b>	<b>2-Aminopyridine-3-carboxylic acid</b>
<b>APCI</b>	<b>Atmospheric Pressure Chemical Ionisation</b>
<b>APOL</b>	<b>2-Aminopyridin-4-ol</b>
<b>BEH</b>	<b>Ethylene Bridged Hybrid silica</b>
<b>BP</b>	<b>Boiling Point</b>
<b>BSA</b>	<b>Benzene sulfonic acid</b>
<b>BTEA</b>	<b>Benzyltriethylammonium</b>
<b>BTEABr</b>	<b>Benzyltriethylammonium Bromide</b>
<b>BTEAC</b>	<b>Benzyltriethylammonium Chloride</b>
<b>BTMAC</b>	<b>Benzyltrimethylammonium Chloride</b>
<b>BTEAI</b>	<b>Benzyltriethylammonium Iodide</b>
<b>CAD</b>	<b>Charged Aerosol Detection</b>
<b>CNLS</b>	<b>Condensation Nucleation Light Scattering Detection</b>
<b>CSH</b>	<b>Charged Surface Hybrid stationary phase</b>
<b>DABS</b>	<b>2,5-Diaminobenzenesulfonic acid</b>
<b>DAD</b>	<b>Diode Array Detector</b>
<b>DMF</b>	<b>Dimethylformamide</b>
<b>DMSO</b>	<b>Dimethylsulfoxide</b>
<b>ESI-MS</b>	<b>Electrospray Mass Spectrometry</b>

<b>ELSD</b>	<b>Evaporative Light Scattering Detection</b>
<b>EPSRC</b>	<b>Engineering and Physical Sciences Research Council</b>
<b>FA</b>	<b>Formic Acid</b>
<b>FIA</b>	<b>Flow Injection Analysis</b>
<b>Fig</b>	<b>Figure</b>
<b>FW</b>	<b>Formula Weight</b>
<b>GC</b>	<b>Gas Chromatography</b>
<b>HBA</b>	<b>4-Hydroxybenzoic Acid</b>
<b>HCl</b>	<b>Hydrogen Chloride</b>
<b>HFBA</b>	<b>Heptafluorobutyric acid</b>
<b>HILIC</b>	<b>Hydrophilic Interaction Chromatography</b>
<b>HPLC</b>	<b>High Performance Liquid Chromatography</b>
<b>ID/i.d.</b>	<b>Internal Diameter</b>
<b>IP</b>	<b>Ion Pairing</b>
<b>IPA</b>	<b>Isopropyl Alcohol</b>
<b>LC</b>	<b>Liquid Chromatography</b>
<b>LOD</b>	<b>Limit Of Detection</b>
<b>LOQ</b>	<b>Limit Of Quantitation</b>
<b>MP</b>	<b>Melting Point</b>
<b>MS</b>	<b>Mass spectrometry</b>
<b>MW</b>	<b>Molecular Weight</b>
<b>NFPA</b>	<b>Nonafluoropentanoic Acid</b>
<b>N,N-DMAC</b>	<b>N,N-dimethylacetamide</b>
<b>NSA</b>	<b>2-Naphthalenesulfonic acid</b>
<b>OA</b>	<b>Open Access</b>
<b>ODS</b>	<b>octadecylsilyl (ligand)</b>
<b>PA</b>	<b>Orthophosphoric acid</b>



<b>Prep</b>	<b>Preparative liquid chromatography</b>
<b>PF</b>	<b>Power Function</b>
<b>RI</b>	<b>Refractive Index (detection)</b>
<b>RMS</b>	<b>Root Mean Squared</b>
<b>RP</b>	<b>Reversed phase liquid chromatography</b>
<b>RPLC</b>	<b>Reversed Phase Liquid Chromatography</b>
<b>RSD</b>	<b>Relative Standard Deviation</b>
<b>SFC</b>	<b>Supercritical Fluid Chromatography</b>
<b>THBA</b>	<b>3,4,5-trihydroxybenzoic acid</b>
<b>TEA</b>	<b>Triethylamine</b>
<b>TEA-MePO3</b>	<b>Triethylamine Methylphosphonate</b>
<b>TEAP</b>	<b>Trimethylamine Phosphate</b>
<b>TFA</b>	<b>Trifluoroacetic acid</b>
<b>TMPAC</b>	<b>Trimethylphenyammonium chloride</b>
<b>TSK</b>	<b>Tosoh Biosciences column brand</b>
<b>UHPLC</b>	<b>Ultra High Performance Liquid Chromatography</b>
<b>USA</b>	<b>United States of America</b>
<b>UV</b>	<b>Ultraviolet (absorbance)</b>
<b>UV-VIS</b>	<b>Ultraviolet-Visible (absorbance)</b>
<b>ZIC-HILIC</b>	<b>Zwitterionic HILIC stationary phase, Merck Sequant brand</b>

## **Appendix II**

### **Presentations and Publications**

## 1. II.1 Poster Presentations

**11 Jan 2013** Centre for Research in Biosciences annual meeting, University of the West of England

*Hydrophilic Interaction Chromatography: A new separation method for the analysis of polar pharmaceuticals and biomedically relevant compounds*

**10 Jan 2014** Centre for Research in Biosciences annual meeting, University of the West of England

*Charged Aerosol Detection for the analysis of pharmaceutical and biologically relevant compounds*

**27 Jun 2014** Faculty of Applied Sciences postgraduate conference, University of the West of England

*Charged Aerosol Detection for pharmaceuticals and biologically relevant compounds*

**11-15 May 2014** 41<sup>st</sup> International Symposium on High Performance Liquid Phase Separations and Related Techniques, New Orleans, USA

*Investigations into Charged Aerosol Detection with Hydrophilic Interaction Chromatography*

**21-25 Jun 2015** 42<sup>nd</sup> International Symposium on High Performance Liquid Phase Separations and Related Techniques, Geneva, Switzerland

*Performance of Charged Aerosol Detection with Hydrophilic Interaction Chromatography*

## 2. II.2 Oral Presentations

**08 May 2013** GlaxoSmithKline industrial partner visit to UWE, Bristol

*Why bother with salt buffer? Peak shapes in HILIC*

**09 May 2013** Centre for Research in Biosciences fortnightly talk, UWE Bristol

*Why bother with salt buffer? Peak shapes in HILIC*

**16 Sep 2013** GlaxoSmithKline and ThermoFisher Scientific industrial partners meeting at UWE, Bristol

*Development of generic methods for the analysis and purification of polar compounds by high performance liquid chromatography: Initial investigations*

**27 Jan 2014** GlaxoSmithKline and ThermoFisher Scientific industrial partners meeting at Thermo, Hemel Hempsted

*Development of generic methods for the analysis and purification of polar compounds by high performance liquid chromatography: HILIC-CAD investigations*

**11 Nov 2014** GlaxoSmithKline industrial partners meeting at UWE, Bristol

*Development of generic methods for the analysis and purification of polar compounds by high performance liquid chromatography: Project update November 2014*

### **3. II.3 Second Author Oral Presentations**

**11-15 May 2014**      41<sup>st</sup> International Symposium on High Performance Liquid Phase Separations  
and Related Techniques, New Orleans, USA

*New Developments in Hydrophilic Interaction Chromatography, presentation with David McCalley and James Heaton*

## 4. II.4 Publications

Meeting report for 'Automated Approaches in Modern Chromatography and Mass Spectrometry'  
Chromsoc spring symposium, *Chromatography Today*, 2013

Meeting report for 'Advances in Clinical Analysis', *Royal Society of Chemistry Separation Science Group website*, 2014

Conference report for '41st symposium of HPLC in New Orleans', *Chromatography Today*, 2014

Comparison of peak shape in hydrophilic interaction chromatography using acidic salt buffers and simple acid solutions. *Journal of chromatography.A*, **1347**, pp. 39-48.

**HEATON, J.C., RUSSELL, J.J., UNDERWOOD, T., BOUGHTFLOWER, R. and MCCALLEY, D.V., 2014.**

Performance of charged aerosol detection with hydrophilic interaction chromatography. *Journal of Chromatography a*, **1405**, pp. 72-84.

**RUSSELL, J.J., HEATON, J.C., UNDERWOOD, T., BOUGHTFLOWER, R. and MCCALLEY, D.V., 2015.**